NASA/CR-1998-206924

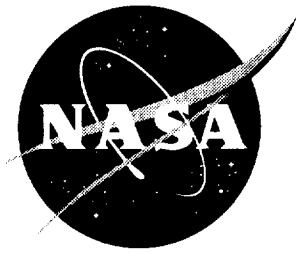

Catalogue of X-Ray Texture Data for Al-Cu-Li Alloy 1460, 2090, 2096 and 2195 Near-Net-Shape Extrusions, Sheet and Plate

Stephen J. Hales, Robert A. Hafley, and Joel A. Alexa
Analytical Services & Materials, Inc., Hampton, Virginia

National Aeronautics and
Space Administration

Langley Research Center
Hampton, Virginia 23681-2199

Prepared for Langley Research Center
under Contract NAS1-19708

February 1998

Available from the following:

NASA Center for AeroSpace Information (CASI)
800 Elkridge Landing Road
Linthicum Heights, MD 21090-2934
(301) 621-0390

National Technical Information Service (NTIS)
5285 Port Royal Road
Springfield, VA 22161-2171
(703) 487-4650

Table of Contents

Table of Contents	iii
List of Tables and Figures	iv
Abstract	1
Symbols and Abbreviations	1
1. Introduction	1
2. Materials	2
3. Procedures	2
4. Results	6
4.1 Alloy 1460	6
4.2 Alloy 2090	47
4.3 Alloy 2096	88
4.4 Alloy 2195	122

List of Tables and Figures

Table 1.	Nominal and specified range of compositions for 1460, 2090, 2096 and 2195 near-net-shape extrusions, sheet and plate.	3
Table 2.	Matrix for collection of x-ray diffraction data as a function of alloy, product form and through-thickness location.	4
Figure 1.	Schematics showing, (a), the dimensions of the near-net-shape extrusions and, (b), the locations of specimen extraction for texture analysis.	5
Figure 2.	Partial pole figures for the 1460-T3 extrusion in the skin @ t/4 [Specimen plane perpendicular to (R)adial axis].	7
Figure 3.	CODF sections for the 1460-T3 extrusion in the skin @ t/4 [Specimen plane perpendicular to (R)adial axis].	8
Figure 4.	Partial pole figures for the 1460-T3 extrusion in the skin @ t/2 [Specimen plane perpendicular to (R)adial axis].	9
Figure 5.	CODF sections for the 1460-T3 extrusion in the skin @ t/2 [Specimen plane perpendicular to (R)adial axis].	10
Figure 6.	Partial pole figures for the 1460-T3 extrusion in the skin @ 3t/4 [Specimen plane perpendicular to (R)adial axis].	11
Figure 7.	CODF sections for the 1460-T3 extrusion in the skin @ 3t/4 [Specimen plane perpendicular to (R)adial axis].	12
Figure 8.	Orientation density, f(g), as a function of location through the cross-section for the 1460-T3 extrusion in the skin region.	13
Figure 9.	Partial pole figures for the 1460-T3 extrusion in the base @ t/2 [Specimen plane perpendicular to (R)adial axis].	14
Figure 10.	CODF sections for the 1460-T3 extrusion in the base @ t/2 [Specimen plane perpendicular to (R)adial axis].	15
Figure 11.	Partial pole figures for the 1460-T3 extrusion in the base @ t/2 [Specimen plane perpendicular to (C)ircumferential axis].	16
Figure 12.	CODF sections for the 1460-T3 extrusion in the base @ t/2 [Specimen plane perpendicular to (C)ircumferential axis].	17
Figure 13.	Partial pole figures for the 1460-T3 extrusion in the web @ t/8 [Specimen plane perpendicular to (C)ircumferential axis].	18
Figure 14.	CODF sections for the 1460-T3 extrusion in the web @ t/8 [Specimen plane perpendicular to (C)ircumferential axis].	19

Figure 15. Partial pole figures for the 1460-T3 extrusion in the web @ 3t/8 [Specimen plane perpendicular to (C)ircumferential axis]. 20

Figure 16. CODF sections for the 1460-T3 extrusion in the web @ 3t/8 [Specimen plane perpendicular to (C)ircumferential axis]. 21

Figure 17. Partial pole figures for the 1460-T3 extrusion in the web @ 5t/8 [Specimen plane perpendicular to (C)ircumferential axis]. 22

Figure 18. CODF sections for the 1460-T3 extrusion in the web @ 5t/8 [Specimen plane perpendicular to (C)ircumferential axis]. 23

Figure 19. Partial pole figures for the 1460-T3 extrusion in the web @ 7t/8 [Specimen plane perpendicular to (C)ircumferential axis]. 24

Figure 20. CODF sections for the 1460-T3 extrusion in the web @ 7t/8 [Specimen plane perpendicular to (C)ircumferential axis]. 25

Figure 21. Partial pole figures for the 1460-T3 extrusion in the cap @ t/4 [Specimen plane perpendicular to (R)adial axis]. 26

Figure 22. CODF sections for the 1460-T3 extrusion in the cap @ t/4 [Specimen plane perpendicular to (R)adial axis]. 27

Figure 23. Partial pole figures for the 1460-T3 extrusion in the cap @ t/2 [Specimen plane perpendicular to (R)adial axis]. 28

Figure 24. CODF sections for the 1460-T3 extrusion in the cap @ t/2 [Specimen plane perpendicular to (R)adial axis]. 29

Figure 25. Partial pole figures for the 1460-T3 extrusion in the cap @ 3t/4 [Specimen plane perpendicular to (R)adial axis]. 30

Figure 26. CODF sections for the 1460-T3 extrusion in the cap @ 3t/4 [Specimen plane perpendicular to (R)adial axis]. 31

Figure 27. Orientation density, f(g), as a function of location through the cross-section for the 1460-T3 extrusion in the cap region. 32

Figure 28. Partial pole figures for 1460-T3 sheet @ t/8 [Specimen plane perpendicular to (S)hort-Transverse axis]. 33

Figure 29. CODF sections for 1460-T3 sheet @ t/8 [Specimen plane perpendicular to (S)hort-Transverse axis]. 34

Figure 30. Partial pole figures for 1460-T3 sheet @ t/4 [Specimen plane perpendicular to (S)hort-Transverse axis]. 35

Figure 31. CODF sections for 1460-T3 sheet @ t/4 [Specimen plane perpendicular to (S)hort-Transverse axis]. 36

Figure 32.	Partial pole figures for 1460-T3 sheet @ t/2 [Specimen plane perpendicular to (S)hort-Transverse axis].	37
Figure 33.	CODF sections for 1460-T3 sheet @ t/2 [Specimen plane perpendicular to (S)hort-Transverse axis].	38
Figure 34.	Orientation density, f(g), as a function of location through the cross-section for the 1460-T3 sheet.	39
Figure 35.	Partial pole figures for 1460-T3 plate @ t/8 [Specimen plane perpendicular to (S)hort-Transverse axis].	40
Figure 36.	CODF sections for 1460-T3 plate @ t/8 [Specimen plane perpendicular to (S)hort-Transverse axis].	41
Figure 37.	Partial pole figures for 1460-T3 plate @ t/4 [Specimen plane perpendicular to (S)hort-Transverse axis].	42
Figure 38.	CODF sections for 1460-T3 plate @ t/4 [Specimen plane perpendicular to (S)hort-Transverse axis].	43
Figure 39.	Partial pole figures for 1460-T3 plate @ t/2 [Specimen plane perpendicular to (S)hort-Transverse axis].	44
Figure 40.	CODF sections for 1460-T3 plate @ t/2 [Specimen plane perpendicular to (S)hort-Transverse axis].	45
Figure 41.	Orientation density, f(g), as a function of location through the cross-section for the 1460-T3 plate.	46
Figure 42.	Partial pole figures for the 2090-T8 extrusion in the skin @ t/4 [Specimen plane perpendicular to (R)adial axis].	48
Figure 43.	CODF sections for the 2090-T8 extrusion in the skin @ t/4 [Specimen plane perpendicular to (R)adial axis].	49
Figure 44.	Partial pole figures for the 2090-T8 extrusion in the skin @ t/2 [Specimen plane perpendicular to (R)adial axis].	50
Figure 45.	CODF sections for the 2090-T8 extrusion in the skin @ t/2 [Specimen plane perpendicular to (R)adial axis].	51
Figure 46.	Partial pole figures for the 2090-T8 extrusion in the skin @ 3t/4 [Specimen plane perpendicular to (R)adial axis].	52
Figure 47.	CODF sections for the 2090-T8 extrusion in the skin @ 3t/4 [Specimen plane perpendicular to (R)adial axis].	53
Figure 48.	Orientation density, f(g), as a function of location through the cross-section for the 2090-T8 extrusion in the skin region.	54

Figure 49. Partial pole figures for the 2090-T8 extrusion in the base @ t/2 [Specimen plane perpendicular to (R)adial axis]. 55

Figure 50. CODF sections for the 2090-T8 extrusion in the base @ t/2 [Specimen plane perpendicular to (R)adial axis]. 56

Figure 51. Partial pole figures for the 2090-T8 extrusion in the base @ t/2 [Specimen plane perpendicular to (C)ircumferential axis]. 57

Figure 52. CODF sections for the 2090-T8 extrusion in the base @ t/2 [Specimen plane perpendicular to (C)ircumferential axis]. 58

Figure 53. Partial pole figures for the 2090-T8 extrusion in the web @ t/8 [Specimen plane perpendicular to (C)ircumferential axis]. 59

Figure 54. CODF sections for the 2090-T8 extrusion in the web @ t/8 [Specimen plane perpendicular to (C)ircumferential axis]. 60

Figure 55. Partial pole figures for the 2090-T8 extrusion in the web @ 3t/8 [Specimen plane perpendicular to (C)ircumferential axis]. 61

Figure 56. CODF sections for the 2090-T8 extrusion in the web @ 3t/8 [Specimen plane perpendicular to (C)ircumferential axis]. 62

Figure 57. Partial pole figures for the 2090-T8 extrusion in the web @ 5t/8 [Specimen plane perpendicular to (C)ircumferential axis]. 63

Figure 58. CODF sections for the 2090-T8 extrusion in the web @ 5t/8 [Specimen plane perpendicular to (C)ircumferential axis]. 64

Figure 59. Partial pole figures for the 2090-T8 extrusion in the web @ 7t/8 [Specimen plane perpendicular to (C)ircumferential axis]. 65

Figure 60. CODF sections for the 2090-T8 extrusion in the web @ 7t/8 [Specimen plane perpendicular to (C)ircumferential axis]. 66

Figure 61. Partial pole figures for the 2090-T8 extrusion in the cap @ t/4 [Specimen plane perpendicular to (R)adial axis]. 67

Figure 62. CODF sections for the 2090-T8 extrusion in the cap @ t/4 [Specimen plane perpendicular to (R)adial axis]. 68

Figure 63. Partial pole figures for the 2090-T8 extrusion in the cap @ t/2 [Specimen plane perpendicular to (R)adial axis]. 69

Figure 64. CODF sections for the 2090-T8 extrusion in the cap @ t/2 [Specimen plane perpendicular to (R)adial axis]. 70

Figure 65. Partial pole figures for the 2090-T8 extrusion in the cap @ 3t/4 [Specimen plane perpendicular to (R)adial axis]. 71

Figure 66. CODF sections for the 2090-T8 extrusion in the cap @ 3t/4 [Specimen plane perpendicular to (R)adial axis]. 72

Figure 67. Orientation density, f(g), as a function of location through the cross-section for the 2090-T8 extrusion in the cap region. 73

Figure 68. Partial pole figures for 2090-T8 sheet @ t/8 [Specimen plane perpendicular to (S)hort-Transverse axis]. 74

Figure 69. CODF sections for 2090-T8 sheet @ t/8 [Specimen plane perpendicular to (S)hort-Transverse axis]. 75

Figure 70. Partial pole figures for 2090-T8 sheet @ t/4 [Specimen plane perpendicular to (S)hort-Transverse axis]. 76

Figure 71. CODF sections for 2090-T8 sheet @ t/4 [Specimen plane perpendicular to (S)hort-Transverse axis]. 77

Figure 72. Partial pole figures for 2090-T8 sheet @ t/2 [Specimen plane perpendicular to (S)hort-Transverse axis]. 78

Figure 73. CODF sections for 2090-T8 sheet @ t/2 [Specimen plane perpendicular to (S)hort-Transverse axis]. 79

Figure 74. Orientation density, f(g), as a function of location through the cross-section for the 2090-T8 sheet. 80

Figure 75. Partial pole figures for 2090-T8 plate @ t/8 [Specimen plane perpendicular to (S)hort-Transverse axis]. 81

Figure 76. CODF sections for 2090-T8 plate @ t/8 [Specimen plane perpendicular to (S)hort-Transverse axis]. 82

Figure 77. Partial pole figures for 2090-T8 plate @ t/4 [Specimen plane perpendicular to (S)hort-Transverse axis]. 83

Figure 78. CODF sections for 2090-T8 plate @ t/4 [Specimen plane perpendicular to (S)hort-Transverse axis]. 84

Figure 79. Partial pole figures for 2090-T8 plate @ t/2 [Specimen plane perpendicular to (S)hort-Transverse axis]. 85

Figure 80. CODF sections for 2090-T8 plate @ t/2 [Specimen plane perpendicular to (S)hort-Transverse axis]. 86

Figure 81. Orientation density, f(g), as a function of location through the cross-section for the 2090-T8 plate. 87

Figure 82. Partial pole figures for the 2096-T3 extrusion in the skin @ t/4 [Specimen plane perpendicular to (R)adial axis]. 89

Figure 83. CODF sections for the 2096-T3 extrusion in the skin @ t/4 [Specimen plane perpendicular to (R)adial axis]. 90

Figure 84. Partial pole figures for the 2096-T3 extrusion in the skin @ t/2 [Specimen plane perpendicular to (R)adial axis]. 91

Figure 85. CODF sections for the 2096-T3 extrusion in the skin @ t/2 [Specimen plane perpendicular to (R)adial axis]. 92

Figure 86. Partial pole figures for the 2096-T3 extrusion in the skin @ 3t/4 [Specimen plane perpendicular to (R)adial axis]. 93

Figure 87. CODF sections for the 2096-T3 extrusion in the skin @ 3t/4 [Specimen plane perpendicular to (R)adial axis]. 94

Figure 88. Orientation density, f(g), as a function of location through the cross-section for the 2096-T3 extrusion in the skin region. 95

Figure 89. Partial pole figures for the 2096-T3 extrusion in the base @ t/2 [Specimen plane perpendicular to (R)adial axis]. 96

Figure 90. CODF sections for the 2096-T3 extrusion in the base @ t/2 [Specimen plane perpendicular to (R)adial axis]. 97

Figure 91. Partial pole figures for the 2096-T3 extrusion in the base @ t/2 [Specimen plane perpendicular to (C)ircumferential axis]. 98

Figure 92. CODF sections for the 2096-T3 extrusion in the base @ t/2 [Specimen plane perpendicular to (C)ircumferential axis]. 99

Figure 93. Partial pole figures for the 2096-T3 extrusion in the web @ t/8 [Specimen plane perpendicular to (C)ircumferential axis]. 100

Figure 94. CODF sections for the 2096-T3 extrusion in the web @ t/8 [Specimen plane perpendicular to (C)ircumferential axis]. 101

Figure 95. Partial pole figures for the 2096-T3 extrusion in the web @ 3t/8 [Specimen plane perpendicular to (C)ircumferential axis]. 102

Figure 96. CODF sections for the 2096-T3 extrusion in the web @ 3t/8 [Specimen plane perpendicular to (C)ircumferential axis]. 103

Figure 97. Partial pole figures for the 2096-T3 extrusion in the web @ 5t/8 [Specimen plane perpendicular to (C)ircumferential axis]. 104

Figure 98. CODF sections for the 2096-T3 extrusion in the web @ 5t/8 [Specimen plane perpendicular to (C)ircumferential axis]. 105

Figure 99. Partial pole figures for the 2096-T3 extrusion in the web @ 7t/8 [Specimen plane perpendicular to (C)ircumferential axis]. 106

Figure 100. CODF sections for the 2096-T3 extrusion in the web @ 7t/8 [Specimen plane perpendicular to (C)ircumferential axis]. 107

Figure 101. Partial pole figures for the 2096-T3 extrusion in the cap @ t/4 [Specimen plane perpendicular to (R)adial axis]. 108

Figure 102. CODF sections for the 2096-T3 extrusion in the cap @ t/4 [Specimen plane perpendicular to (R)adial axis]. 109

Figure 103. Partial pole figures for the 2096-T3 extrusion in the cap @ t/2 [Specimen plane perpendicular to (R)adial axis]. 110

Figure 104. CODF sections for the 2096-T3 extrusion in the cap @ t/2 [Specimen plane perpendicular to (R)adial axis]. 111

Figure 105. Partial pole figures for the 2096-T3 extrusion in the cap @ 3t/4 [Specimen plane perpendicular to (R)adial axis]. 112

Figure 106. CODF sections for the 2096-T3 extrusion in the cap @ 3t/4 [Specimen plane perpendicular to (R)adial axis]. 113

Figure 107. Orientation density, f(g), as a function of location through the cross-section for the 2096-T3 extrusion in the cap region. 114

Figure 108. Partial pole figures for 2096-T8 sheet @ t/8 [Specimen plane perpendicular to (S)hort-Transverse axis]. 115

Figure 109. CODF sections for 2096-T8 sheet @ t/8 [Specimen plane perpendicular to (S)hort-Transverse axis]. 116

Figure 110. Partial pole figures for 2096-T8 sheet @ t/4 [Specimen plane perpendicular to (S)hort-Transverse axis]. 117

Figure 111. CODF sections for 2096-T8 sheet @ t/4 [Specimen plane perpendicular to (S)hort-Transverse axis]. 118

Figure 112. Partial pole figures for 2096-T8 sheet @ t/2 [Specimen plane perpendicular to (S)hort-Transverse axis]. 119

Figure 113. CODF sections for 2096-T8 sheet @ t/2 [Specimen plane perpendicular to (S)hort-Transverse axis]. 120

Figure 114. Orientation density, f(g), as a function of location through the cross-section for the 2096-T8 sheet. 121

Figure 115. Partial pole figures for the 2195-T3 extrusion in the skin @ t/4 [Specimen plane perpendicular to (R)adial axis]. 123

Figure 116. CODF sections for the 2195-T3 extrusion in the skin @ t/4 [Specimen plane perpendicular to (R)adial axis]. 124

Figure 117. Partial pole figures for the 2195-T3 extrusion in the skin @ t/2 [Specimen plane perpendicular to (R)adial axis]. 125

Figure 118. CODF sections for the 2195-T3 extrusion in the skin @ t/2 [Specimen plane perpendicular to (R)adial axis]. 126

Figure 119. Partial pole figures for the 2195-T3 extrusion in the skin @ 3t/4 [Specimen plane perpendicular to (R)adial axis]. 127

Figure 120. CODF sections for the 2195-T3 extrusion in the skin @ 3t/4 [Specimen plane perpendicular to (R)adial axis]. 128

Figure 121. Orientation density, f(g), as a function of location through the cross-section for the 2195-T3 extrusion in the skin region. 129

Figure 122. Partial pole figures for the 2195-T3 extrusion in the base @ t/2 [Specimen plane perpendicular to (R)adial axis]. 130

Figure 123. CODF sections for the 2195-T3 extrusion in the base @ t/2 [Specimen plane perpendicular to (R)adial axis]. 131

Figure 124. Partial pole figures for the 2195-T3 extrusion in the base @ t/2 [Specimen plane perpendicular to (C)ircumferential axis]. 132

Figure 125. CODF sections for the 2195-T3 extrusion in the base @ t/2 [Specimen plane perpendicular to (C)ircumferential axis]. 133

Figure 126. Partial pole figures for the 2195-T3 extrusion in the web @ t/8 [Specimen plane perpendicular to (C)ircumferential axis]. 134

Figure 127. CODF sections for the 2195-T3 extrusion in the web @ t/8 [Specimen plane perpendicular to (C)ircumferential axis]. 135

Figure 128. Partial pole figures for the 2195-T3 extrusion in the web @ 3t/8 [Specimen plane perpendicular to (C)ircumferential axis]. 136

Figure 129. CODF sections for the 2195-T3 extrusion in the web @ 3t/8 [Specimen plane perpendicular to (C)ircumferential axis]. 137

Figure 130. Partial pole figures for the 2195-T3 extrusion in the web @ 5t/8 [Specimen plane perpendicular to (C)ircumferential axis]. 138

Figure 131. CODF sections for the 2195-T3 extrusion in the web @ 5t/8 [Specimen plane perpendicular to (C)ircumferential axis]. 139

Figure 132. Partial pole figures for the 2195-T3 extrusion in the web @ 7t/8 [Specimen plane perpendicular to (C)ircumferential axis]. 140

Figure 133. CODF sections for the 2195-T3 extrusion in the web @ 7t/8 [Specimen plane perpendicular to (C)ircumferential axis]. 141

Figure 134. Partial pole figures for the 2195-T3 extrusion in the cap @ t/4 [Specimen plane perpendicular to (R)adial axis]. 142

Figure 135. CODF sections for the 2195-T3 extrusion in the cap @ t/4 [Specimen plane perpendicular to (R)adial axis]. 143

Figure 136. Partial pole figures for the 2195-T3 extrusion in the cap @ t/2 [Specimen plane perpendicular to (R)adial axis]. 144

Figure 137. CODF sections for the 2195-T3 extrusion in the cap @ t/2 [Specimen plane perpendicular to (R)adial axis]. 145

Figure 138. Partial pole figures for the 2195-T3 extrusion in the cap @ 3t/4 [Specimen plane perpendicular to (R)adial axis]. 146

Figure 139. CODF sections for the 2195-T3 extrusion in the cap @ 3t/4 [Specimen plane perpendicular to (R)adial axis]. 147

Figure 140. Orientation density, f(g), as a function of location through the cross-section for the 2195-T3 extrusion in the cap region. 148

Figure 141. Partial pole figures for 2195-T8 plate @ t/8 [Specimen plane perpendicular to (S)hort-Transverse axis]. 149

Figure 142. CODF sections for 2195-T8 plate @ t/8 [Specimen plane perpendicular to (S)hort-Transverse axis]. 150

Figure 143. Partial pole figures for 2195-T8 plate @ t/4 [Specimen plane perpendicular to (S)hort-Transverse axis]. 151

Figure 144. CODF sections for 2195-T8 plate @ t/4 [Specimen plane perpendicular to (S)hort-Transverse axis]. 152

Figure 145. Partial pole figures for 2195-T8 plate @ t/2 [Specimen plane perpendicular to (S)hort-Transverse axis]. 153

Figure 146. CODF sections for 2195-T8 plate @ t/2 [Specimen plane perpendicular to (S)hort-Transverse axis]. 154

Figure 147. Orientation density, f(g), as a function of location through the cross-section for the 2195-T8 plate. 155

Catalogue of X-Ray Texture Data for Al-Cu-Li Alloy 1460, 2090, 2096 and 2195 Near-Net-Shape Extrusions, Sheet and Plate

Stephen J. Hales, Robert A. Hafley and Joel A. Alexa

Abstract

The effect of crystallographic texture on the mechanical properties of near-net-shape extrusions is of major interest if these products are to find application in launch vehicle or aircraft structures. The objective of this research was to produce a catalogue containing quantitative texture information for extruded product, sheet and plate. The material characterized was extracted from wide, integrally stiffened panels fabricated from the Al-Cu-Li alloys 1460, 2090, 2096 and 2195. The textural characteristics of sheet and plate products of the same alloys were determined for comparison purposes. The approach involved using x-ray diffraction to generate pole figures in combination with crystallite orientation distribution function analysis. The data were compiled as a function of location in the extruded and wrought product cross-sections and the variation in the major deformation- and recrystallization-related texture components was identified.

* This research was conducted in the Materials Division at NASA Langley Research Center under Contract # NAS1-19708 with Mr. Keith Bird as technical monitor.

Symbols and Abbreviations

OD : Outside diameter
ID : Inside diameter
R : Specimen plane perpendicular to the original radial axis of the stovepipe extrusion
C : Specimen plane perpendicular to the original circumferential axis of the stovepipe extrusion
ED : Extrusion direction
RD : Rolling direction in sheet and plate
S : Specimen plane perpendicular to the short-transverse axis of sheet and plate
TD : Transverse direction
t : Thickness (e.g. t/2 corresponds to mid-plane of cross-section)
CODF : Crystallite orientation distribution function

φ_1, ϕ, φ_2 : Euler angles using Bunge notation

1. Introduction

A variety of Al-Cu-Li alloy products are candidates for future launch vehicle and aircraft structures. The improved specific properties of these alloys compared to conventional Al alloys can be translated into structural weight savings and reduced operational costs. Because Al-Cu-Li alloys are more expensive than conventional alloys, fabrication methods which reduce manufacturing costs are also being considered. The current Space Shuttle External Tank is fabricated from integrally machined plate and the use of near-net-shape extrusions creates the potential to reduce material expenses by lowering the scrap rate. When considering different product forms for service, the relationship between crystallographic texture and mechanical properties is an important issue. Although this relationship is not addressed here, there is a need to develop a database of texture information on extruded product. The objective of this research was to document the variation in texture of near-net-shape extrusions as a function of location through the cross-section.

In parallel, data outlining the textural characteristics of sheet and plate were compiled for comparison.

2. Materials

The compositions of the Al-Cu-Li alloys studied in this investigation are listed in Table 1. The sequence of events leading to production of the near-net-shape extrusions is as follows. The alloys were cast into rectangular ingots which were then machined to circular cross-section and forged into hollow cylindrical billets with dimensions 16.5in OD, 12in ID and 25in long. Subsequently, "stove pipe" extrusions 157in long were produced using an extrusion temperature of 680-825°F at a rate of 16-24in/min. The extruded cross-section comprised a 15 in diameter cylinder, 0.18in thick, with 8 equi-spaced integral "J" stiffeners on the outer surface. These cylinders were then split lengthwise and processed into flat panels 32in wide and 118in long using a combination of mechanical unfolding and rolling. Finally, the extrusions were cold stretched to the T3 temper condition. The dimensions of a typical section of the extruded product are shown in Figure 1(a). The sheet and plate product obtained for comparison were rolled by conventional means to the various gages specified and examined in either a T3 or T8 temper.

3. Procedures

The locations for extraction of specimens from the extruded cross-sections suitable for x-ray diffraction analysis are outlined in Figure 1(b). The nomenclature used to describe the principal regions in the cross-section comprise the skin, base, web and cap of the integrally "J" stiffened extrusion. Square coupons, 0.75in x 0.75in, were extracted and metallographically prepared to the appropriate depth location for analysis. In order to confine analysis in the base to the region of interest, multiple sections were extracted and laminated together to produce the desired coupon dimensions. Initial specimen preparation involved rough mechanical polishing down to the desired depth followed by final polishing through 0.05μm colloidal silica, macroetching with a 10% caustic solution for 15 secs at 150°F and de-smutting with concentrated nitric acid.

The x-ray diffraction data were collected using the Schultz backward reflection technique with the specimen mounted in a computer-driven Eulerian cradle and a sample oscillation of 10mm. The data were collected in accordance with the matrix outlined in Table 2 using x-ray diffraction equipment with software suitable for quantitative texture analysis. The data were collected using Cu Kα radiation with tube settings of 40kV/30mA and a slit width of 1.8mm. The raw data were corrected with respect to background intensity and defocussing errors using data collected from a randomly-textured, pure Al powder specimen using the same equipment settings. The data were reduced to {111}, {200} and {220} partial pole figures, CODF's calculated and represented graphically in Euler space using the Bunge notation.

4. Results

Quantitative texture data for the alloys and product forms described above are shown in Figures 2-41 for 1460, Figures 42-81 for 2090, Figures 82-114 for 2096 and Figures 115-147 for 2195. The information presented comprises pole figures, CODF data and plots showing the variation in the intensities of the prominent deformation- and recrystallization-related texture components as a function of depth through the product cross-section. This latter analysis, which is only valid when the extrusion/rolling direction is contained within the specimen plane, was only performed on data collected with the specimen plane normal to the radial axis of the extrusion and the plate and sheet.

Alloy	Composition, wt%							
	Element	Cu	Li	Mg	Ag	Zr	Sc	Al
1460	Range	2.6/3.3	2.0/2.5	< 0.05	--	0.06/0.15	0.04/0.14	Bal.
	Nominal	2.9	2.1	--	--	0.11	0.04	Bal.
2090	Range	2.4/3.0	1.9/2.6	< 0.25	--	0.08/0.15	--	Bal.
	Nominal	2.7	2.0	--	--	0.12	--	Bal.
2096	Range	2.3/3.0	1.3/1.9	0.25/0.8	0.25/0.6	0.04/0.18	--	Bal.
	Nominal	2.8	1.4	0.5	0.3	0.13	--	Bal.
2195	Range	3.7/4.3	0.8/1.2	0.25/0.8	0.25/0.6	0.08/0.16	--	Bal.
	Nominal	4.3	1.0	0.4	0.5	0.12	--	Bal.

Table 1. Nominal and specified range of compositions for 1460, 2090, 2096 and 2195 near-net-shape extrusions, sheet and plate.

Alloy	Product	Location	t/8	t/4	3t/8	t/2	5t/8	3t/4	7t/8	Plane*
1460-T3	Extrusion	Skin		•		•		•		R
		Base				••				R/C
		Web	•		•		•		•	C
		Cap		•		•		•		R
1460-T3	0.060" Sheet		•	•		•				S
1460-T3	0.285" Plate		•	•		•				S
2090-T8	Extrusion	Skin		•		•		•		R
		Base				••				R/C
		Web	•		•		•		•	C
		Cap		•		•		•		R
2090-T8	0.120" Sheet		•	•		•				S
2090-T8	0.750" Plate		•	•		•				S
2096-T3	Extrusion	Skin		•		•		•		R
		Base				••				R/C
		Web	•		•		•		•	C
		Cap		•		•		•		R
2096-T8	0.090" Sheet		•	•		•				S
2195-T3	Extrusion	Skin		•		•		•		R
		Base				••				R/C
		Web	•		•		•		•	C
		Cap		•		•		•		R
2195-T8	0.250" Plate		•	•		•				S

Table 2. Matrix for collection of x-ray diffraction data as a function of alloy, product form and through-thickness location. * = Orientation of specimen plane: R - perpendicular to radial axis; C - perpendicular to circumferential axis of near-net-shape extrusion and S - perpendicular to short-transverse axis of rolled product.

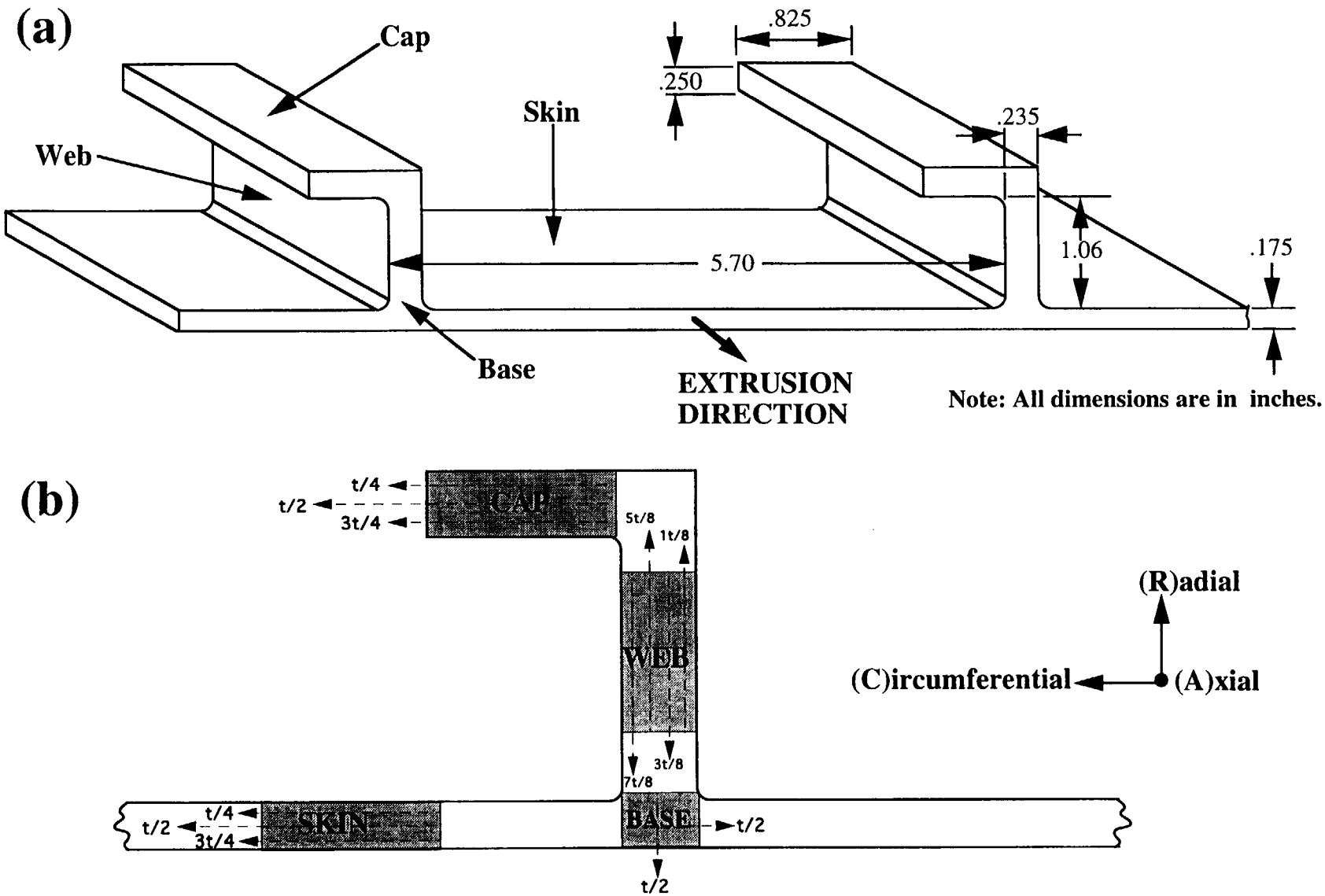

Figure 1. Schematics showing, (a), the dimensions of the near-net-shape extrusions and, (b), the locations of specimen extraction for texture analysis.

4.1 Alloy 1460

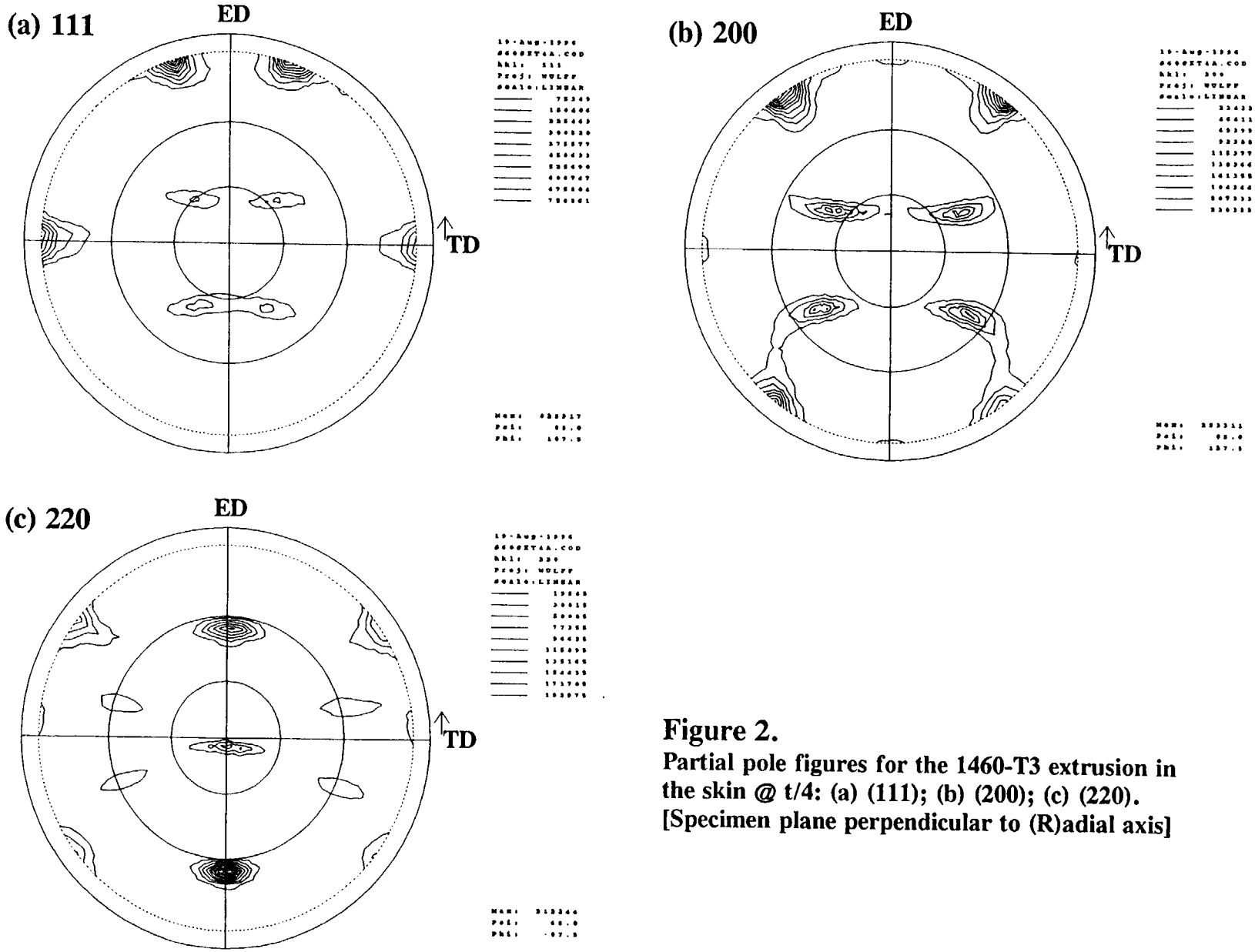

Figure 2.
Partial pole figures for the 1460-T3 extrusion in the skin @ t/4: (a) (111); (b) (200); (c) (220). [Specimen plane perpendicular to (R)adial axis]

(a) Sections: φ_2= 0 - 90°

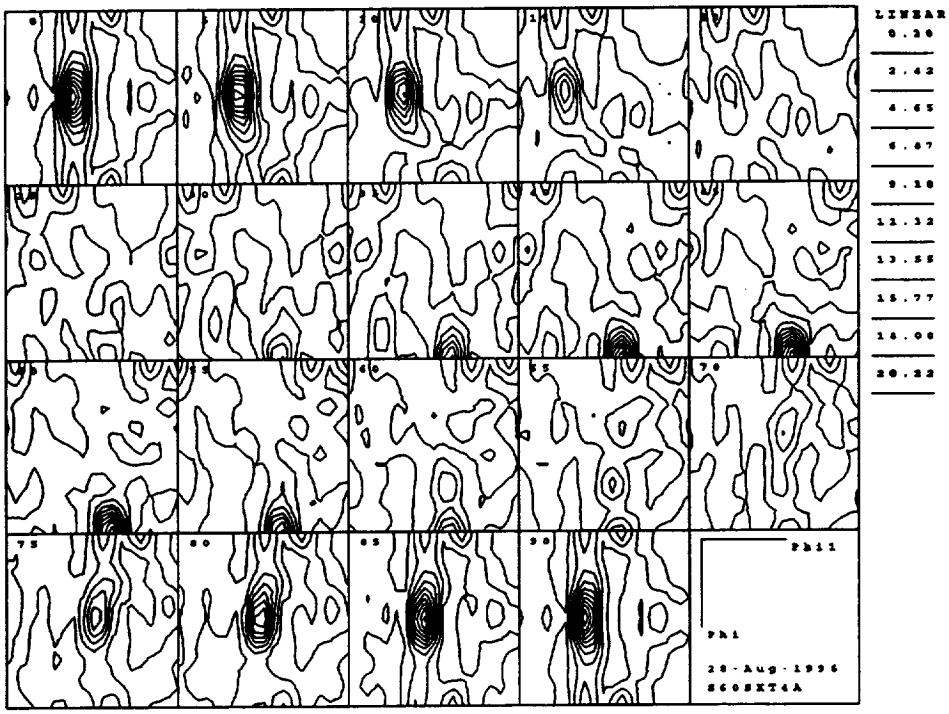

(b) Sections: φ_2= 45°; φ_2= 90°

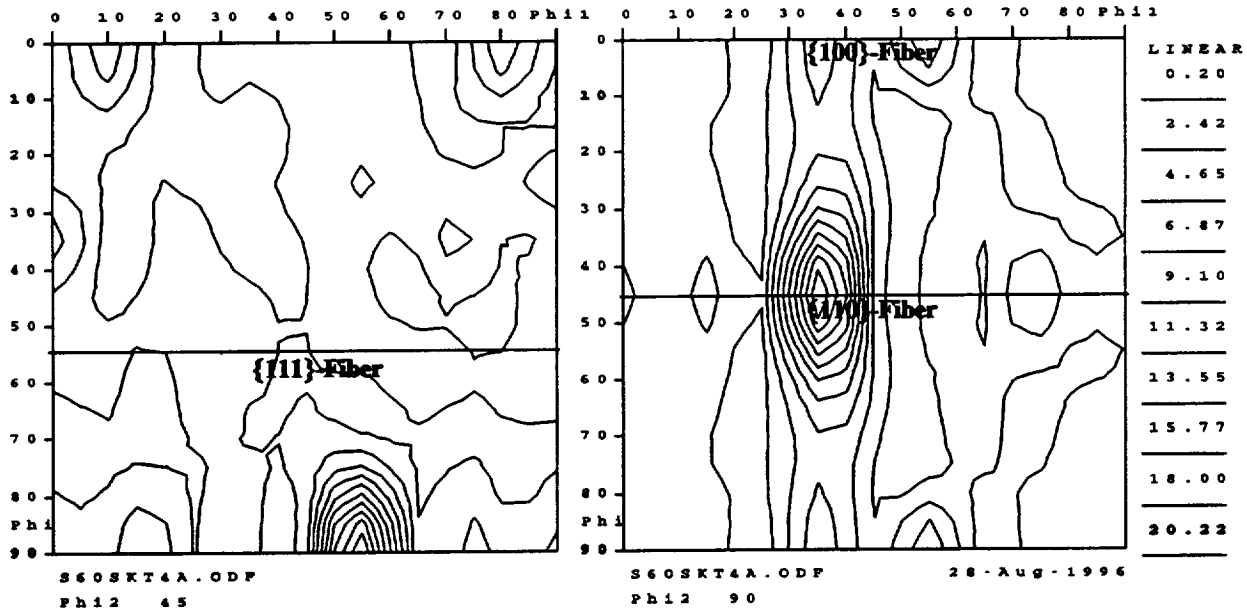

Figure 3. CODF sections for the 1460-T3 extrusion in the skin @ t/4; (a), Complete sections: φ_2= 0, 5, 10 ..... 90°; and (b), enlarged φ_2= 45° and φ_2= 90° sections. The locations of the {100}-fiber, {110}-fiber and {111}-fiber are shown.
[Specimen plane perpendicular to (R)adial axis]

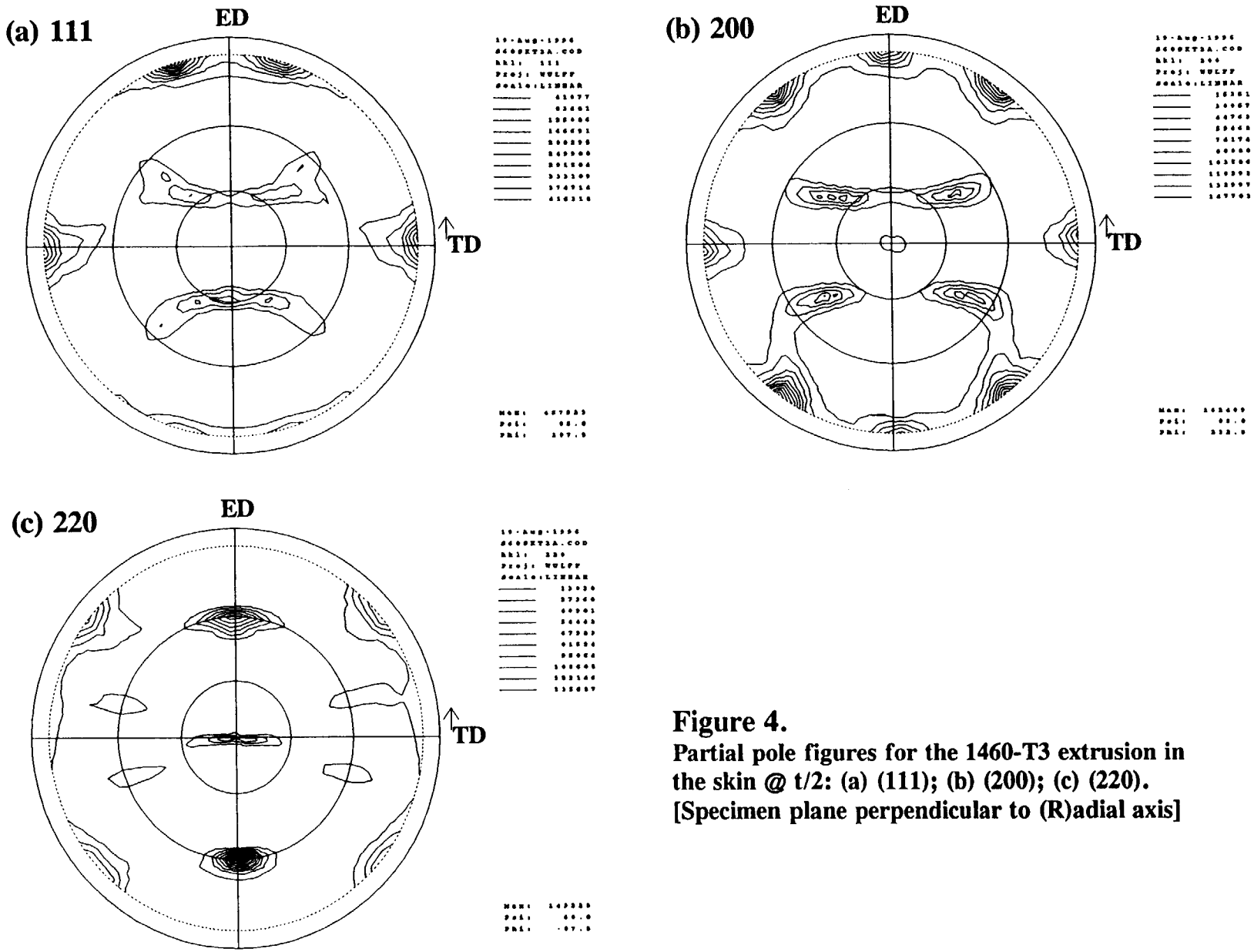

Figure 4.
Partial pole figures for the 1460-T3 extrusion in the skin @ t/2: (a) (111); (b) (200); (c) (220). [Specimen plane perpendicular to (R)adial axis]

(a) Sections: φ_2= 0 - 90°

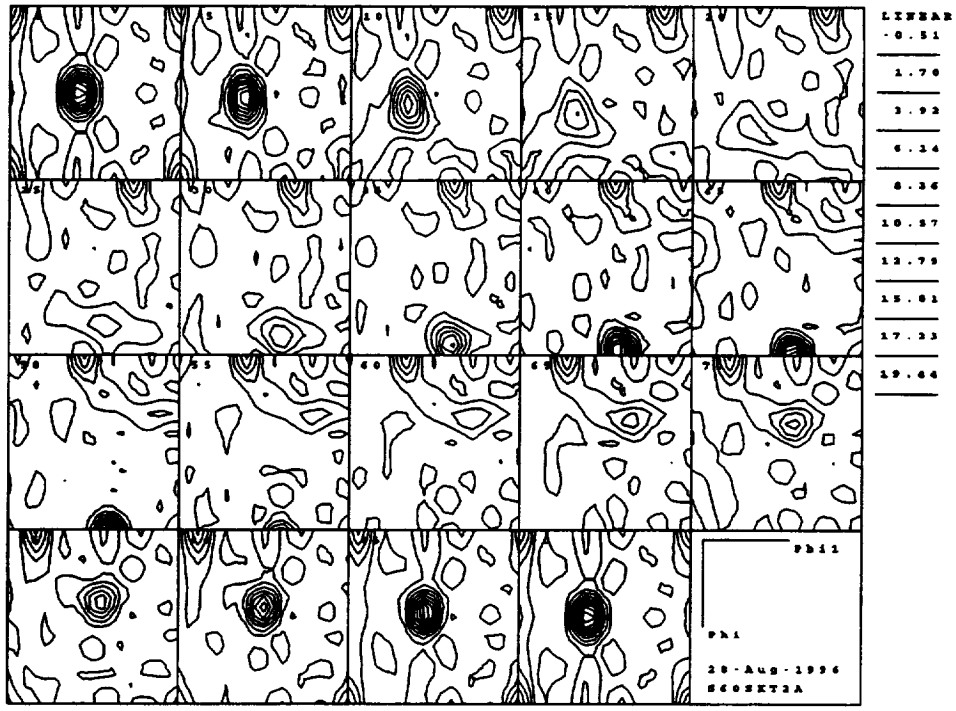

(b) Sections: φ_2= 45°; φ_2= 90°

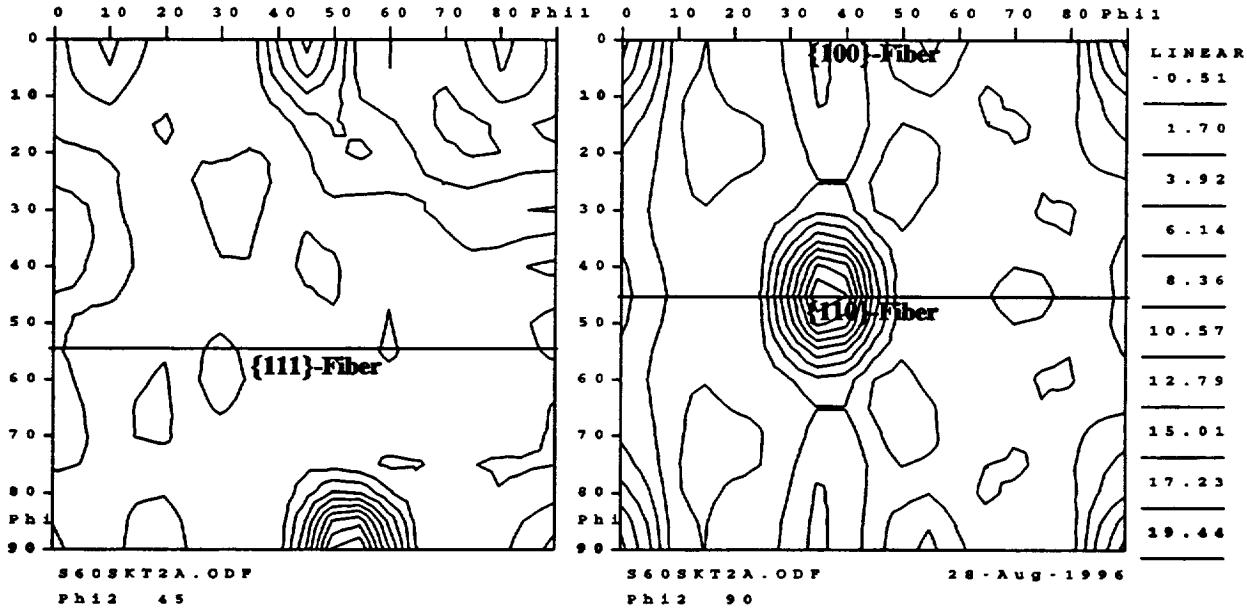

Figure 5. CODF sections for the 1460-T3 extrusion in the skin @ t/2; (a), Complete sections: φ_2= 0, 5, 10 ..... 90°; and (b), enlarged φ_2= 45° and φ_2= 90° sections. The locations of the {100}-fiber, {110}-fiber and {111}-fiber are shown.
[Specimen plane perpendicular to (R)adial axis]

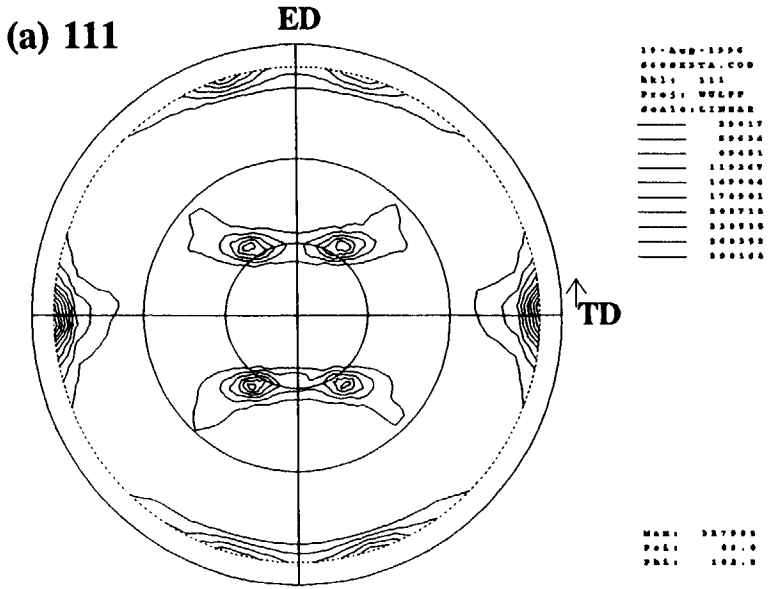

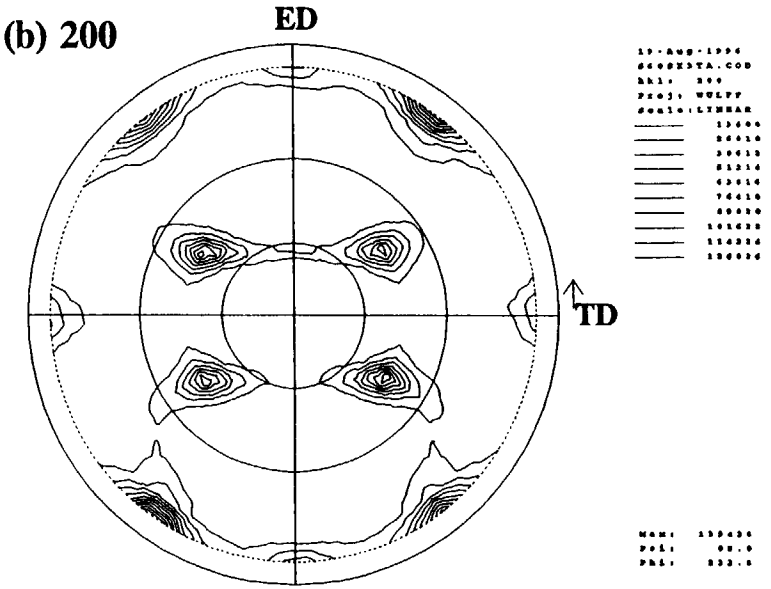

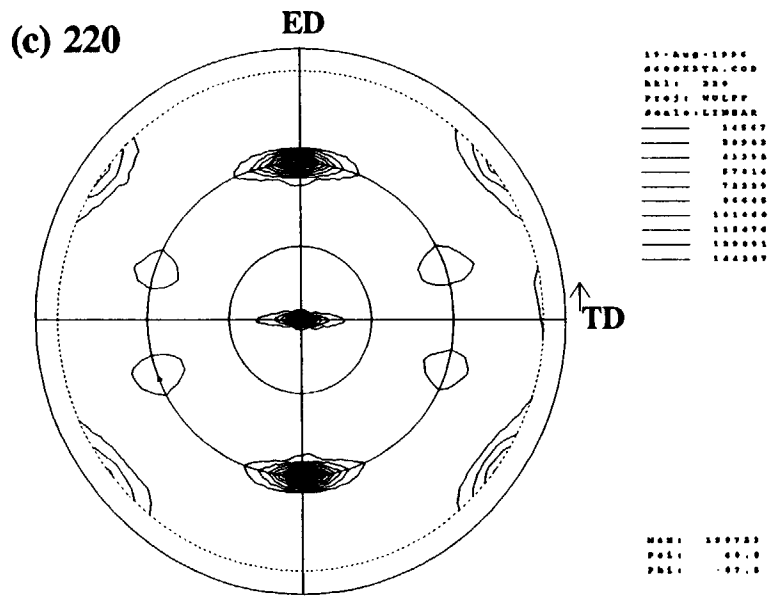

Figure 6.
Partial pole figures for the 1460-T3 extrusion in the skin @ 3t/4: (a) (111); (b) (200); (c) (220). [Specimen plane perpendicular to (R)adial axis]

(a) Sections: φ_2= 0 - 90°

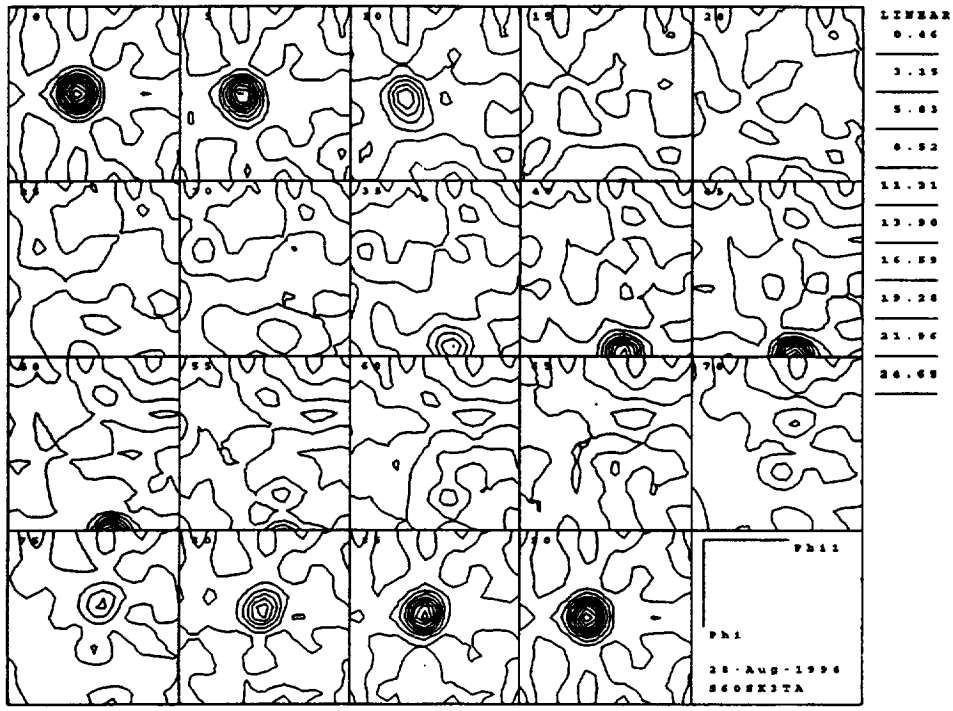

(b) Sections: φ_2= 45°; φ_2= 90°

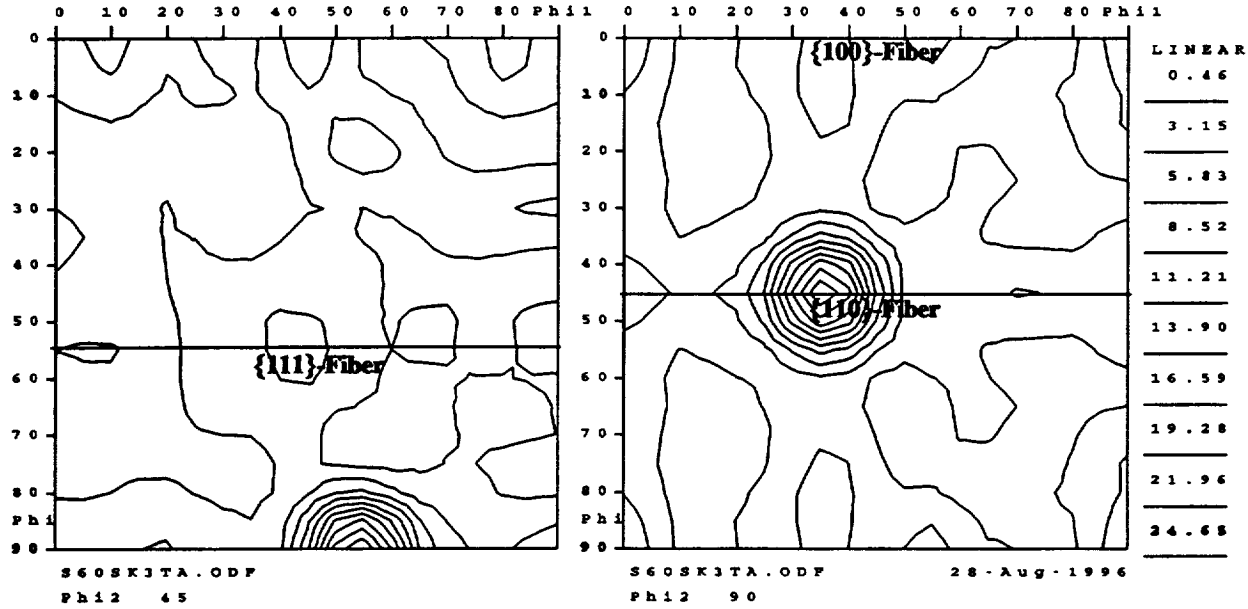

Figure 7. CODF sections for the 1460-T3 extrusion in the skin @ 3t/4; (a), Complete sections: φ_2= 0, 5, 10 ..... 90°; and (b), enlarged φ_2= 45° and φ_2= 90° sections. The locations of the {100}-fiber, {110}-fiber and {111}-fiber are shown.
[Specimen plane perpendicular to (R)adial axis]

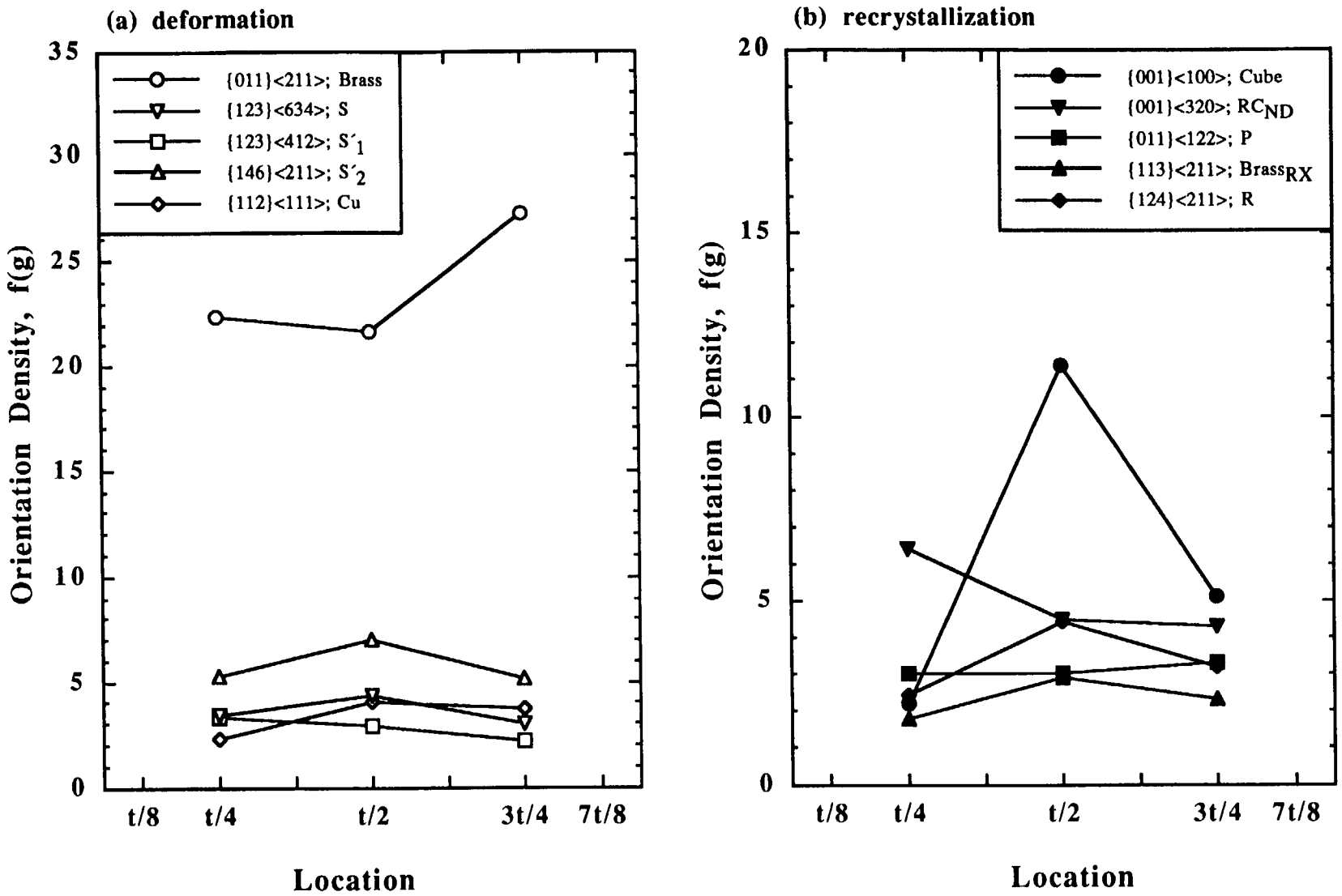

Figure 8. Orientation density, f(g), as a function of location through the cross-section for the 1460-T3 extrusion in the skin region: (a) Deformation-related components; (b) Recrystallization-related components.

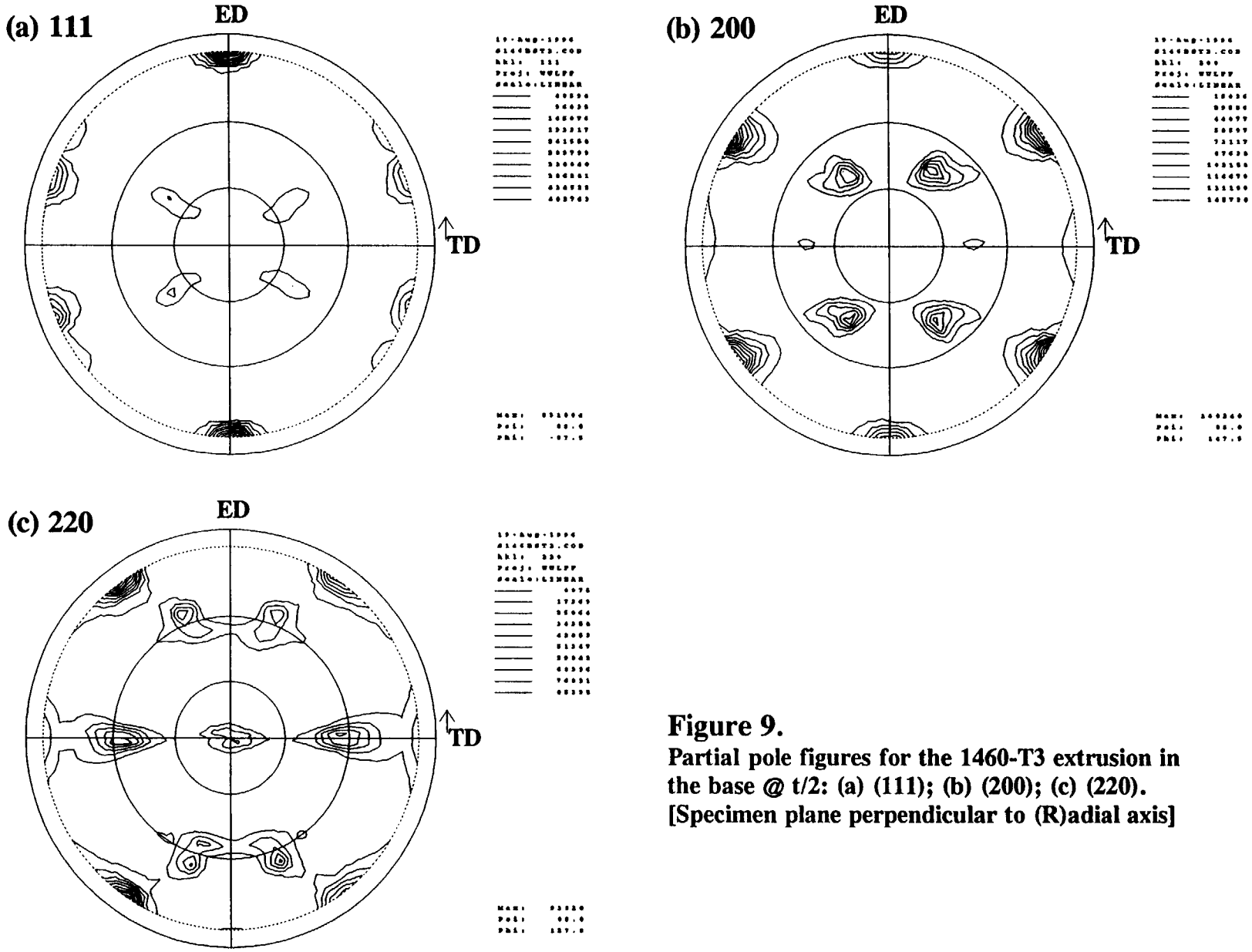

Figure 9.
Partial pole figures for the 1460-T3 extrusion in the base @ t/2: (a) (111); (b) (200); (c) (220). [Specimen plane perpendicular to (R)adial axis]

(a) Sections: φ_2= 0 - 90°

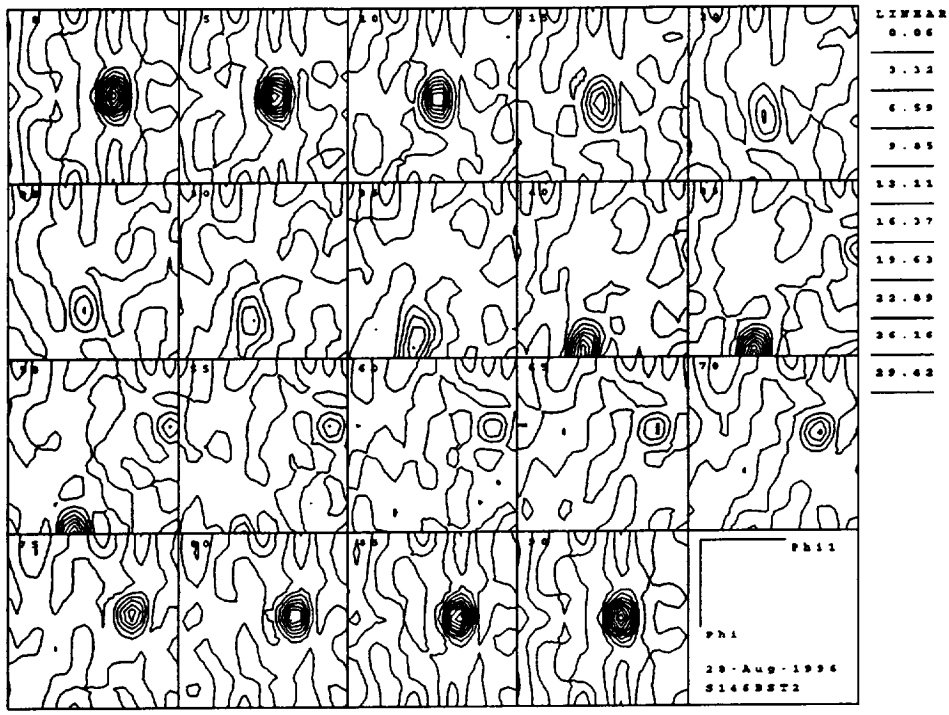

(b) Sections: φ_2= 45°; φ_2= 90°

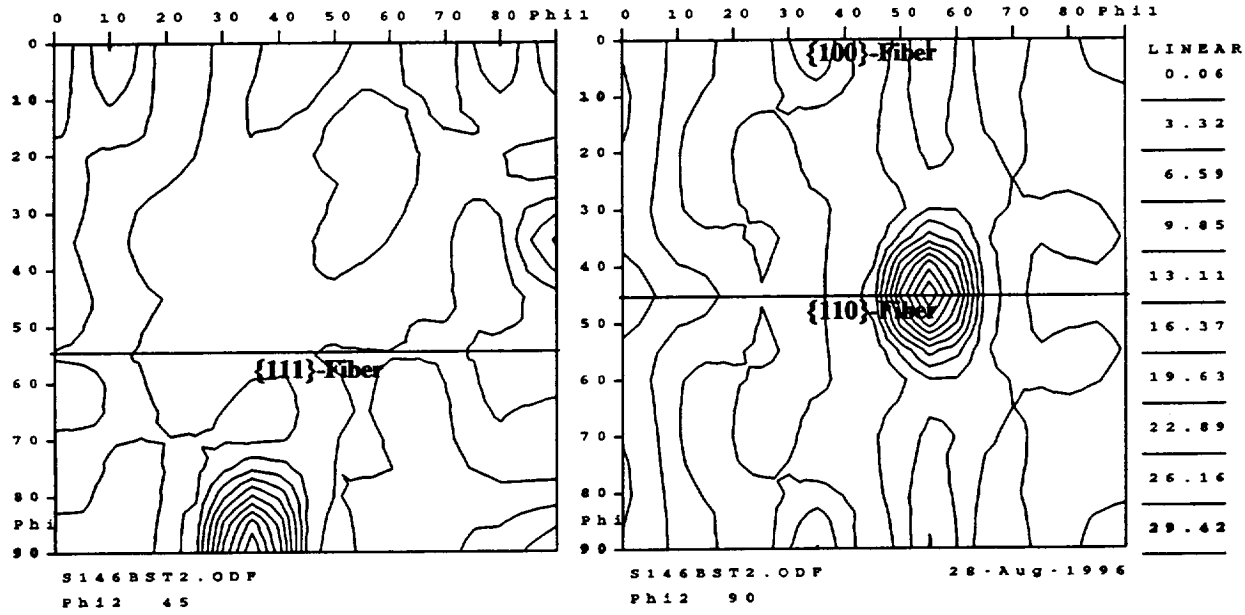

Figure 10. CODF sections for the 1460-T3 extrusion in the base @ t/2; (a), Complete sections: φ_2= 0, 5, 10 ..... 90°; and (b), enlarged φ_2= 45° and φ_2= 90° sections. The locations of the {100}-fiber, {110}-fiber and {111}-fiber are shown.
[Specimen plane perpendicular to (R)adial axis]

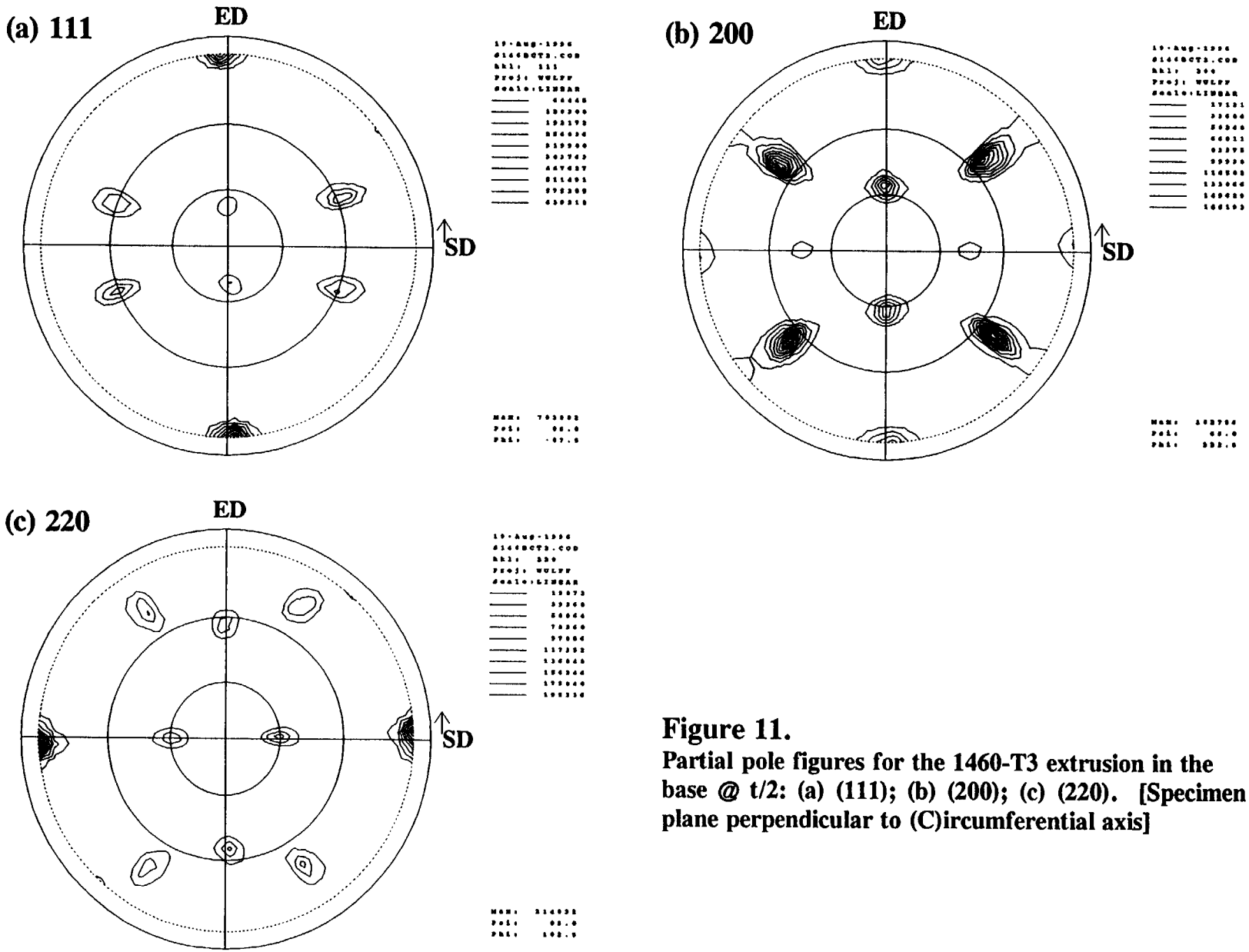

Figure 11.
Partial pole figures for the 1460-T3 extrusion in the base @ t/2: (a) (111); (b) (200); (c) (220). [Specimen plane perpendicular to (C)ircumferential axis]

(a) Sections: φ_2= 0 - 90°

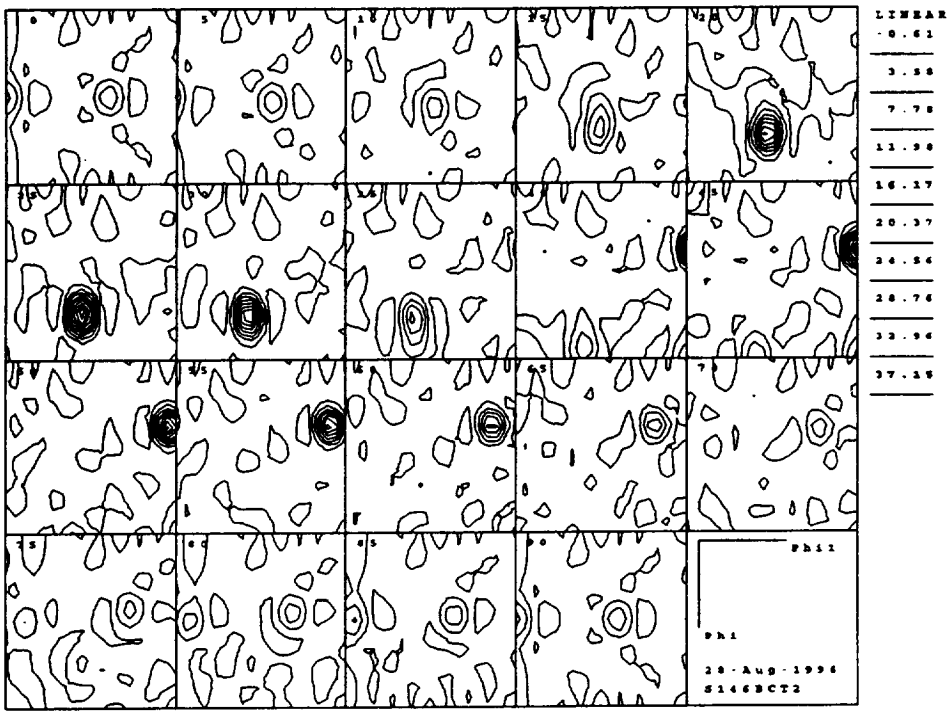

(b) Sections: φ_2= 45°; φ_2= 90°

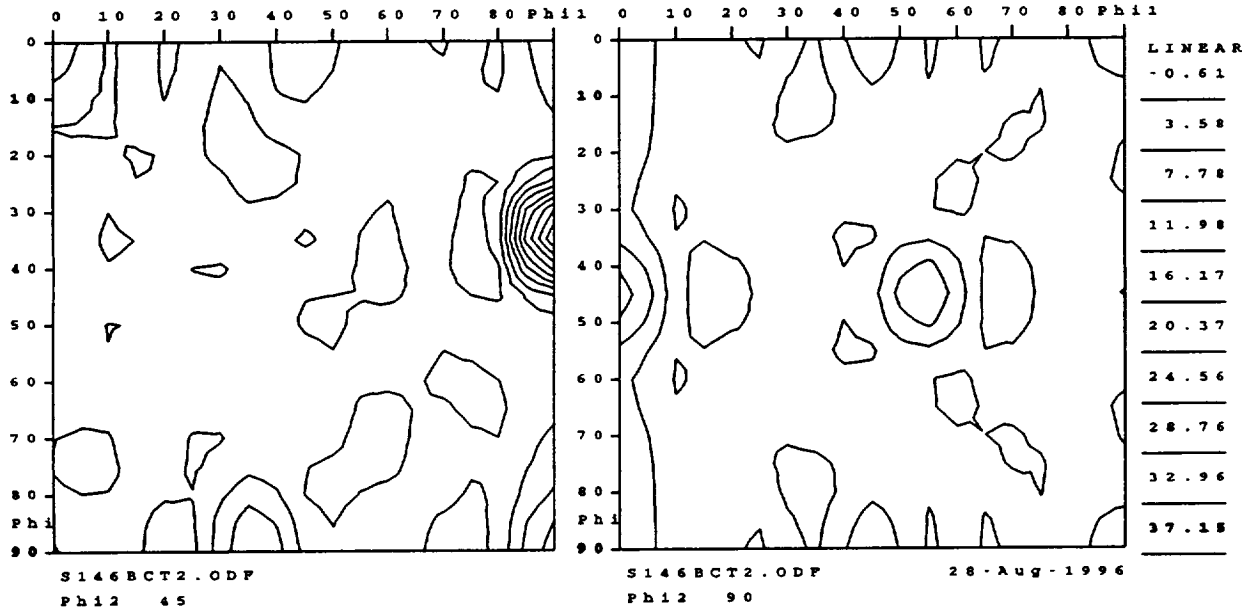

Figure 12. CODF sections for the 1460-T3 extrusion in the base @ t/2; (a), Complete sections: φ_2= 0, 5, 10 ..... 90°; and (b), enlarged φ_2= 45° and φ_2= 90° sections. [Specimen plane perpendicular to (C)ircumferential axis]

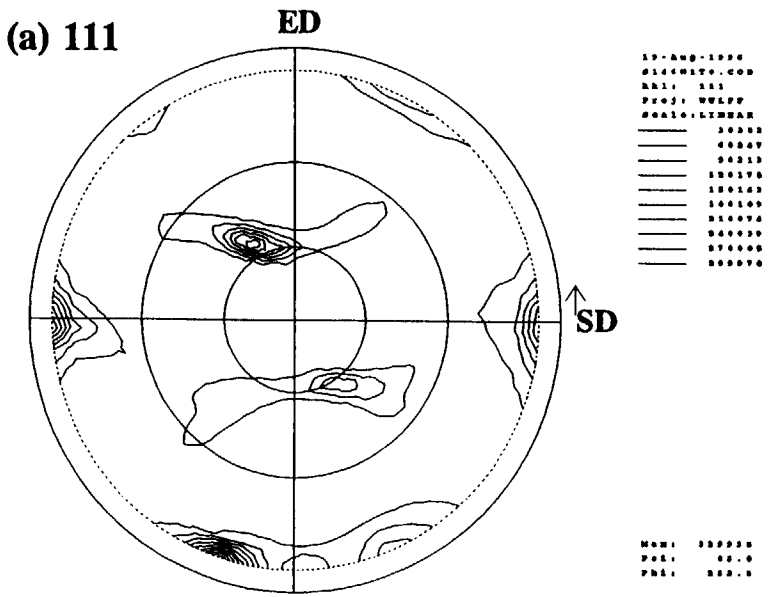

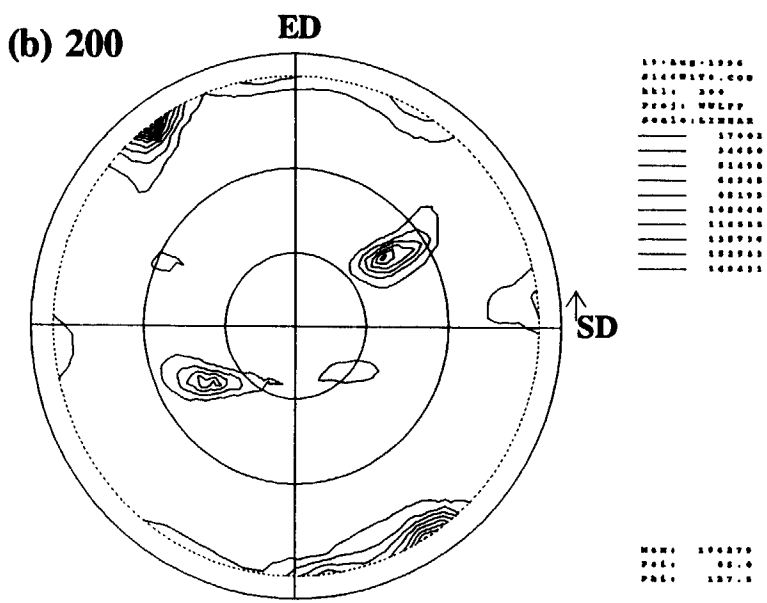

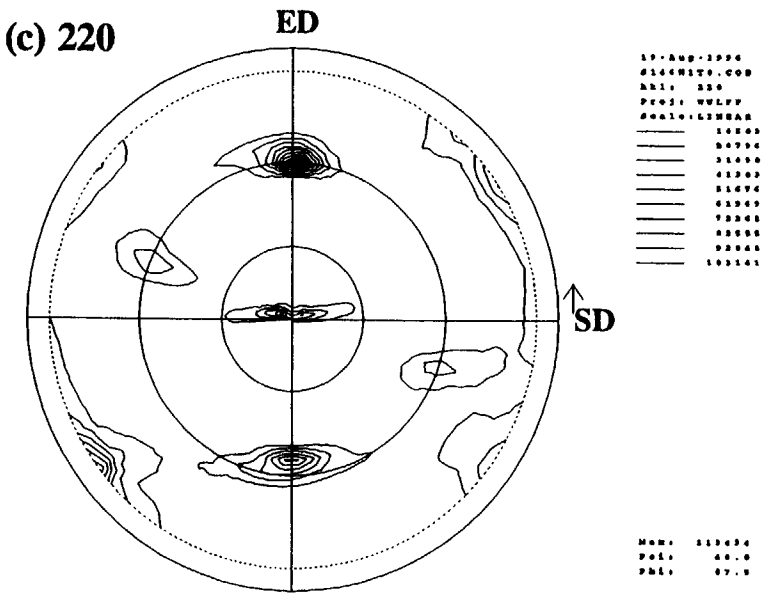

Figure 13.
Partial pole figures for the 1460-T3 extrusion in the web @ t/8: (a) (111); (b) (200); (c) (220). [Specimen plane perpendicular to (C)ircumferential axis]

(a) Sections: $\varphi_2 = 0 - 90°$

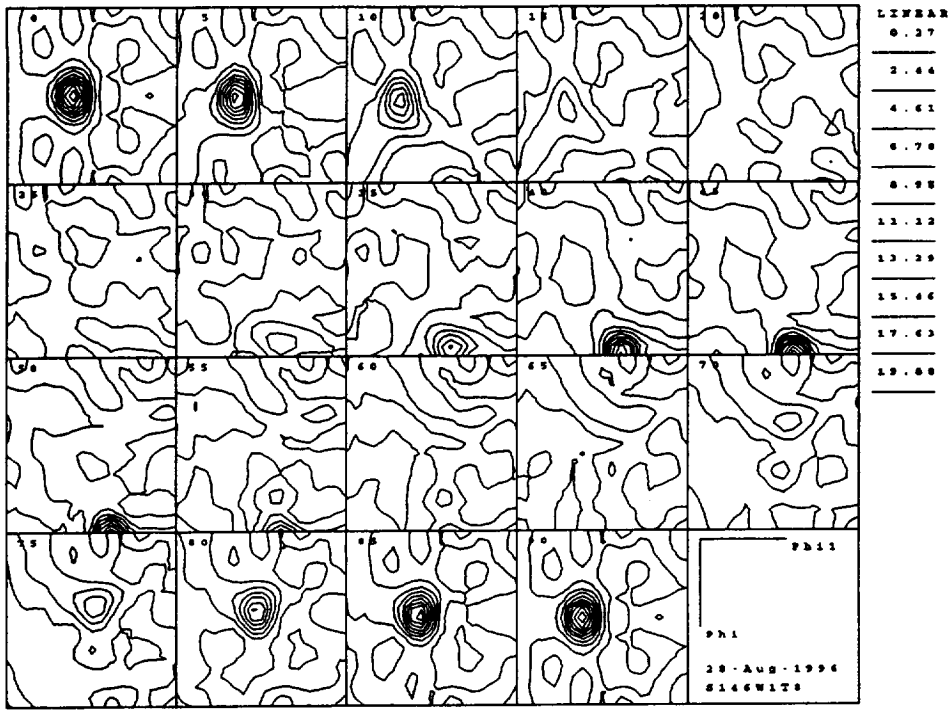

(b) Sections: $\varphi_2 = 45°$; $\varphi_2 = 90°$

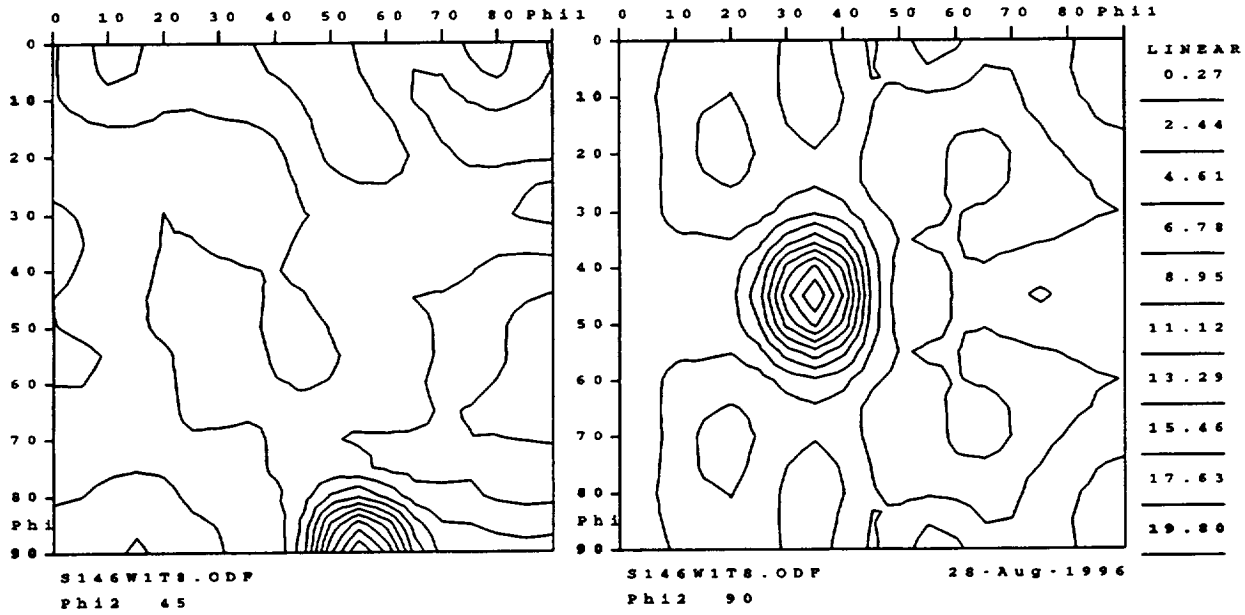

Figure 14. CODF sections for the 1460-T3 extrusion in the web @ t/8; (a), Complete sections: $\varphi_2 = 0, 5, 10 \ldots\ldots 90°$; and (b), enlarged $\varphi_2 = 45°$ and $\varphi_2 = 90°$ sections. [Specimen plane perpendicular to (C)ircumferential axis]

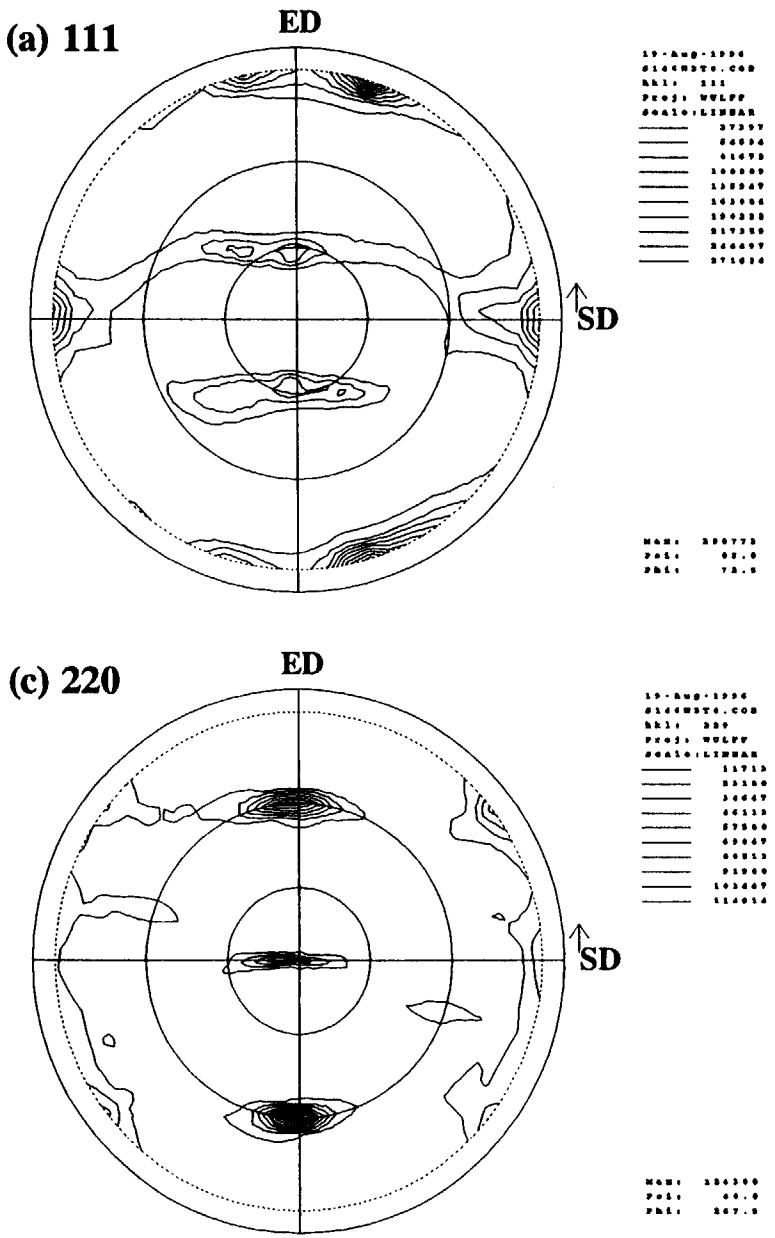

Figure 15.
Partial pole figures for the 1460-T3 extrusion in the web @ 3t/8: (a) (111); (b) (200); (c) (220). [Specimen plane perpendicular to (C)ircumferential axis]

(a) Sections: φ_2= 0 - 90°

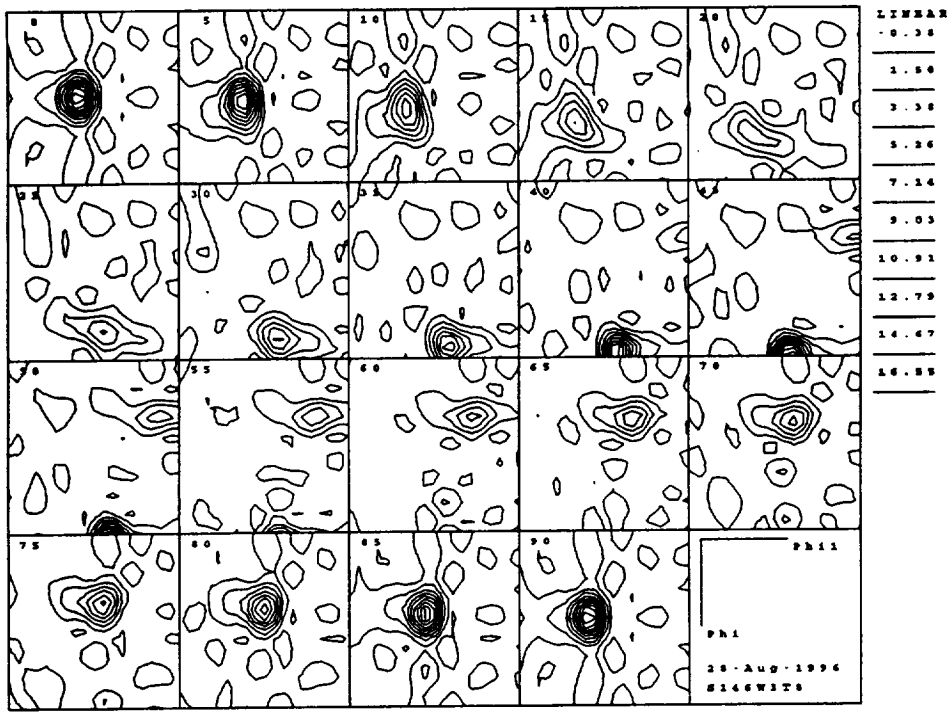

(b) Sections: φ_2= 45°; φ_2= 90°

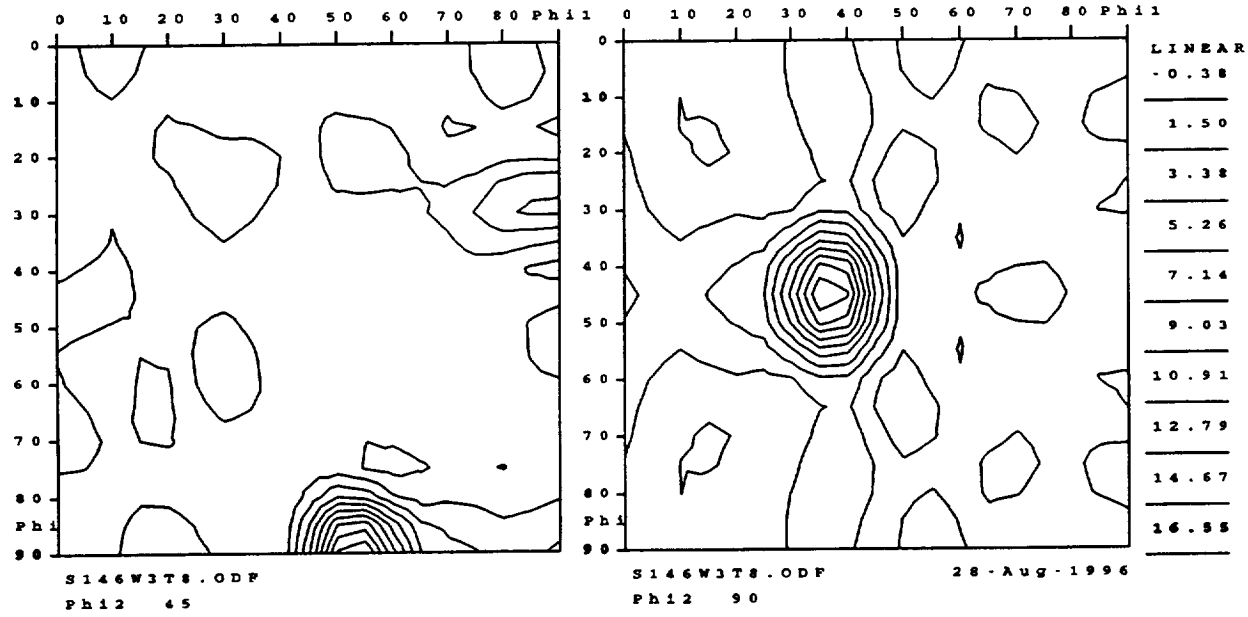

Figure 16. CODF sections for the 1460-T3 extrusion in the web @ 3t/8; (a), Complete sections: φ_2= 0, 5, 10 ..... 90°; and (b), enlarged φ_2= 45° and φ_2= 90° sections. [Specimen plane perpendicular to (C)ircumferential axis]

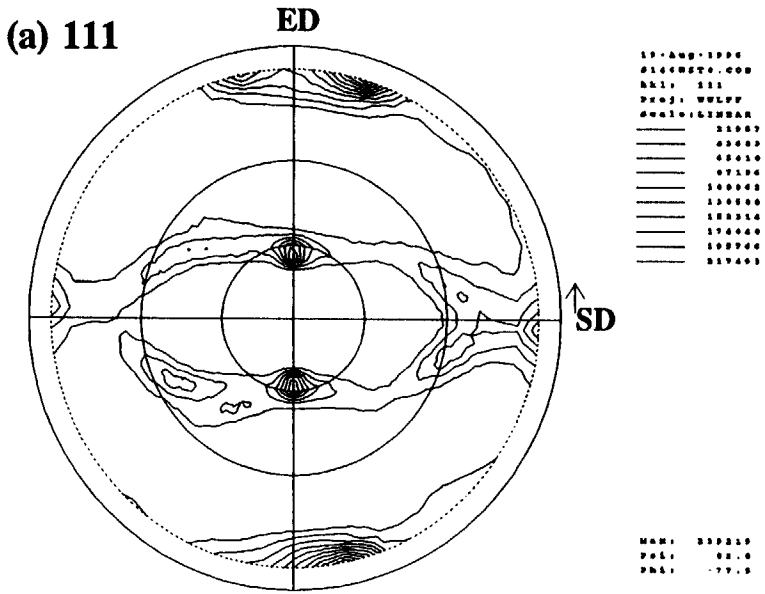

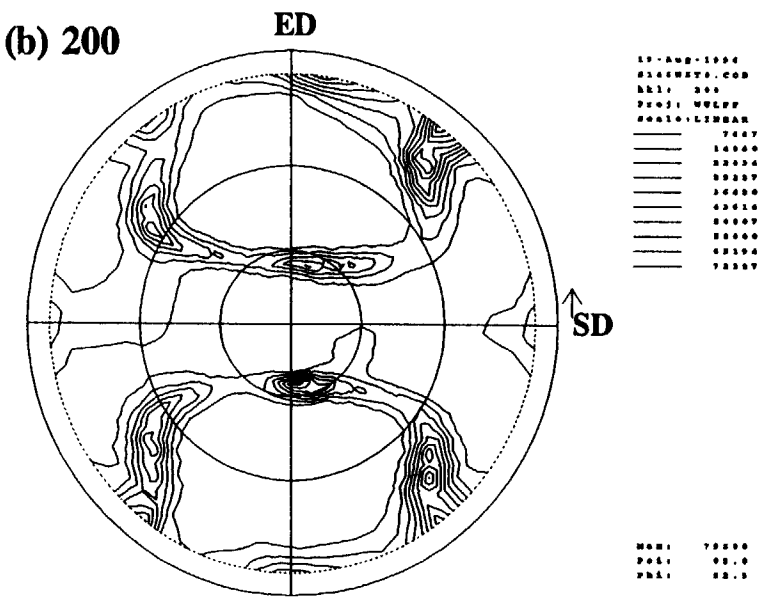

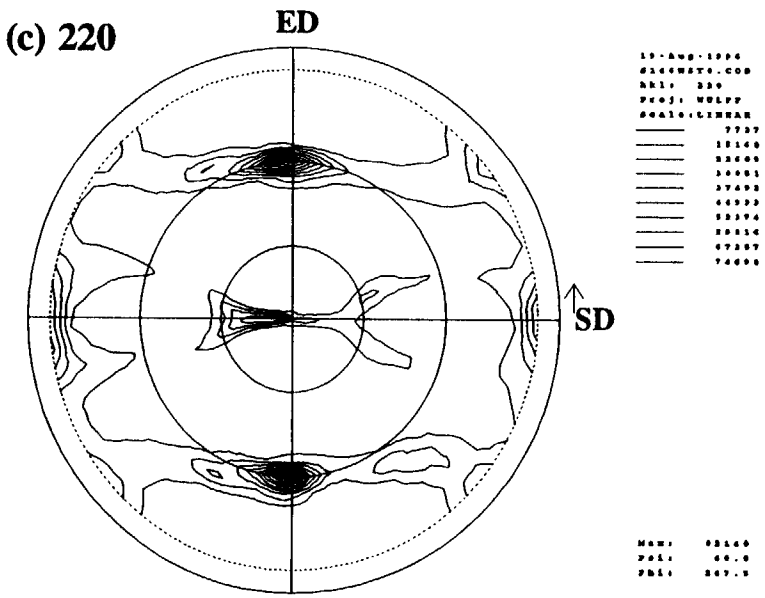

Figure 17.
Partial pole figures for the 1460-T3 extrusion in the web @ 5t/8: (a) (111); (b) (200); (c) (220). [Specimen plane perpendicular to (C)ircumferential axis]

(a) Sections: $\varphi_2 = 0 - 90°$

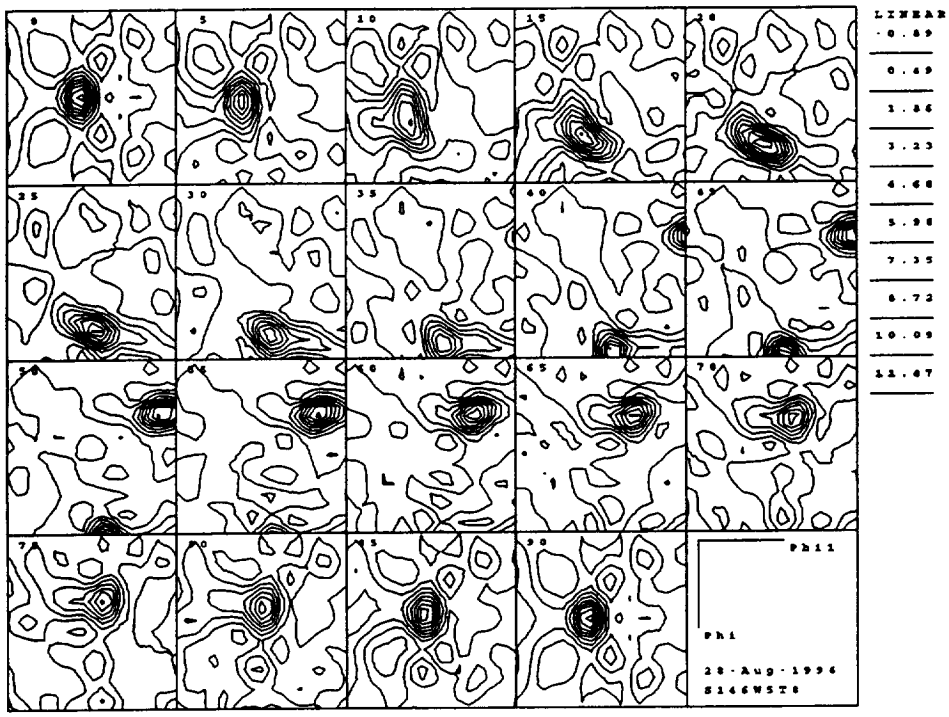

(b) Sections: $\varphi_2 = 45°$; $\varphi_2 = 90°$

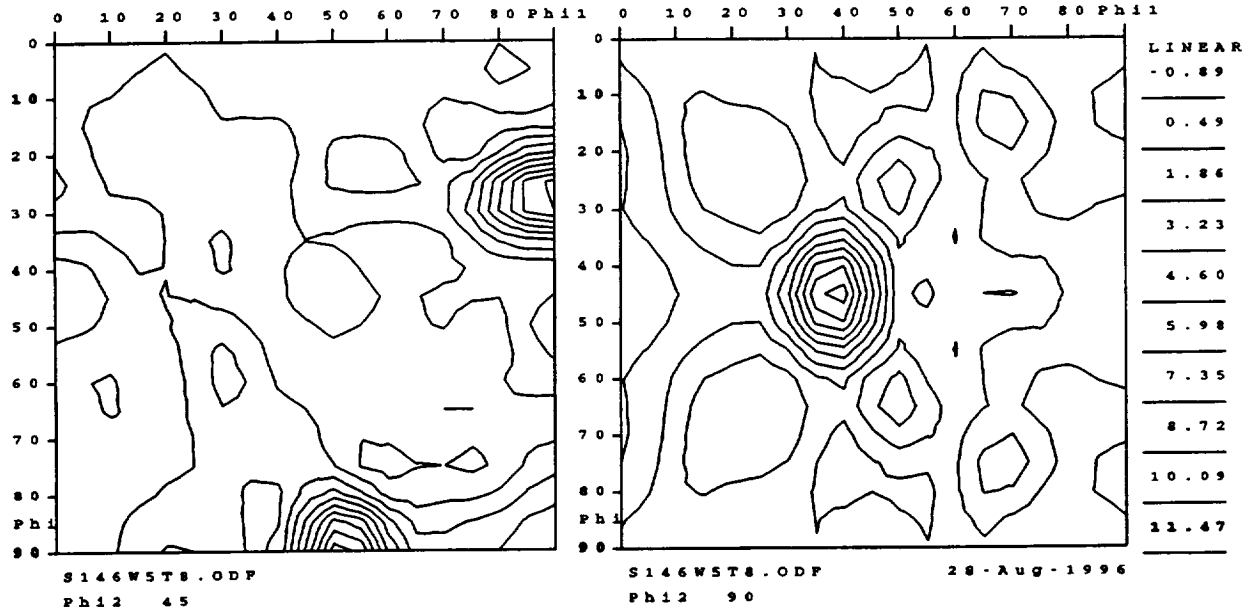

Figure 18. CODF sections for the 1460-T3 extrusion in the web @ 5t/8; (a), Complete sections: $\varphi_2 = 0, 5, 10 \ldots\ldots 90°$; and (b), enlarged $\varphi_2 = 45°$ and $\varphi_2 = 90°$ sections. [Specimen plane perpendicular to (C)ircumferential axis]

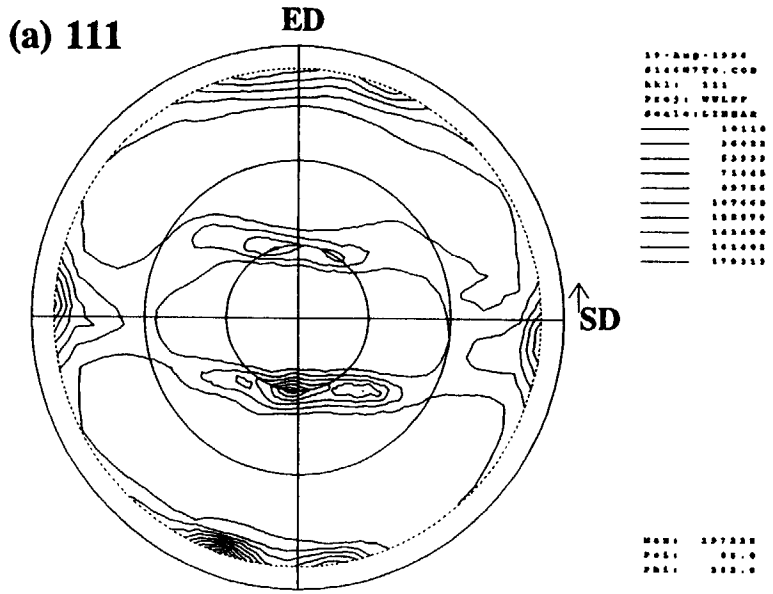

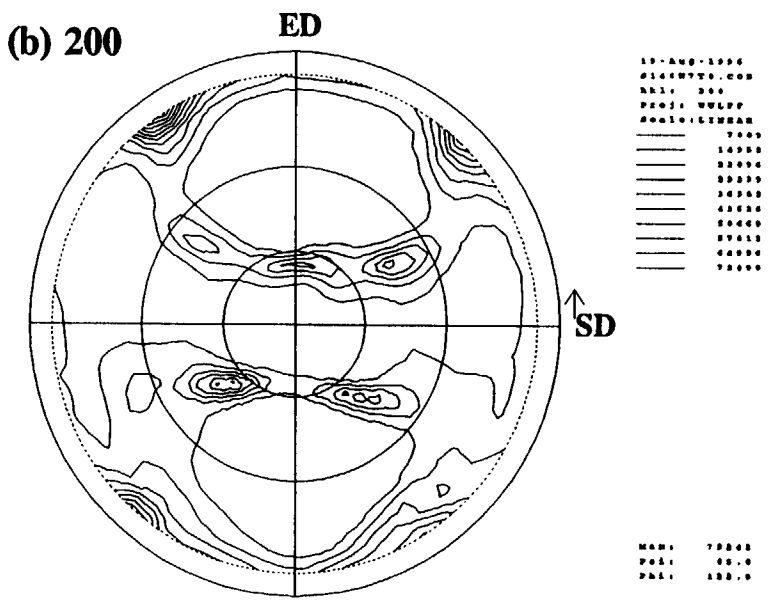

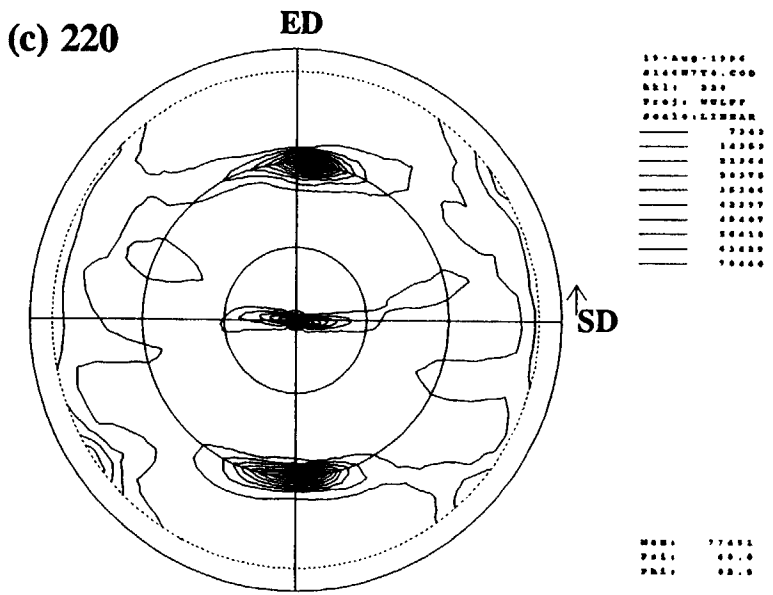

Figure 19.
Partial pole figures for the 1460-T3 extrusion in the web @ 7t/8: (a) (111); (b) (200); (c) (220). [Specimen plane perpendicular to (C)ircumferential axis]

(a) Sections: φ_2= 0 - 90°

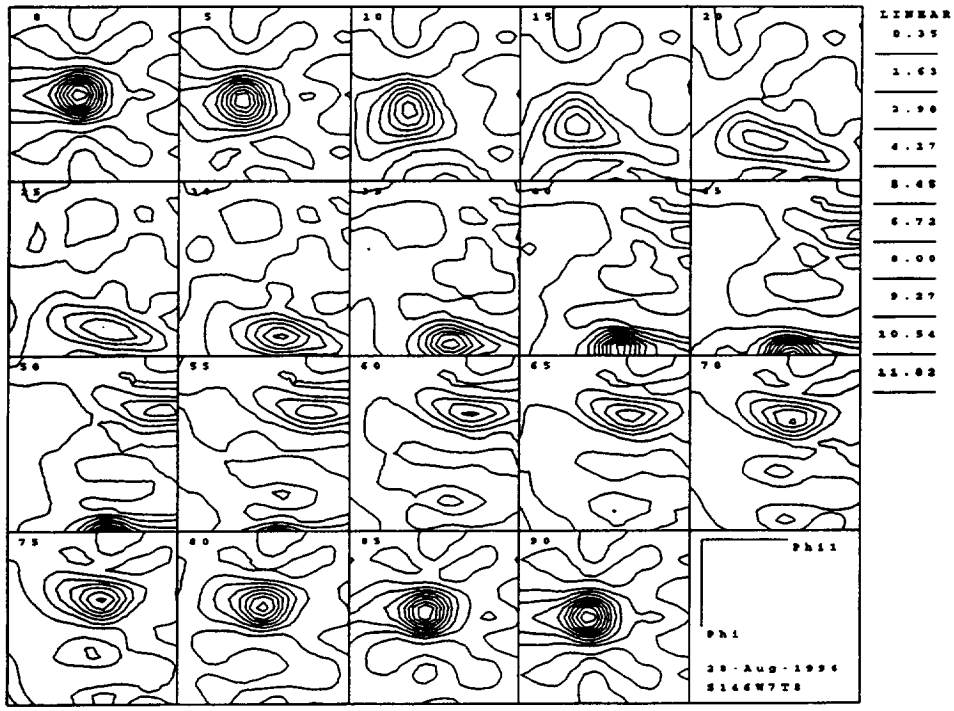

(b) Sections: φ_2= 45°; φ_2= 90°

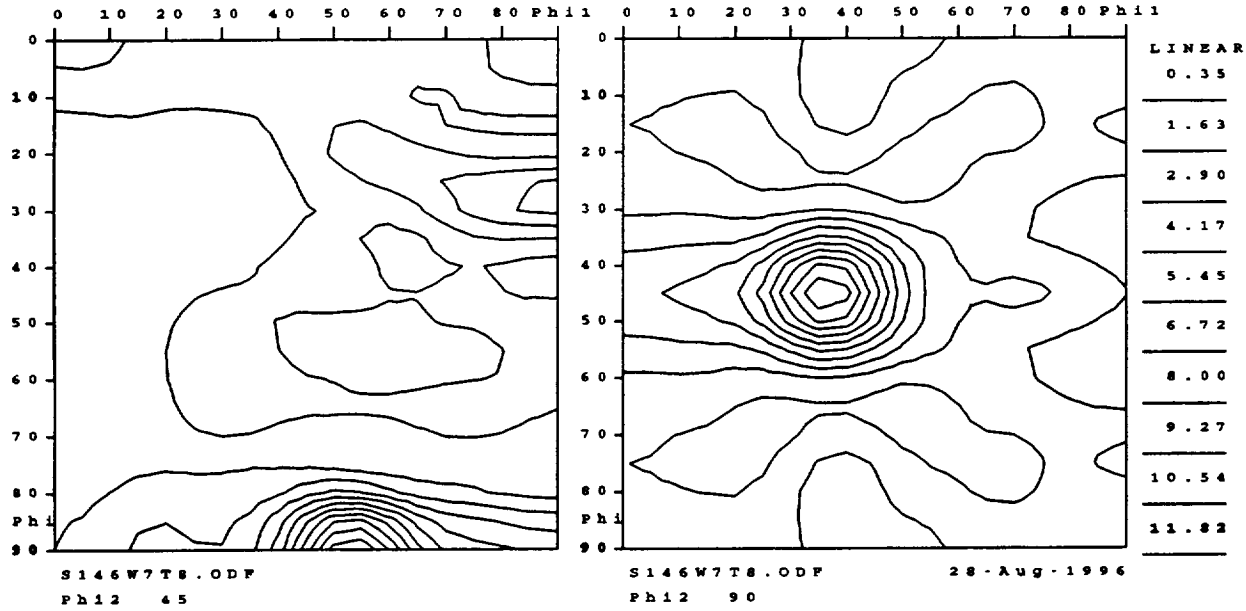

Figure 20. CODF sections for the 1460-T3 extrusion in the web @ 7t/8; (a), Complete sections: φ_2= 0, 5, 10 ..... 90°; and (b), enlarged φ_2= 45° and φ_2= 90° sections. [Specimen plane perpendicular to (C)ircumferential axis]

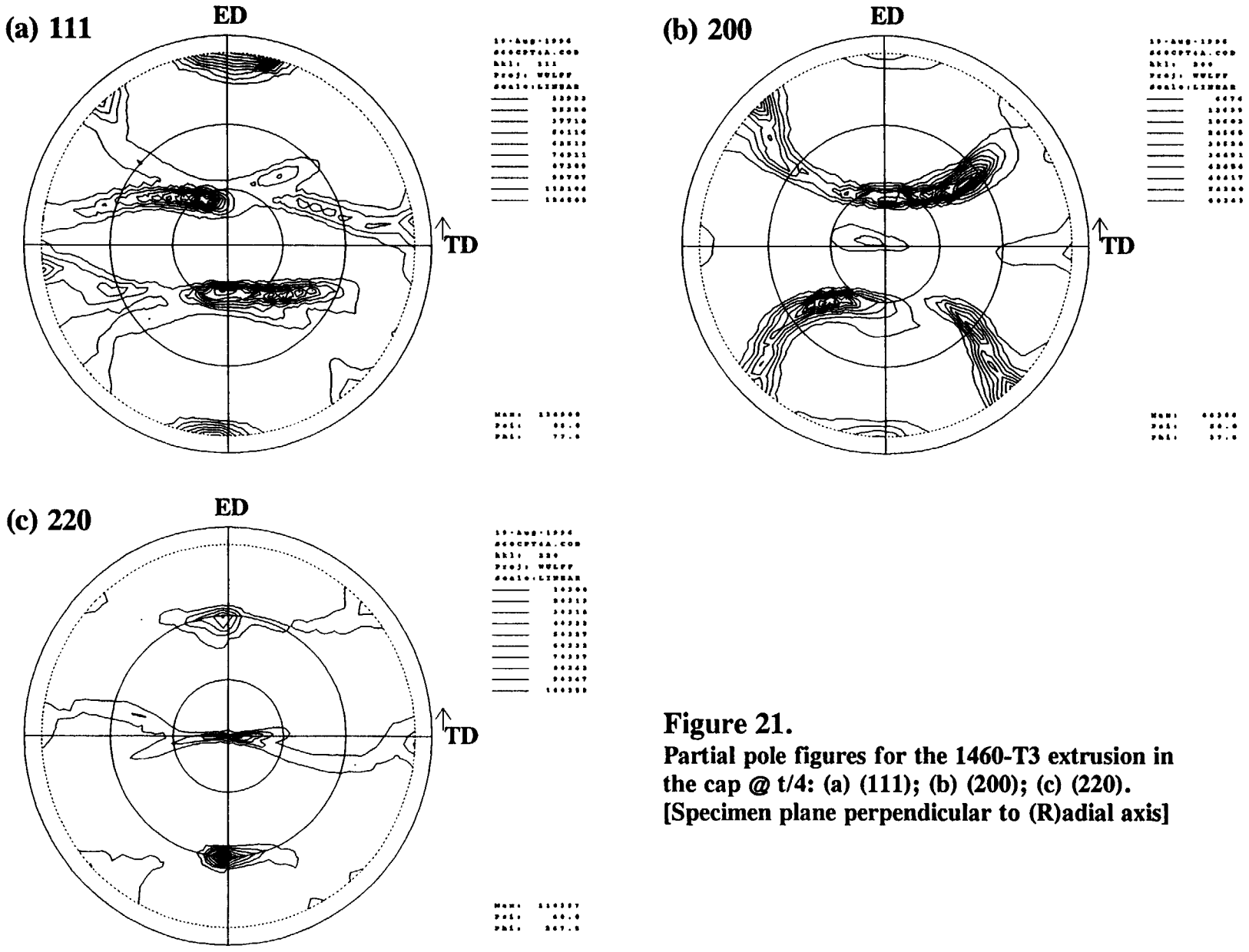

Figure 21.
Partial pole figures for the 1460-T3 extrusion in the cap @ t/4: (a) (111); (b) (200); (c) (220). [Specimen plane perpendicular to (R)adial axis]

(a) Sections: φ_2= 0 - 90°

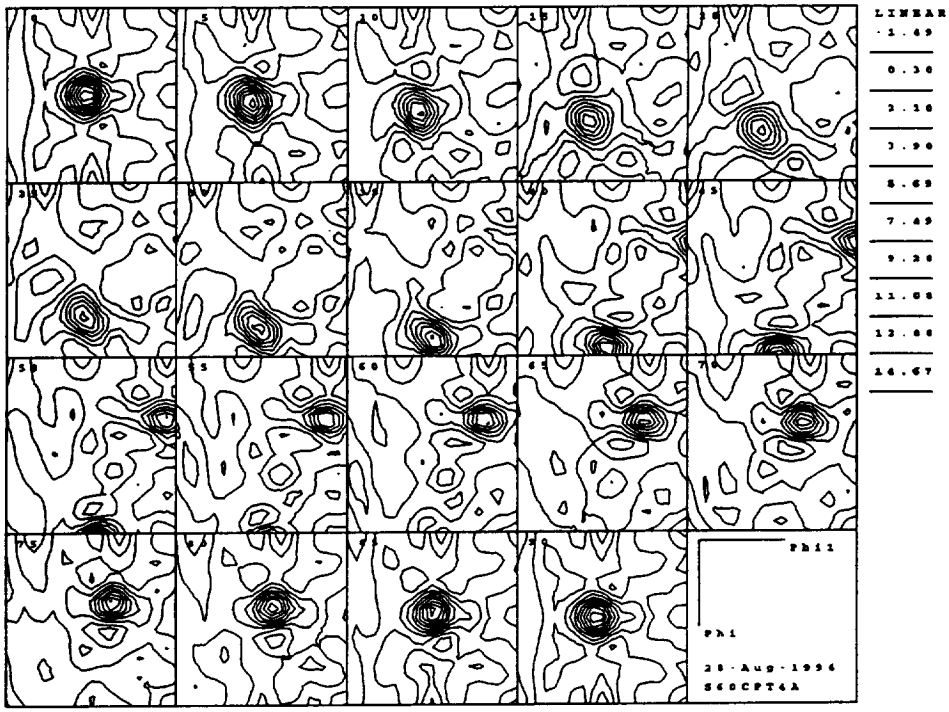

(b) Sections: φ_2= 45°; φ_2= 90°

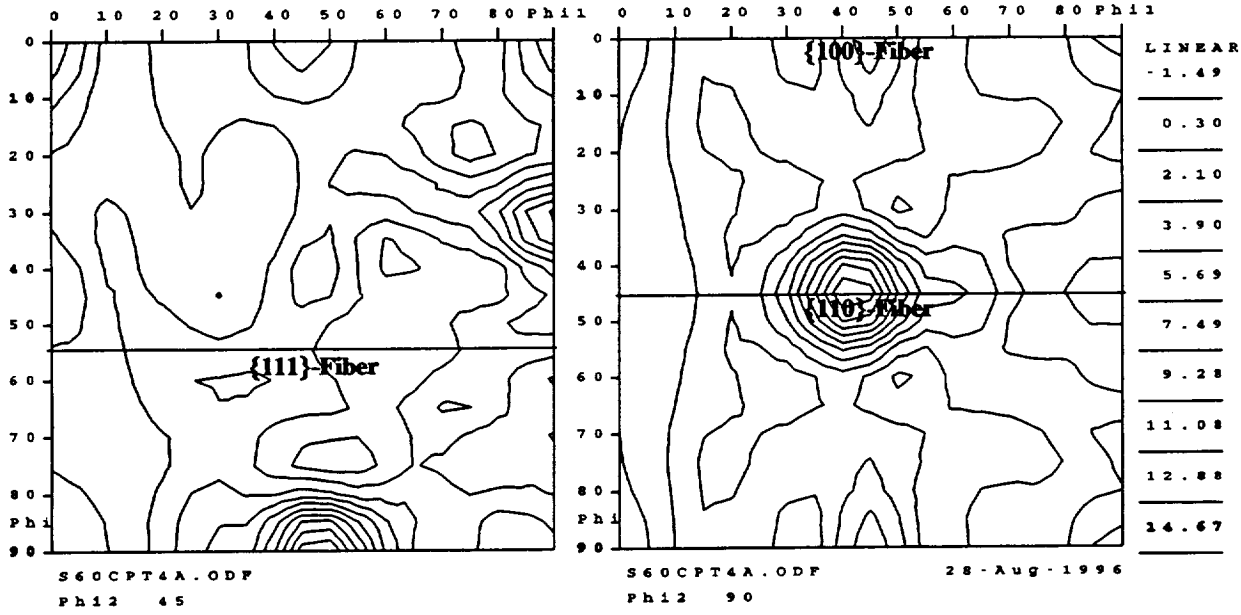

Figure 22. CODF sections for the 1460-T3 extrusion in the cap @ t/4; (a), Complete sections: φ_2= 0, 5, 10 ..... 90°; and (b), enlarged φ_2= 45° and φ_2= 90° sections. The locations of the {100}-fiber, {110}-fiber and {111}-fiber are shown.
[Specimen plane perpendicular to (R)adial axis]

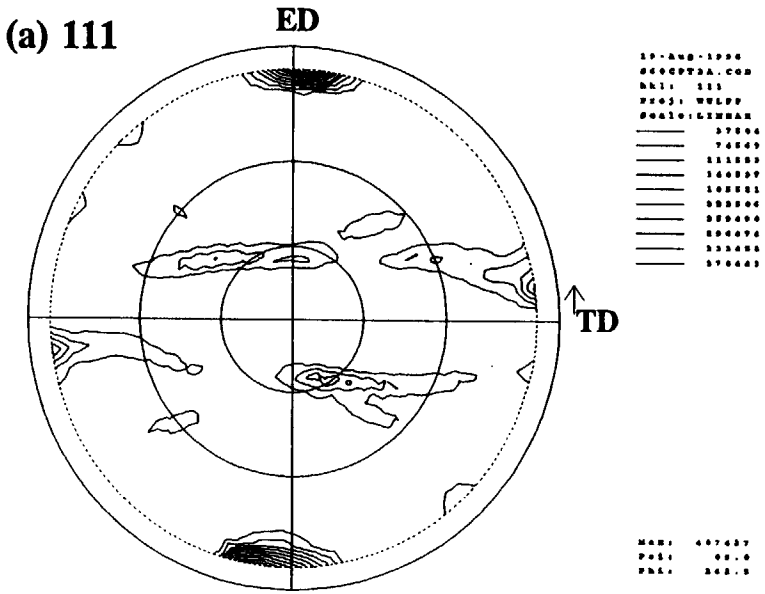

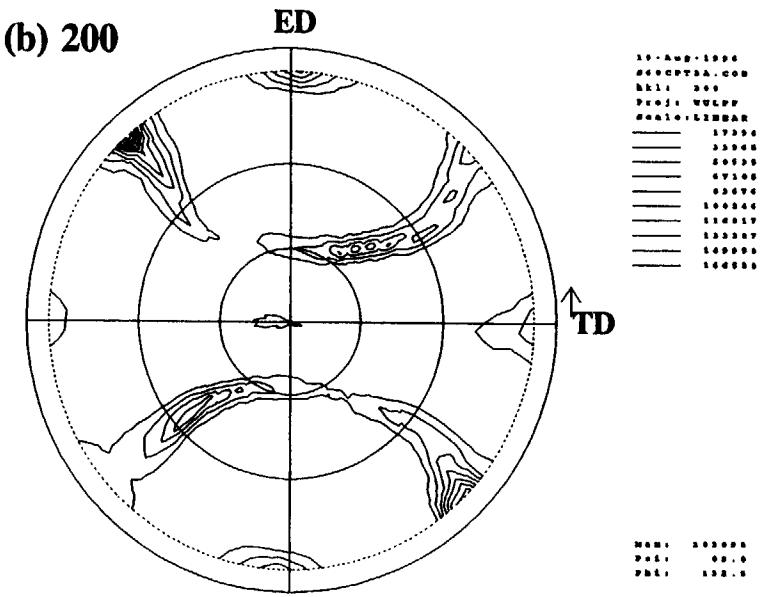

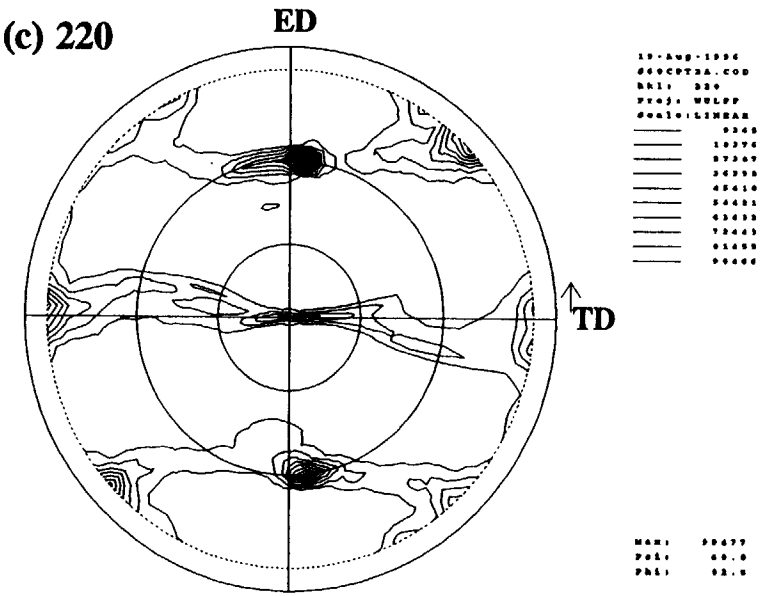

Figure 23.
Partial pole figures for the 1460-T3 extrusion in the cap @ t/2: (a) (111); (b) (200); (c) (220). [Specimen plane perpendicular to (R)adial axis]

(a) Sections: φ_2= 0 - 90°

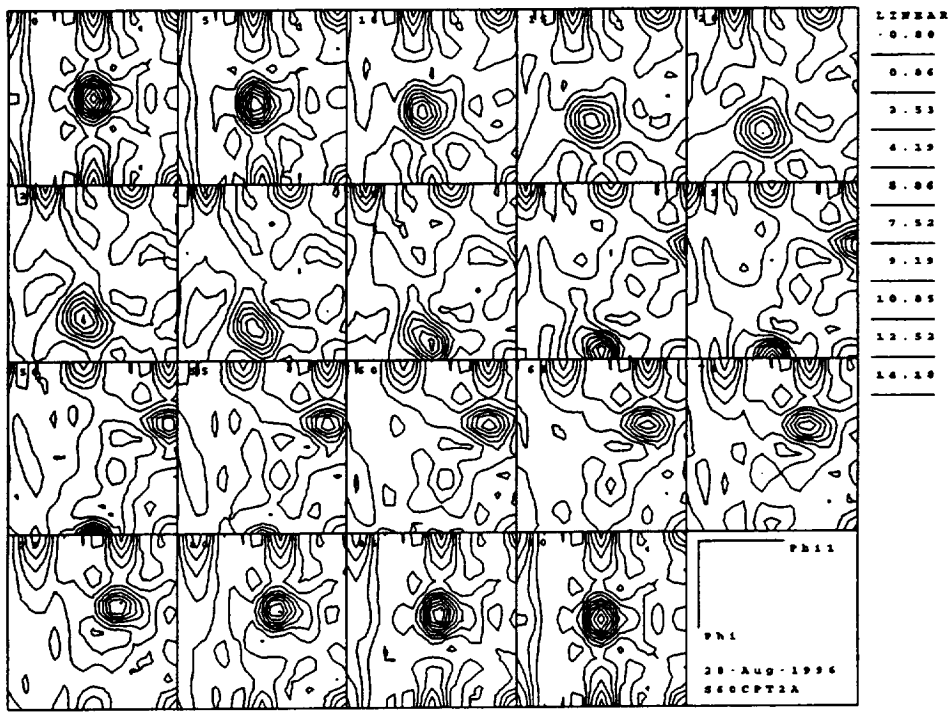

(b) Sections: φ_2= 45°; φ_2= 90°

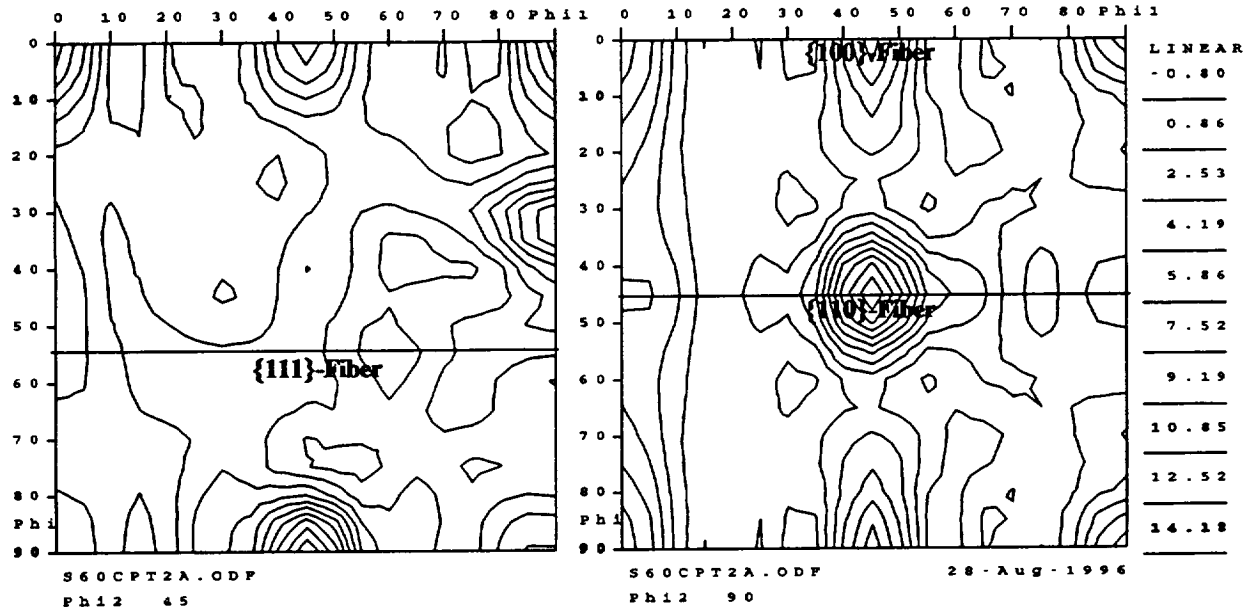

Figure 24. CODF sections for the 1460-T3 extrusion in the cap @ t/2; (a), Complete sections: φ_2= 0, 5, 10 ..... 90°; and (b), enlarged φ_2= 45° and φ_2= 90° sections. The locations of the {100}-fiber, {110}-fiber and {111}-fiber are shown.
[Specimen plane perpendicular to (R)adial axis]

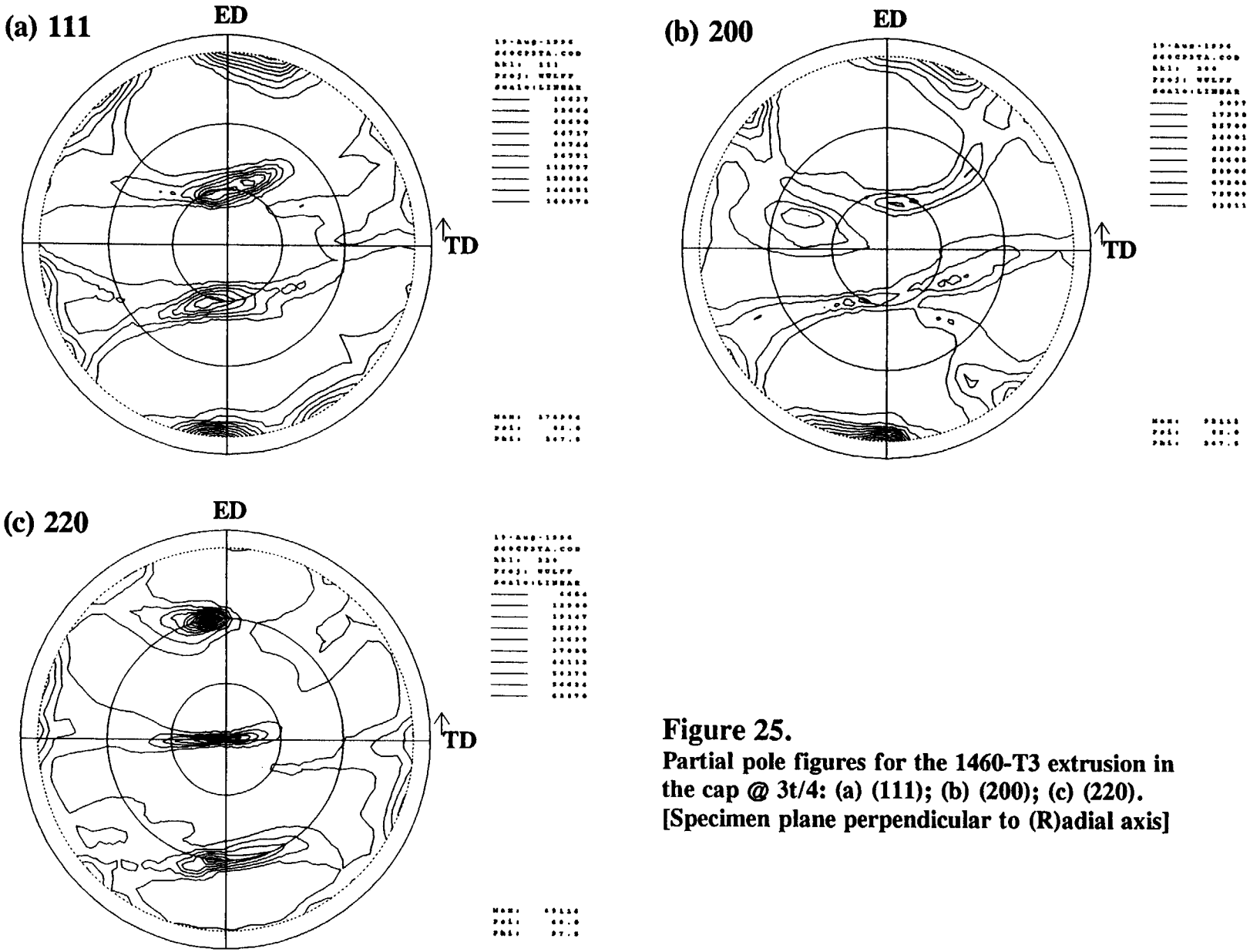

Figure 25.
Partial pole figures for the 1460-T3 extrusion in the cap @ 3t/4: (a) (111); (b) (200); (c) (220). [Specimen plane perpendicular to (R)adial axis]

(a) Sections: $\varphi_2 = 0 - 90°$

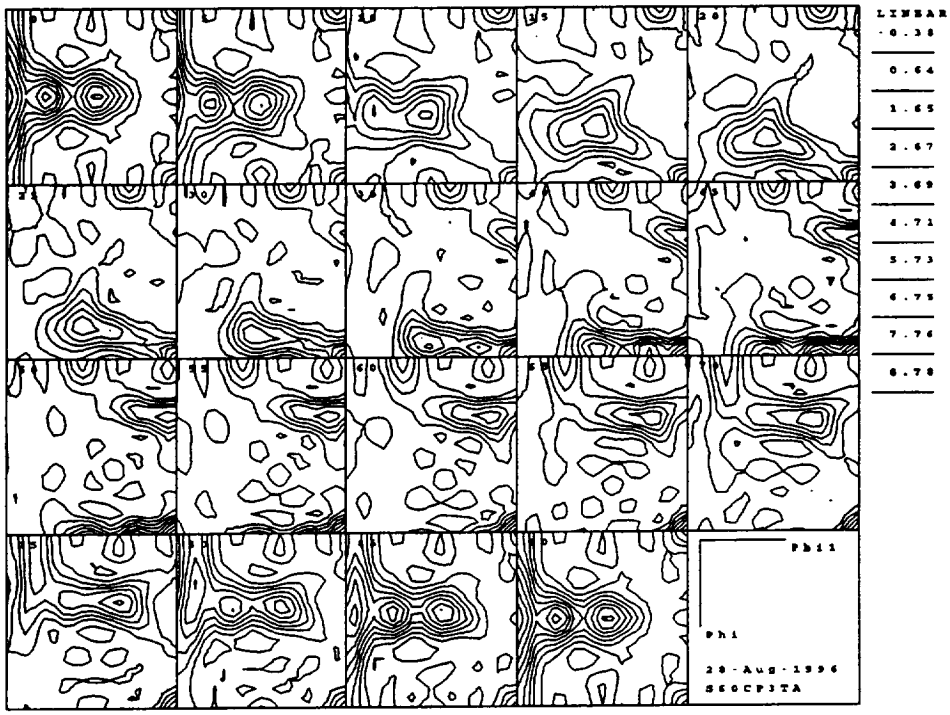

(b) Sections: $\varphi_2 = 45°$; $\varphi_2 = 90°$

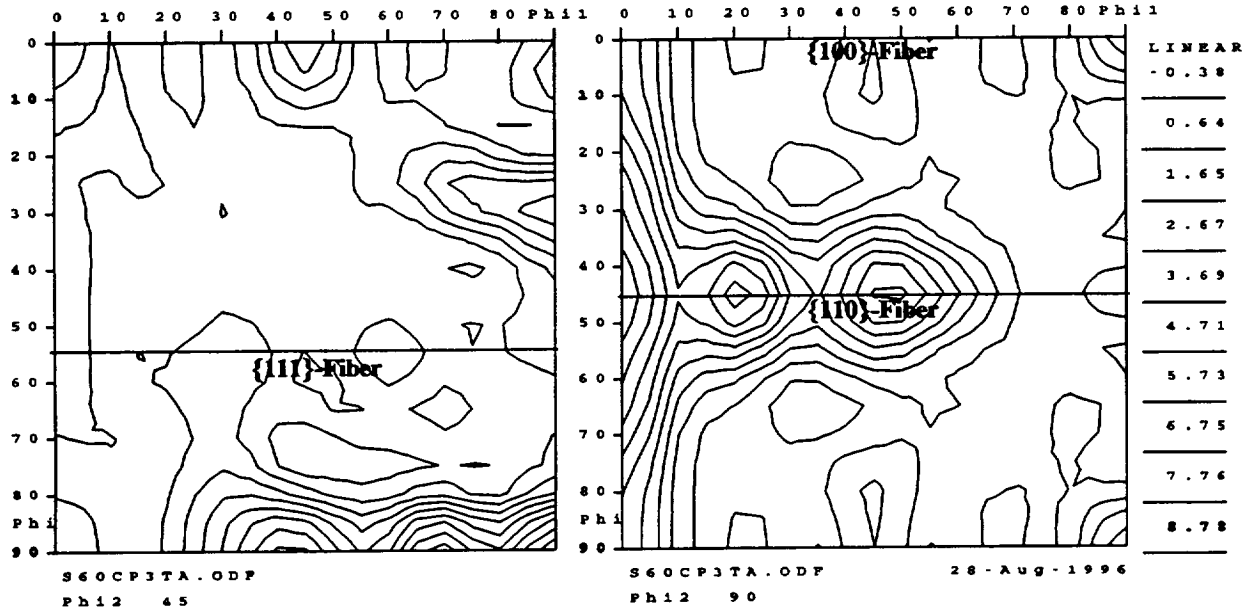

Figure 26. CODF sections for the 1460-T3 extrusion in the cap @ 3t/4; (a), Complete sections: $\varphi_2 = 0, 5, 10 \ldots\ldots 90°$; and (b), enlarged $\varphi_2 = 45°$ and $\varphi_2 = 90°$ sections. The locations of the {100}-fiber, {110}-fiber and {111}-fiber are shown.
[Specimen plane perpendicular to (R)adial axis]

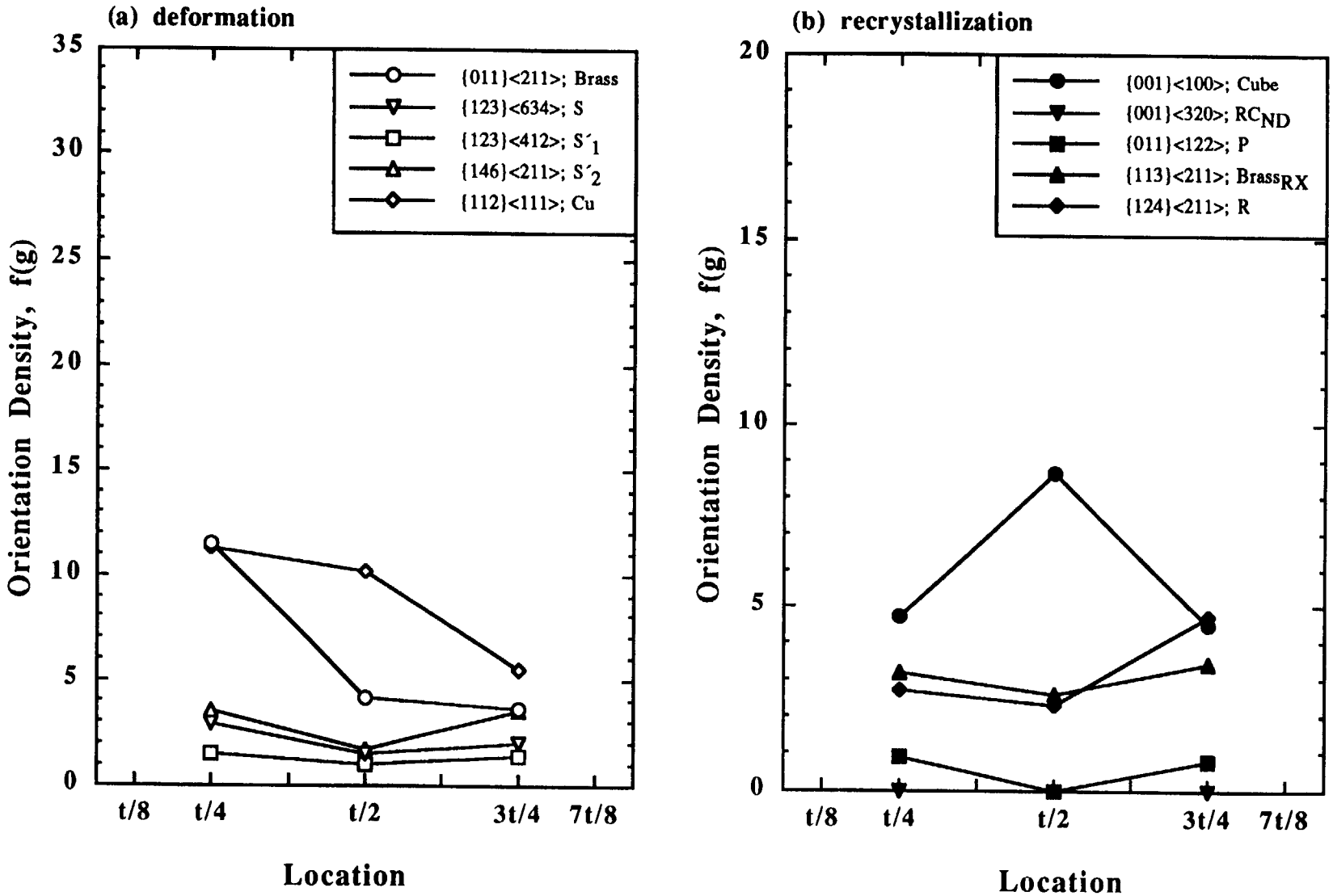

Figure 27. Orientation density, f(g), as a function of location through the cross-section for the 1460-T3 extrusion in the cap region: (a) Deformation-related components; (b) Recrystallization-related components.

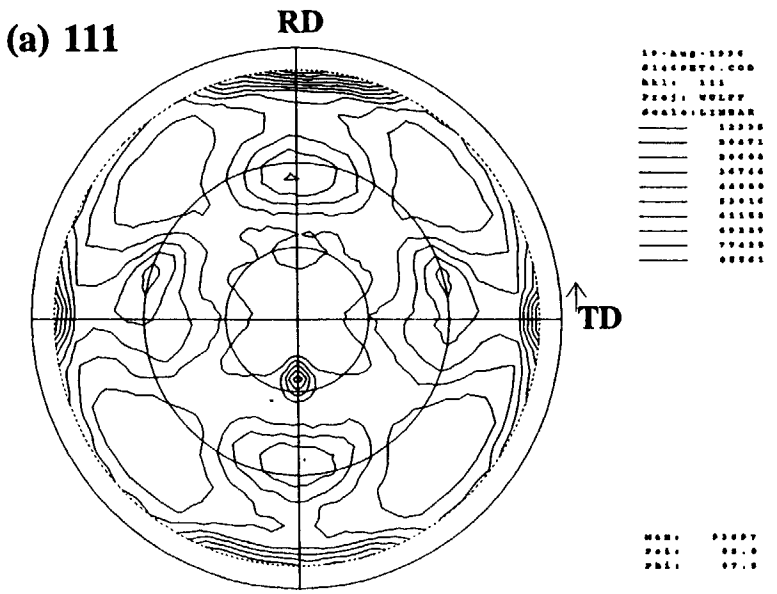

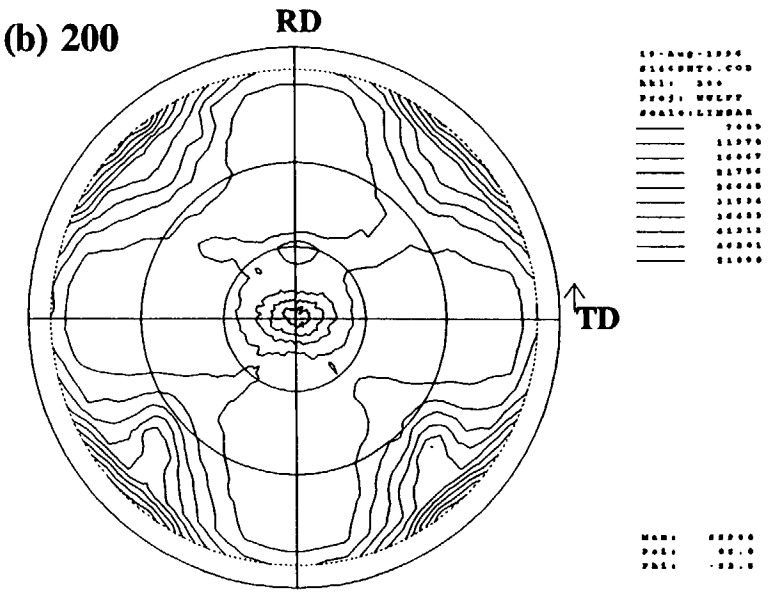

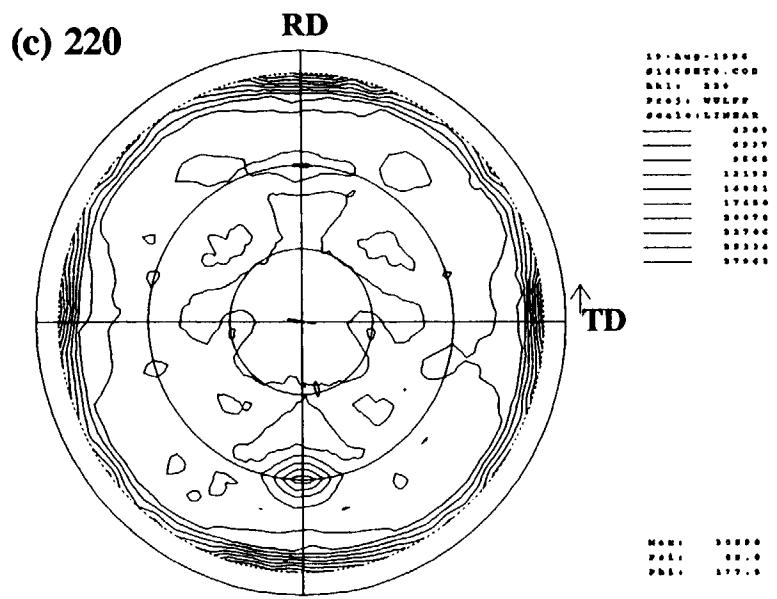

Figure 28.
Partial pole figures for 1460-T3 sheet @ t/8: (a) (111); (b) (200); (c) (220). [Specimen plane perpendicular to (S)hort-Transverse axis]

(a) Sections: $\varphi_2 = 0 - 90°$

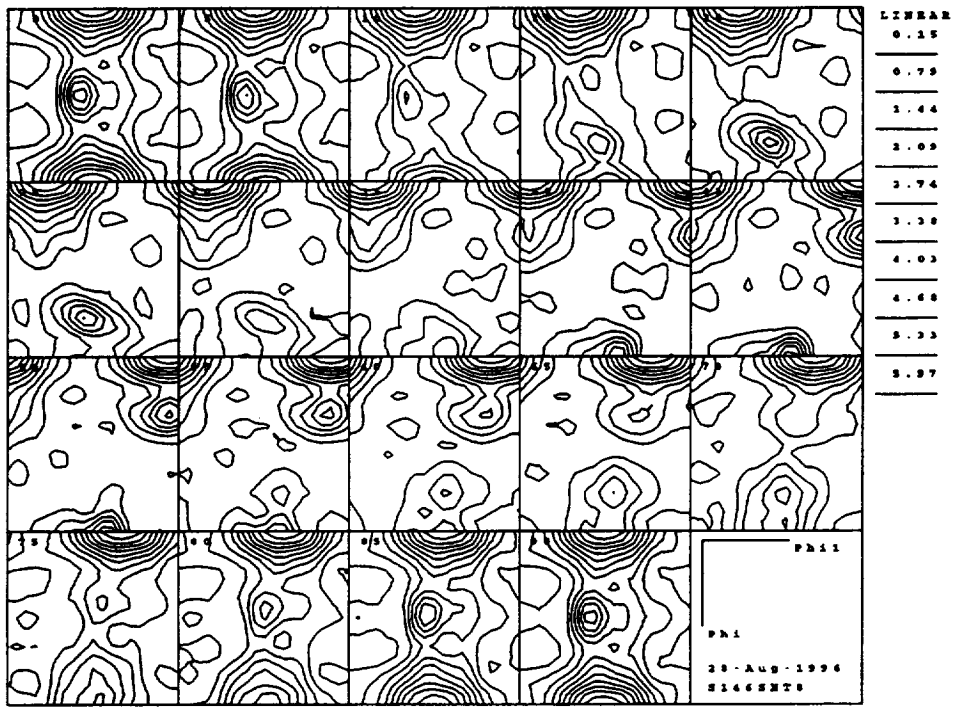

(b) Sections: $\varphi_2 = 45°$; $\varphi_2 = 90°$

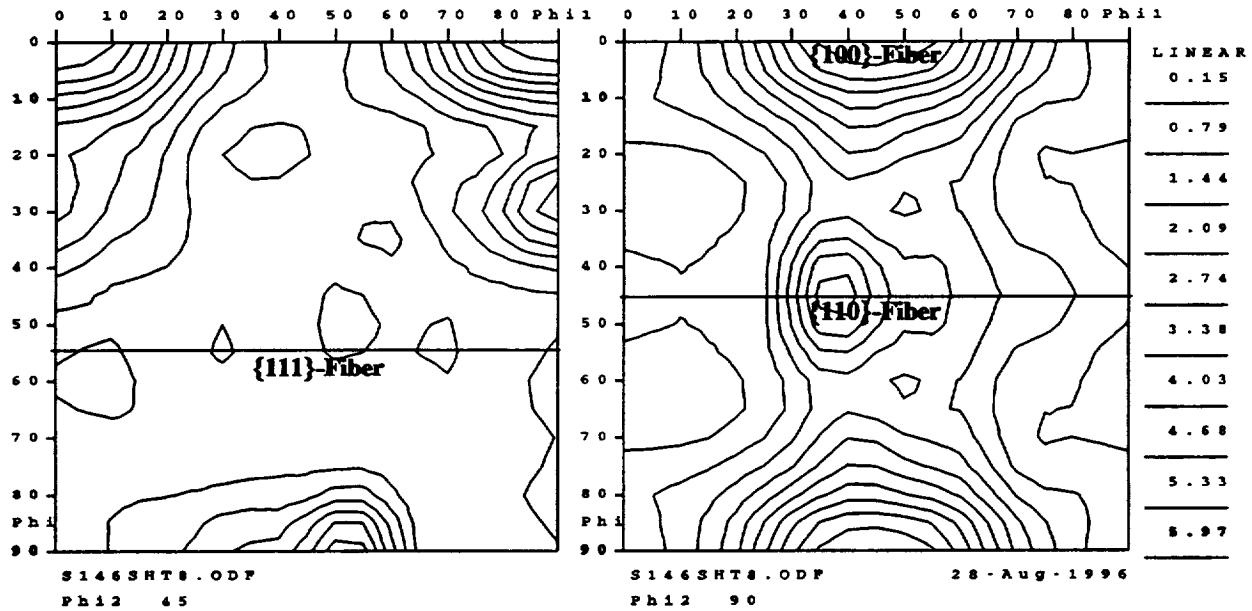

Figure 29. CODF sections for 1460-T3 sheet @ t/8; (a), Complete sections: $\varphi_2 = 0, 5, 10$ ..... 90°; and (b), enlarged $\varphi_2 = 45°$ and $\varphi_2 = 90°$ sections. The locations of the {100}-fiber, {110}-fiber and {111}-fiber are shown.
[Specimen plane perpendicular to (S)hort-Transverse axis]

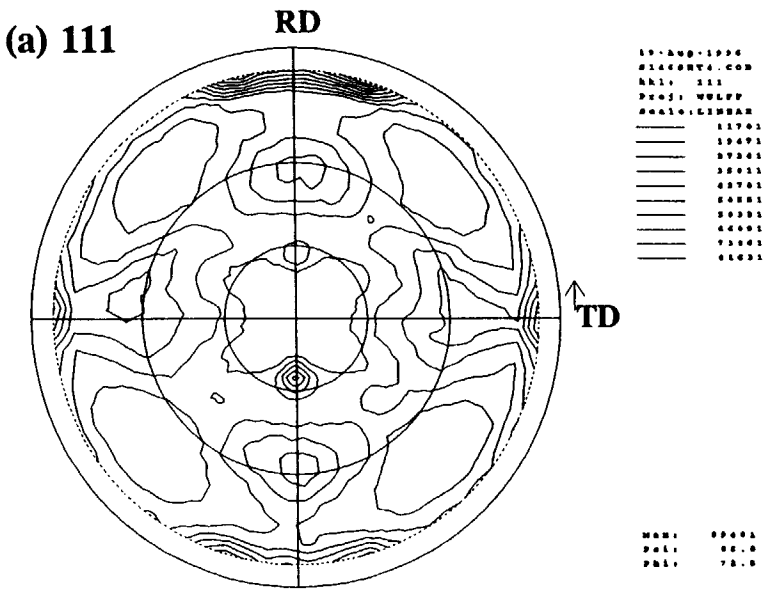

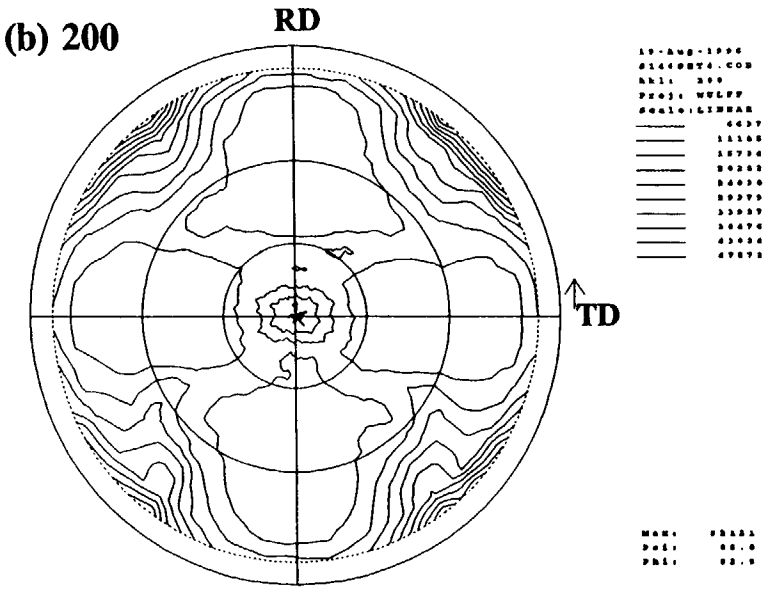

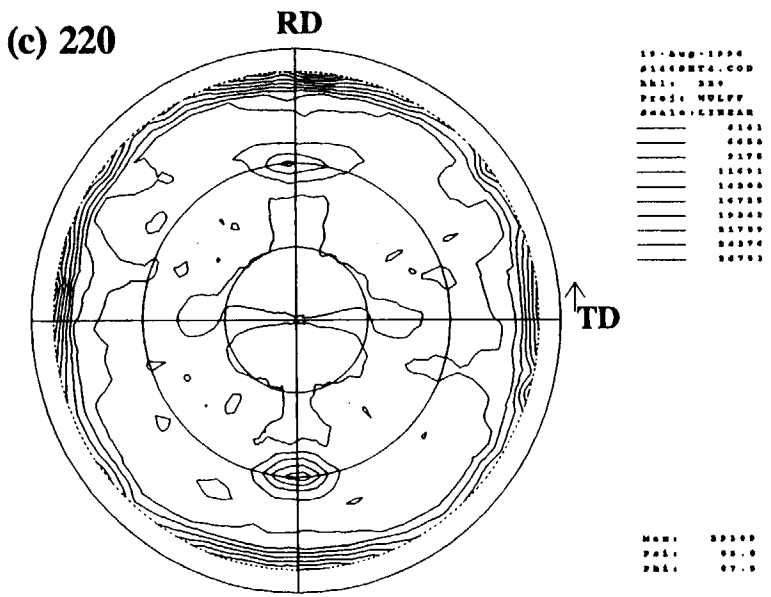

Figure 30.
Partial pole figures for 1460-T3 sheet @ t/4: (a) (111); (b) (200); (c) (220). [Specimen plane perpendicular to (S)hort-Transverse axis]

(a) Sections: $\varphi_2 = 0 - 90°$

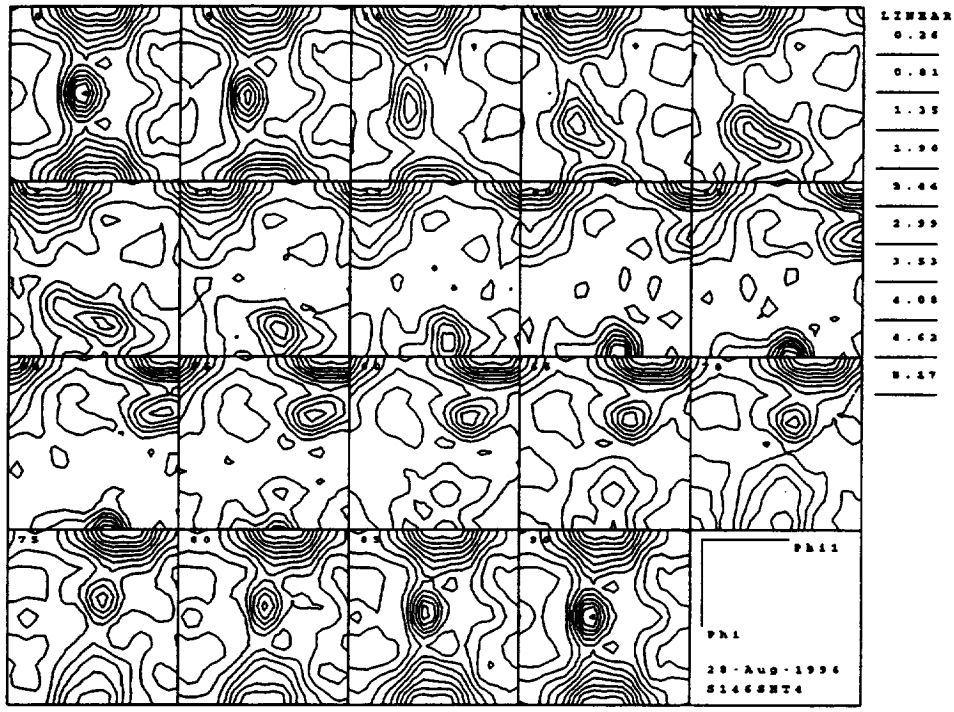

(b) Sections: $\varphi_2 = 45°$; $\varphi_2 = 90°$

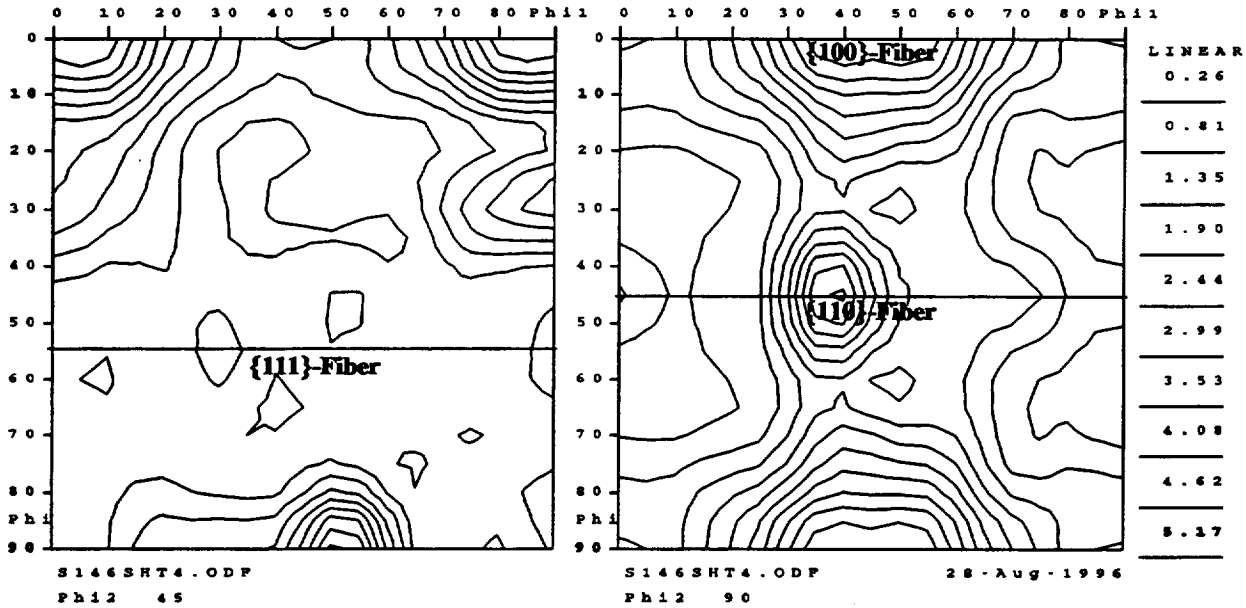

Figure 31. CODF sections for 1460-T3 sheet @ t/4; (a), Complete sections: $\varphi_2 = 0, 5, 10$ ..... 90°; and (b), enlarged $\varphi_2 = 45°$ and $\varphi_2 = 90°$ sections. The locations of the {100}-fiber, {110}-fiber and {111}-fiber are shown.
[Specimen plane perpendicular to (S)hort-Transverse axis]

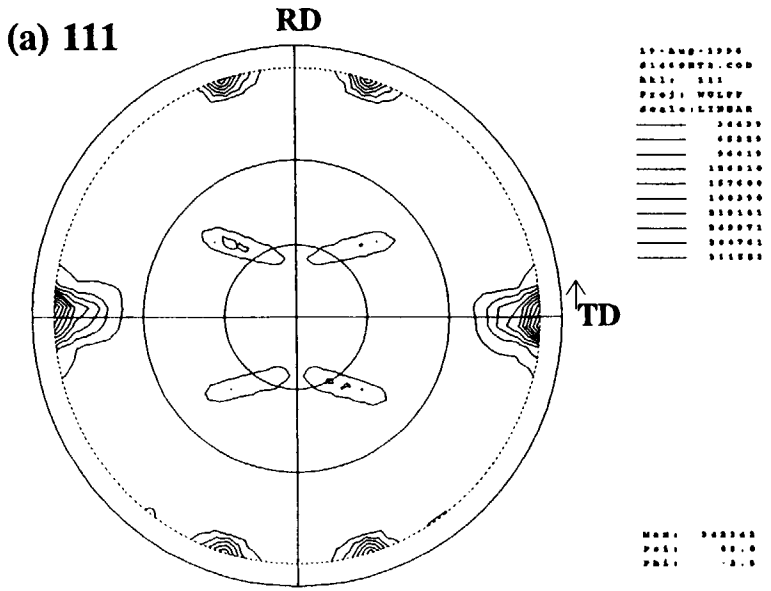

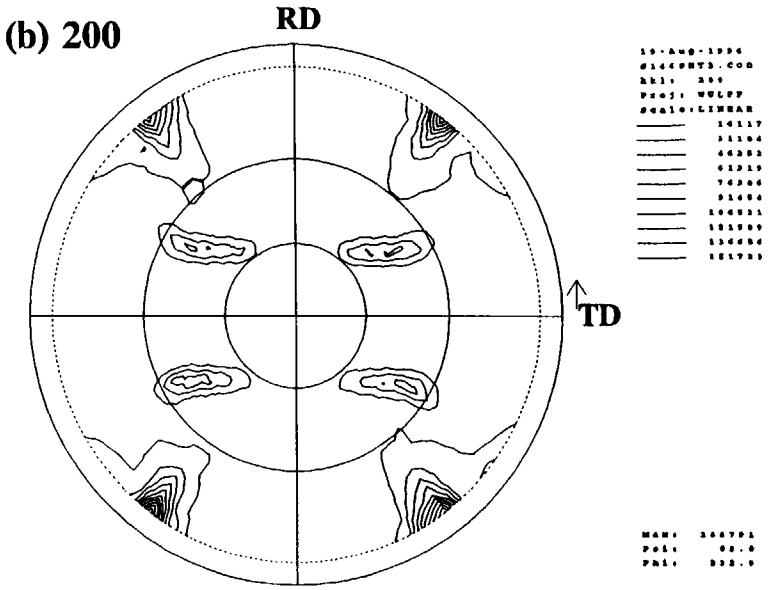

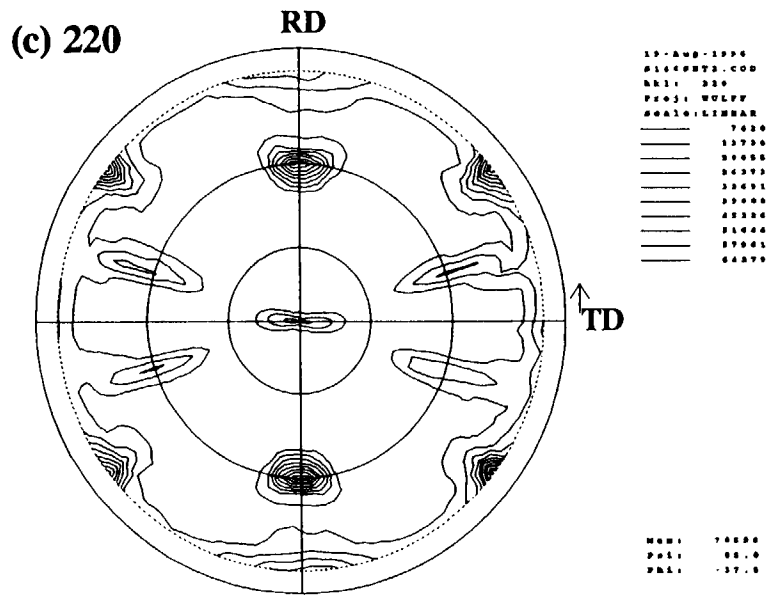

Figure 32.
Partial pole figures for 1460-T3 sheet @ t/2: (a) (111); (b) (200); (c) (220). [Specimen plane perpendicular to (S)hort-Transverse axis]

(a) Sections: φ_2= 0 - 90°

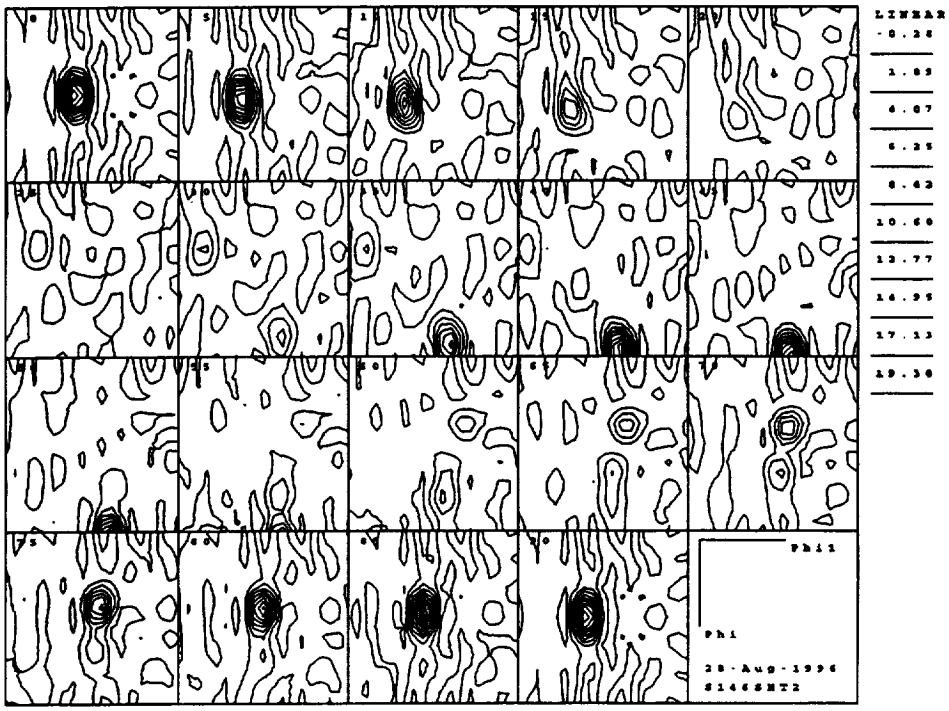

(b) Sections: φ_2= 45°; φ_2= 90°

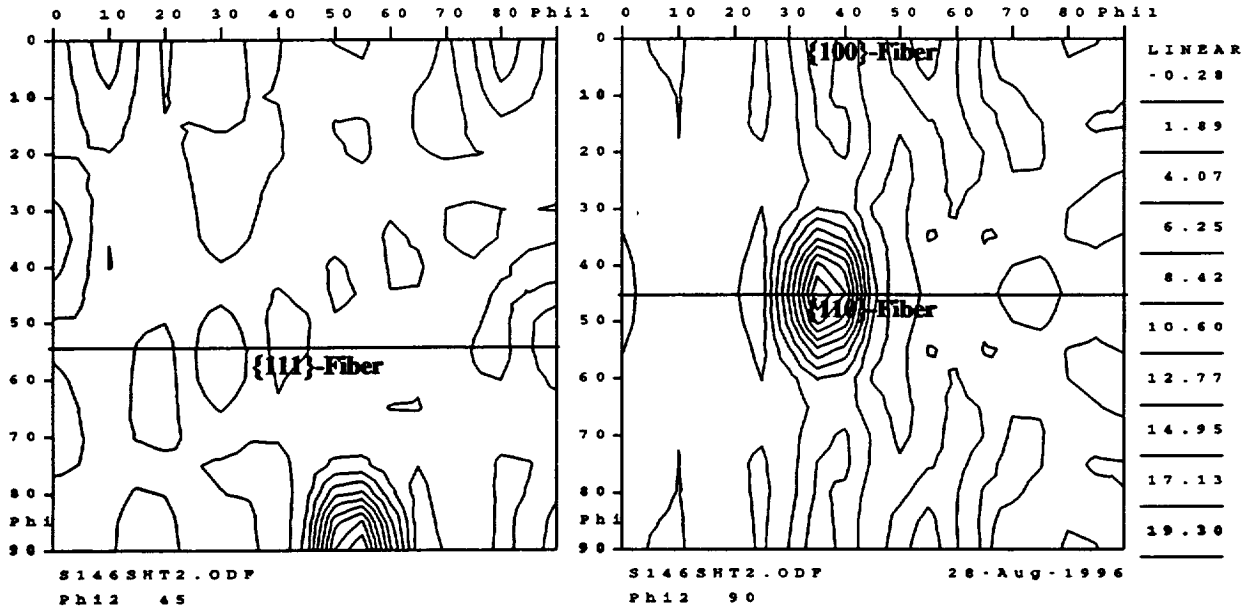

Figure 33. CODF sections for 1460-T3 sheet @ t/2; (a), Complete sections: φ_2= 0, 5, 10 ..... 90°; and (b), enlarged φ_2= 45° and φ_2= 90° sections. The locations of the {100}-fiber, {110}-fiber and {111}-fiber are shown.
[Specimen plane perpendicular to (S)hort-Transverse axis]

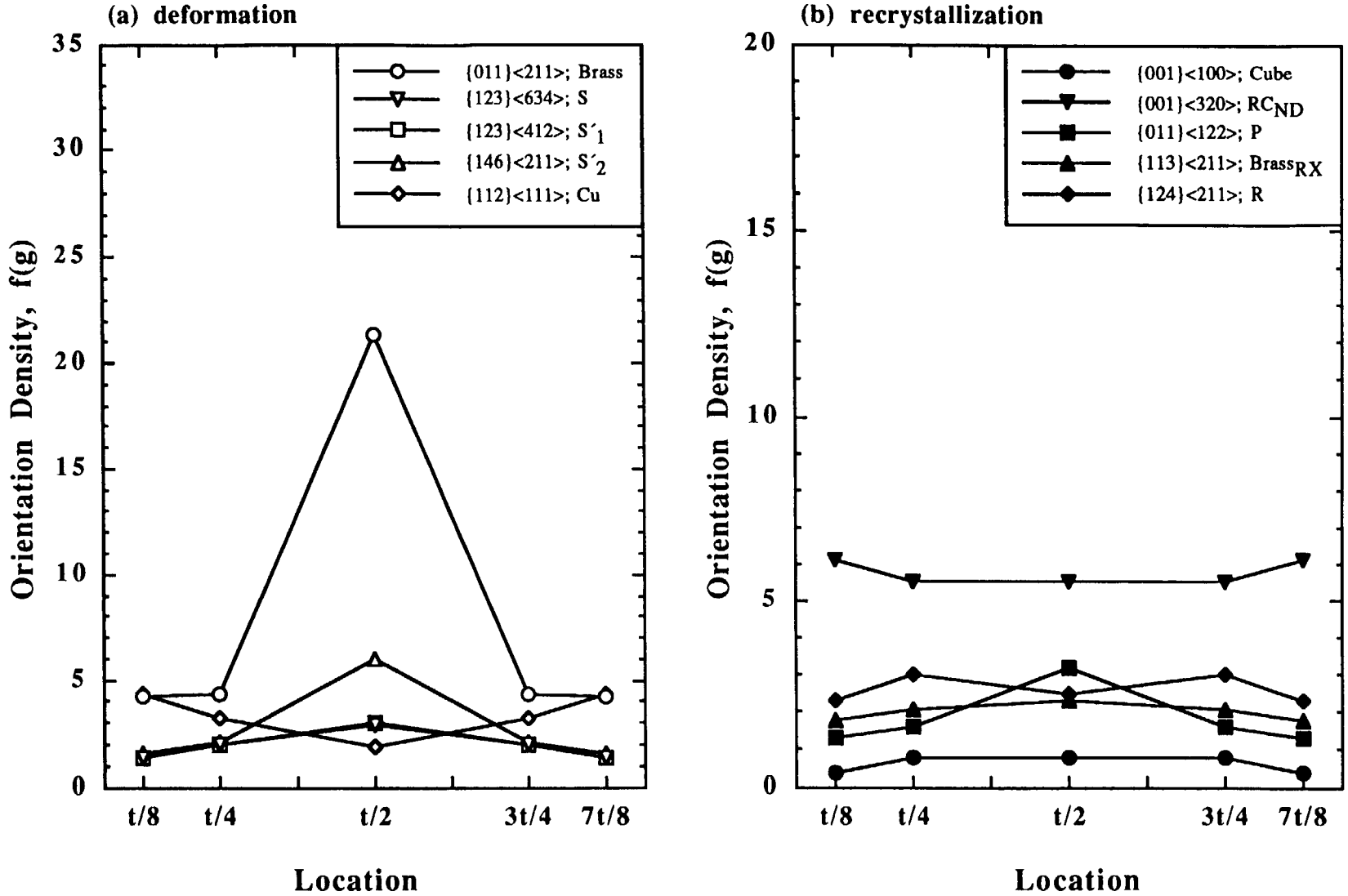

Figure 34. Orientation density, f(g), as a function of location through the cross-section for the 1460-T3 sheet: (a) Deformation-related components; (b) Recrystallization-related components.

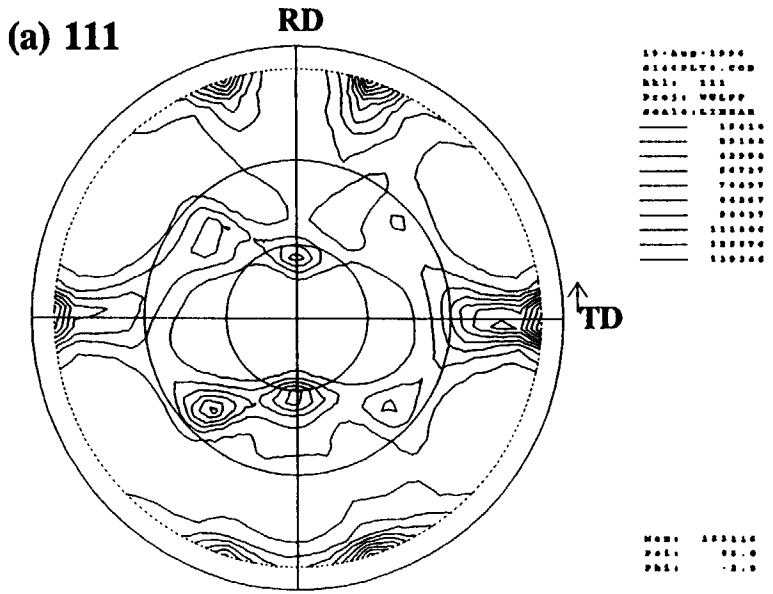

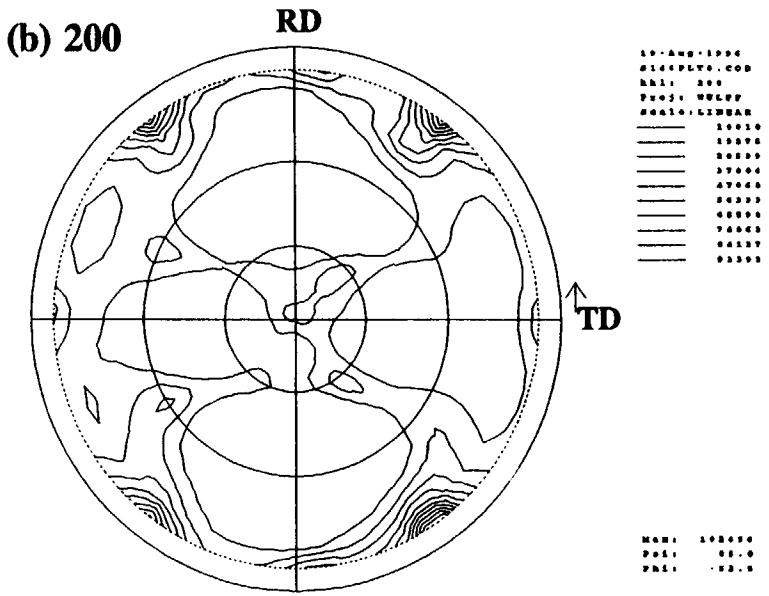

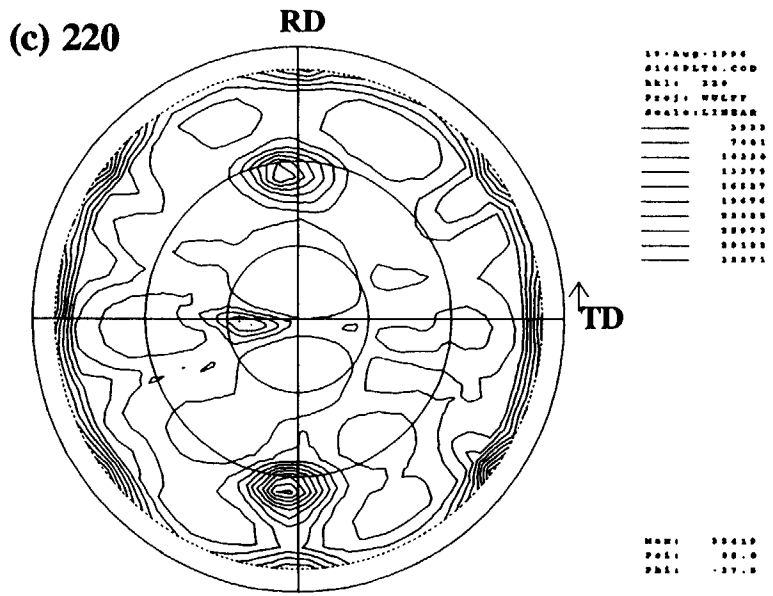

Figure 35.
Partial pole figures for 1460-T3 plate @ t/8: (a) (111); (b) (200); (c) (220). [Specimen plane perpendicular to (S)hort-Transverse axis]

(a) Sections: φ_2= 0 - 90°

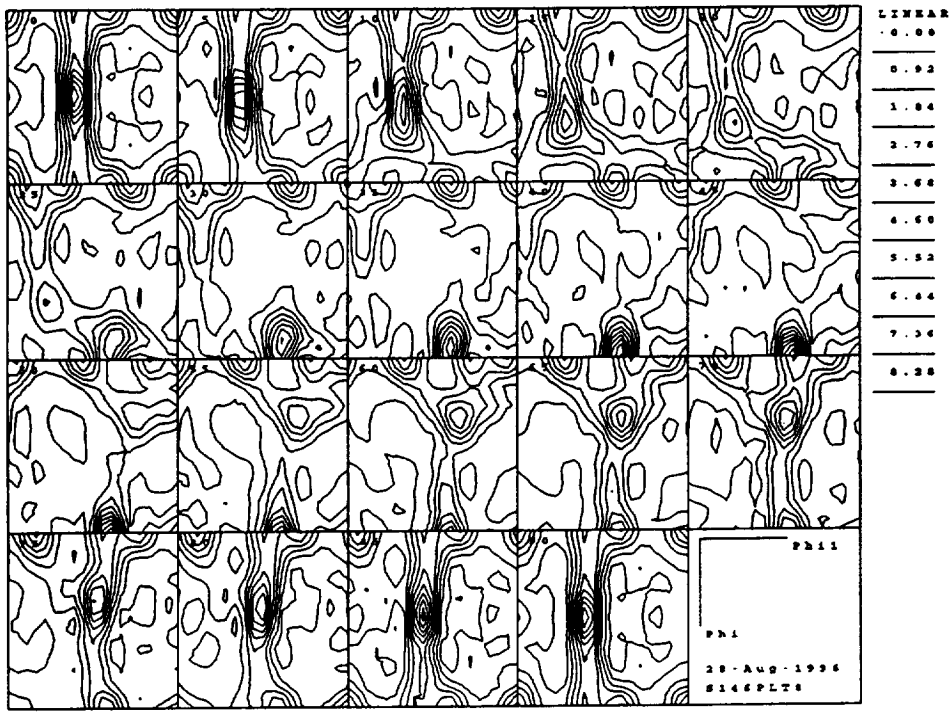

(b) Sections: φ_2= 45°; φ_2= 90°

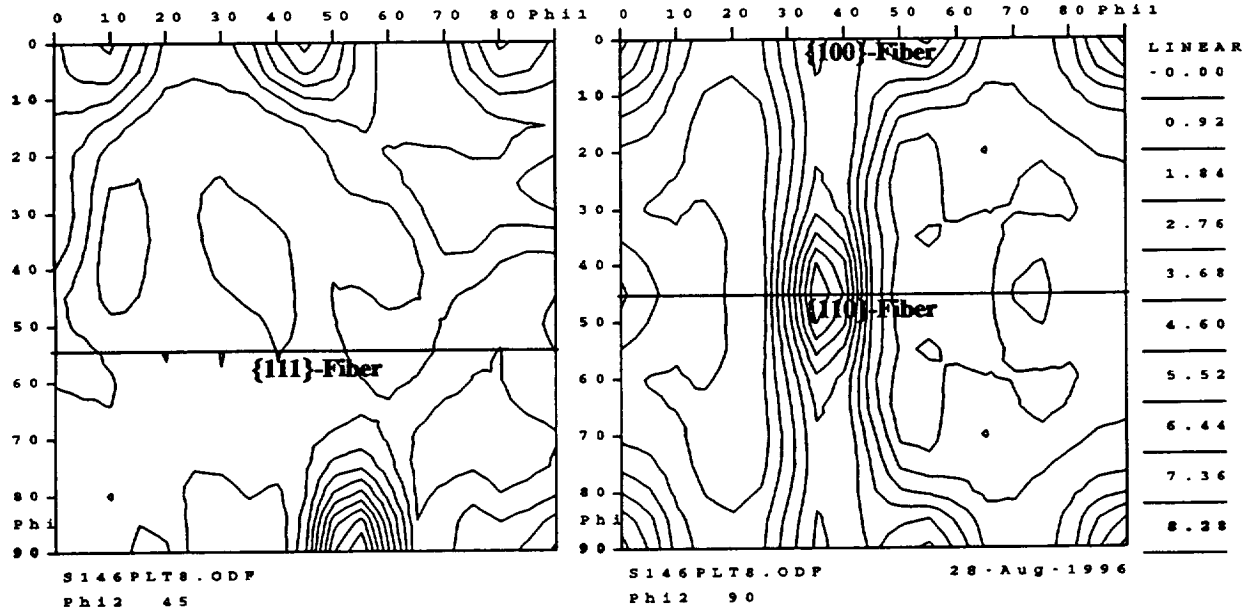

Figure 36. CODF sections for 1460-T3 plate @ t/8; (a), Complete sections: φ_2= 0, 5, 10 ..... 90°; and (b), enlarged φ_2= 45° and φ_2= 90° sections. The locations of the {100}-fiber, {110}-fiber and {111}-fiber are shown.
[Specimen plane perpendicular to (S)hort-Transverse axis]

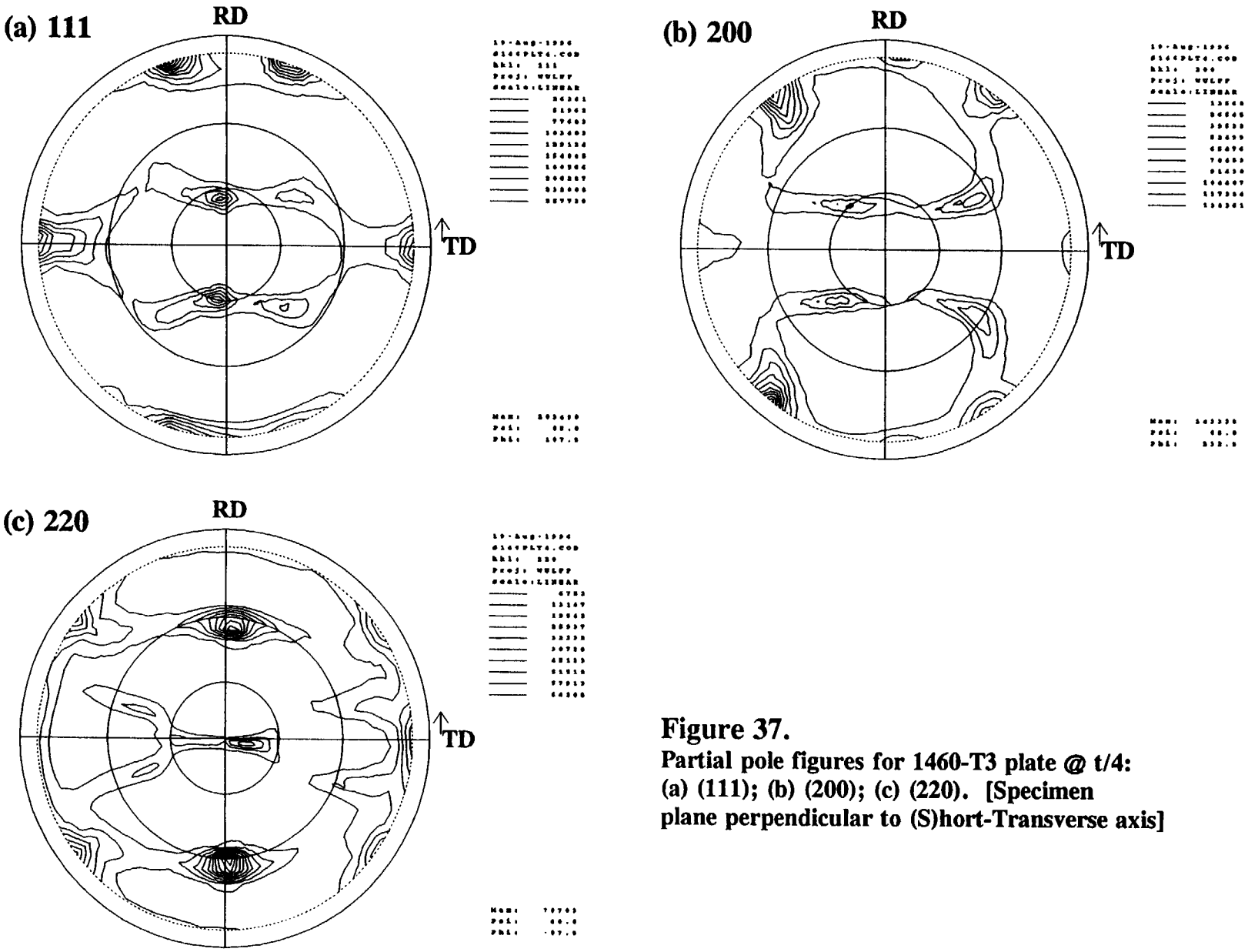

Figure 37.
Partial pole figures for 1460-T3 plate @ t/4: (a) (111); (b) (200); (c) (220). [Specimen plane perpendicular to (S)hort-Transverse axis]

(a) Sections: φ_2= 0 - 90°

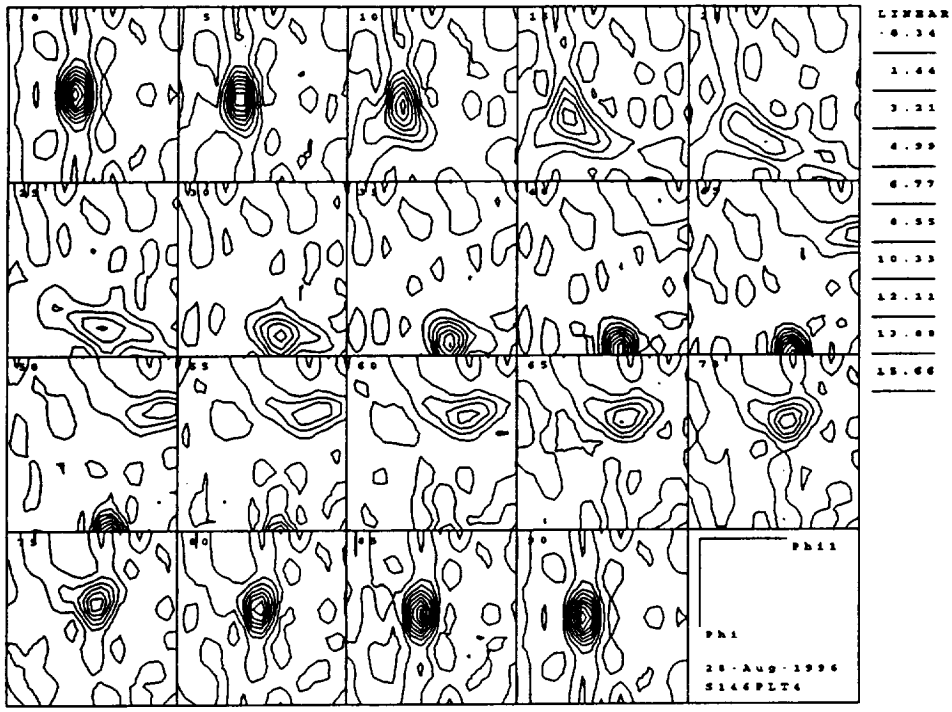

(b) Sections: φ_2= 45°; φ_2= 90°

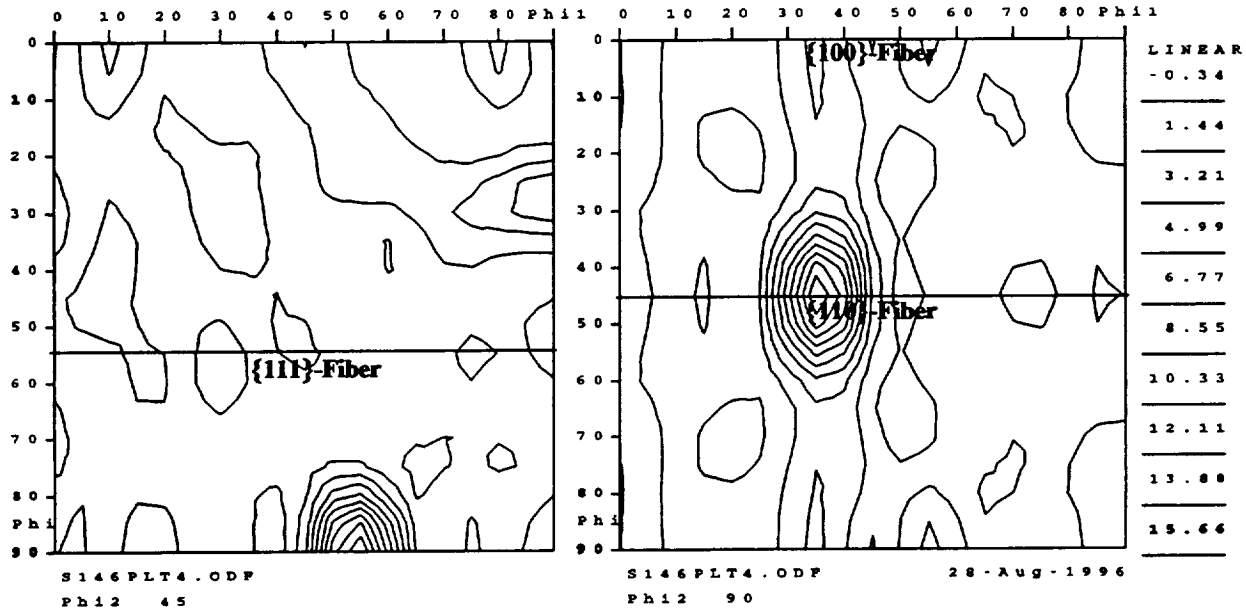

Figure 38. CODF sections for 1460-T3 plate @ t/4; (a), Complete sections: φ_2= 0, 5, 10 ..... 90°; and (b), enlarged φ_2= 45° and φ_2= 90° sections. The locations of the {100}-fiber, {110}-fiber and {111}-fiber are shown.
[Specimen plane perpendicular to (S)hort-Transverse axis]

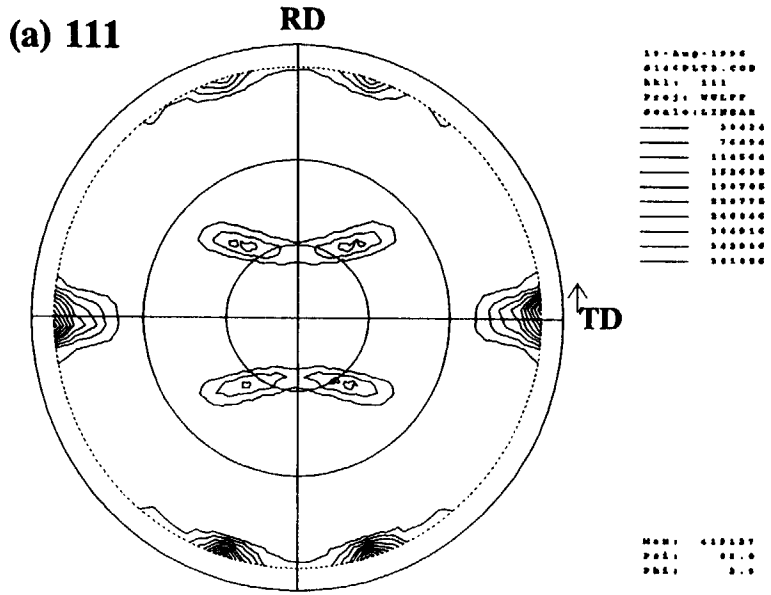

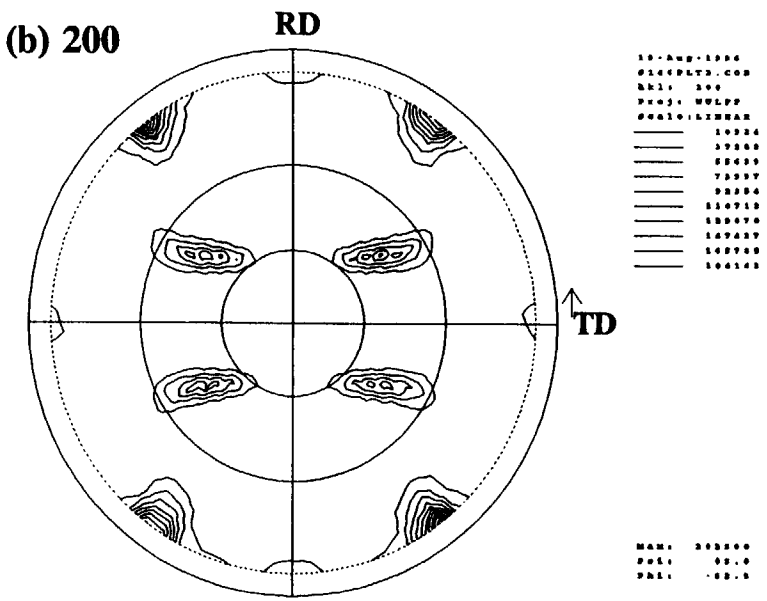

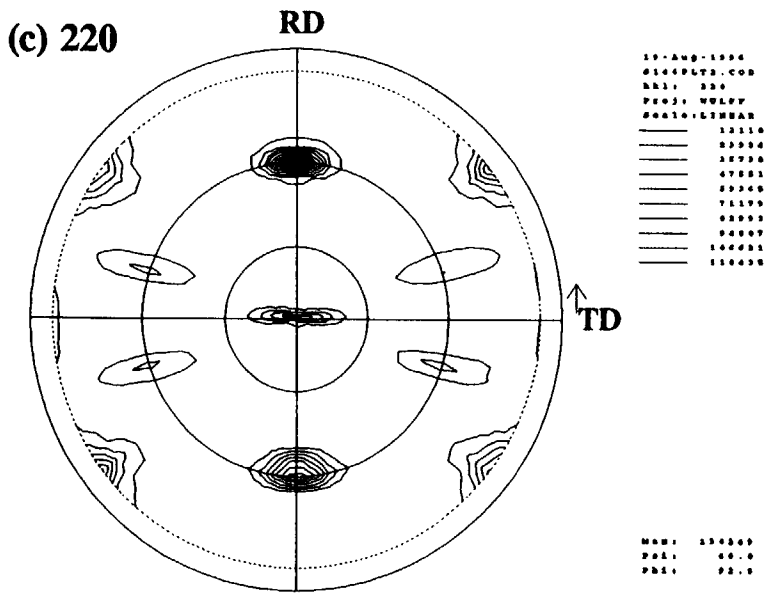

Figure 39.
Partial pole figures for 1460-T3 plate @ t/2: (a) (111); (b) (200); (c) (220). [Specimen plane perpendicular to (S)hort-Transverse axis]

(a) Sections: φ_2= 0 - 90°

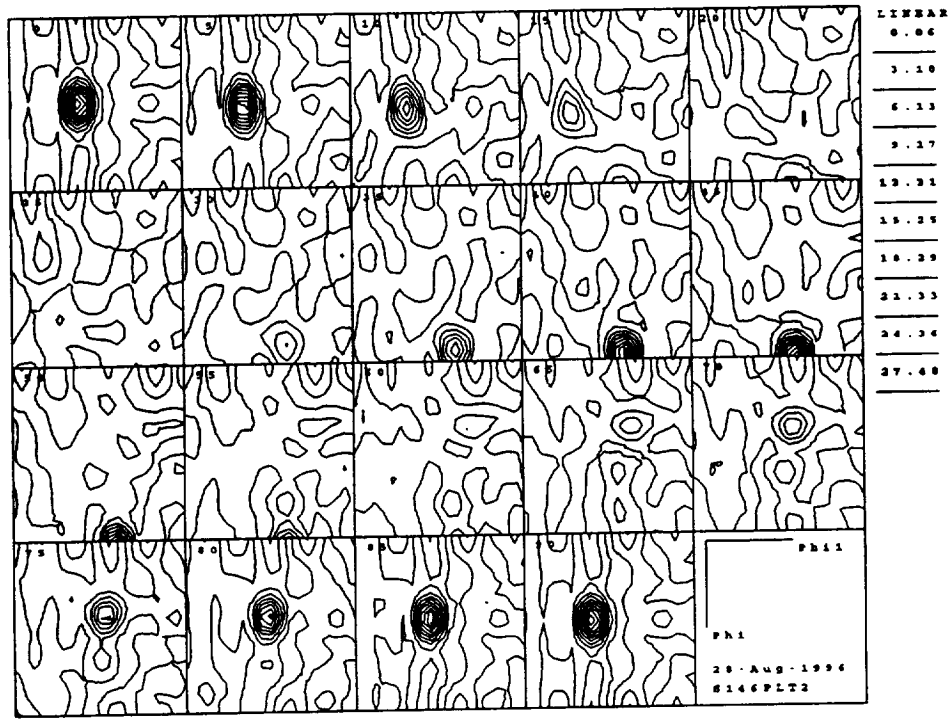

(b) Sections: φ_2= 45°; φ_2= 90°

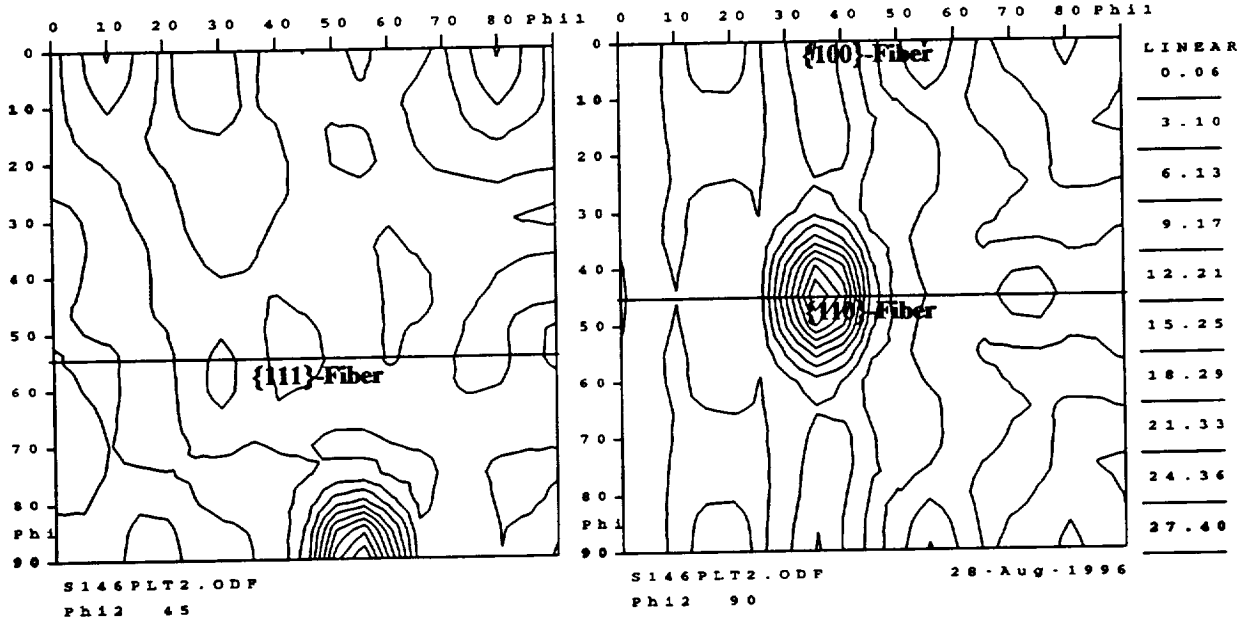

Figure 40. CODF sections for 1460-T3 plate @ t/2; (a), Complete sections: φ_2= 0, 5, 10 ..... 90°; and (b), enlarged φ_2= 45° and φ_2= 90° sections. The locations of the {100}-fiber, {110}-fiber and {111}-fiber are shown.
[Specimen plane perpendicular to (S)hort-Transverse axis]

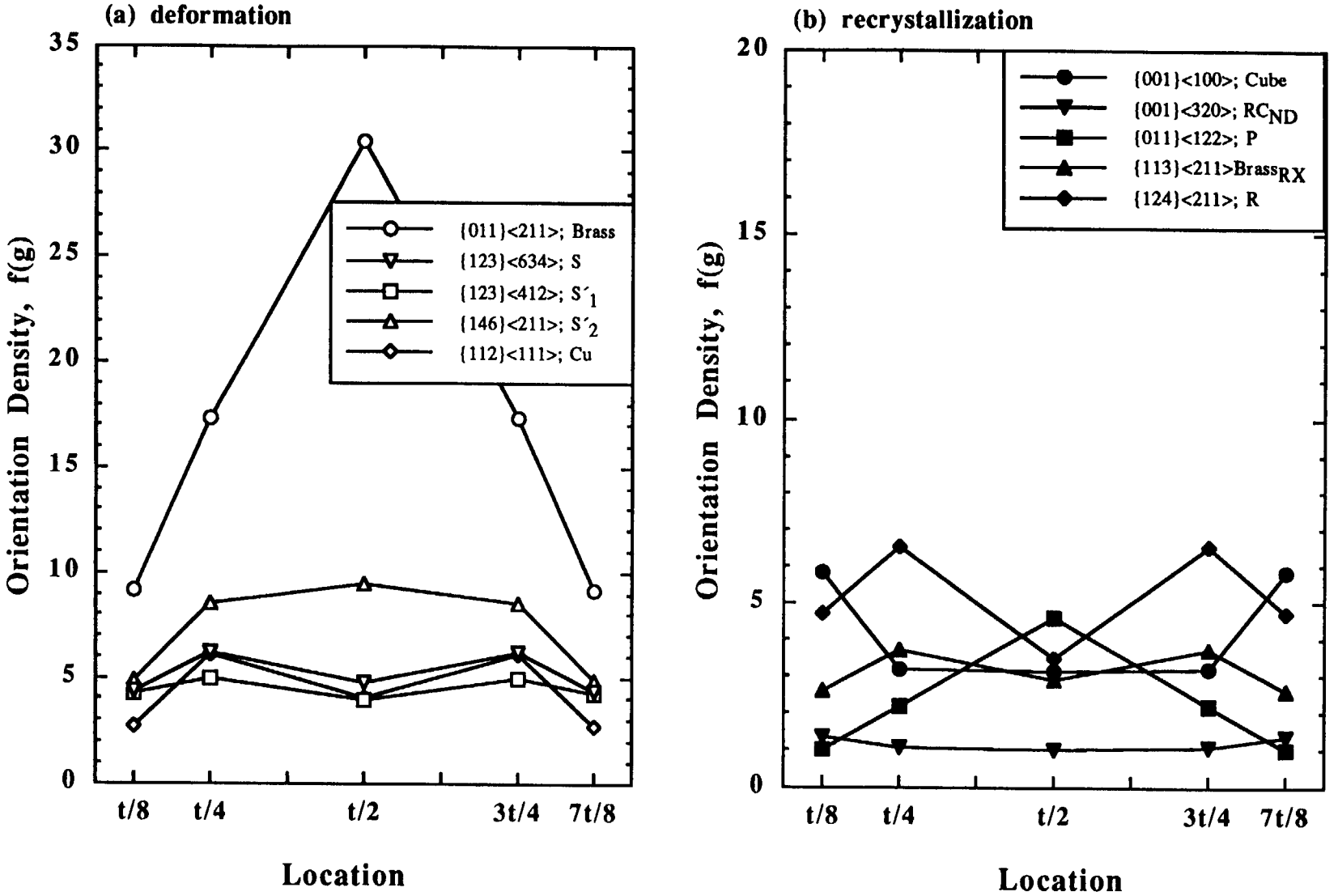

Figure 41. Orientation density, f(g), as a function of location through the cross-section for the 1460-T3 plate: (a) Deformation-related components; (b) Recrystallization-related components.

4.2 Alloy 2090

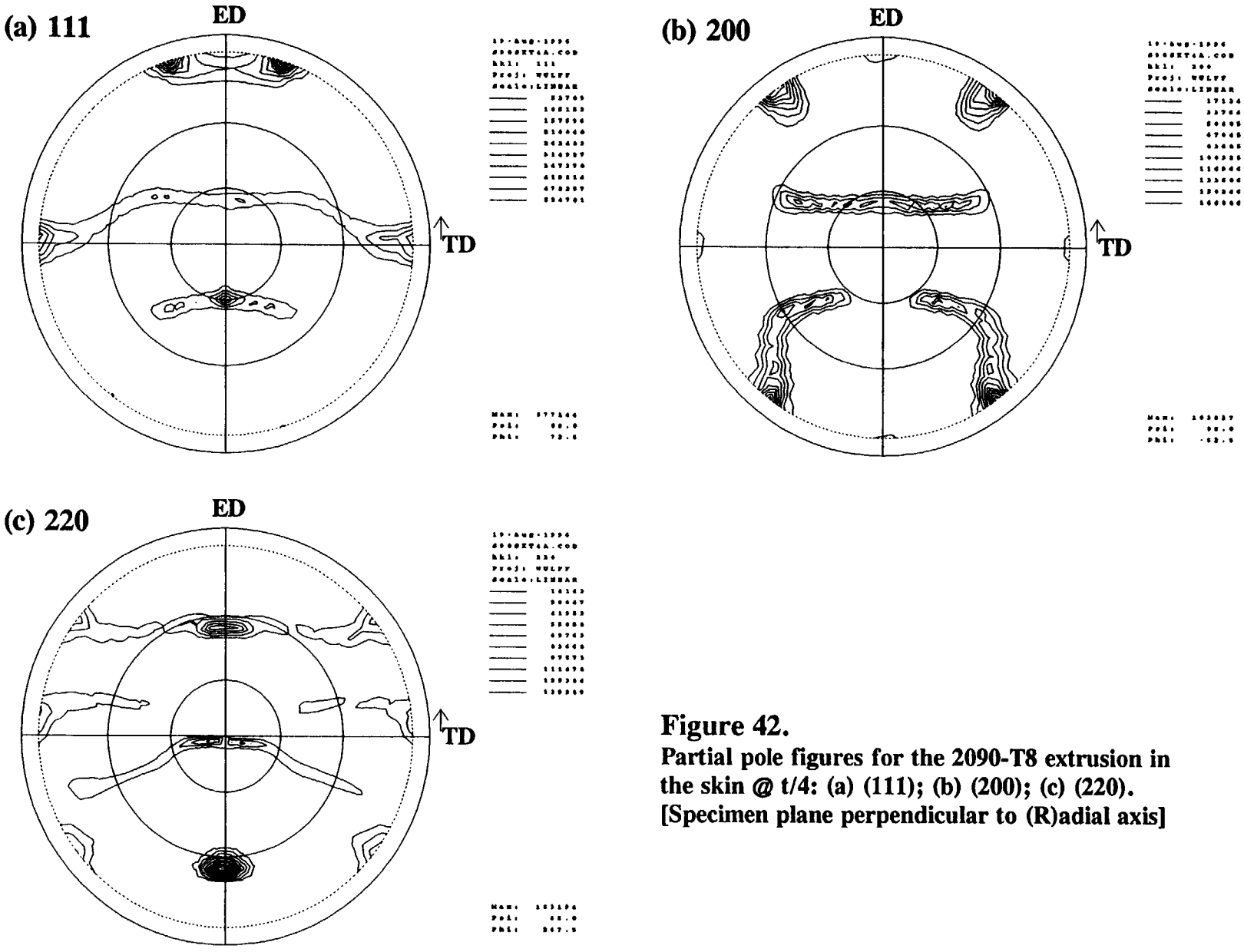

Figure 42.
Partial pole figures for the 2090-T8 extrusion in the skin @ t/4: (a) (111); (b) (200); (c) (220). [Specimen plane perpendicular to (R)adial axis]

(a) Sections: φ_2= 0 - 90°

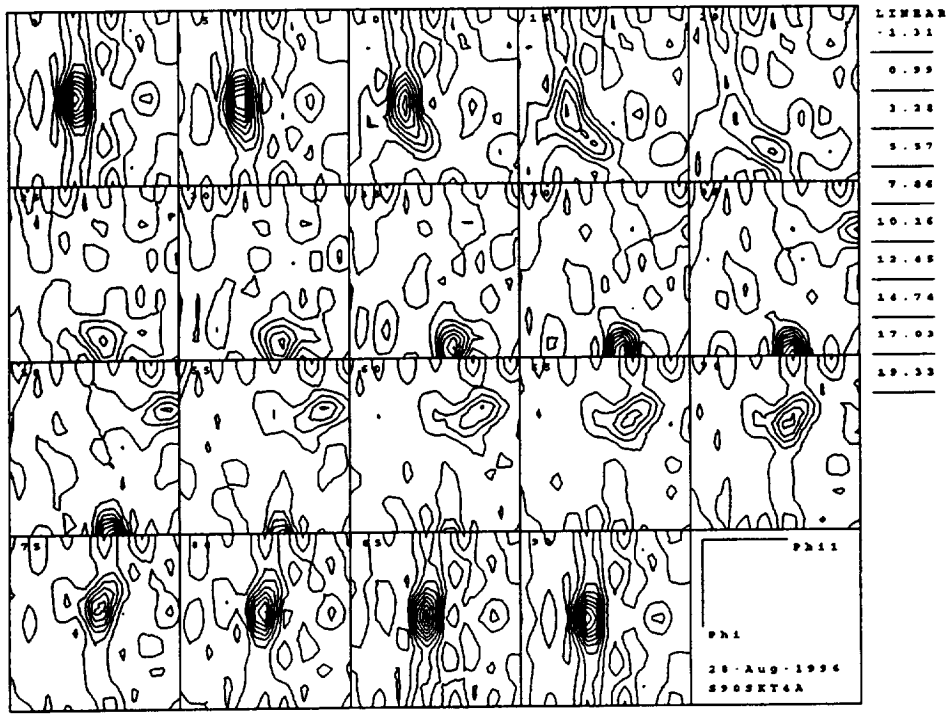

(b) Sections: φ_2= 45°; φ_2= 90°

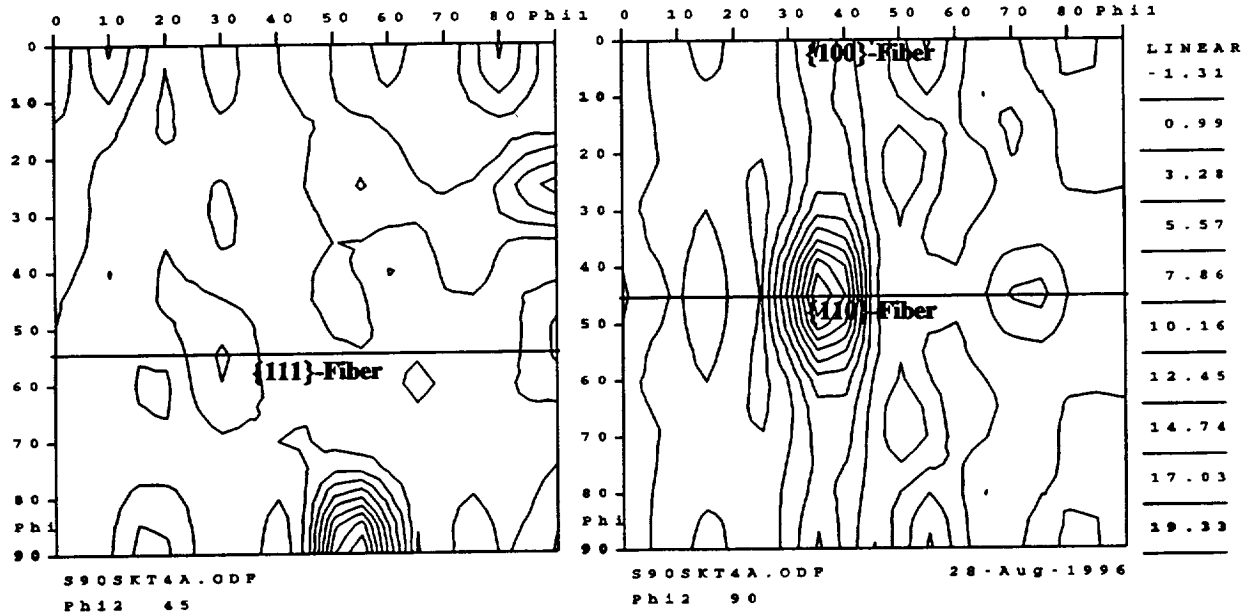

Figure 43. CODF sections for the 2090-T8 extrusion in the skin @ t/4; (a), Complete sections: φ_2= 0, 5, 10 ..... 90°; and (b), enlarged φ_2= 45° and φ_2= 90° sections. The locations of the {100}-fiber, {110}-fiber and {111}-fiber are shown.
[Specimen plane perpendicular to (R)adial axis]

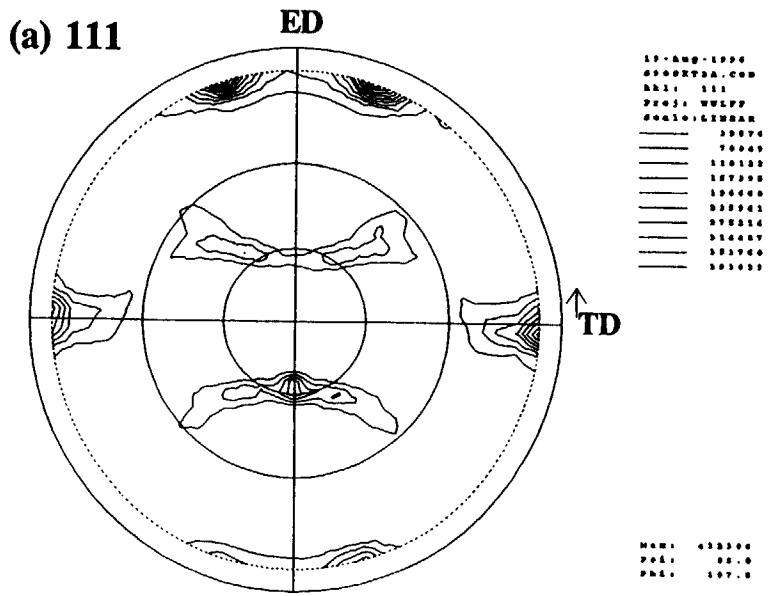

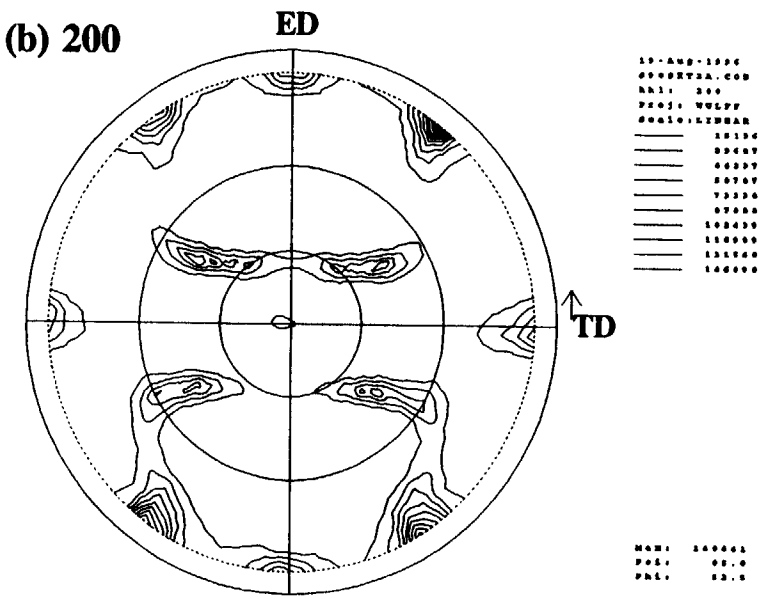

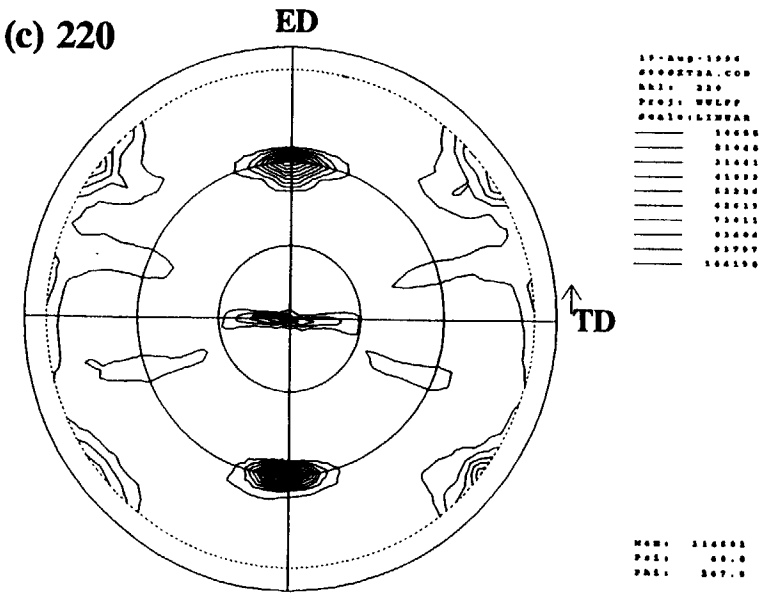

Figure 44.
Partial pole figures for the 2090-T8 extrusion in the skin @ t/2: (a) (111); (b) (200); (c) (220). [Specimen plane perpendicular to (R)adial axis]

(a) Sections: φ_2= 0 - 90°

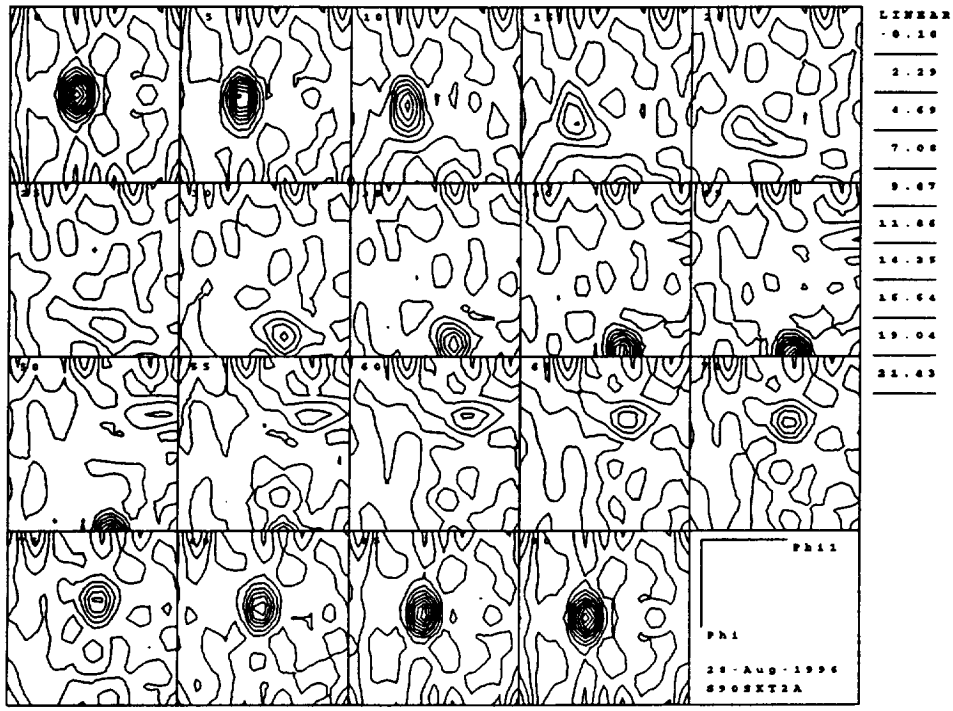

(b) Sections: φ_2= 45°; φ_2= 90°

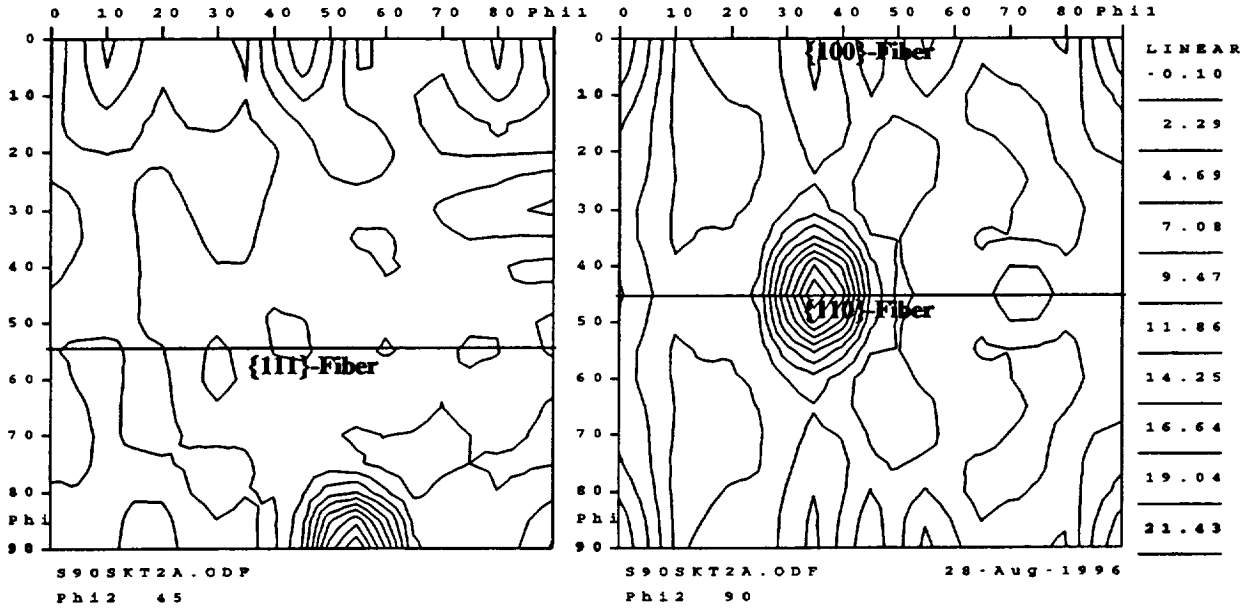

Figure 45. CODF sections for the 2090-T8 extrusion in the skin @ t/2; (a), Complete sections: φ_2= 0, 5, 10 ..... 90°; and (b), enlarged φ_2= 45° and φ_2= 90° sections. The locations of the {100}-fiber, {110}-fiber and {111}-fiber are shown.
[Specimen plane perpendicular to (R)adial axis]

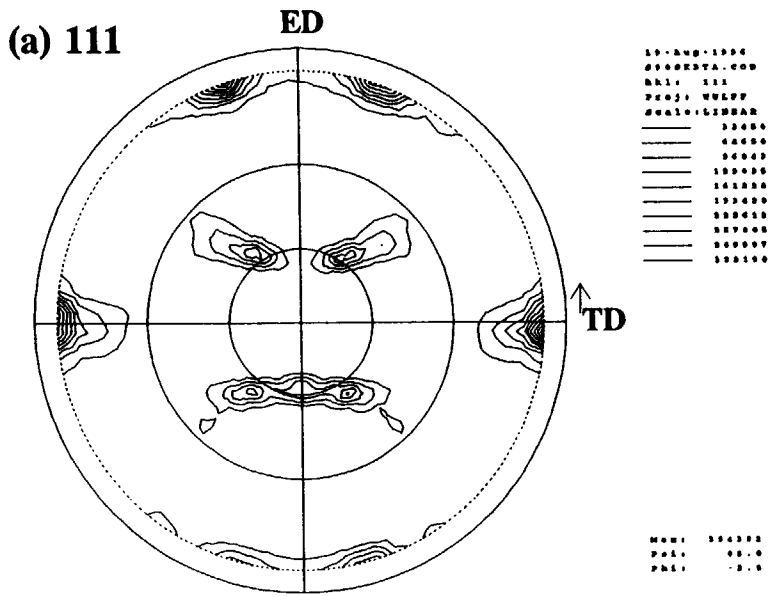

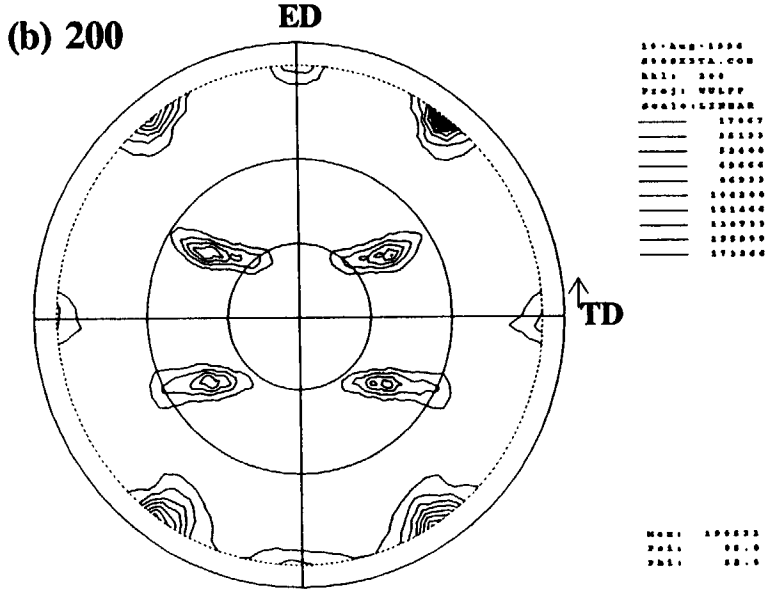

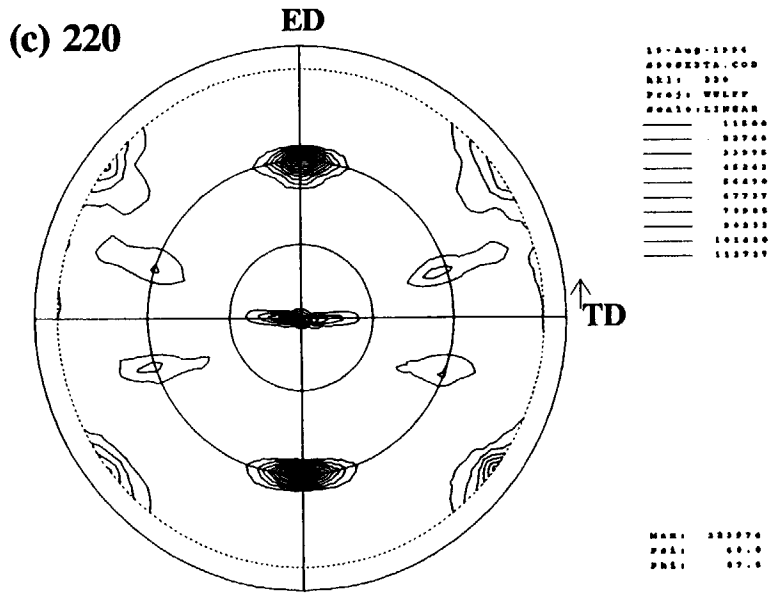

Figure 46.
Partial pole figures for the 2090-T8 extrusion in the skin @ 3t/4: (a) (111); (b) (200); (c) (220). [Specimen plane perpendicular to (R)adial axis]

(a) Sections: φ_2= 0 - 90°

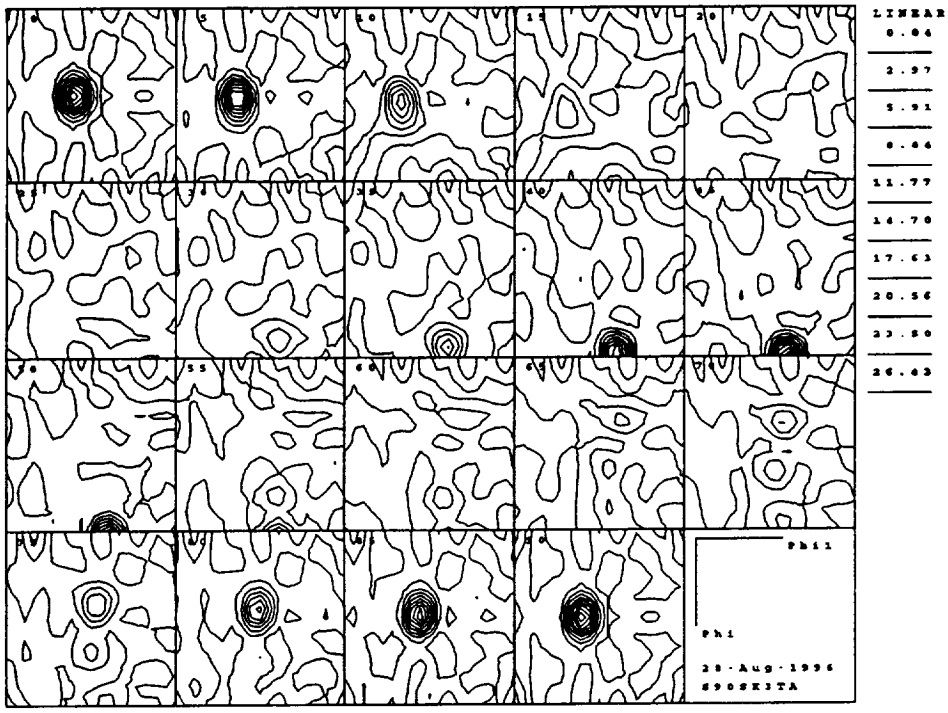

(b) Sections: φ_2= 45°; φ_2= 90°

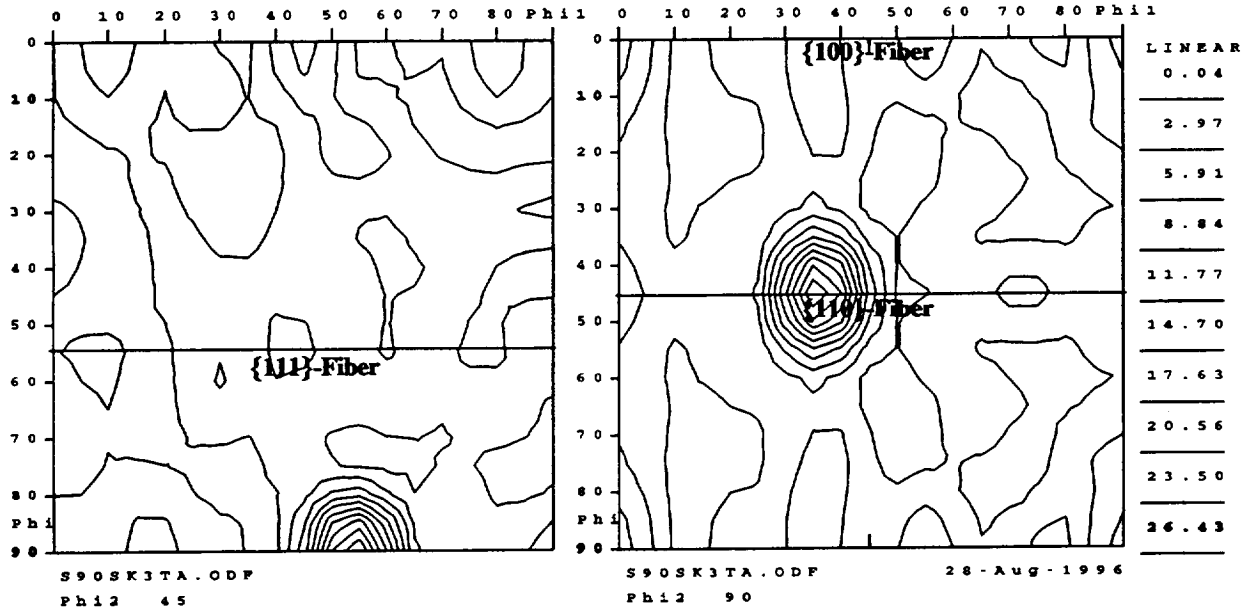

Figure 47. CODF sections for the 2090-T8 extrusion in the skin @ 3t/4; (a), Complete sections: φ_2= 0, 5, 10 ..... 90°; and (b), enlarged φ_2= 45° and φ_2= 90° sections. The locations of the {100}-fiber, {110}-fiber and {111}-fiber are shown.
[Specimen plane perpendicular to (R)adial axis]

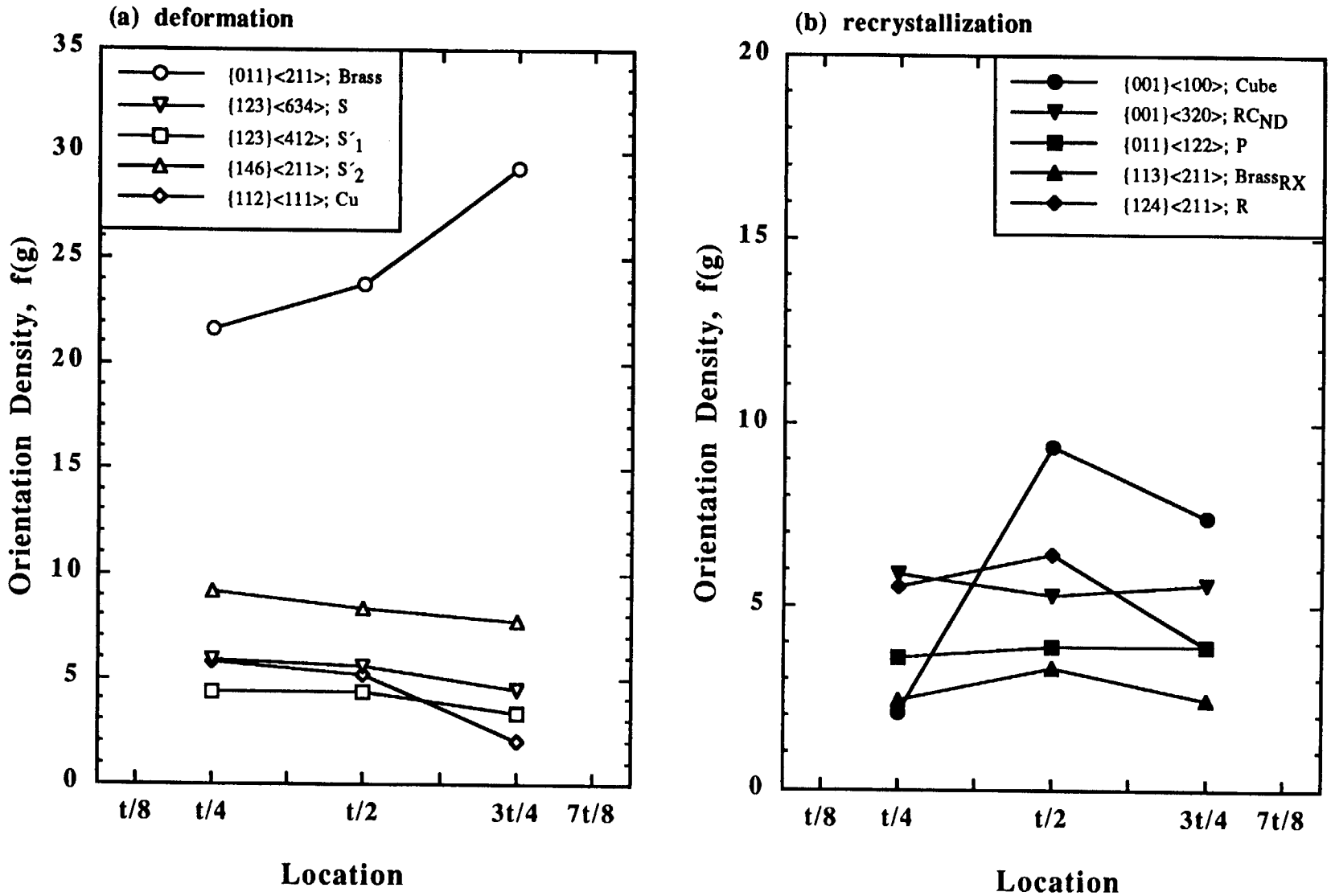

Figure 48. Orientation density, f(g), as a function of location through the cross-section for the 2090-T8 extrusion in the skin region: (a) Deformation-related components; (b) Recrystallization-related components.

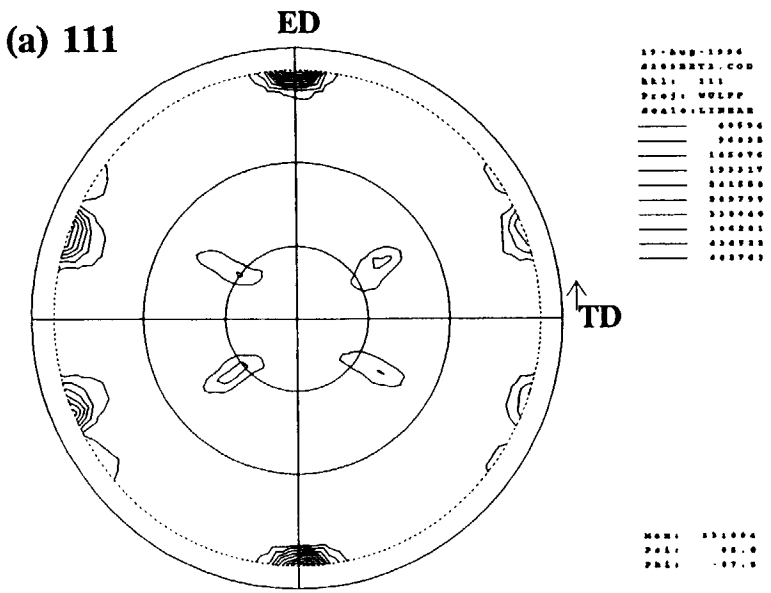

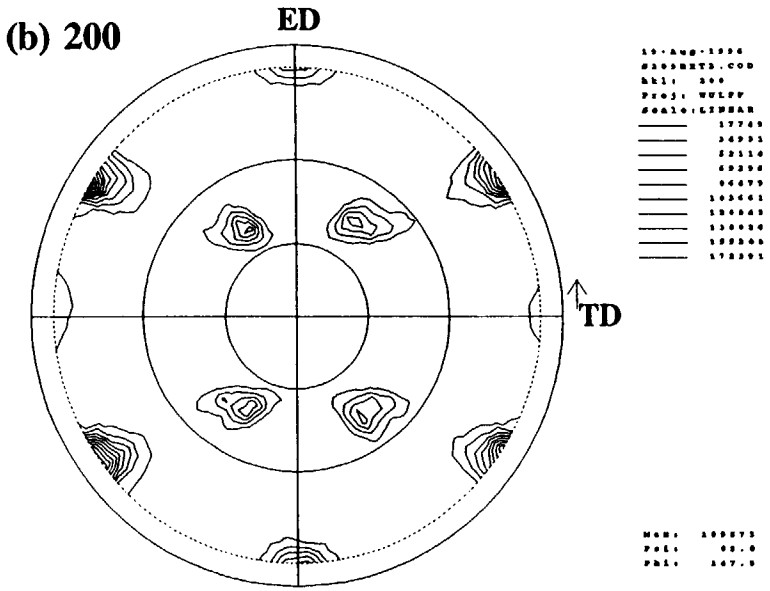

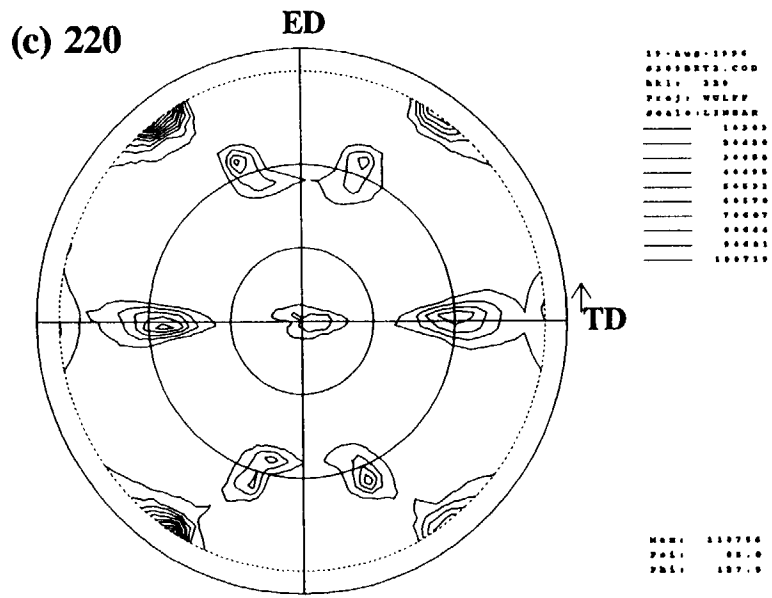

Figure 49.
Partial pole figures for the 2090-T8 extrusion in the base @ t/2: (a) (111); (b) (200); (c) (220). [Specimen plane perpendicular to (R)adial axis]

(a) Sections: φ_2= 0 - 90°

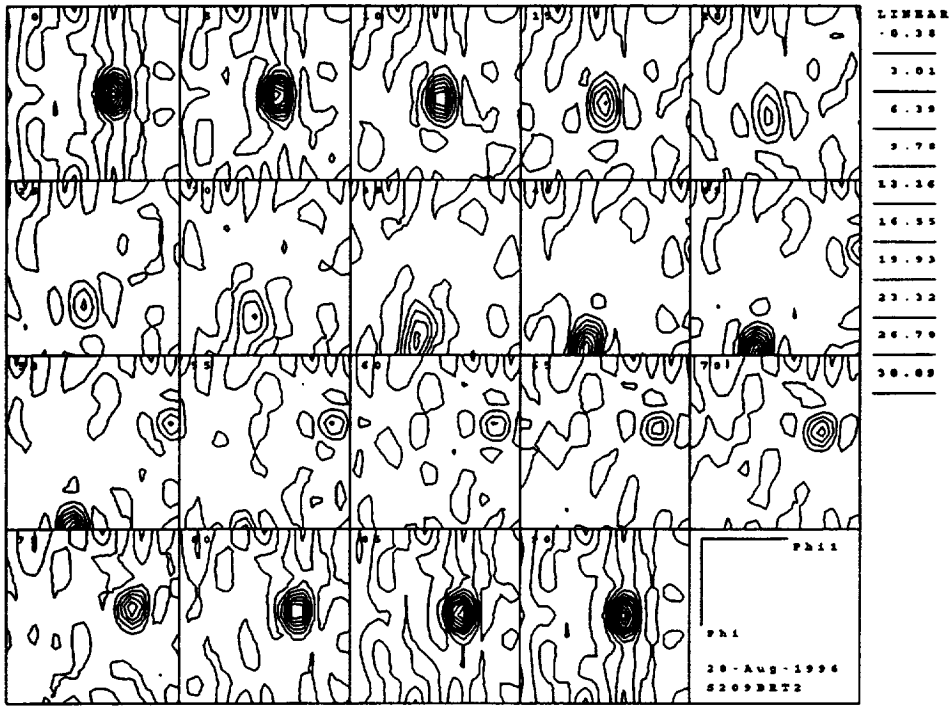

(b) Sections: φ_2= 45°; φ_2= 90°

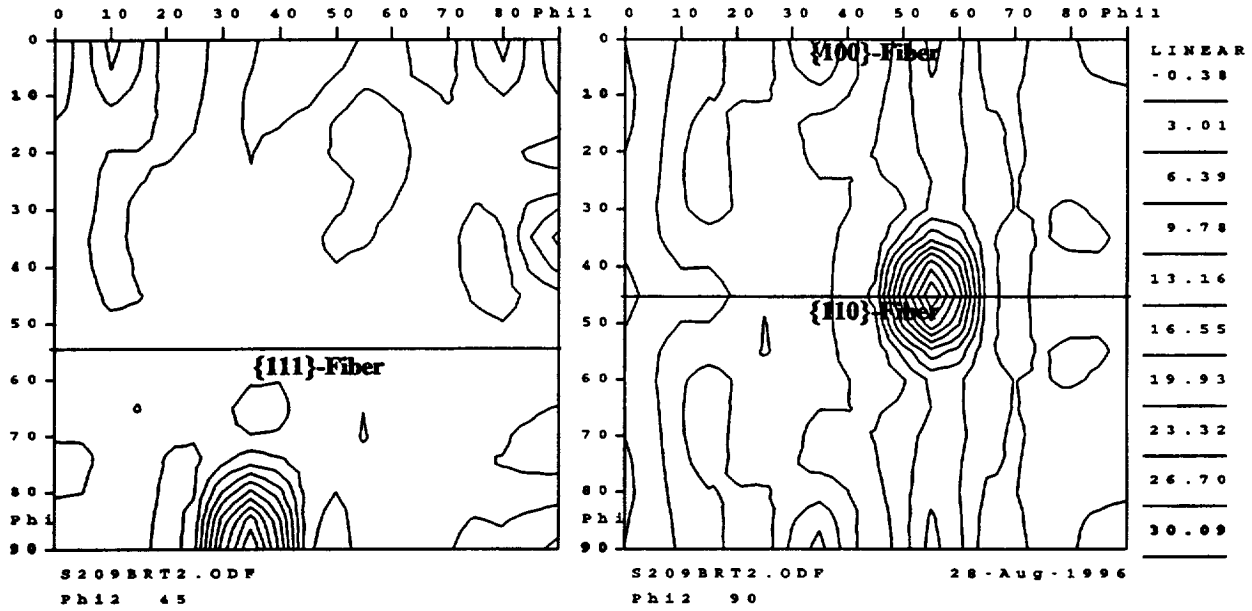

Figure 50. CODF sections for the 2090-T8 extrusion in the base @ t/2; (a), Complete sections: φ_2= 0, 5, 10 ..... 90°; and (b), enlarged φ_2= 45° and φ_2= 90° sections. The locations of the {100}-fiber, {110}-fiber and {111}-fiber are shown.
[Specimen plane perpendicular to (R)adial axis]

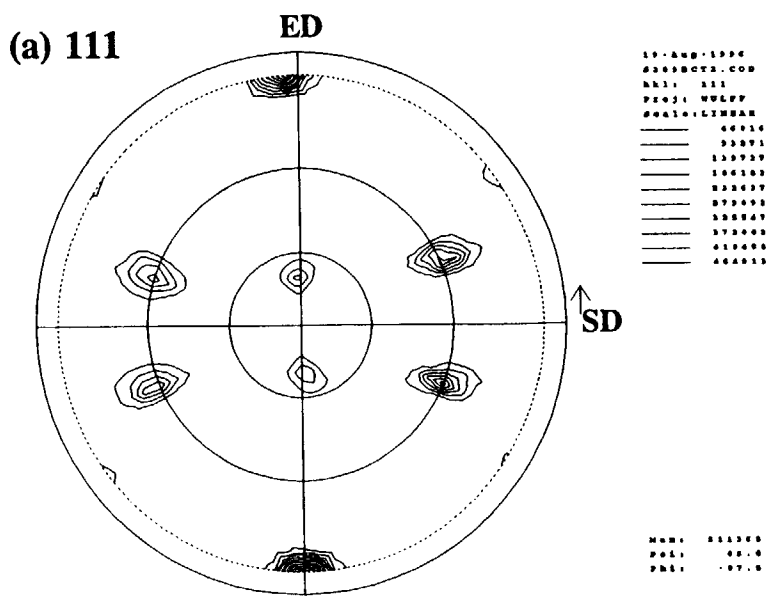

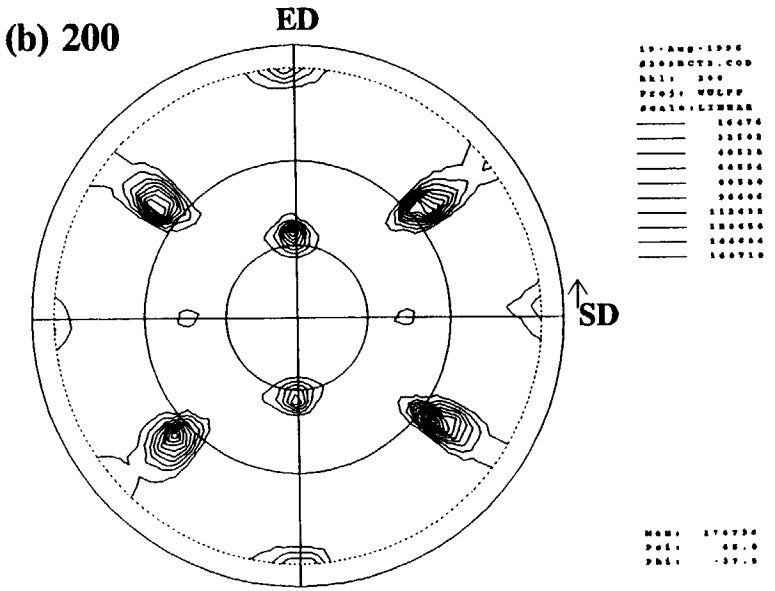

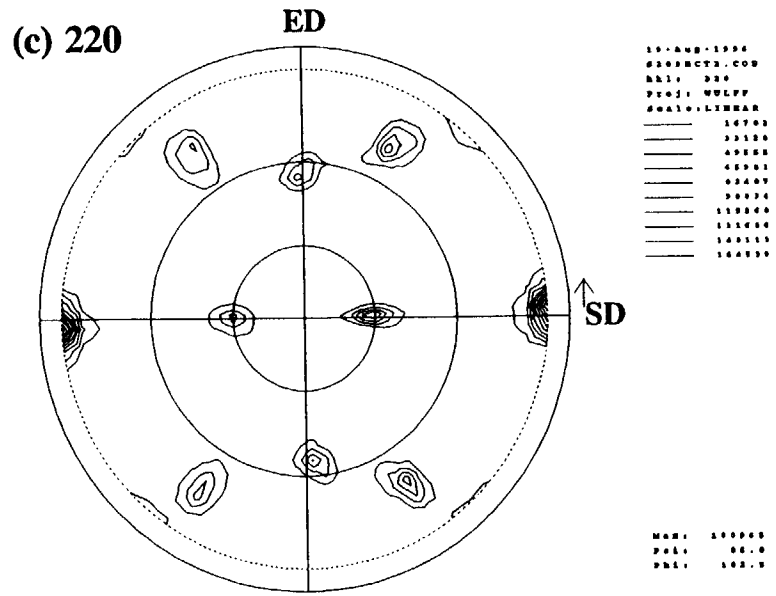

Figure 51.
Partial pole figures for the 2090-T8 extrusion in the base @ t/2: (a) (111); (b) (200); (c) (220). [Specimen plane perpendicular to (C)ircumferential axis]

(a) Sections: $\varphi_2 = 0 - 90°$

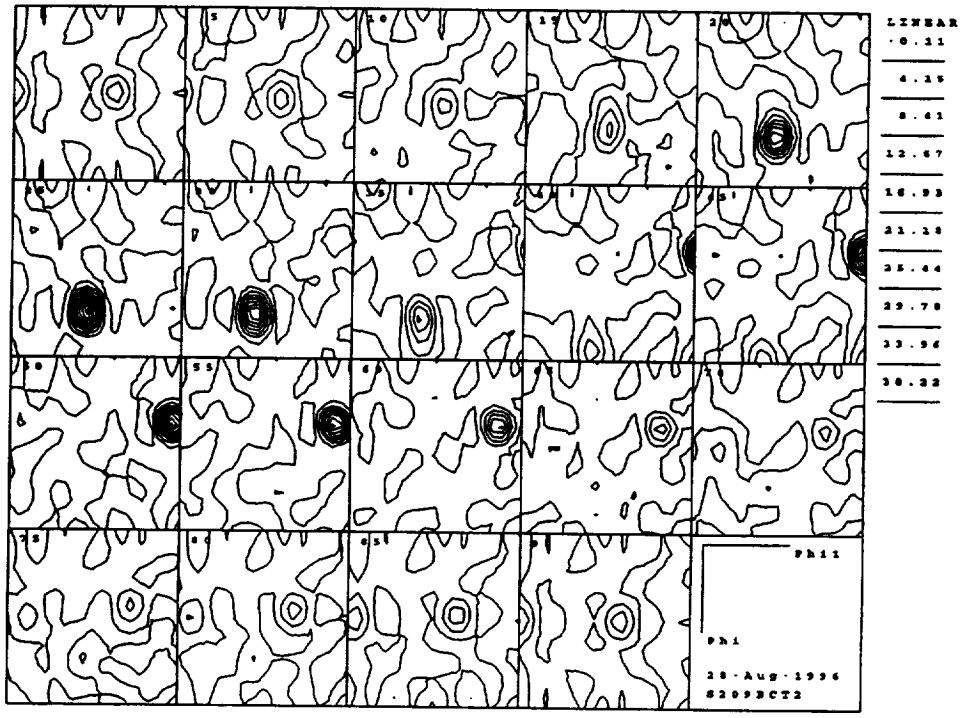

(b) Sections: $\varphi_2 = 45°$; $\varphi_2 = 90°$

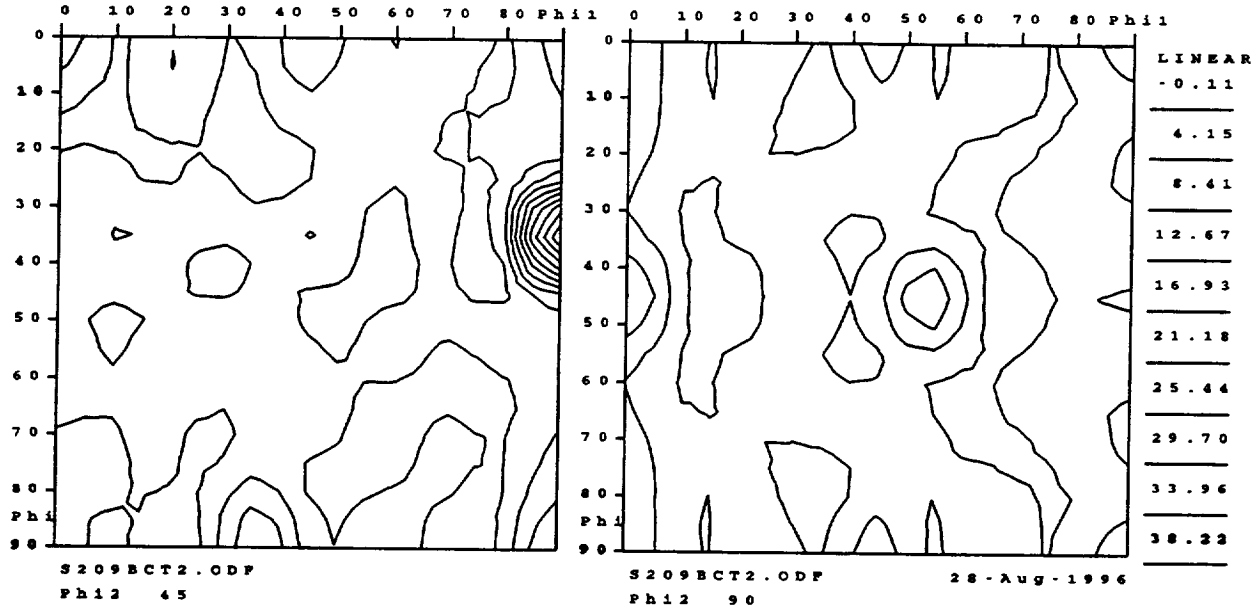

Figure 52. CODF sections for the 2090-T8 extrusion in the base @ t/2; (a), Complete sections: $\varphi_2 = 0, 5, 10 \ldots 90°$; and (b), enlarged $\varphi_2 = 45°$ and $\varphi_2 = 90°$ sections. [Specimen plane perpendicular to (C)ircumferential axis]

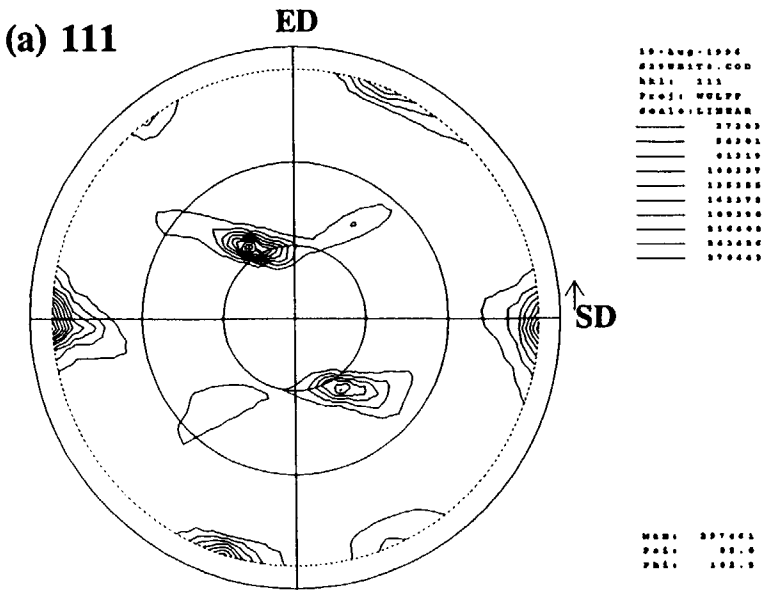

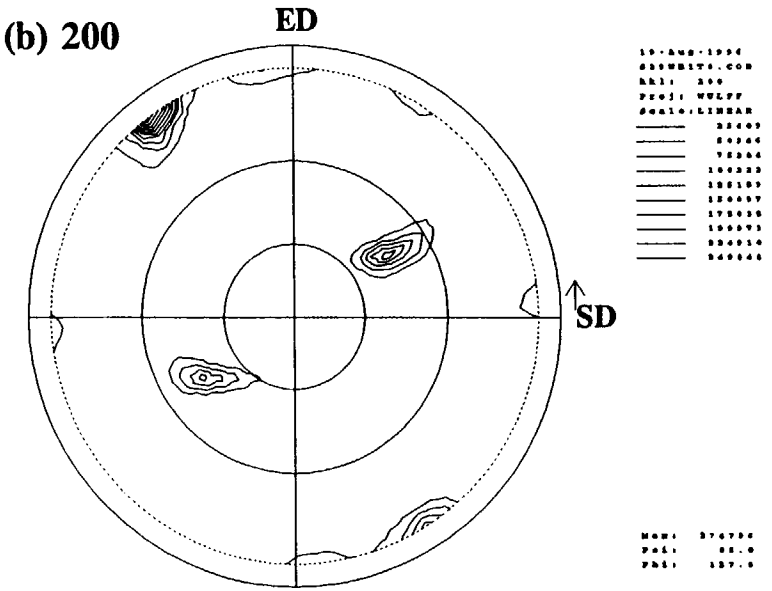

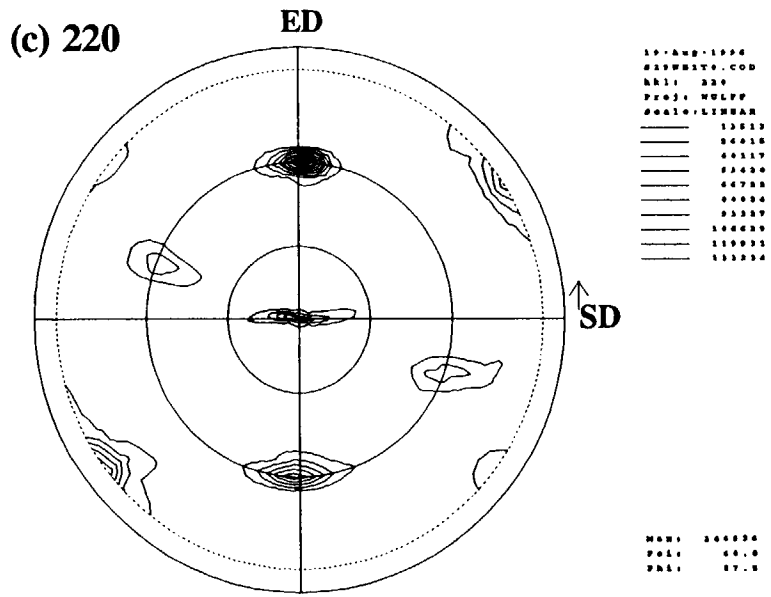

Figure 53.
Partial pole figures for the 2090-T8 extrusion in the web @ t/8: (a) (111); (b) (200); (c) (220). [Specimen plane perpendicular to (C)ircumferential axis]

(a) Sections: $\varphi_2 = 0 - 90°$

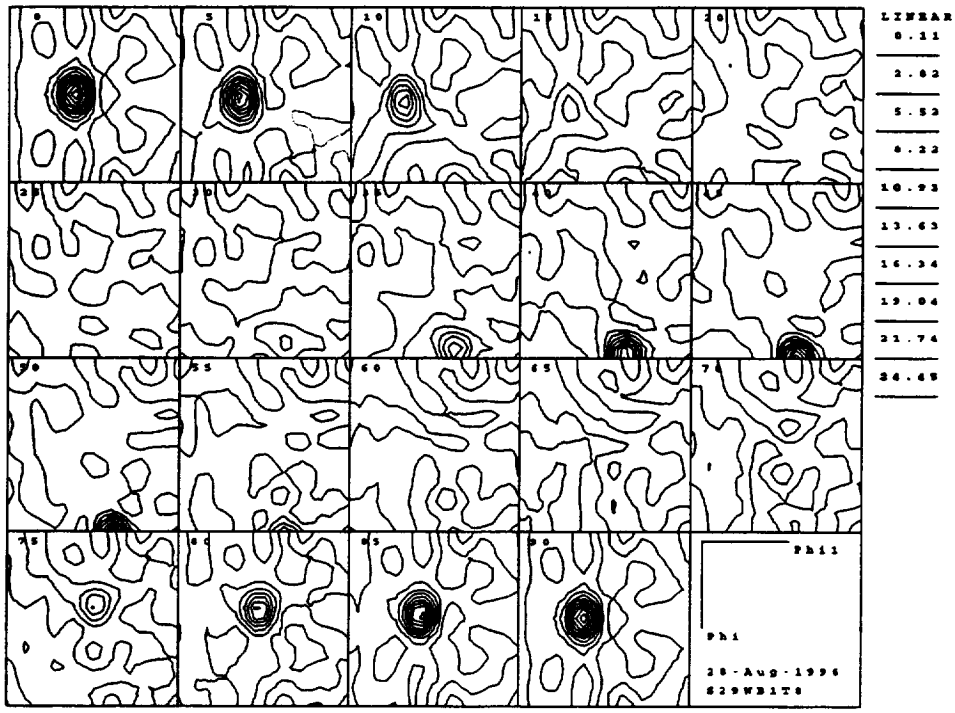

(b) Sections: $\varphi_2 = 45°$; $\varphi_2 = 90°$

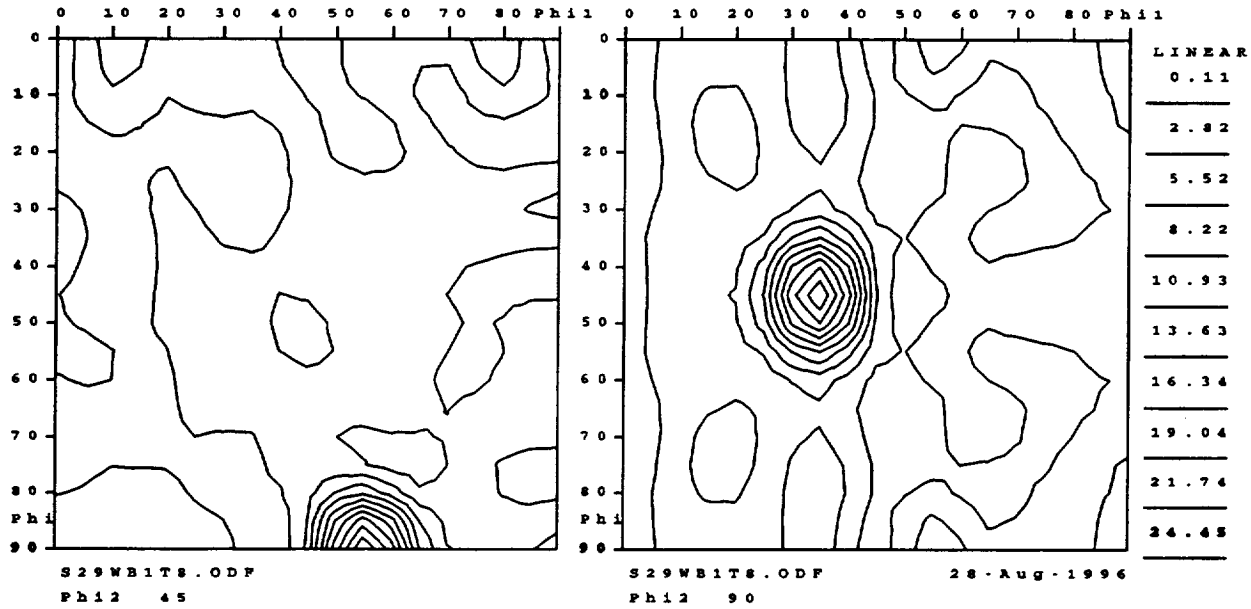

Figure 54. CODF sections for the 2090-T8 extrusion in the web @ t/8; (a), Complete sections: $\varphi_2 = 0, 5, 10 \ldots\ldots 90°$; and (b), enlarged $\varphi_2 = 45°$ and $\varphi_2 = 90°$ sections. [Specimen plane perpendicular to (C)ircumferential axis]

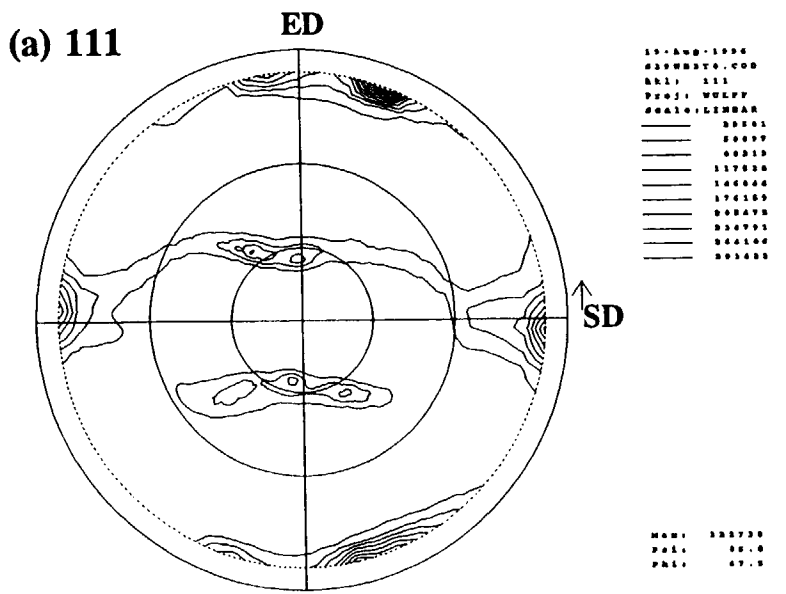

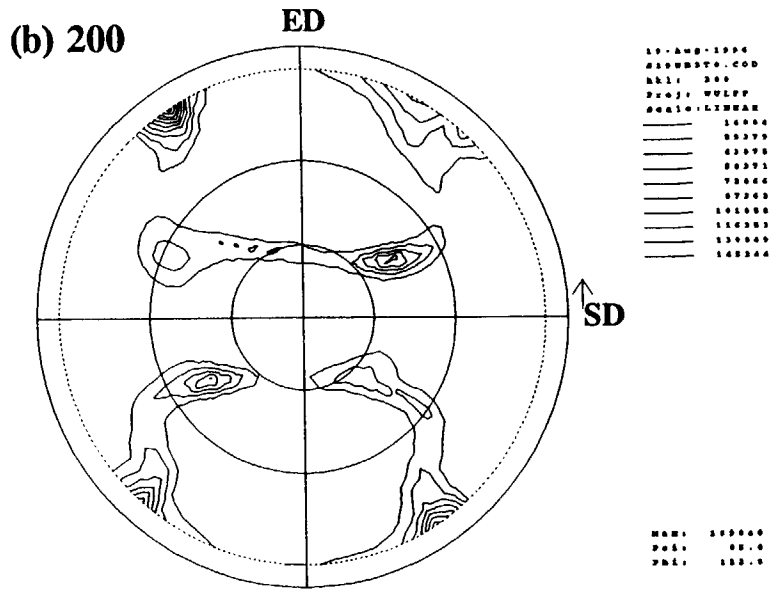

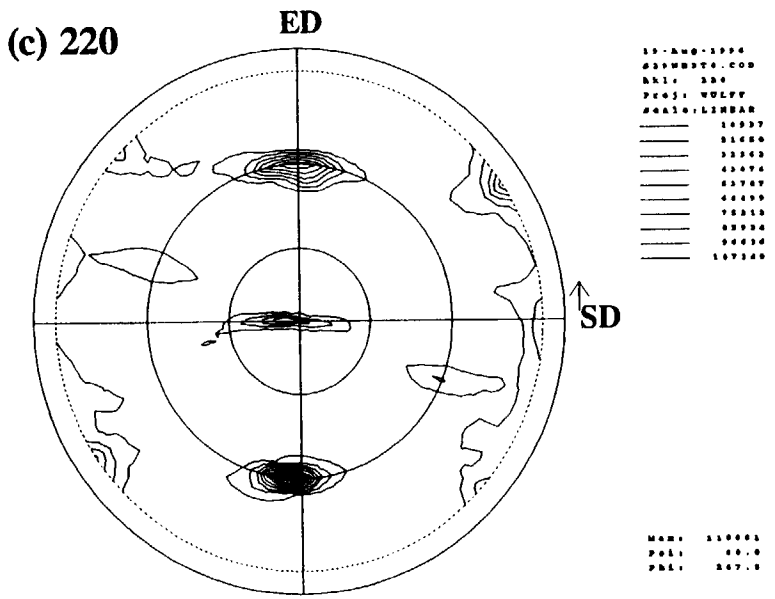

Figure 55.
Partial pole figures for the 2090-T8 extrusion in the web @ 3t/8: (a) (111); (b) (200); (c) (220). [Specimen plane perpendicular to (C)ircumferential axis]

(a) Sections: φ_2= 0 - 90°

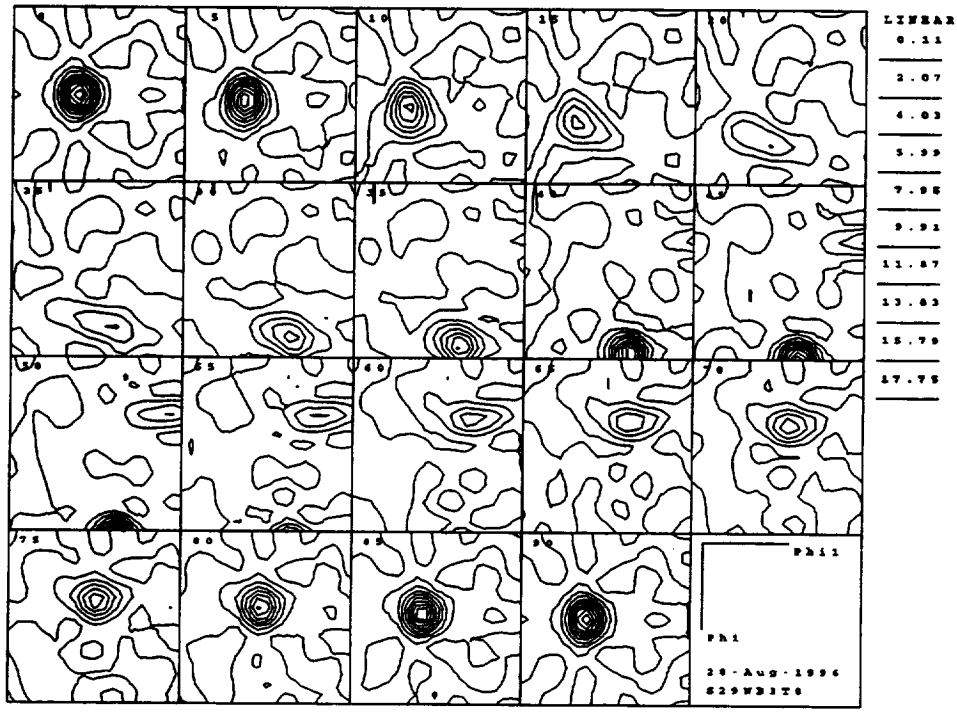

(b) Sections: φ_2= 45°; φ_2= 90°

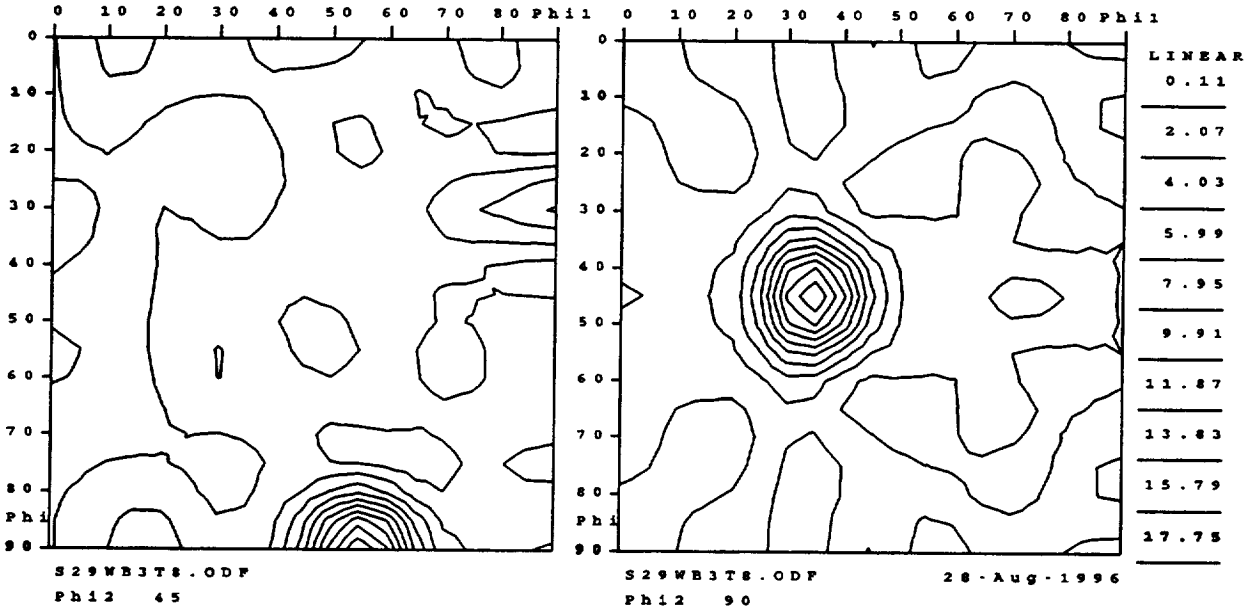

Figure 56. CODF sections for the 2090-T8 extrusion in the web @ 3t/8; (a), Complete sections: φ_2= 0, 5, 10 ..... 90°; and (b), enlarged φ_2= 45° and φ_2= 90° sections. [Specimen plane perpendicular to (C)ircumferential axis]

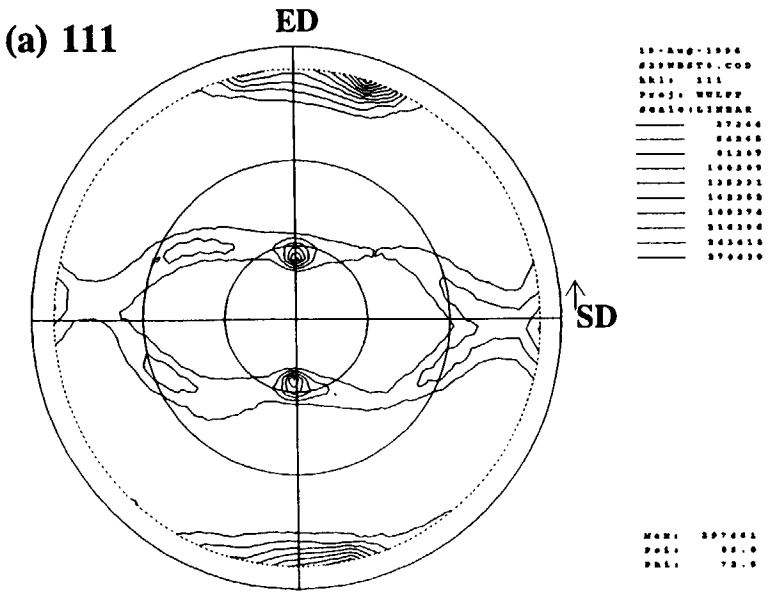

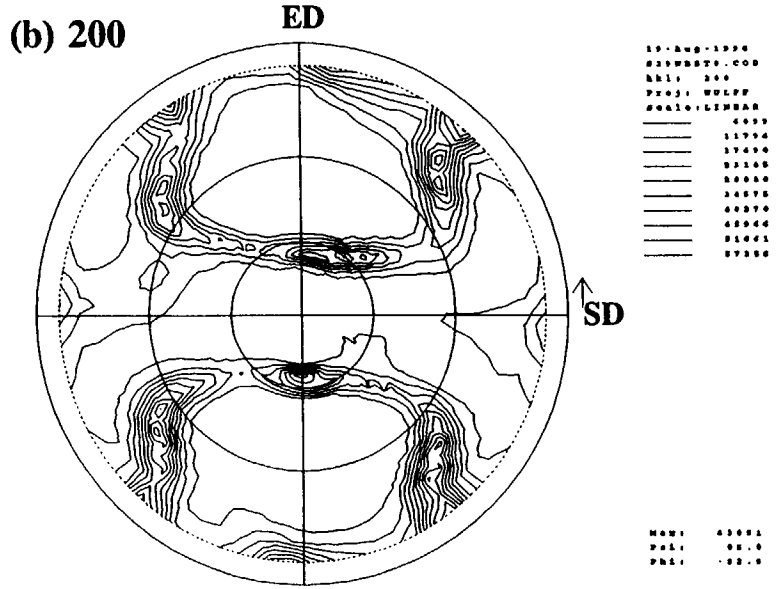

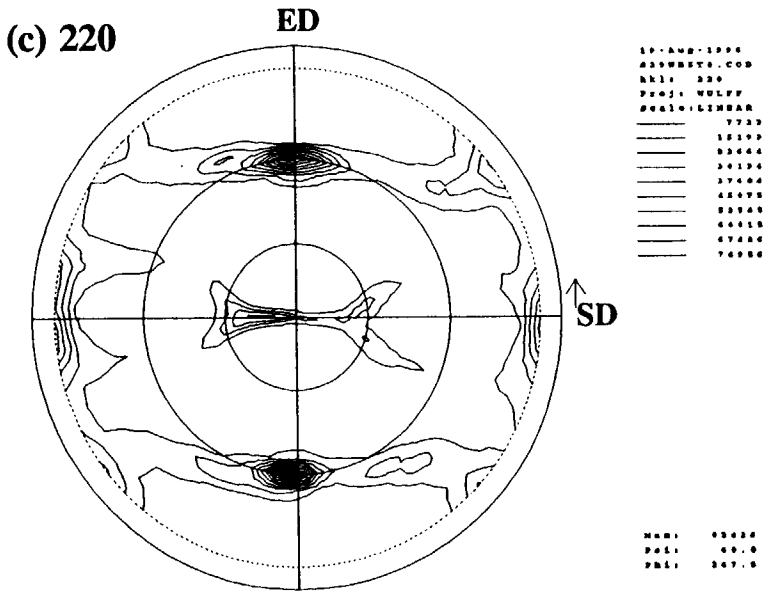

Figure 57.
Partial pole figures for the 2090-T8 extrusion in the web @ 5t/8: (a) (111); (b) (200); (c) (220). [Specimen plane perpendicular to (C)ircumferential axis]

(a) Sections: φ_2= 0 - 90°

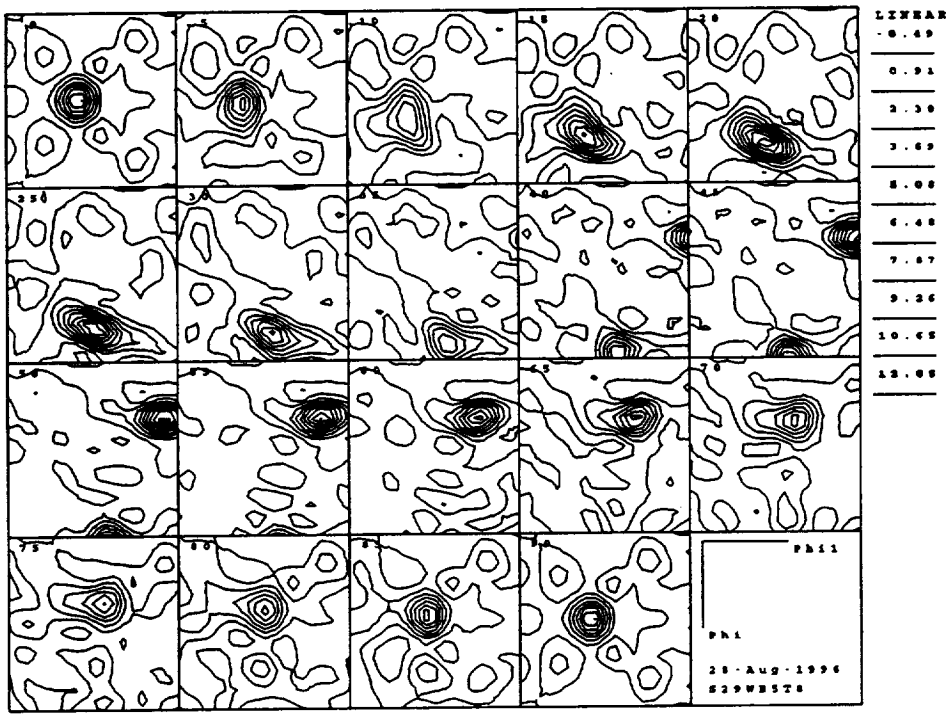

(b) Sections: φ_2= 45°; φ_2= 90°

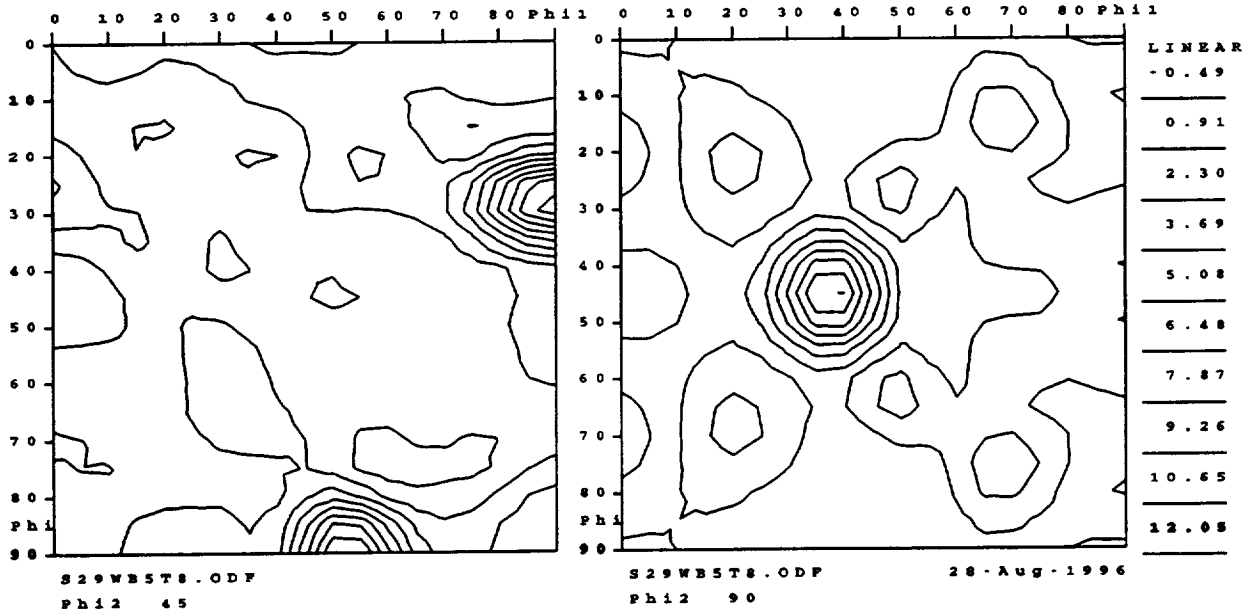

Figure 58. CODF sections for the 2090-T8 extrusion in the web @ 5t/8; (a), Complete sections: φ_2= 0, 5, 10 ..... 90°; and (b), enlarged φ_2= 45° and φ_2= 90° sections. [Specimen plane perpendicular to (C)ircumferential axis]

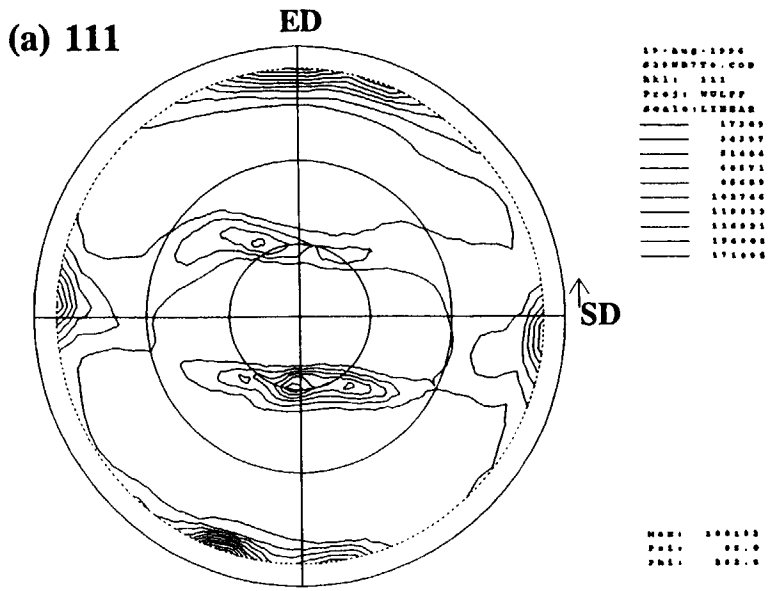

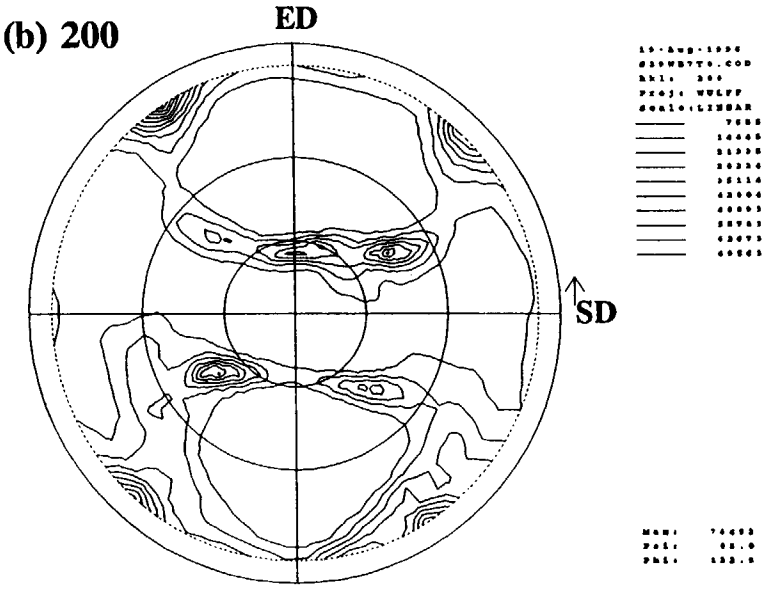

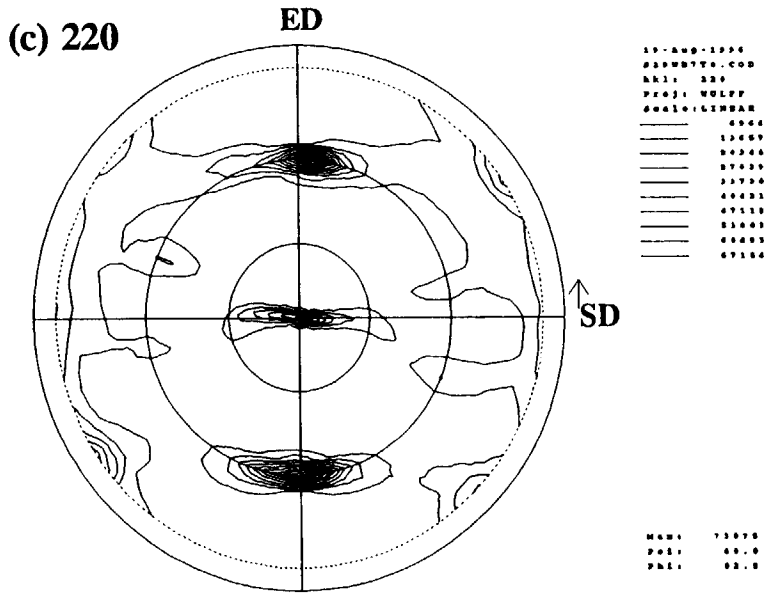

Figure 59.
Partial pole figures for the 2090-T8 extrusion in the web @ 7t/8: (a) (111); (b) (200); (c) (220). [Specimen plane perpendicular to (C)ircumferential axis]

(a) Sections: $\varphi_2 = 0 - 90°$

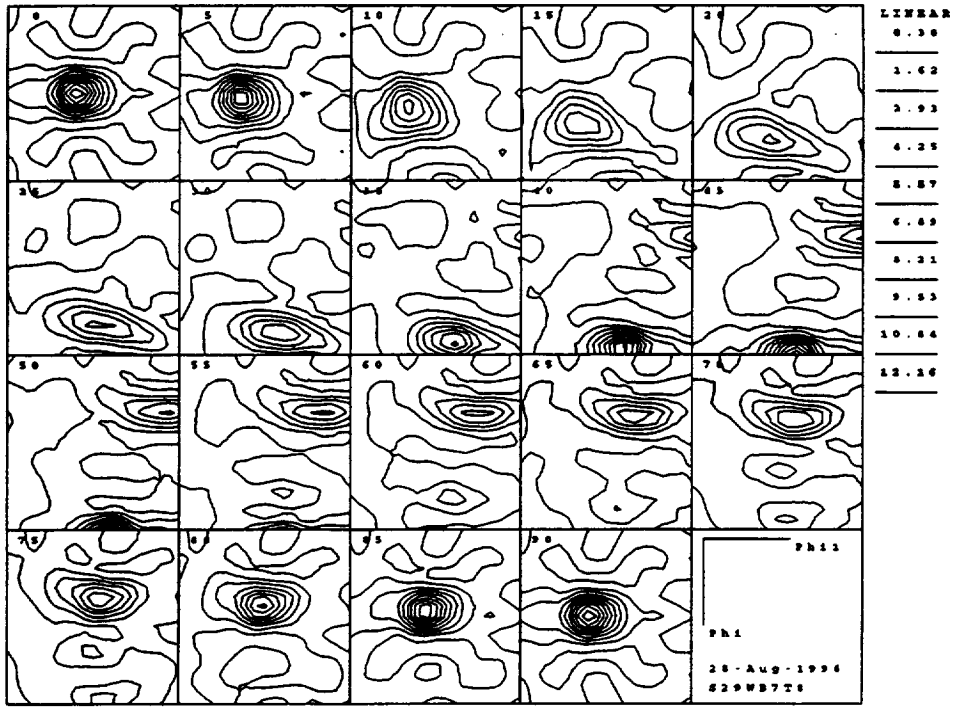

(b) Sections: $\varphi_2 = 45°$; $\varphi_2 = 90°$

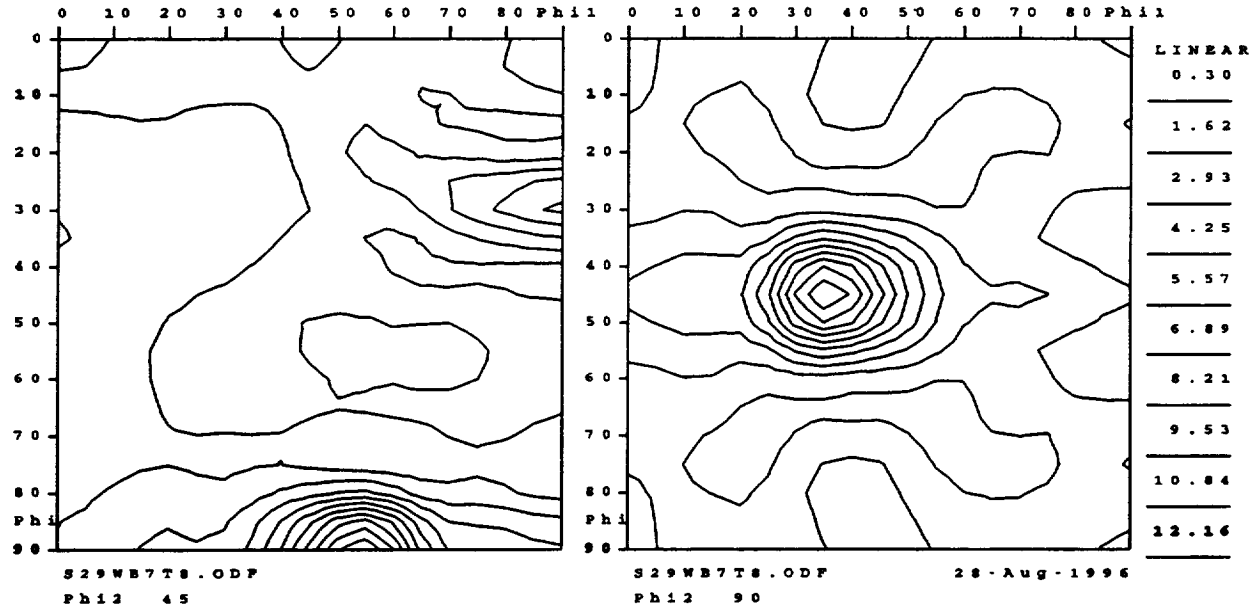

Figure 60. CODF sections for the 2090-T8 extrusion in the web @ 7t/8; (a), Complete sections: $\varphi_2 = 0, 5, 10 \ldots 90°$; and (b), enlarged $\varphi_2 = 45°$ and $\varphi_2 = 90°$ sections. [Specimen plane perpendicular to (C)ircumferential axis]

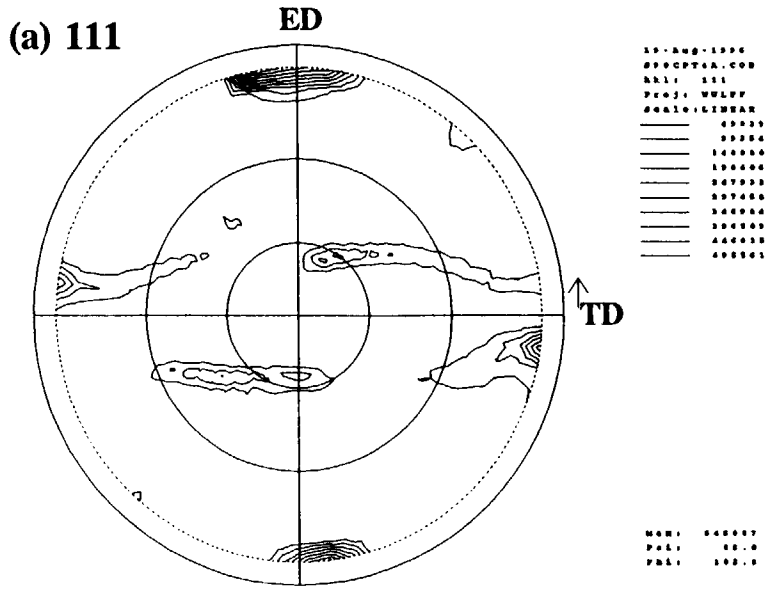

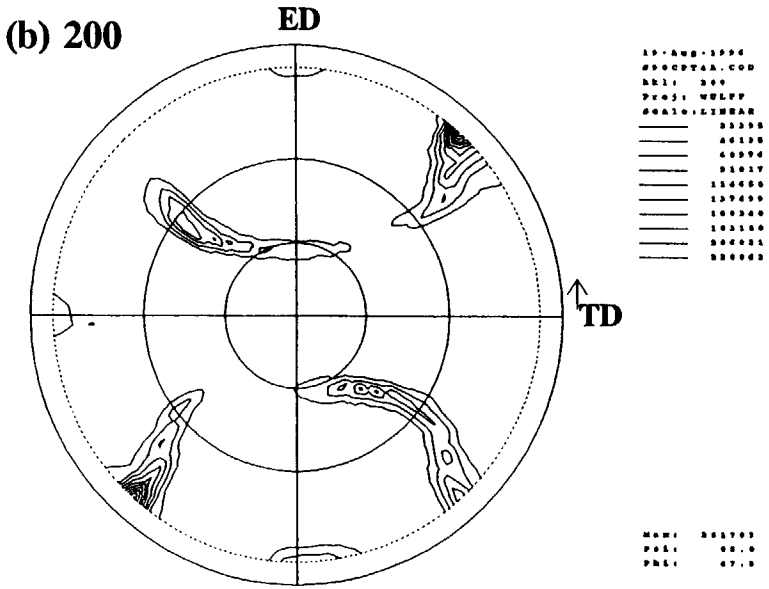

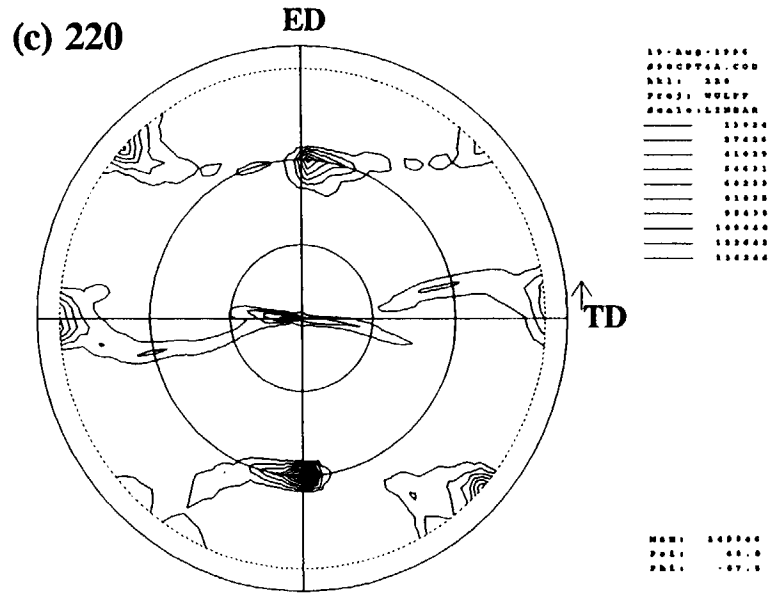

Figure 61.
Partial pole figures for the 2090-T8 extrusion in the cap @ t/4: (a) (111); (b) (200); (c) (220). [Specimen plane perpendicular to (R)adial axis]

(a) Sections: $\varphi_2 = 0 - 90°$

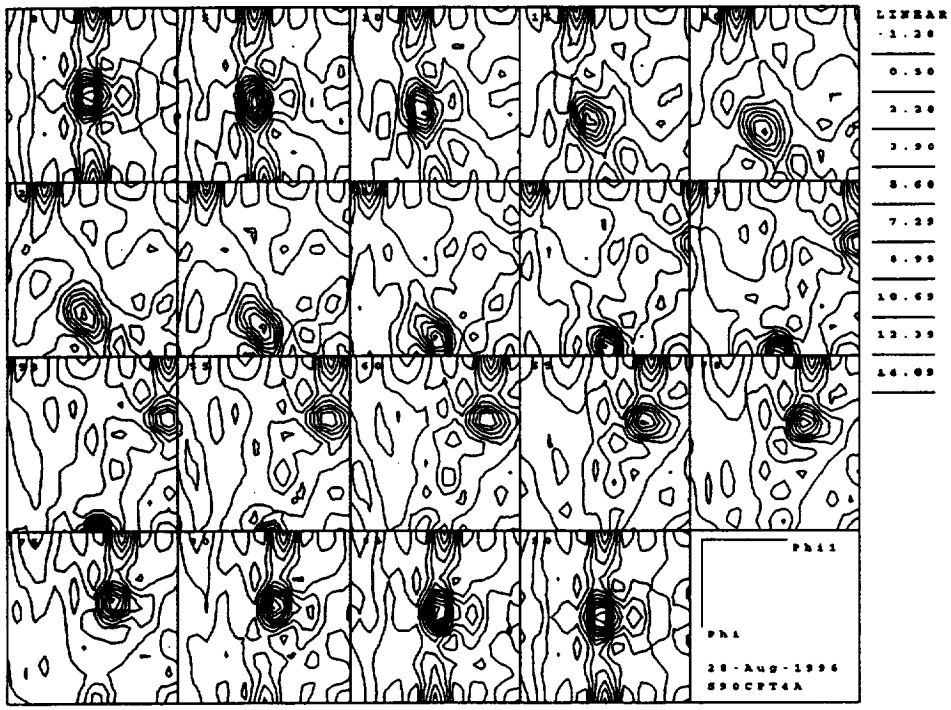

(b) Sections: $\varphi_2 = 45°$; $\varphi_2 = 90°$

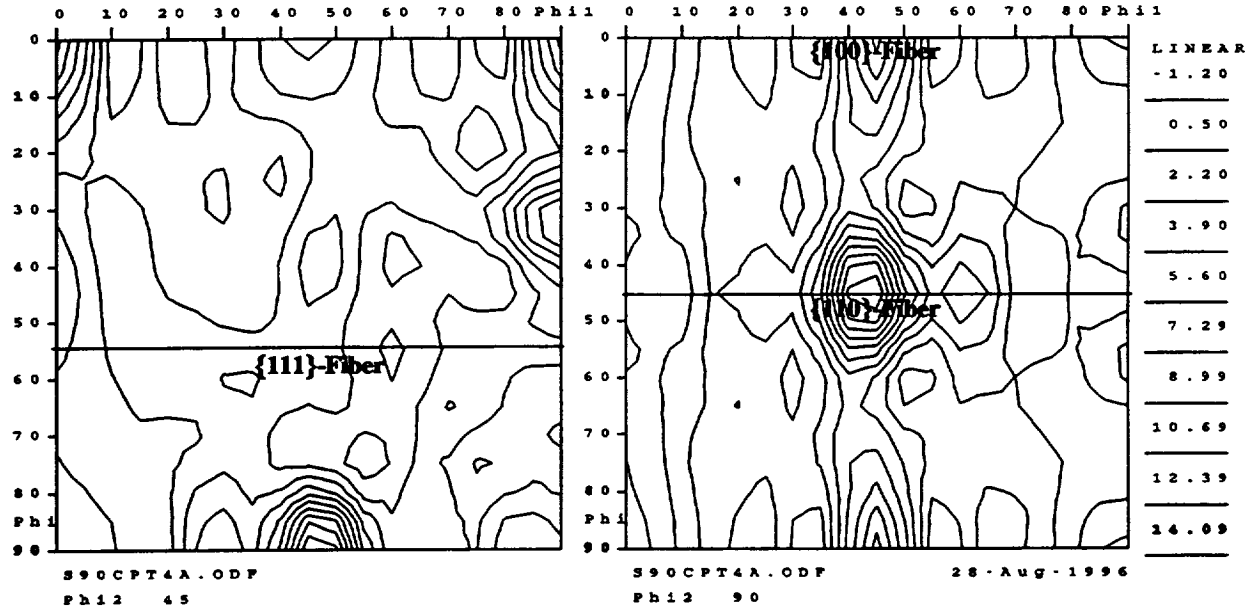

Figure 62. CODF sections for the 2090-T8 extrusion in the cap @ t/4; (a), Complete sections: $\varphi_2 = 0, 5, 10 \ldots\ldots 90°$; and (b), enlarged $\varphi_2 = 45°$ and $\varphi_2 = 90°$ sections. The locations of the {100}-fiber, {110}-fiber and {111}-fiber are shown.
[Specimen plane perpendicular to (R)adial axis]

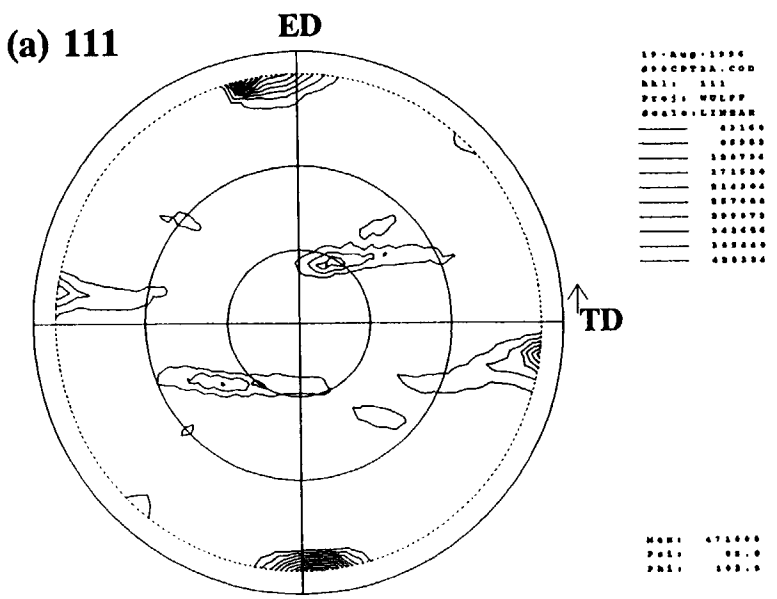

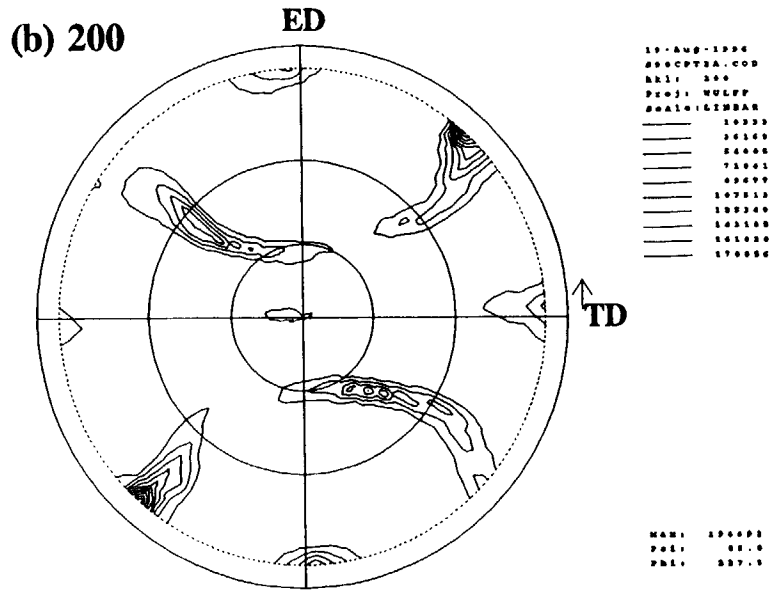

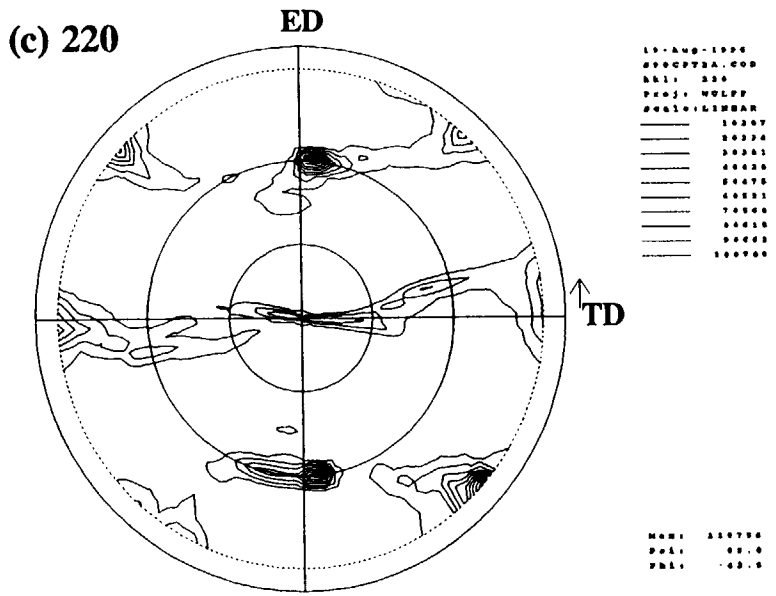

Figure 63.
Partial pole figures for the 2090-T8 extrusion in the cap @ t/2: (a) (111); (b) (200); (c) (220). [Specimen plane perpendicular to (R)adial axis]

(a) Sections: φ_2= 0 - 90°

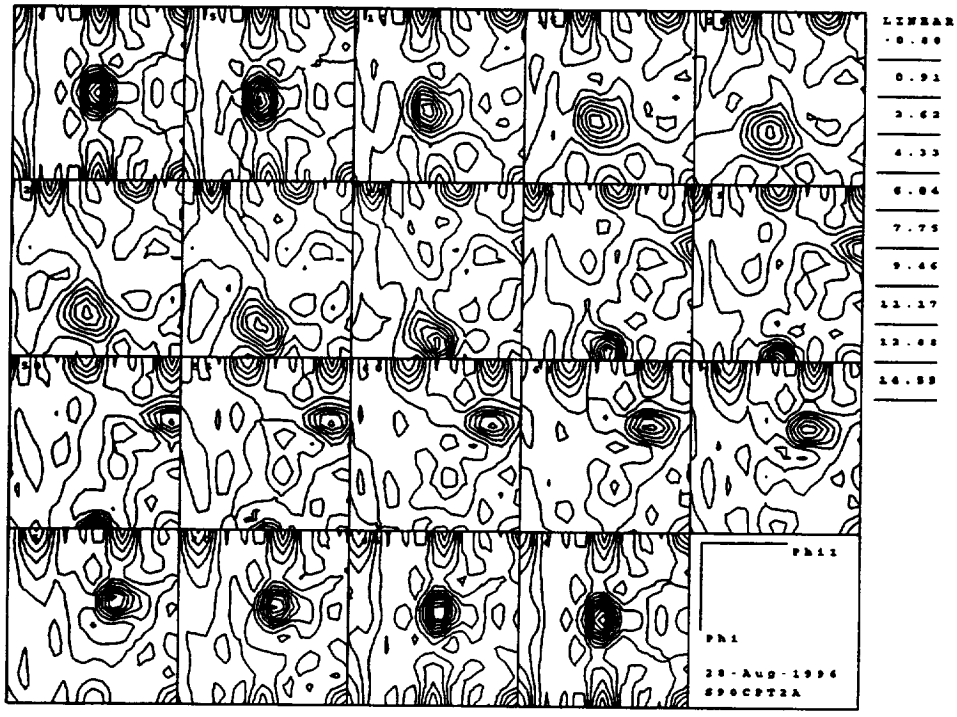

(b) Sections: φ_2= 45°; φ_2= 90°

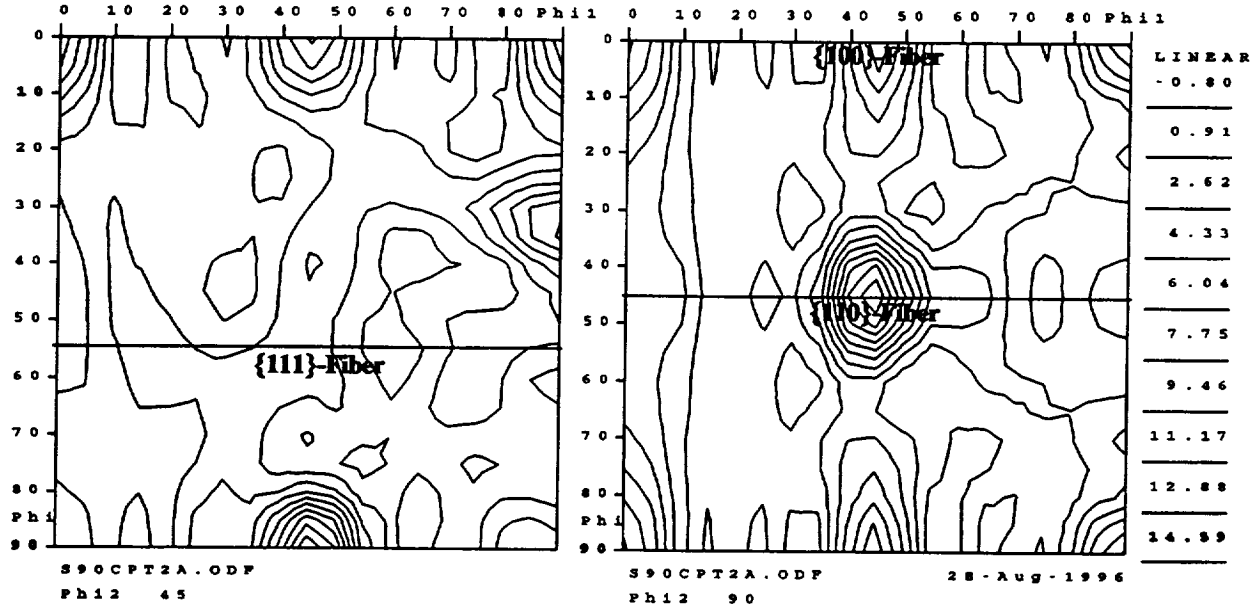

Figure 64. CODF sections for the 2090-T8 extrusion in the cap @ t/2; (a), Complete sections: φ_2= 0, 5, 10 ..... 90°; and (b), enlarged φ_2= 45° and φ_2= 90° sections. The locations of the {100}-fiber, {110}-fiber and {111}-fiber are shown.
[Specimen plane perpendicular to (R)adial axis]

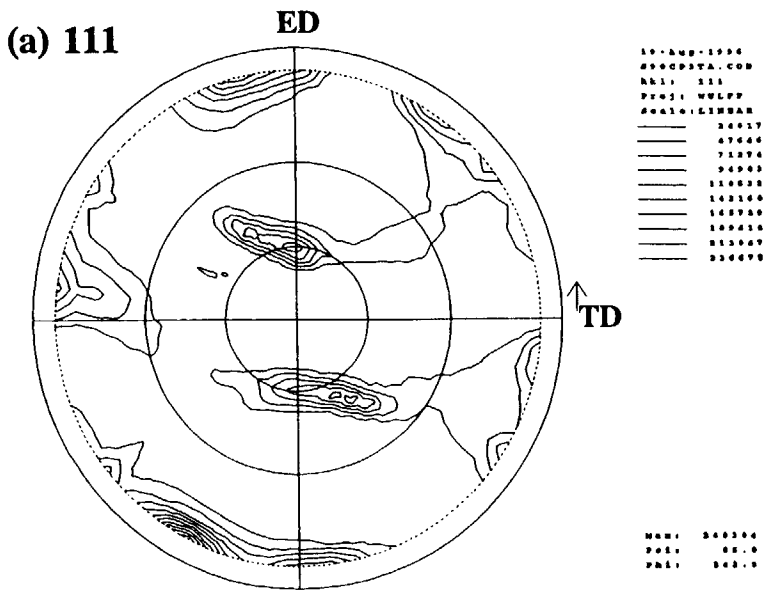

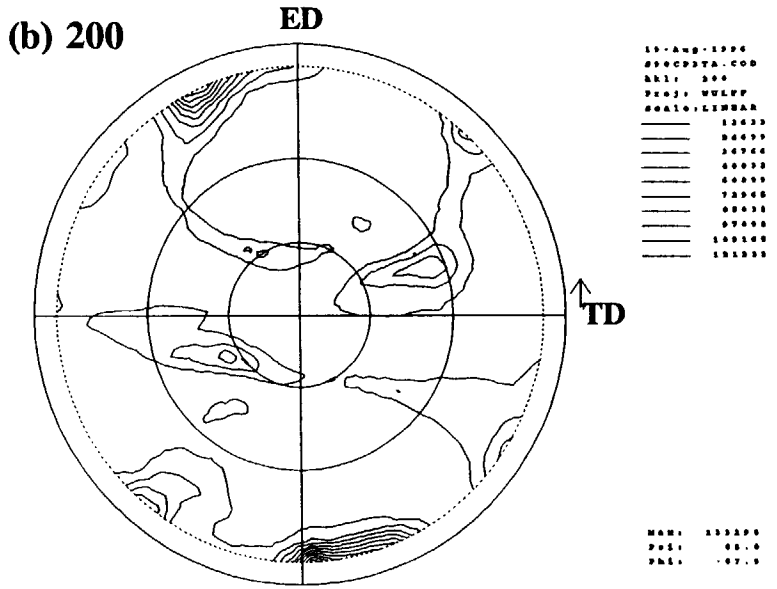

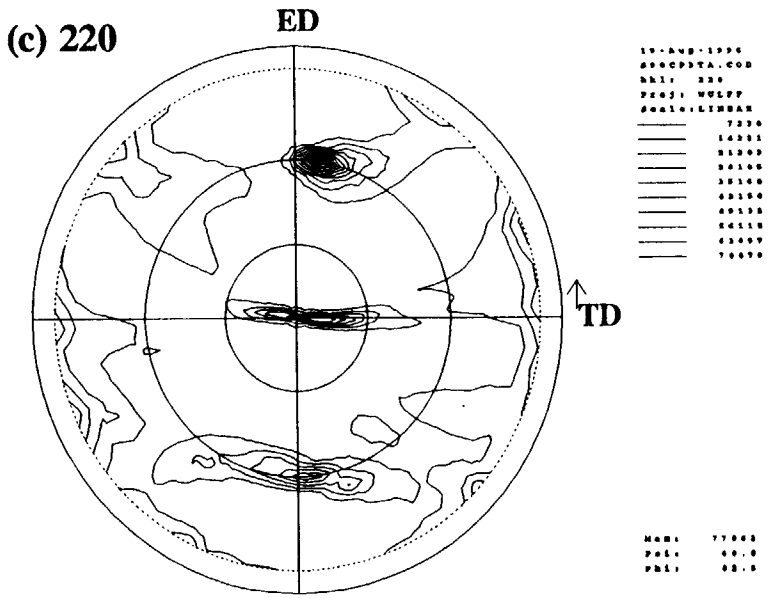

Figure 65.
Partial pole figures for the 2090-T8 extrusion in the cap @ 3t/4: (a) (111); (b) (200); (c) (220). [Specimen plane perpendicular to (R)adial axis]

(a) Sections: φ_2= 0 - 90°

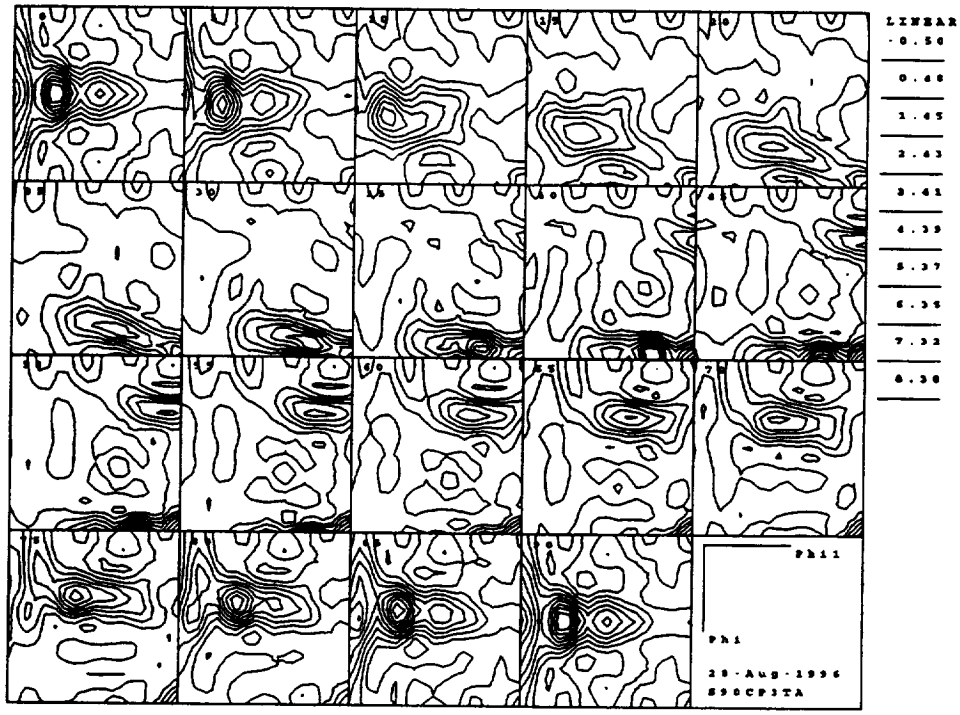

(b) Sections: φ_2= 45°; φ_2= 90°

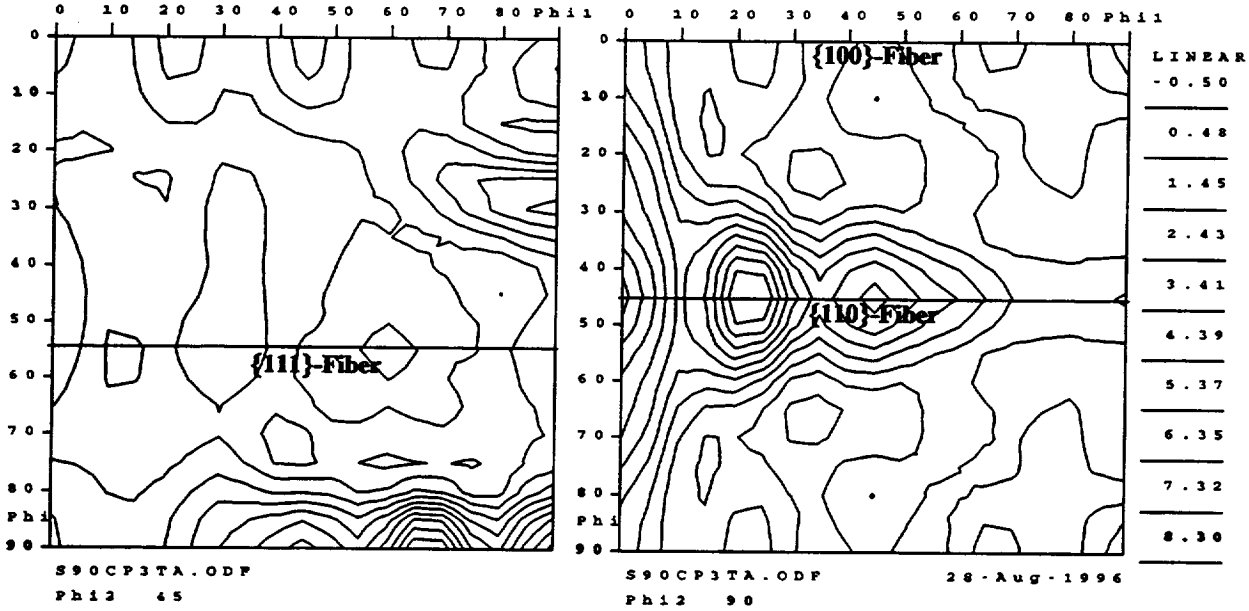

Figure 66. CODF sections for the 2090-T8 extrusion in the cap @ 3t/4; (a), Complete sections: φ_2= 0, 5, 10 ..... 90°; and (b), enlarged φ_2= 45° and φ_2= 90° sections. The locations of the {100}-fiber, {110}-fiber and {111}-fiber are shown.
[Specimen plane perpendicular to (R)adial axis]

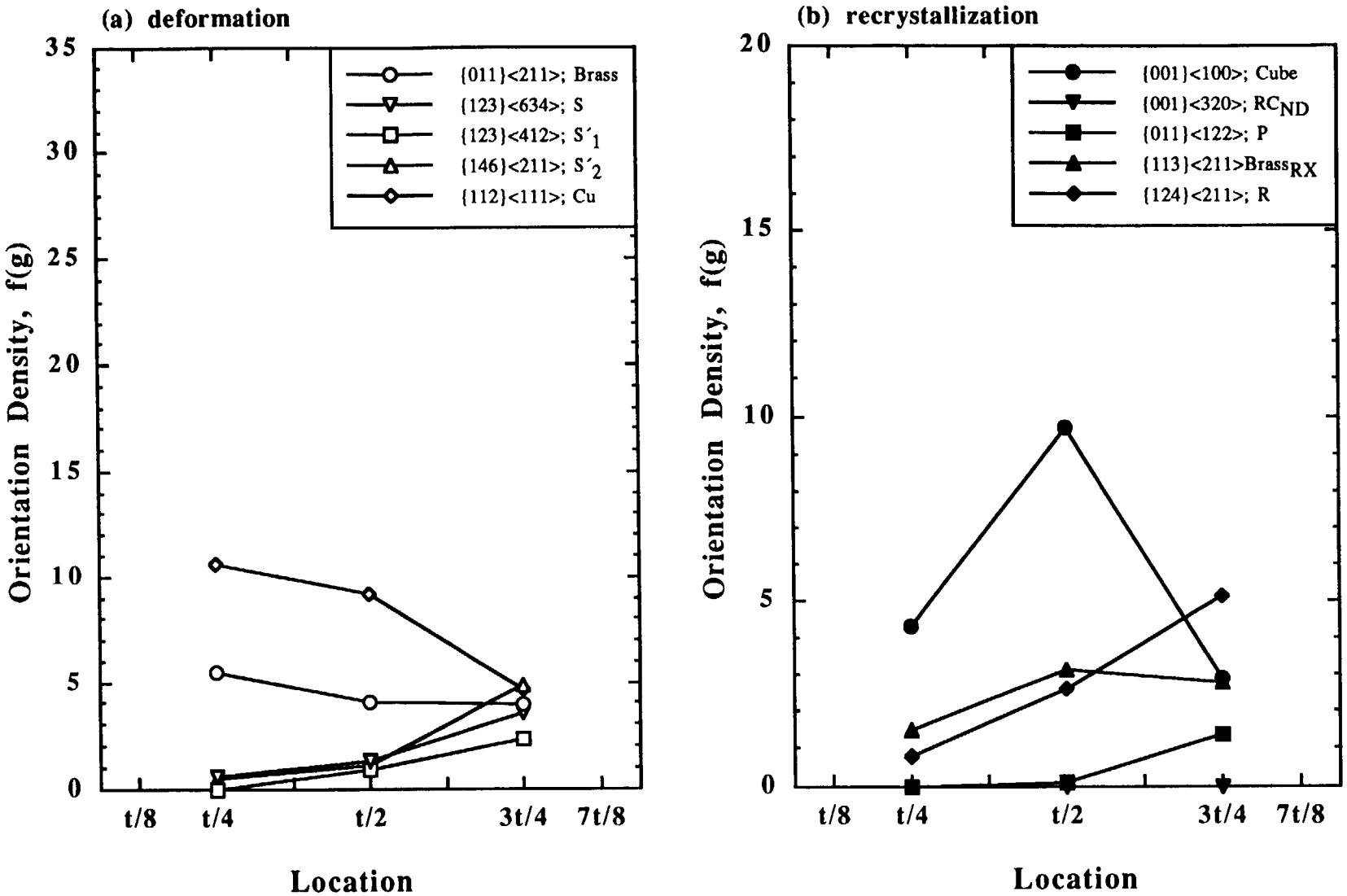

Figure 67. Orientation density, f(g), as a function of location through the cross-section for the 2090-T8 extrusion in the cap region: (a) Deformation-related components; (b) Recrystallization-related components.

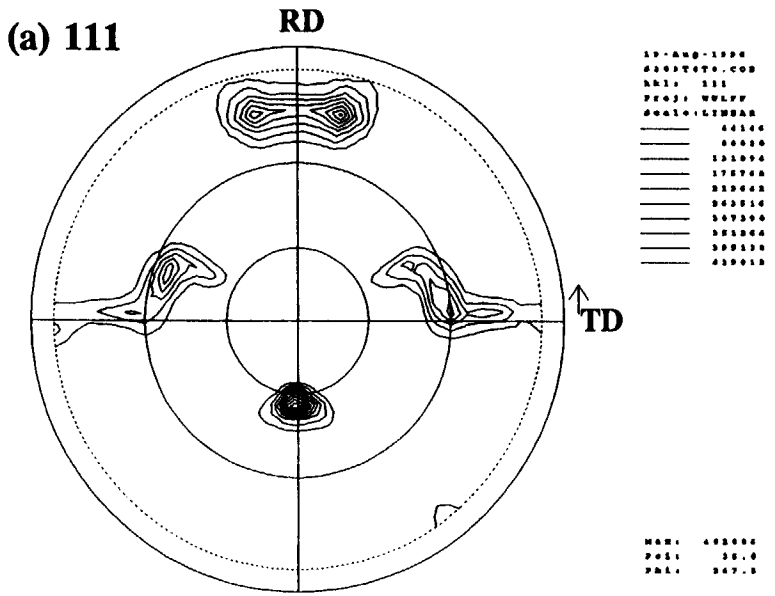

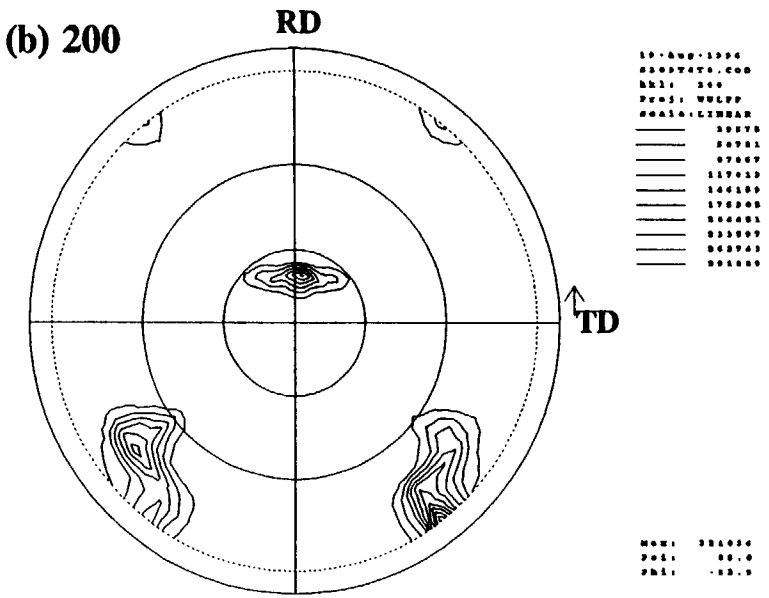

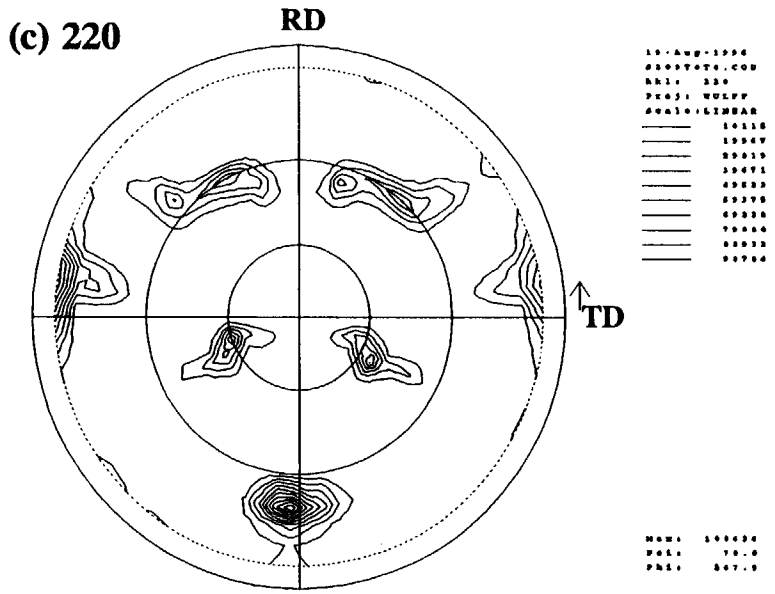

Figure 68.
Partial pole figures for 2090-T8 sheet @ t/8: (a) (111); (b) (200); (c) (220). [Specimen plane perpendicular to (S)hort-Transverse axis]

(a) Sections: $\varphi_2 = 0 - 90°$

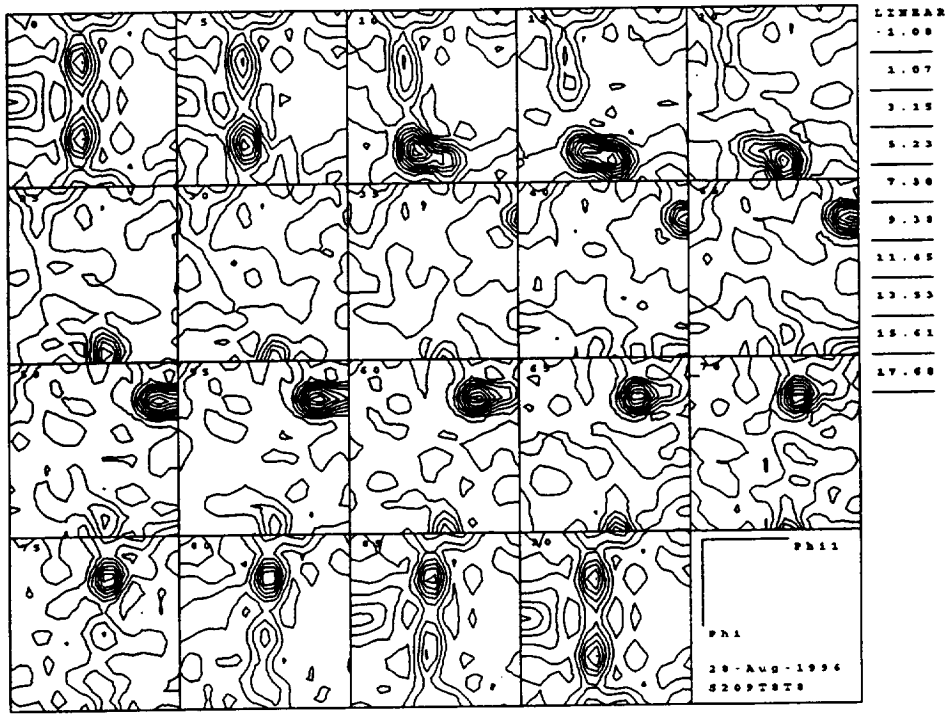

(b) Sections: $\varphi_2 = 45°$; $\varphi_2 = 90°$

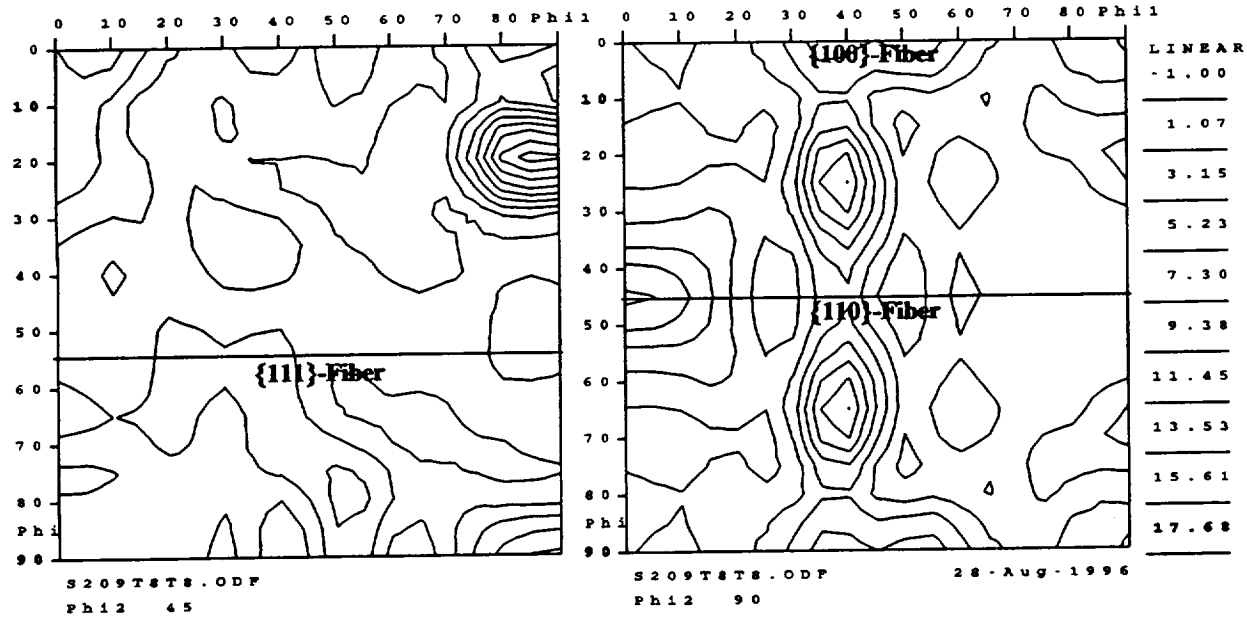

Figure 69. CODF sections for 2090-T8 sheet @ t/8; (a), Complete sections: $\varphi_2 = 0, 5, 10$ ..... 90°; and (b), enlarged $\varphi_2 = 45°$ and $\varphi_2 = 90°$ sections. The locations of the {100}-fiber, {110}-fiber and {111}-fiber are shown.
[Specimen plane perpendicular to (S)hort-Transverse axis]

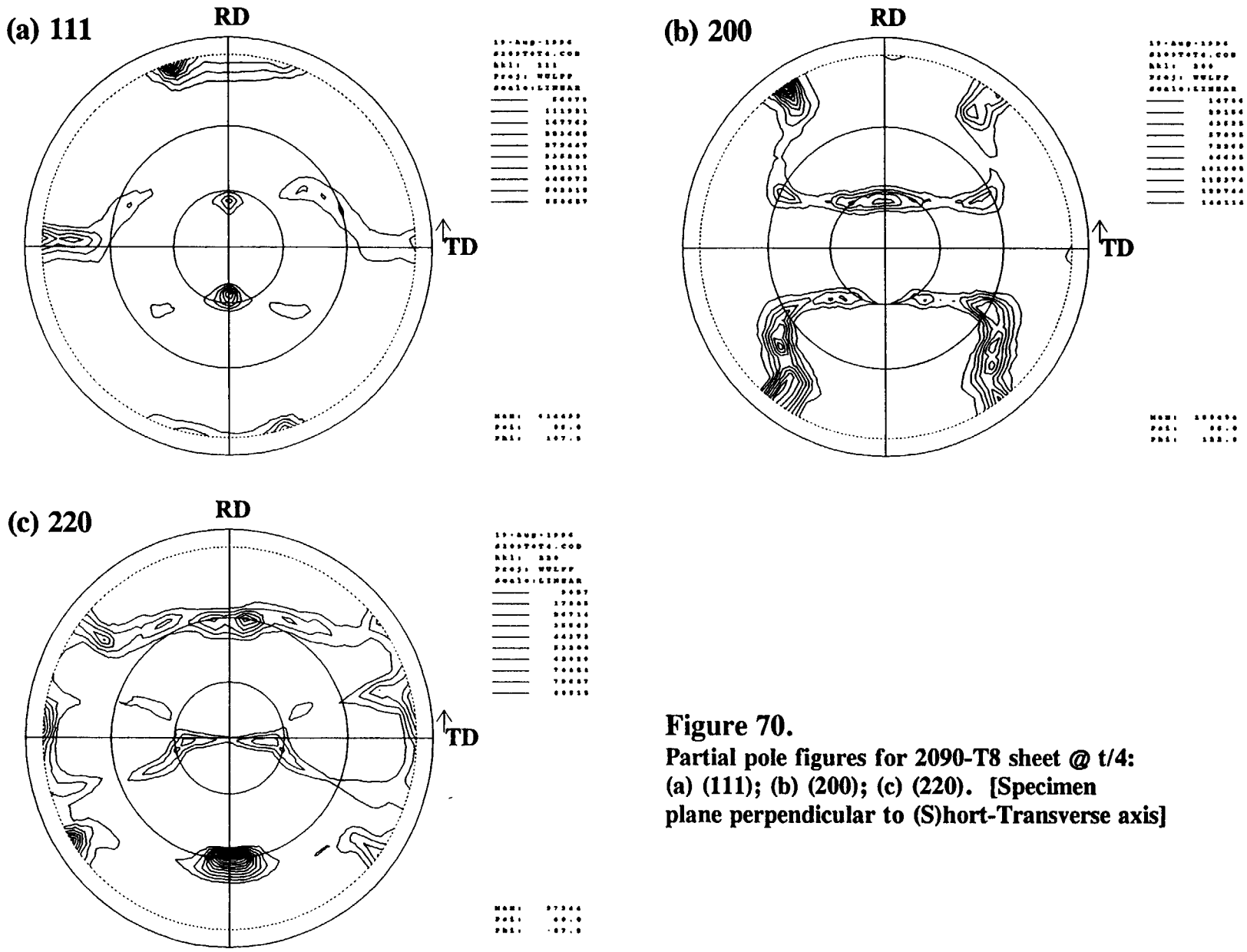

Figure 70.
Partial pole figures for 2090-T8 sheet @ t/4: (a) (111); (b) (200); (c) (220). [Specimen plane perpendicular to (S)hort-Transverse axis]

(a) Sections: φ_2= 0 - 90°

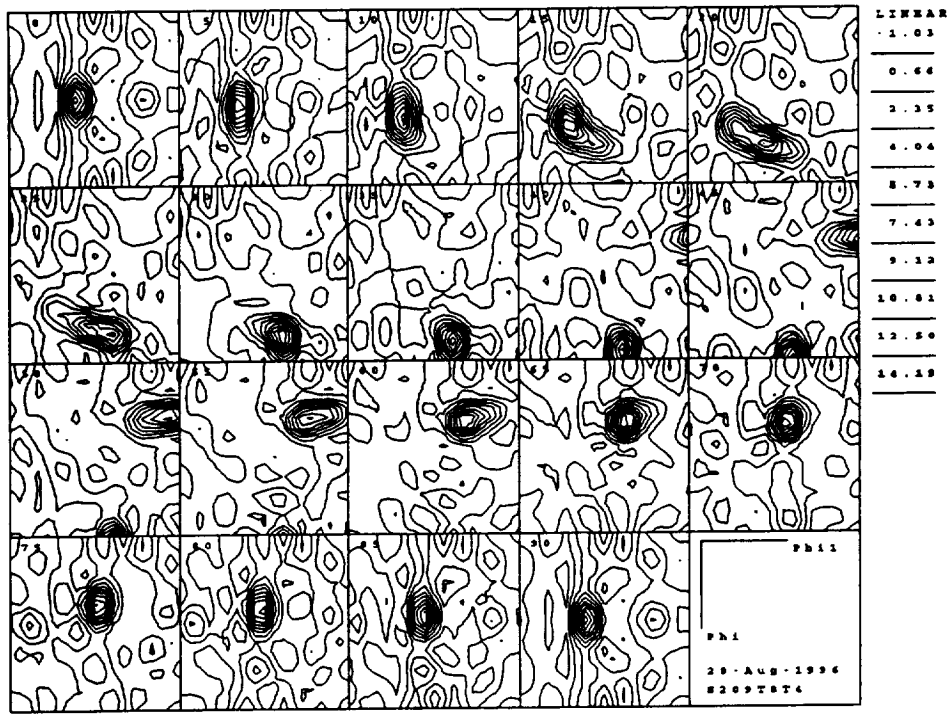

(b) Sections: φ_2= 45°; φ_2= 90°

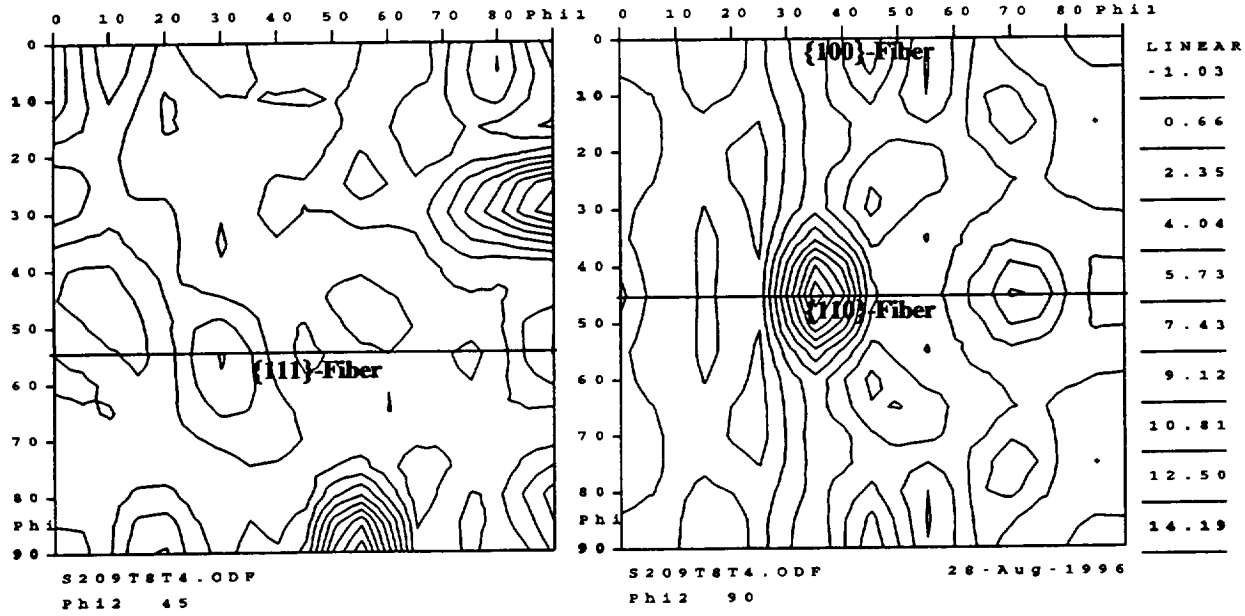

Figure 71. CODF sections for 2090-T8 sheet @ t/4; (a), Complete sections: φ_2= 0, 5, 10 ..... 90°; and (b), enlarged φ_2= 45° and φ_2= 90° sections. The locations of the {100}-fiber, {110}-fiber and {111}-fiber are shown.
[Specimen plane perpendicular to (S)hort-Transverse axis]

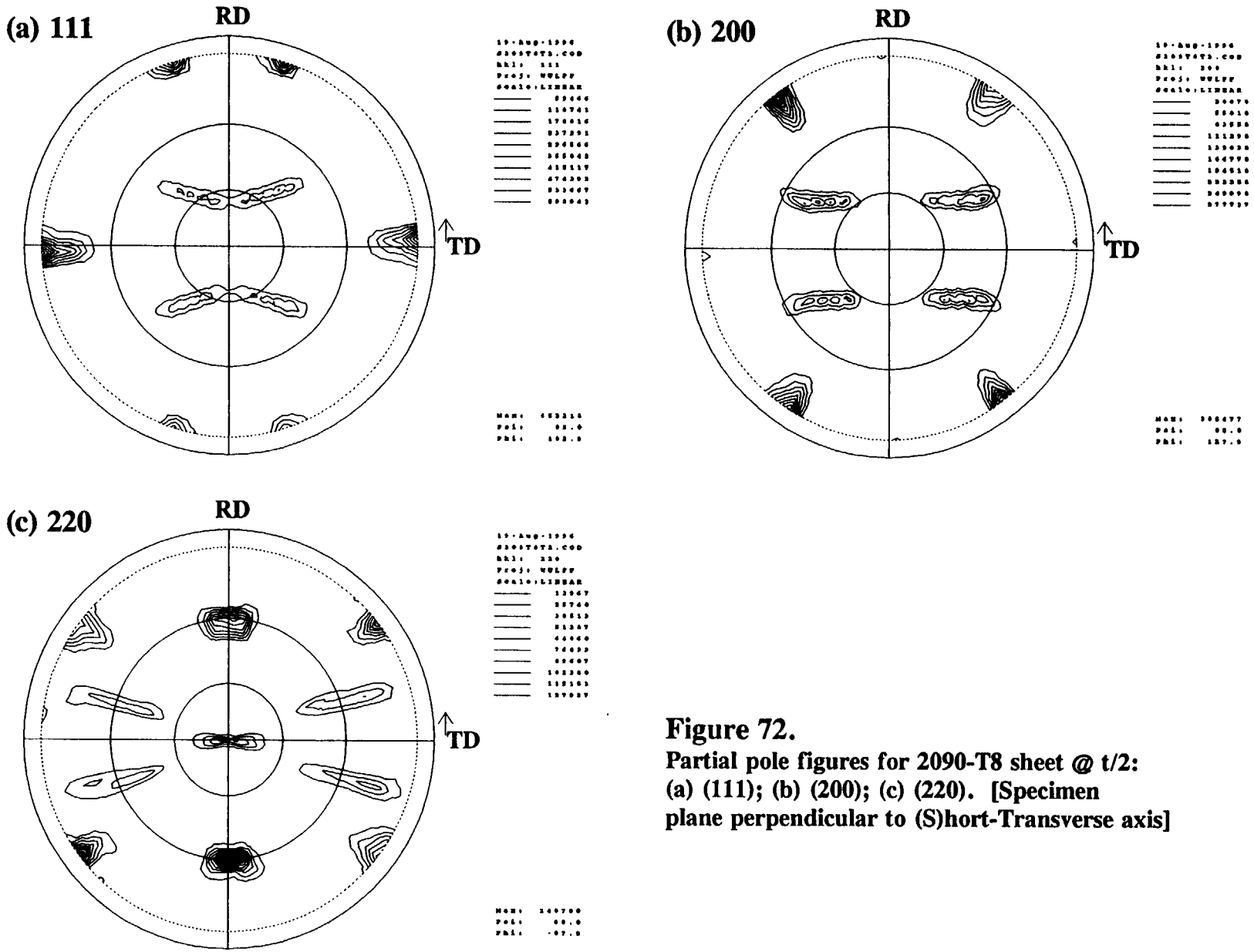

Figure 72.
Partial pole figures for 2090-T8 sheet @ t/2: (a) (111); (b) (200); (c) (220). [Specimen plane perpendicular to (S)hort-Transverse axis]

(a) Sections: $\varphi_2 = 0 - 90°$

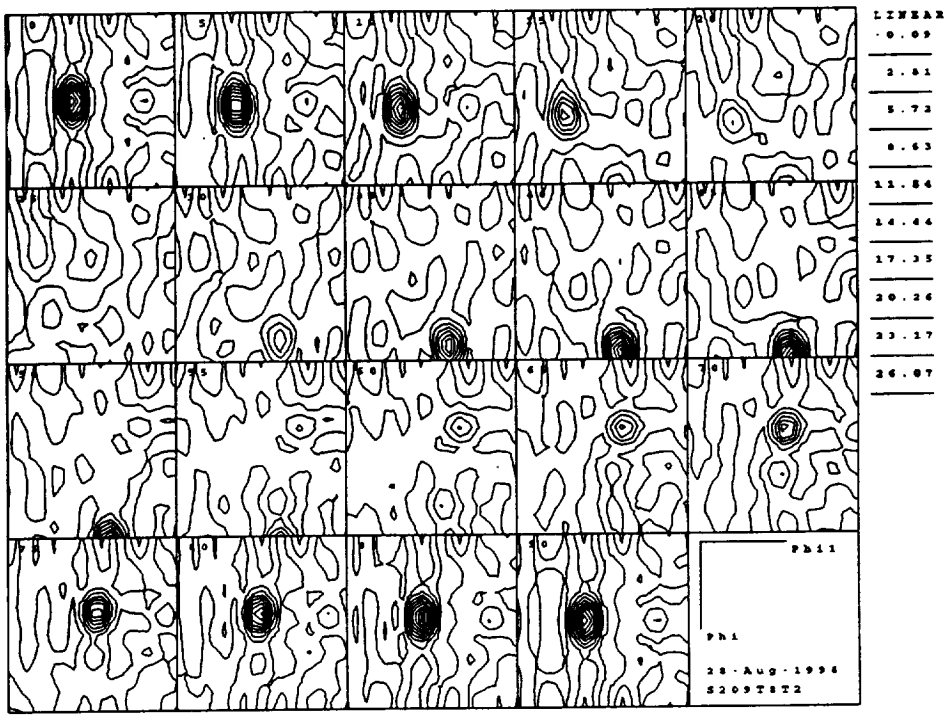

(b) Sections: $\varphi_2 = 45°$; $\varphi_2 = 90°$

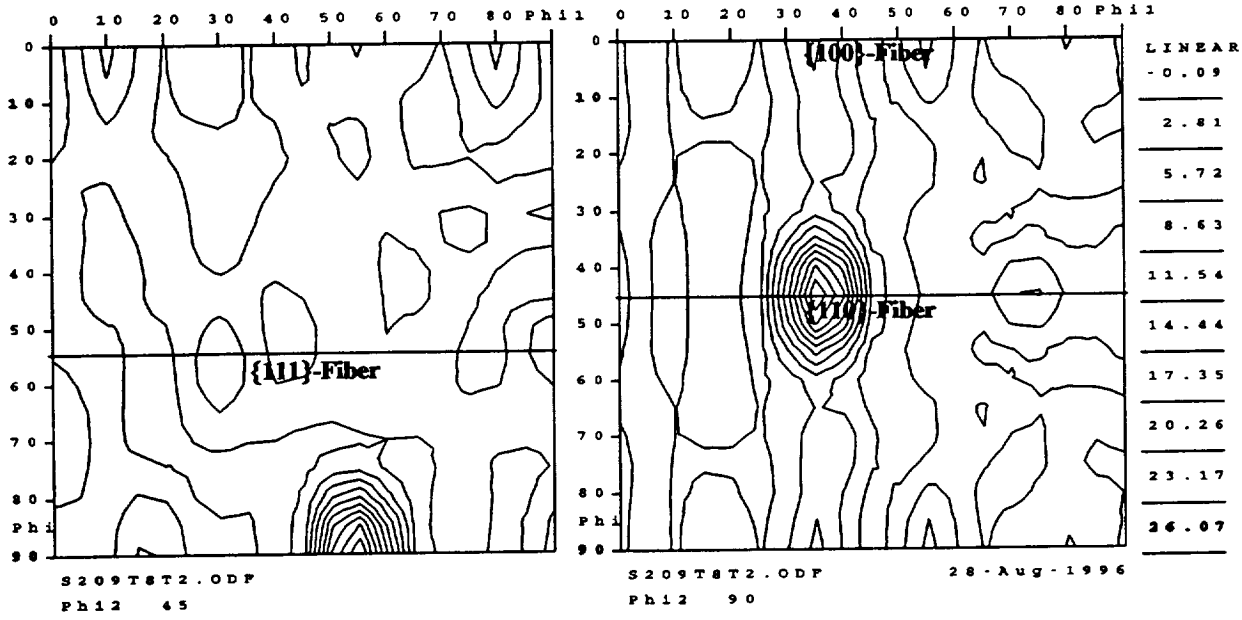

Figure 73. CODF sections for 2090-T8 sheet @ t/2; (a), Complete sections: $\varphi_2 = 0, 5, 10$ ..... 90°; and (b), enlarged $\varphi_2 = 45°$ and $\varphi_2 = 90°$ sections. The locations of the {100}-fiber, {110}-fiber and {111}-fiber are shown.
[Specimen plane perpendicular to (S)hort-Transverse axis]

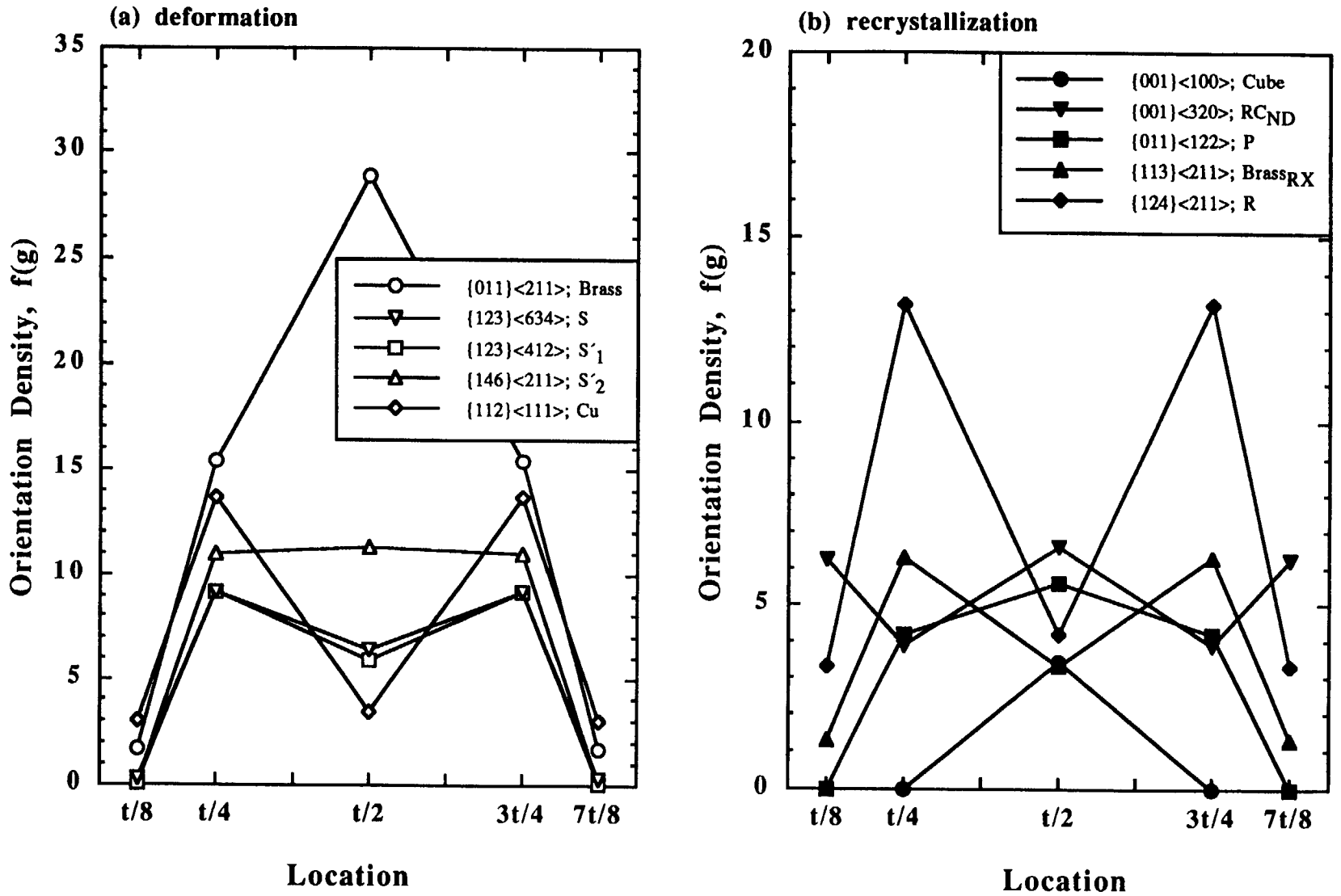

Figure 74. Orientation density, f(g), as a function of location through the cross-section for the 2090-T8 sheet: (a) Deformation-related components; (b) Recrystallization-related components.

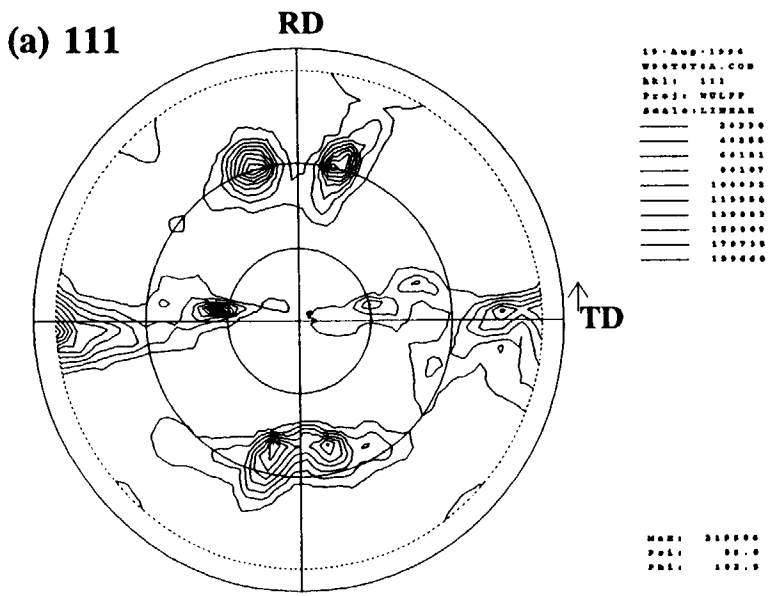

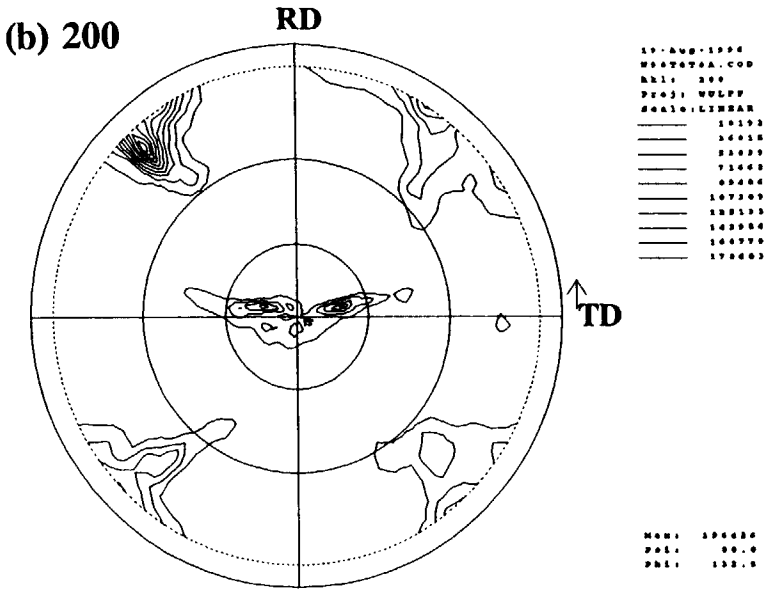

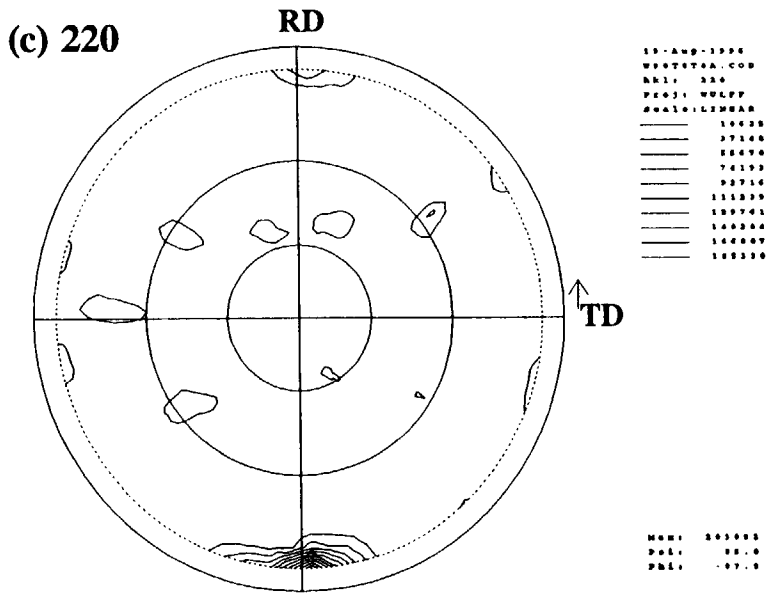

Figure 75.
Partial pole figures for 2090-T8 plate @ t/8: (a) (111); (b) (200); (c) (220). [Specimen plane perpendicular to (S)hort-Transverse axis]

(a) Sections: φ_2= 0 - 90°

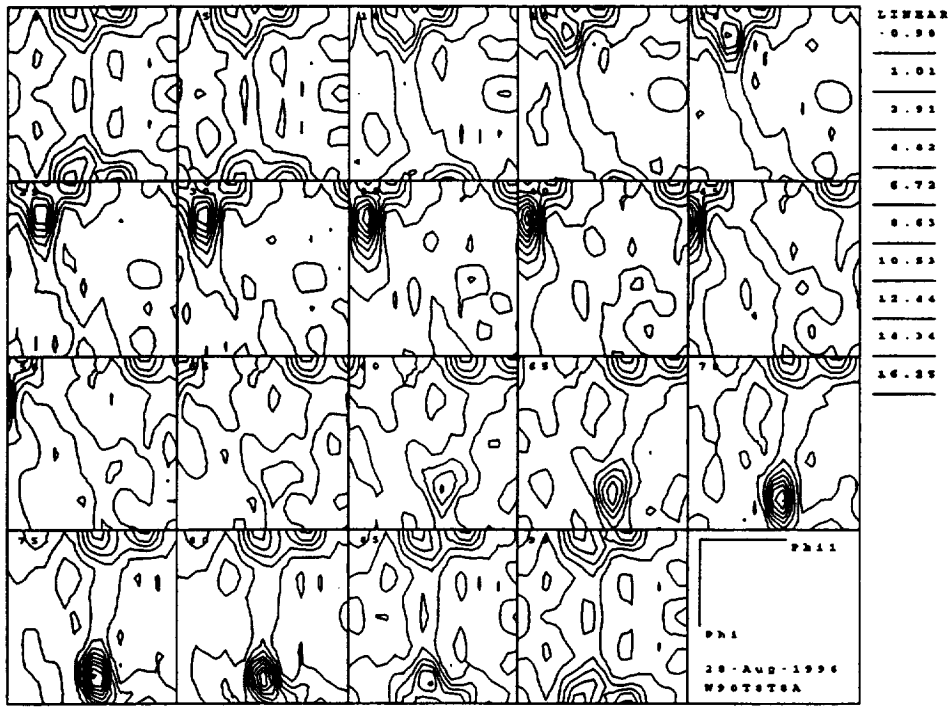

(b) Sections: φ_2= 45°; φ_2= 90°

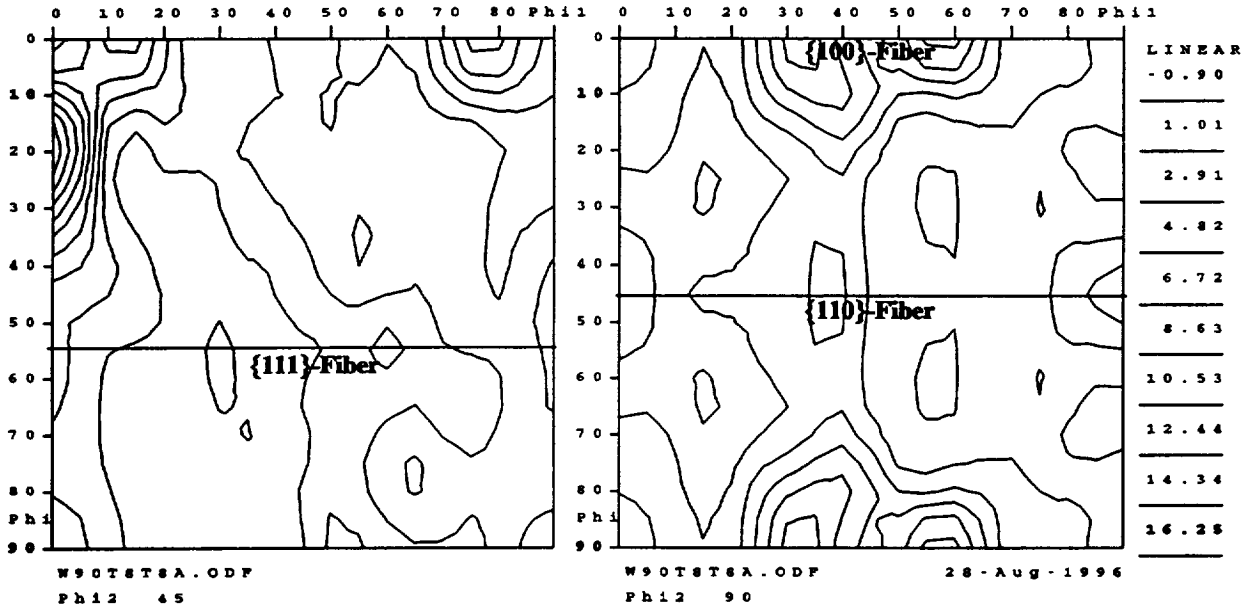

Figure 76. CODF sections for 2090-T8 plate @ t/8; (a), Complete sections: φ_2= 0, 5, 10 ..... 90°; and (b), enlarged φ_2= 45° and φ_2= 90° sections. The locations of the {100}-fiber, {110}-fiber and {111}-fiber are shown.
[Specimen plane perpendicular to (S)hort-Transverse axis]

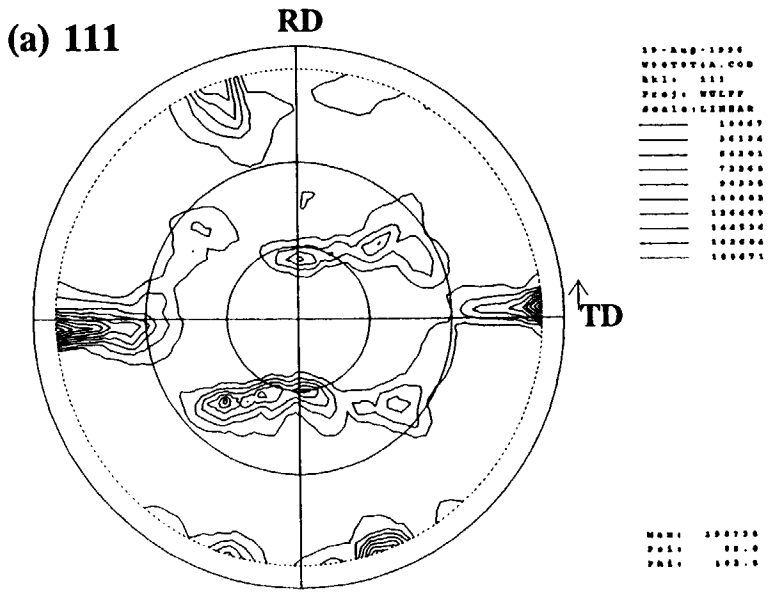

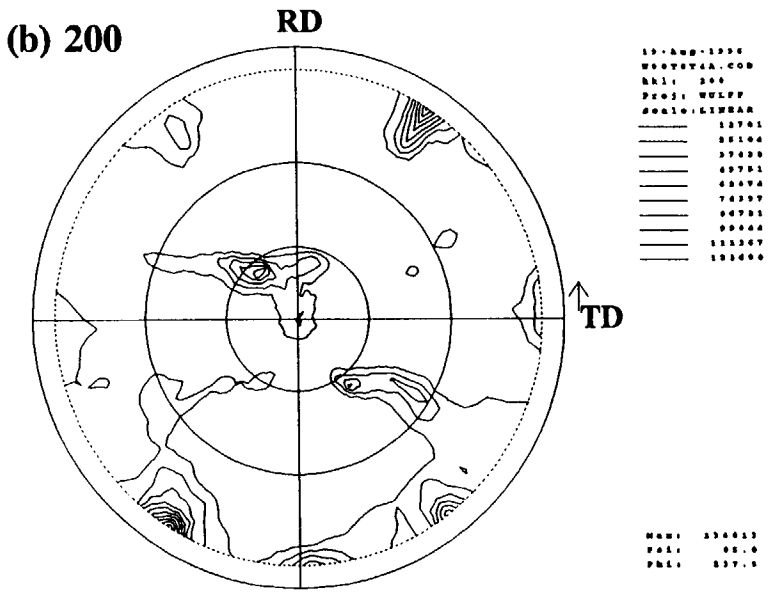

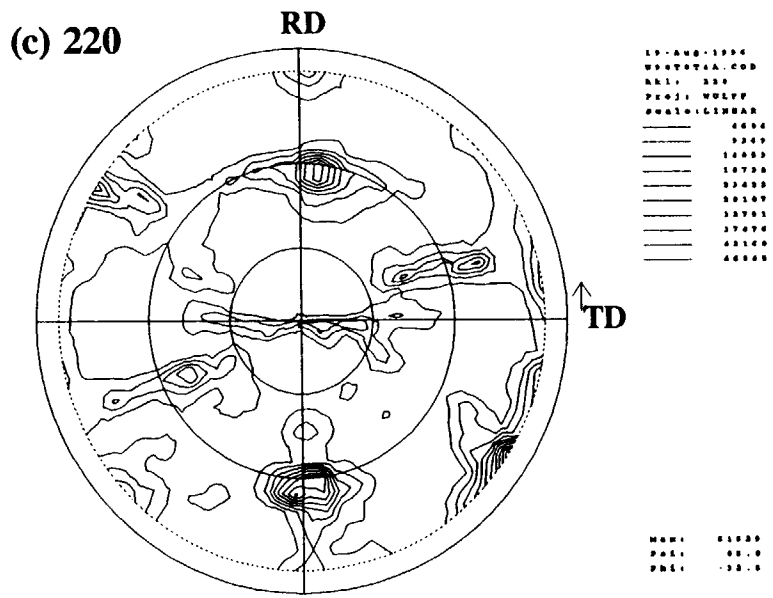

Figure 77.
Partial pole figures for 2090-T8 plate @ t/4: (a) (111); (b) (200); (c) (220). [Specimen plane perpendicular to (S)hort-Transverse axis]

(a) Sections: φ_2= 0 - 90°

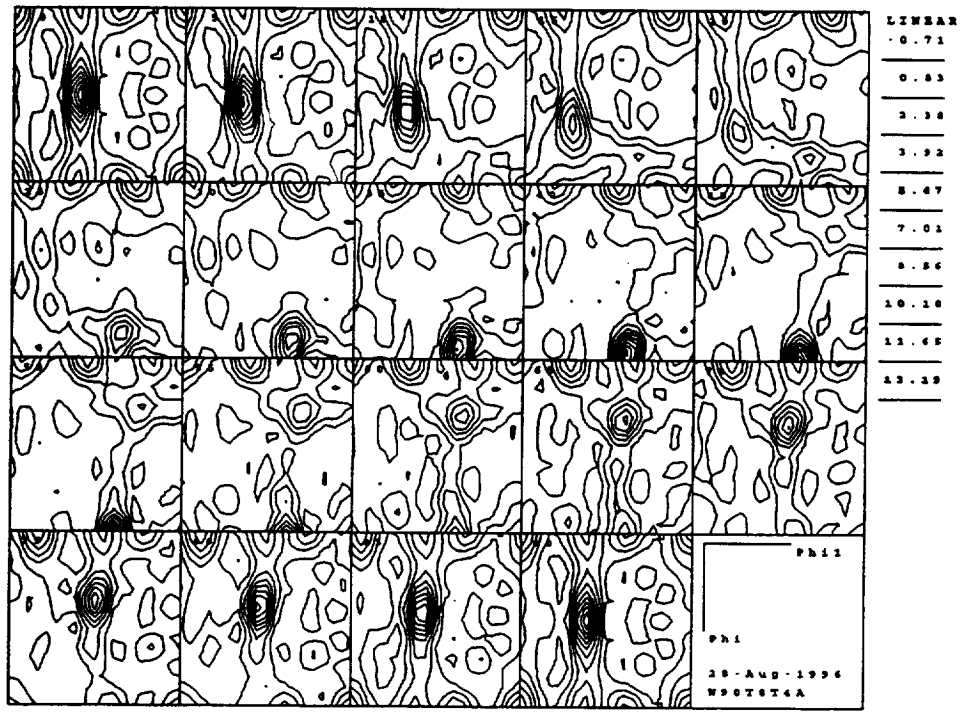

(b) Sections: φ_2= 45°; φ_2= 90°

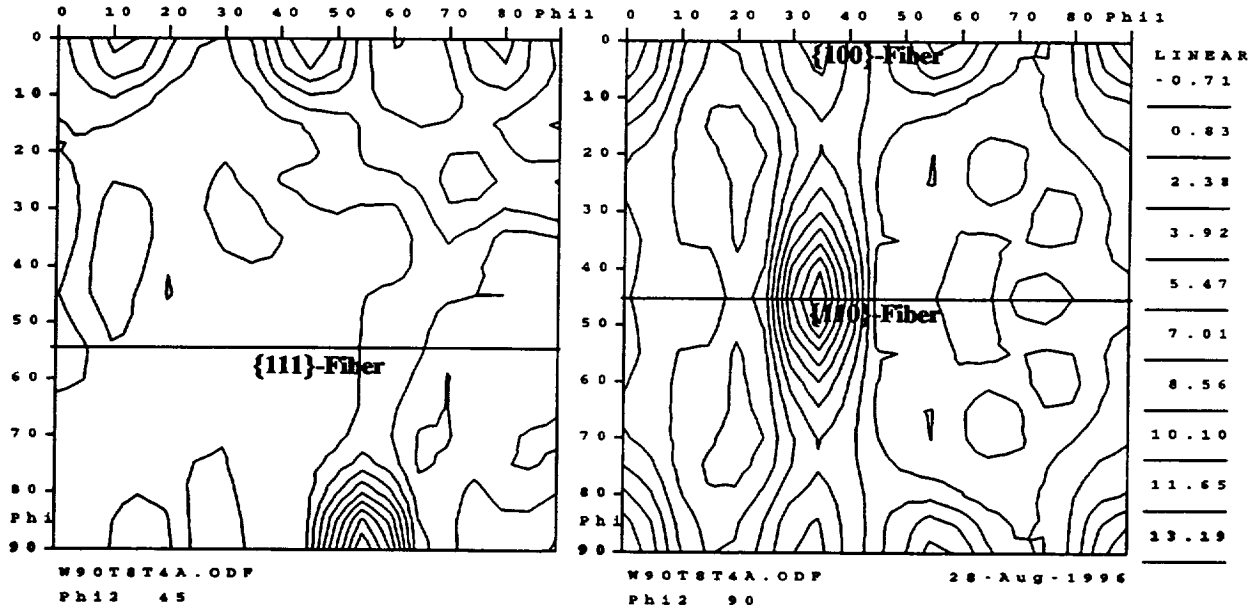

Figure 78. CODF sections for 2090-T8 plate @ t/4; (a), Complete sections: φ_2= 0, 5, 10 ..... 90°; and (b), enlarged φ_2= 45° and φ_2= 90° sections. The locations of the {100}-fiber, {110}-fiber and {111}-fiber are shown.
[Specimen plane perpendicular to (S)hort-Transverse axis]

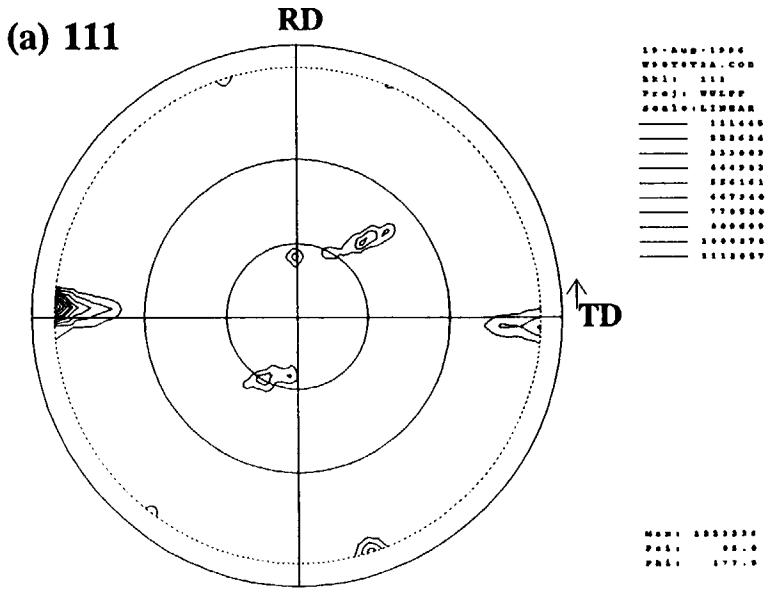

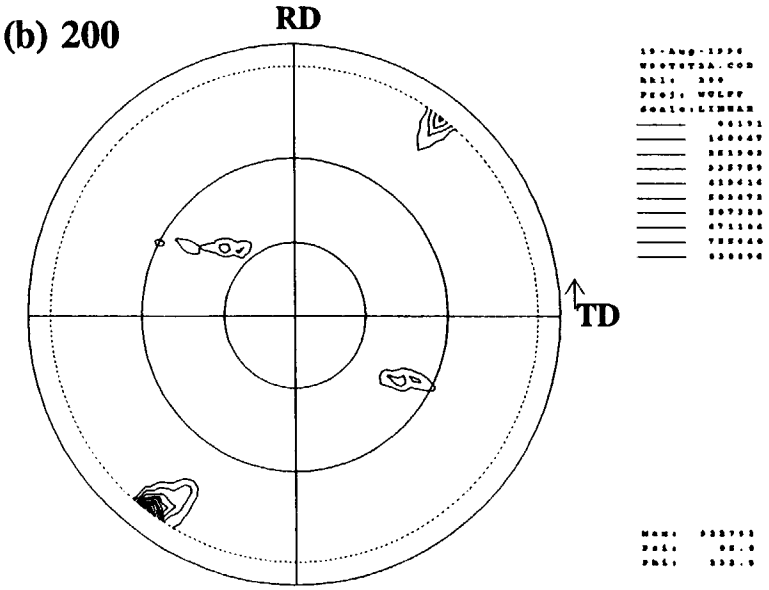

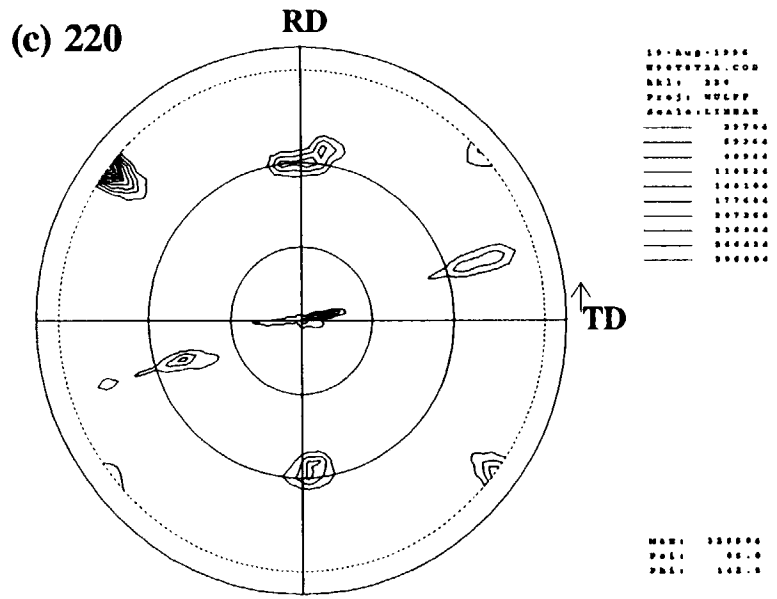

Figure 79.
Partial pole figures for 2090-T8 plate @ t/2: (a) (111); (b) (200); (c) (220). [Specimen plane perpendicular to (S)hort-Transverse axis]

(a) Sections: φ_2= 0 - 90°

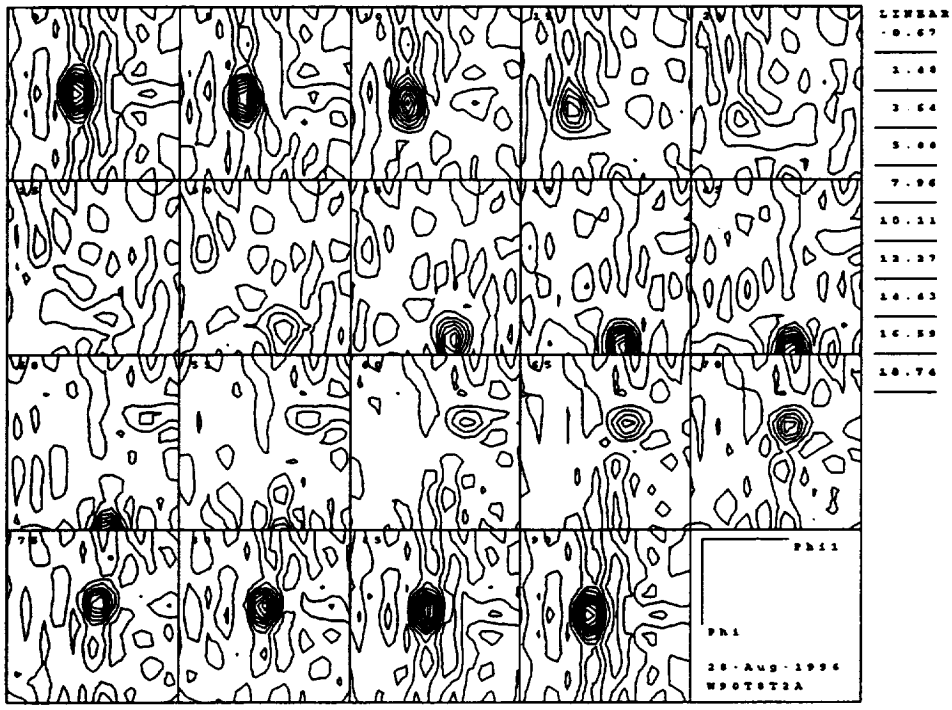

(b) Sections: φ_2= 45°; φ_2= 90°

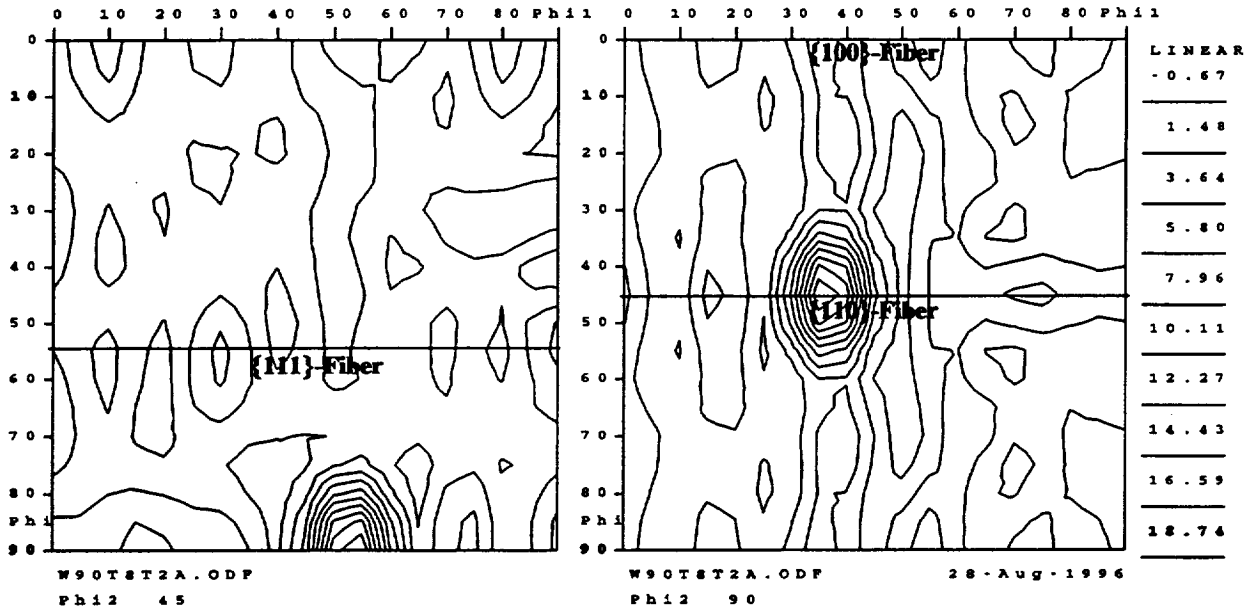

Figure 80. CODF sections for 2090-T8 plate @ t/2; (a), Complete sections: φ_2= 0, 5, 10 ..... 90°; and (b), enlarged φ_2= 45° and φ_2= 90° sections. The locations of the {100}-fiber, {110}-fiber and {111}-fiber are shown.
[Specimen plane perpendicular to (S)hort-Transverse axis]

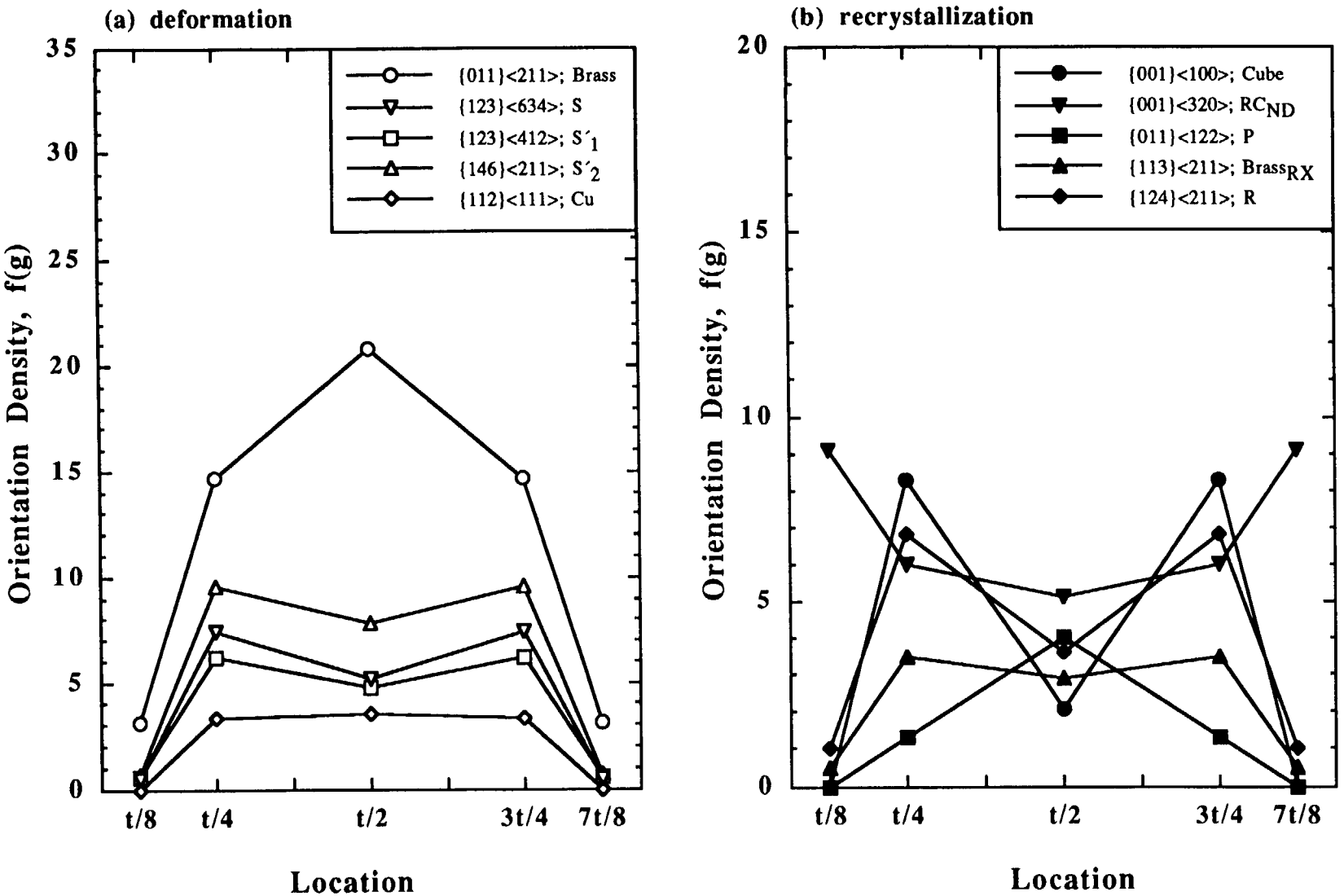

Figure 81. Orientation density, f(g), as a function of location through the cross-section for the 2090-T8 plate: (a) Deformation-related components; (b) Recrystallization-related components.

4.3 Alloy 2096

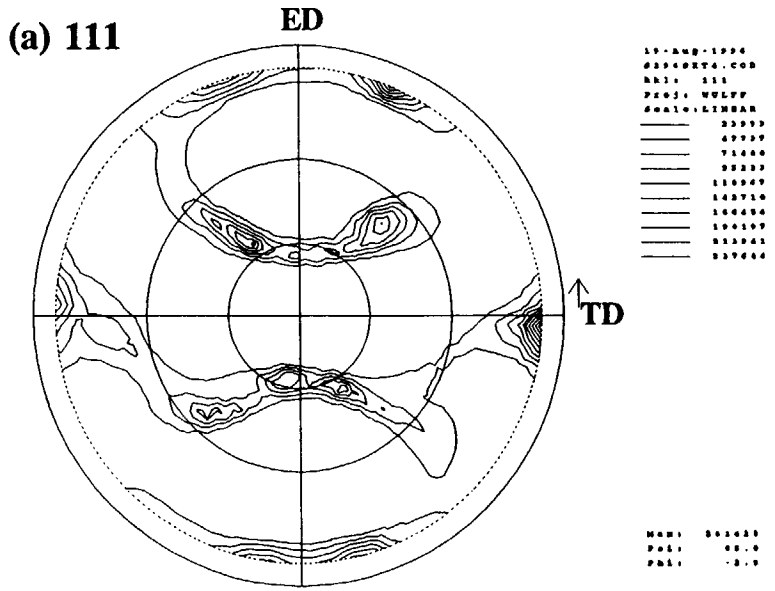

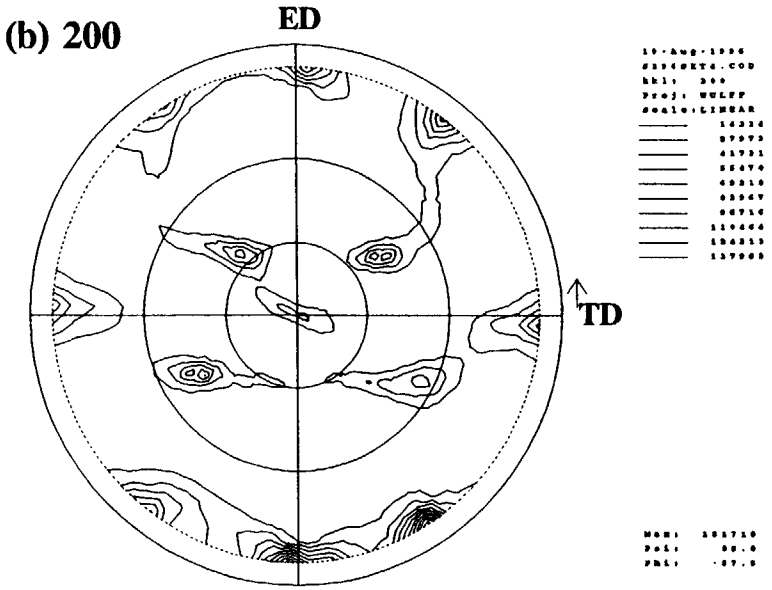

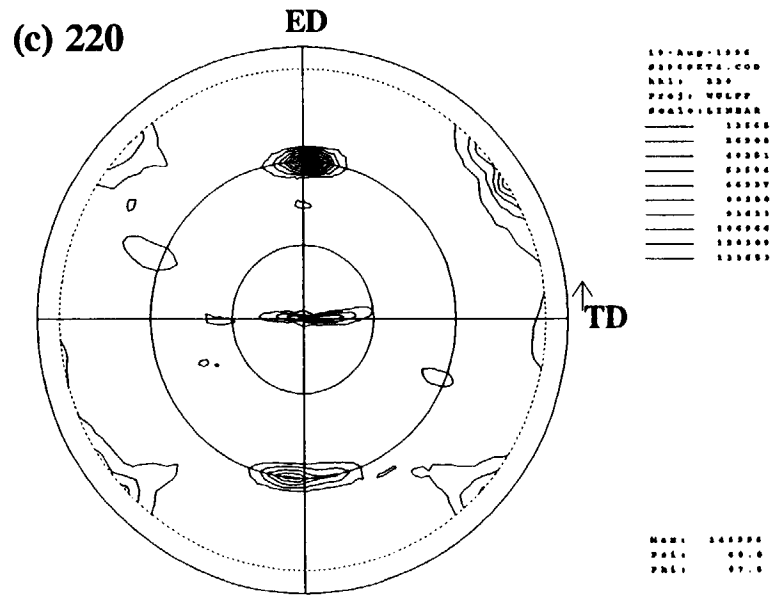

Figure 82.
Partial pole figures for the 2096-T3 extrusion in the skin @ t/4: (a) (111); (b) (200); (c) (220). [Specimen plane perpendicular to (R)adial axis]

(a) Sections: φ_2= 0 - 90°

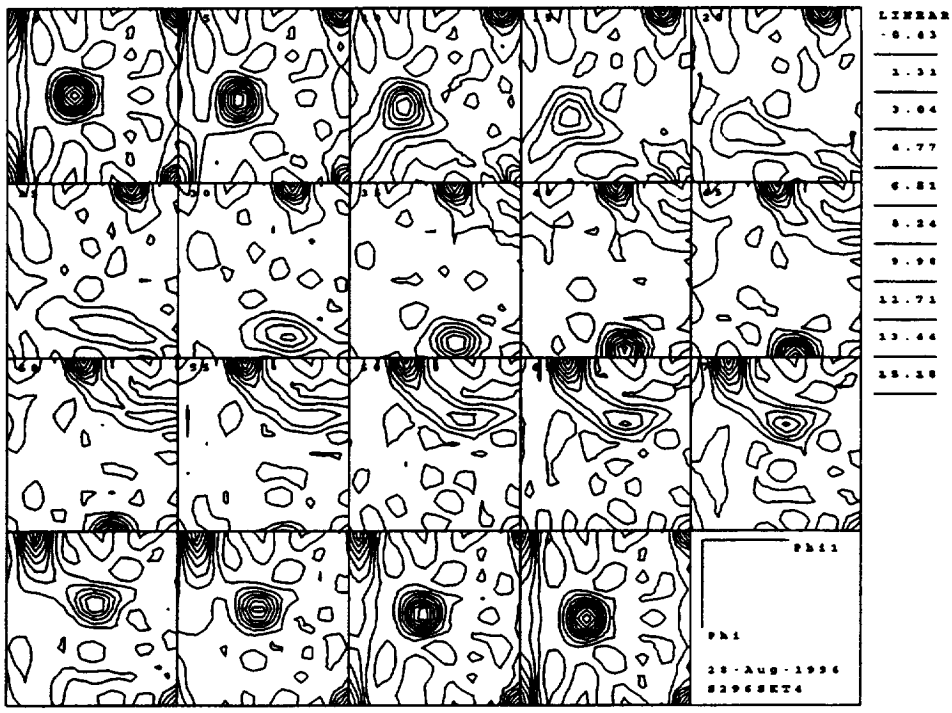

(b) Sections: φ_2= 45°; φ_2= 90°

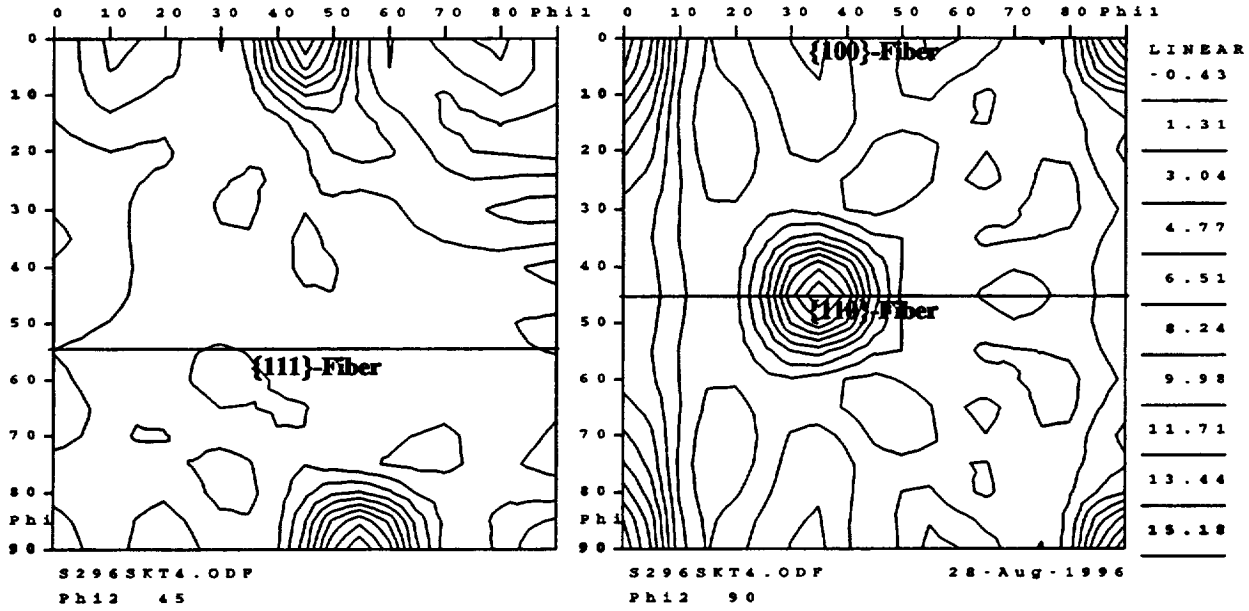

Figure 83. CODF sections for the 2096-T3 extrusion in the skin @ t/4; (a), Complete sections: φ_2= 0, 5, 10 ..... 90°; and (b), enlarged φ_2= 45° and φ_2= 90° sections. The locations of the {100}-fiber, {110}-fiber and {111}-fiber are shown.
[Specimen plane perpendicular to (R)adial axis]

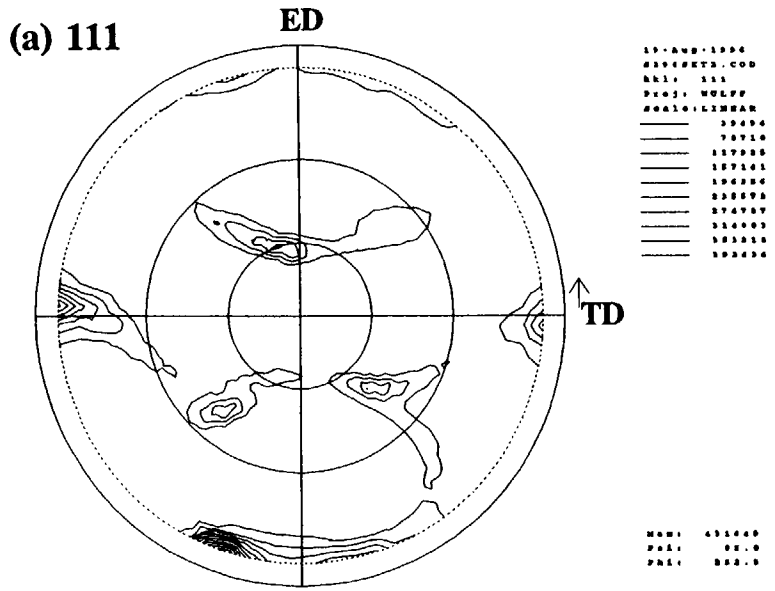

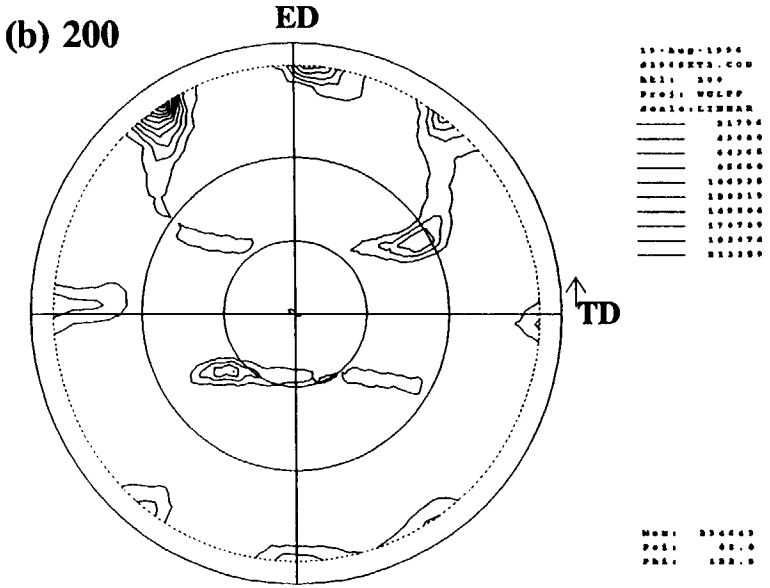

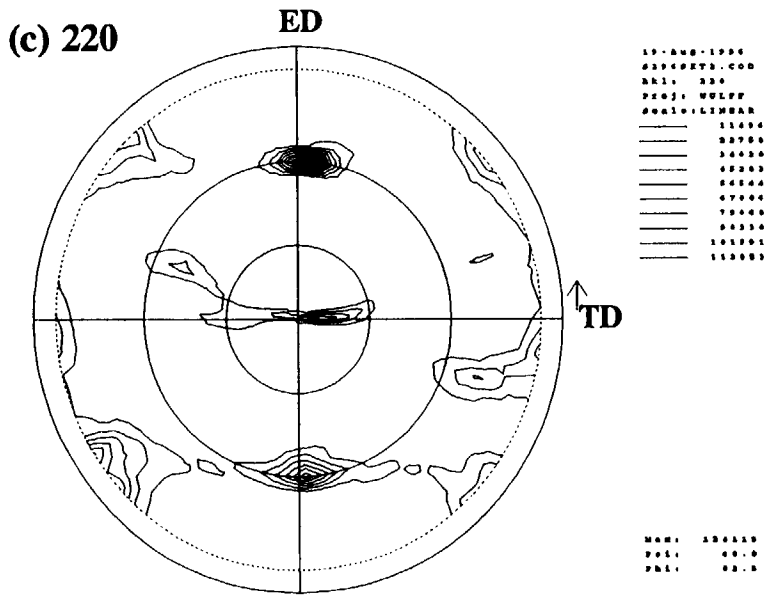

Figure 84.
Partial pole figures for the 2096-T3 extrusion in the skin @ t/2: (a) (111); (b) (200); (c) (220). [Specimen plane perpendicular to (R)adial axis]

(a) Sections: φ_2= 0 - 90°

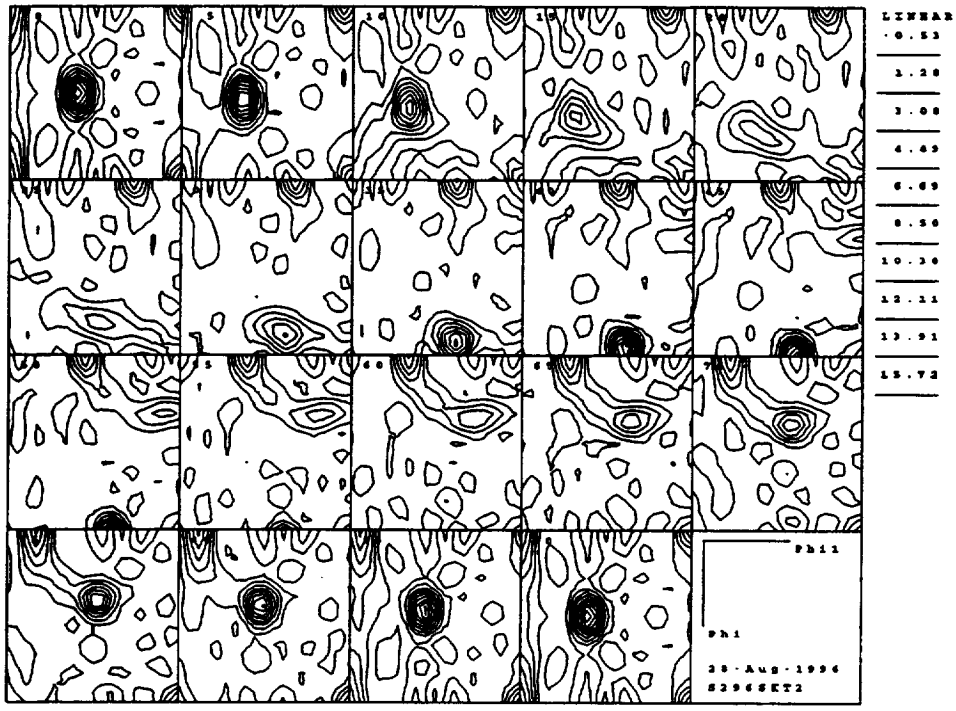

(b) Sections: φ_2= 45°; φ_2= 90°

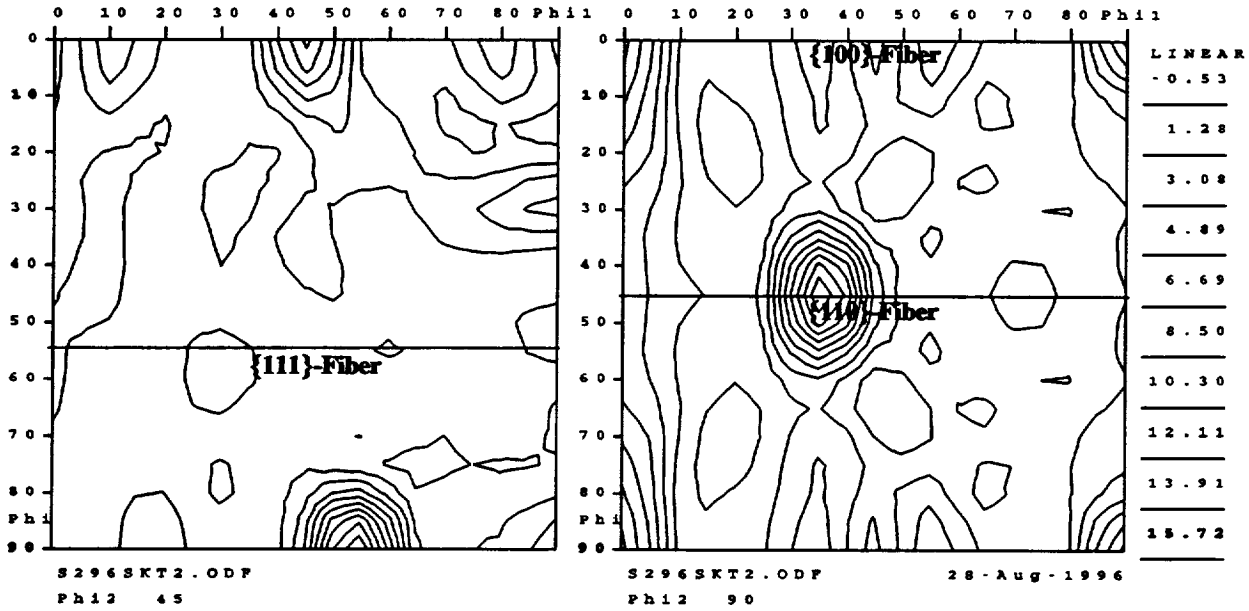

Figure 85. CODF sections for the 2096-T3 extrusion in the skin @ t/2; (a), Complete sections: φ_2= 0, 5, 10 ..... 90°; and (b), enlarged φ_2= 45° and φ_2= 90° sections. The locations of the {100}-fiber, {110}-fiber and {111}-fiber are shown.
[Specimen plane perpendicular to (R)adial axis]

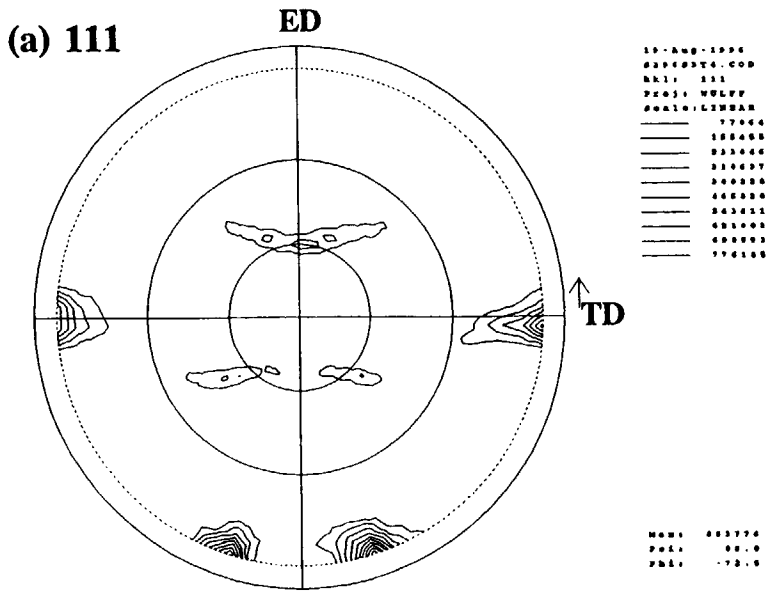

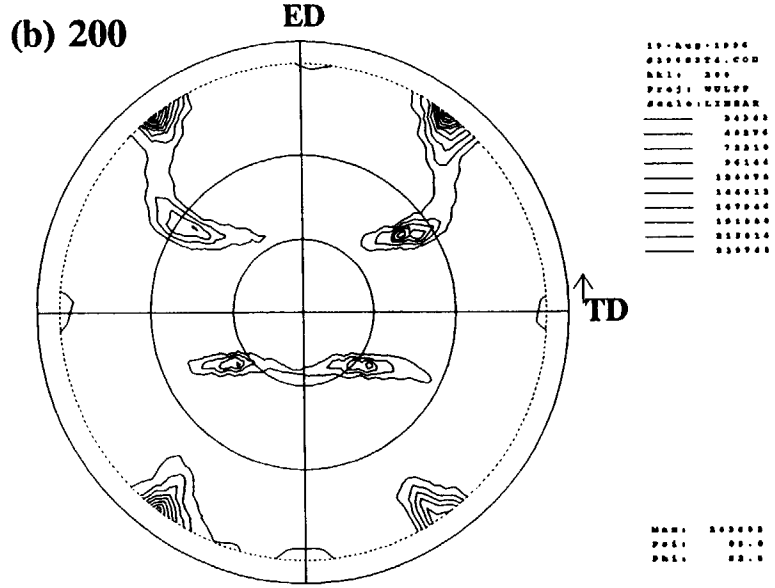

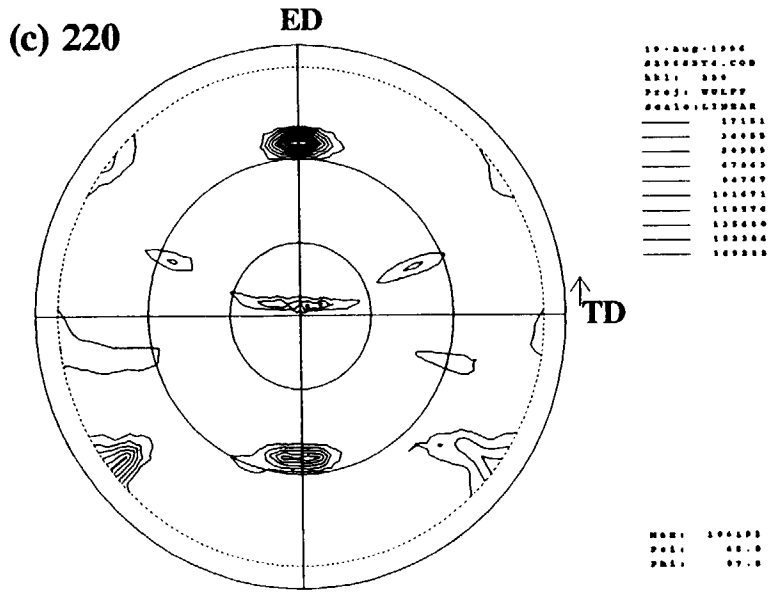

Figure 86.
Partial pole figures for the 2096-T3 extrusion in the skin @ 3t/4: (a) (111); (b) (200); (c) (220). [Specimen plane perpendicular to (R)adial axis]

(a) Sections: φ_2= 0 - 90°

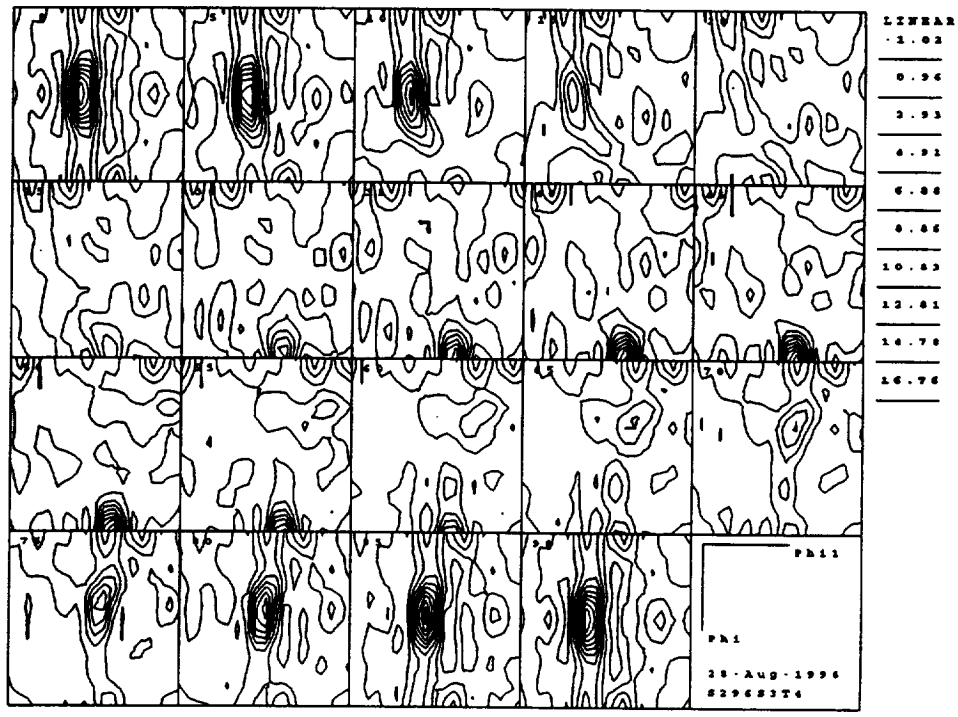

(b) Sections: φ_2= 45°; φ_2= 90°

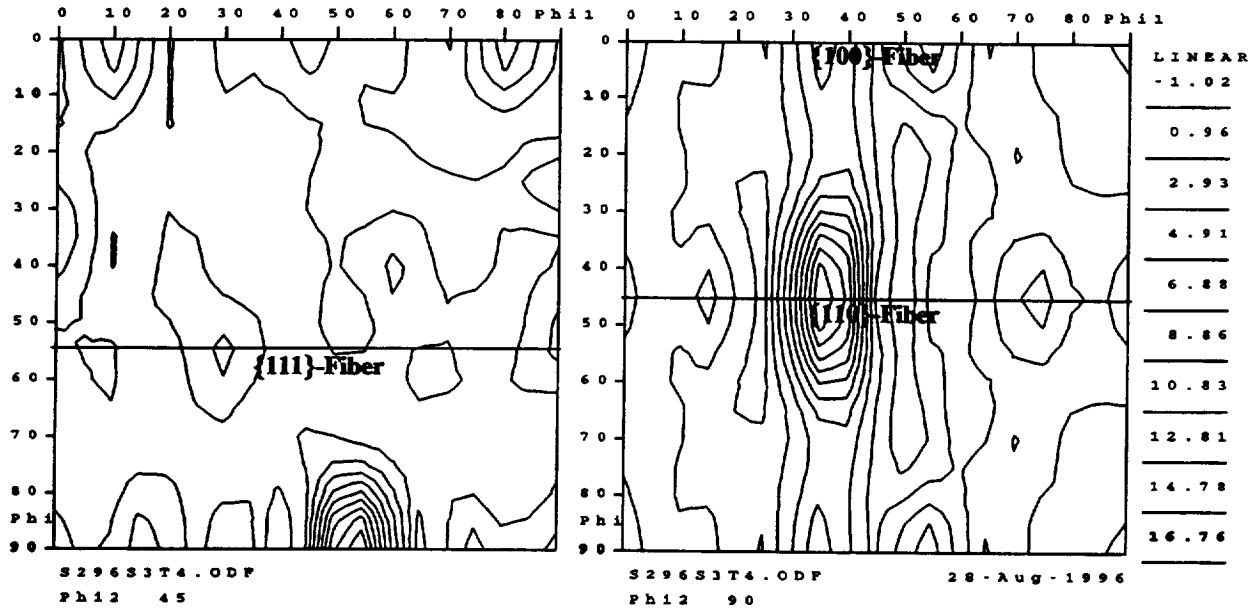

Figure 87. CODF sections for the 2096-T3 extrusion in the skin @ 3t/4; (a), Complete sections: φ_2= 0, 5, 10 ..... 90°; and (b), enlarged φ_2= 45° and φ_2= 90° sections. The locations of the {100}-fiber, {110}-fiber and {111}-fiber are shown.
[Specimen plane perpendicular to (R)adial axis]

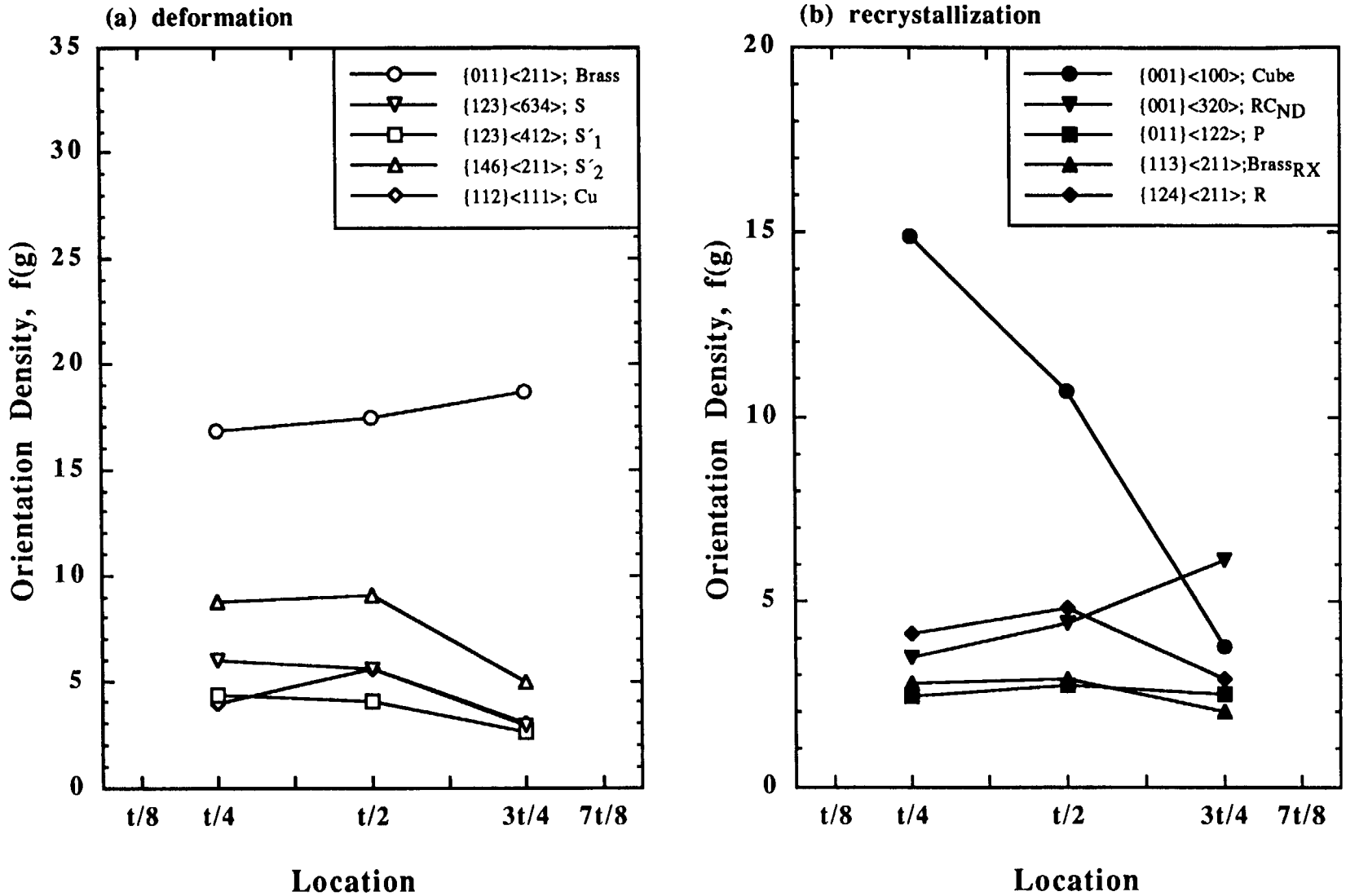

Figure 88. Orientation density, f(g), as a function of location through the cross-section for the 2096-T3 extrusion in the skin region: (a) Deformation-related components; (b) Recrystallization-related components.

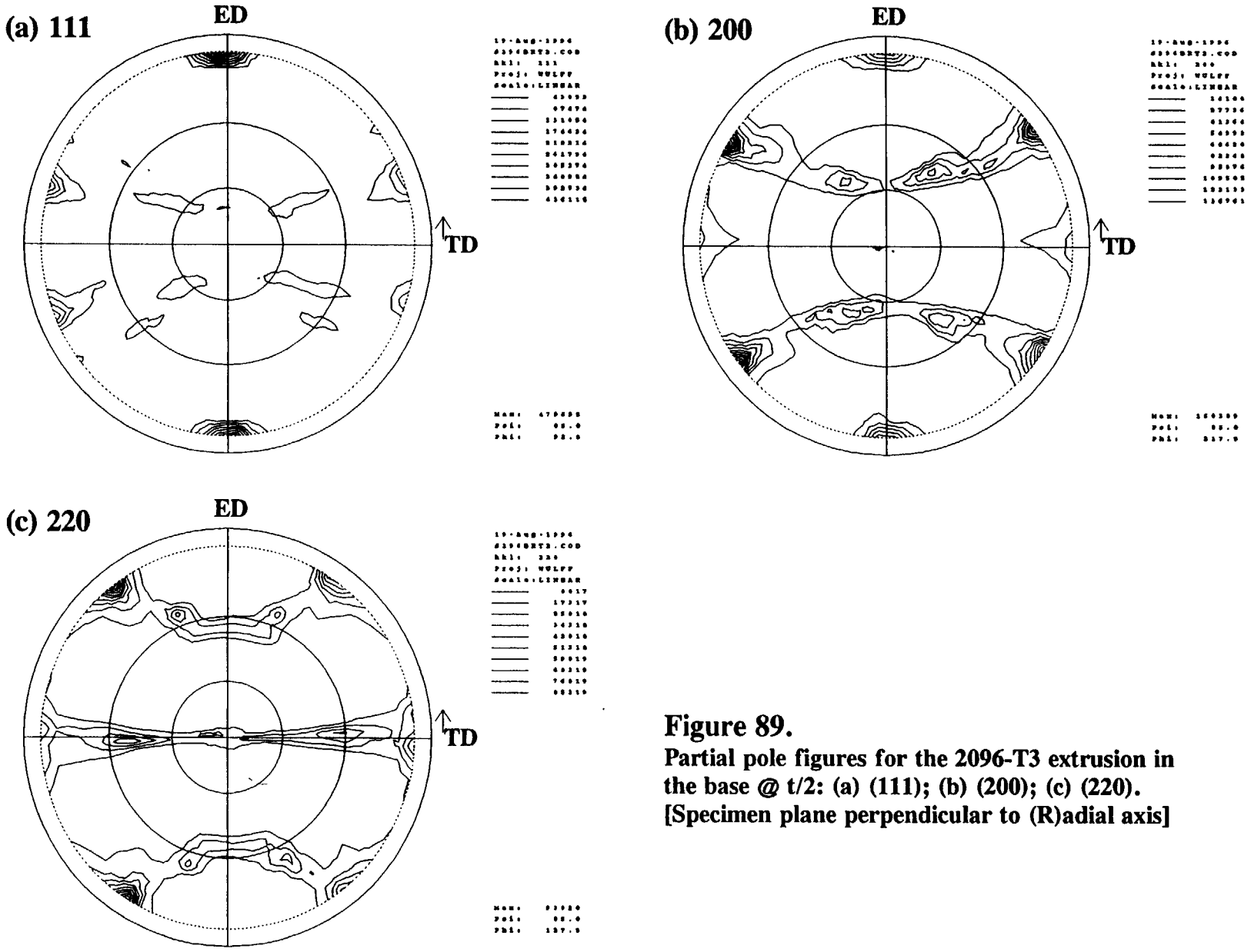

Figure 89.
Partial pole figures for the 2096-T3 extrusion in the base @ t/2: (a) (111); (b) (200); (c) (220). [Specimen plane perpendicular to (R)adial axis]

(a) Sections: φ_2= 0 - 90°

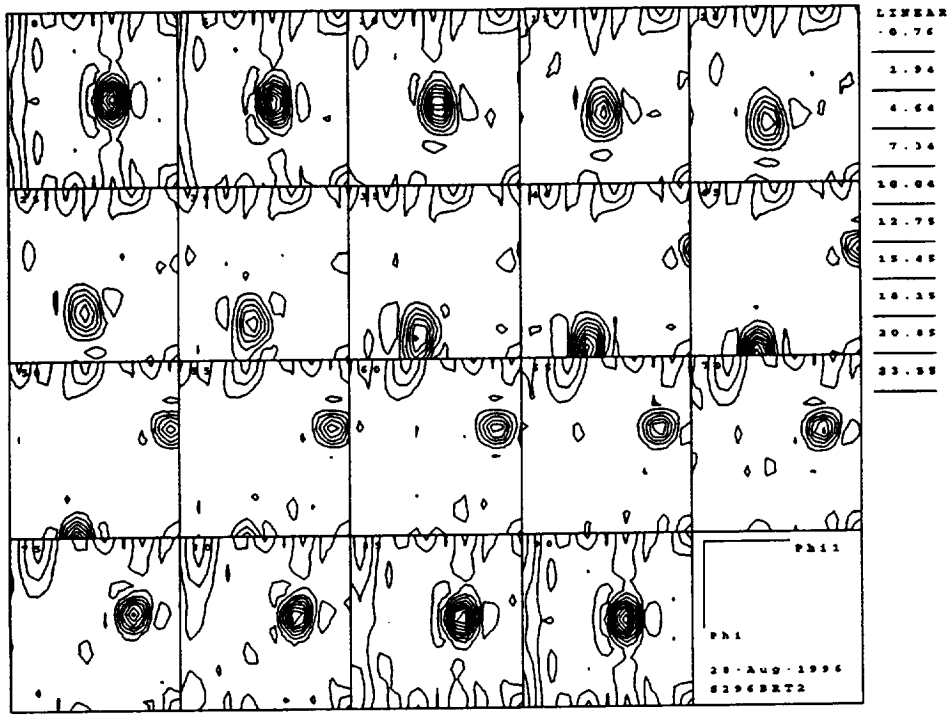

(b) Sections: φ_2= 45°; φ_2= 90°

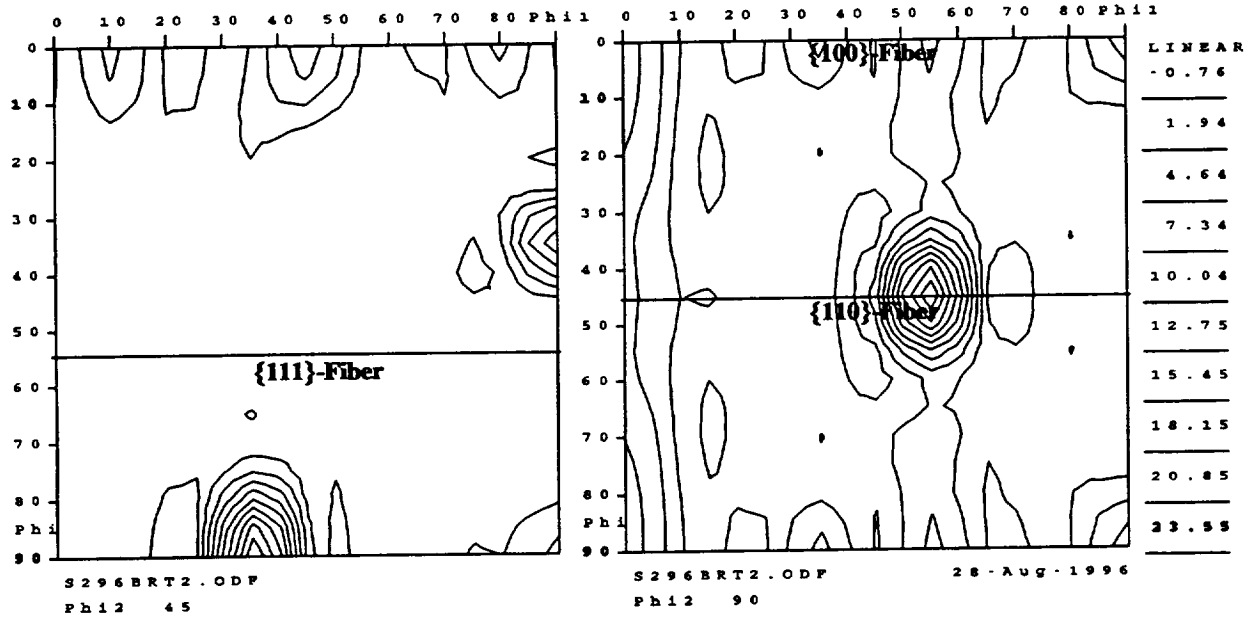

Figure 90. CODF sections for the 2096-T3 extrusion in the base @ t/2; (a), Complete sections: φ_2= 0, 5, 10 ..... 90°; and (b), enlarged φ_2= 45° and φ_2= 90° sections. The locations of the {100}-fiber, {110}-fiber and {111}-fiber are shown.
[Specimen plane perpendicular to (R)adial axis]

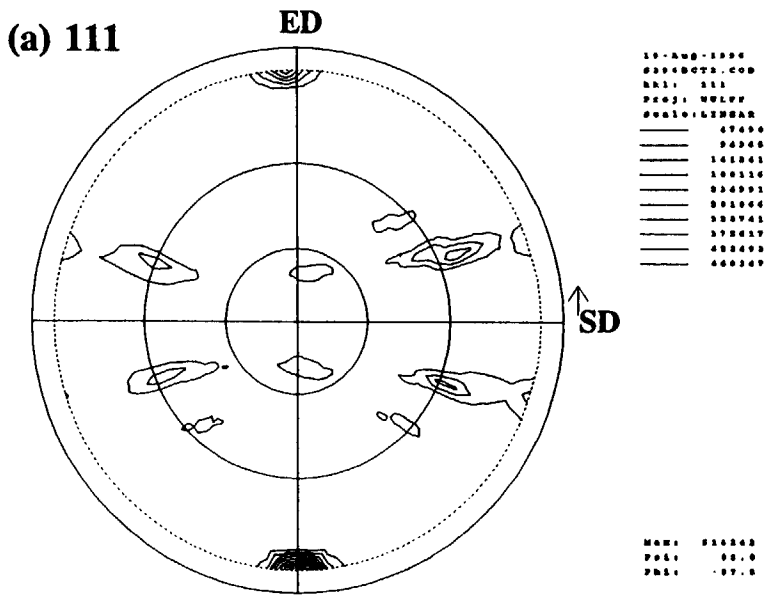

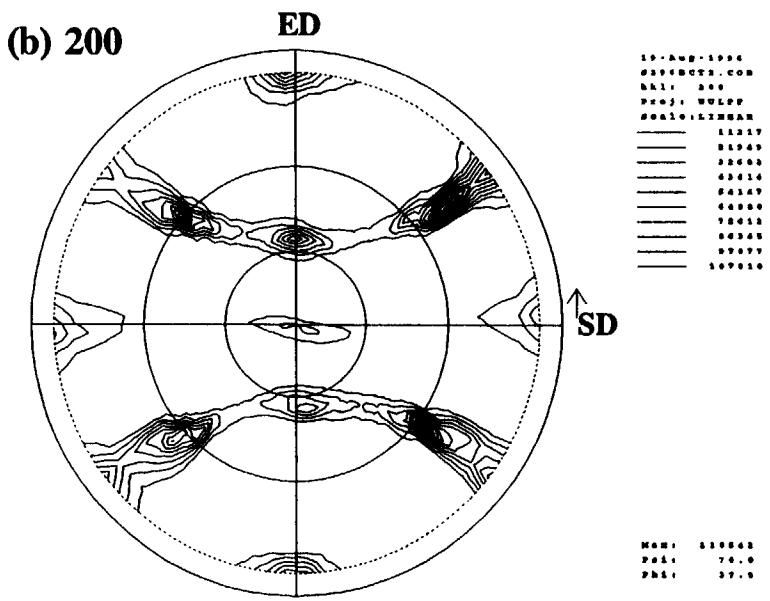

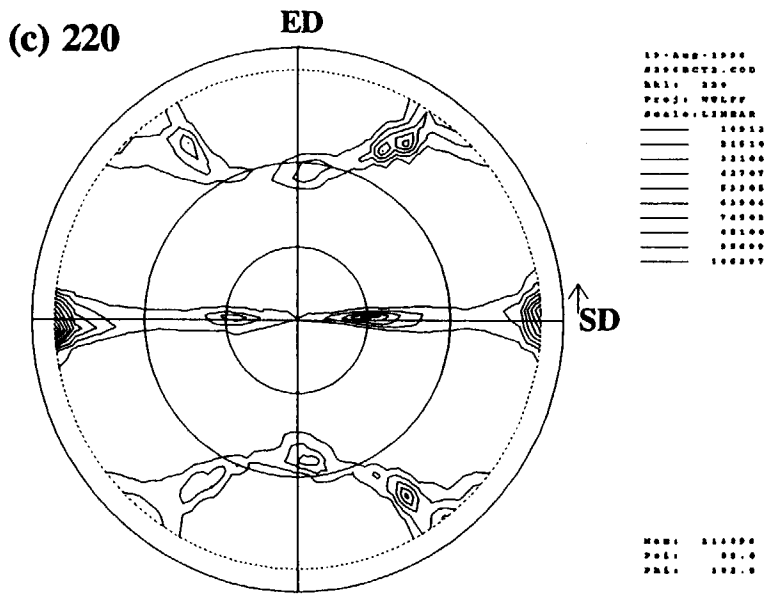

Figure 91.
Partial pole figures for the 2096-T3 extrusion in the base @ t/2: (a) (111); (b) (200); (c) (220). [Specimen plane perpendicular to (C)ircumferential axis]

(a) Sections: φ_2= 0 - 90°

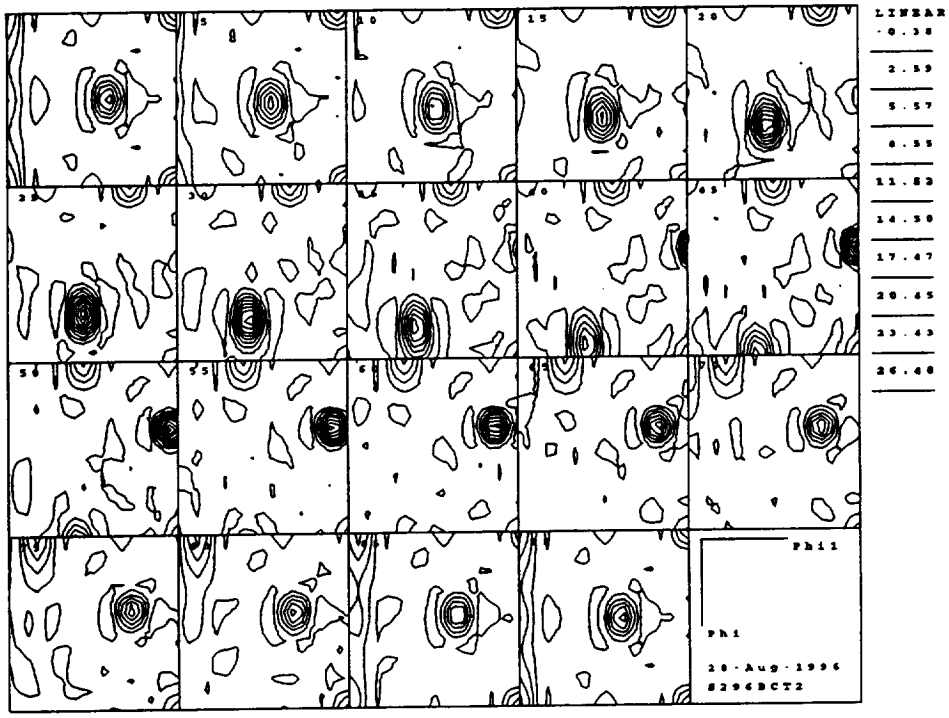

(b) Sections: φ_2= 45°; φ_2= 90°

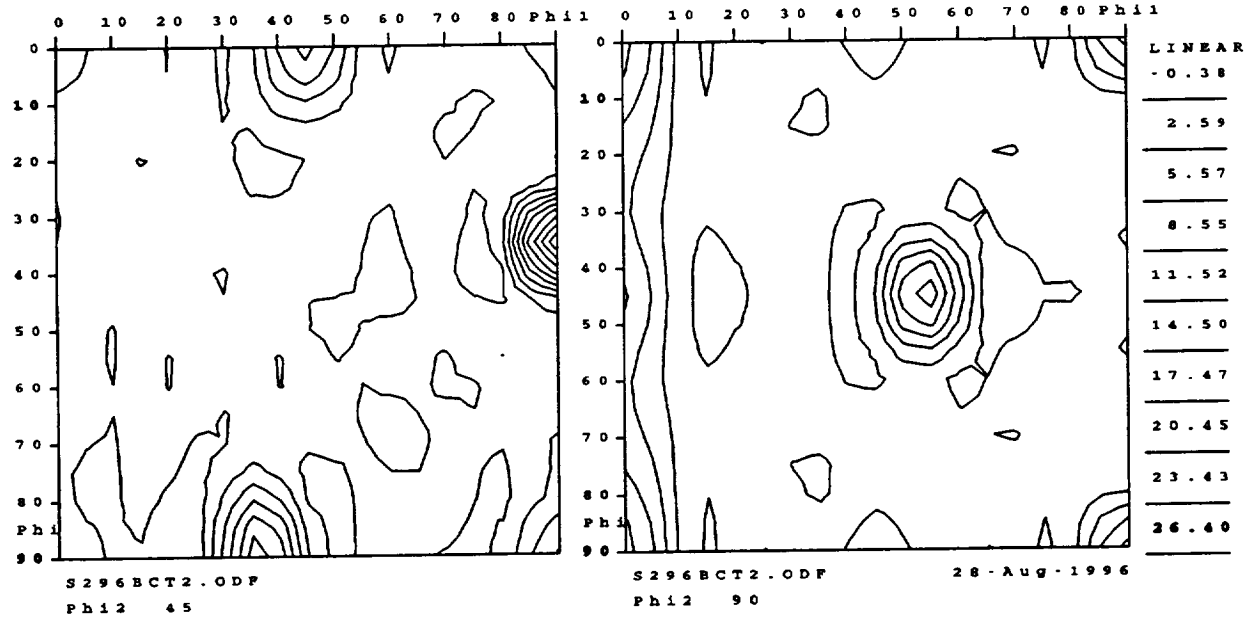

Figure 92. CODF sections for the 2096-T3 extrusion in the base @ t/2; (a), Complete sections: φ_2= 0, 5, 10 ..... 90°; and (b), enlarged φ_2= 45° and φ_2= 90° sections. [Specimen plane perpendicular to (C)ircumferential axis]

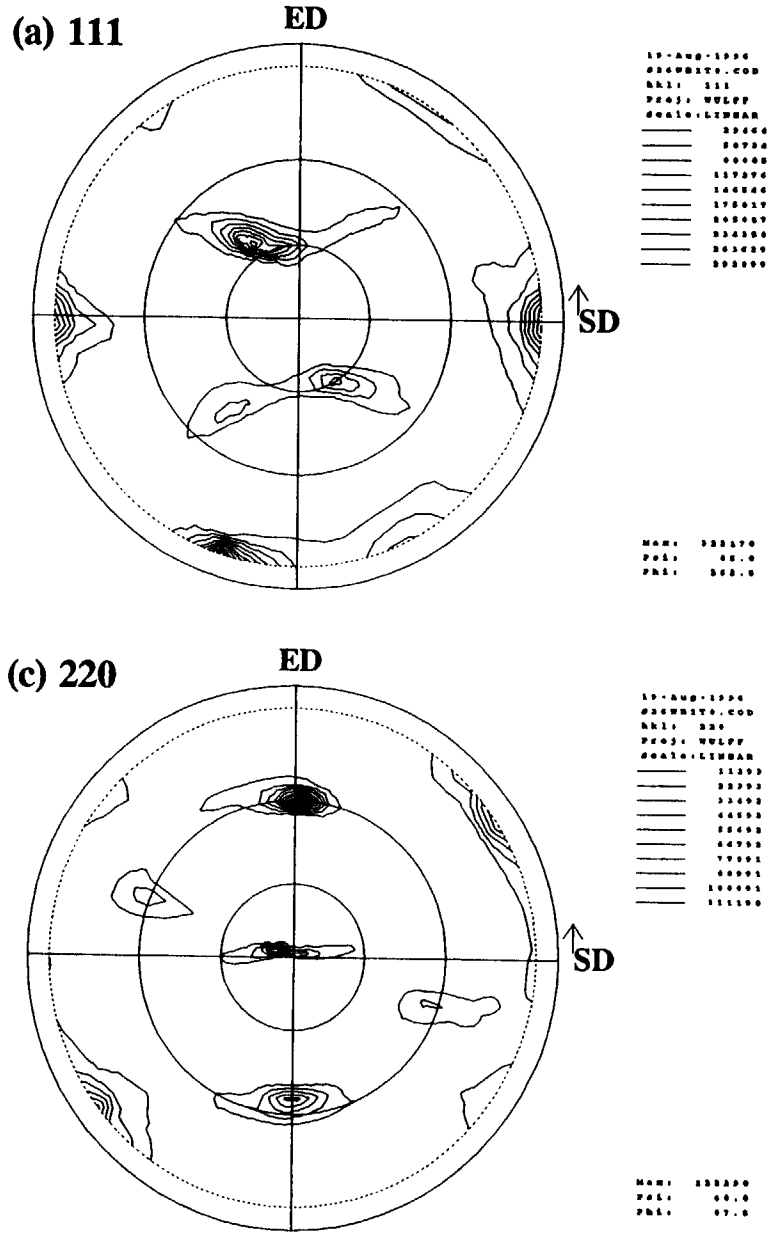

Figure 93.
Partial pole figures for the 2096-T3 extrusion in the web @ t/8: (a) (111); (b) (200); (c) (220). [Specimen plane perpendicular to (C)ircumferential axis]

(a) Sections: φ_2= 0 - 90°

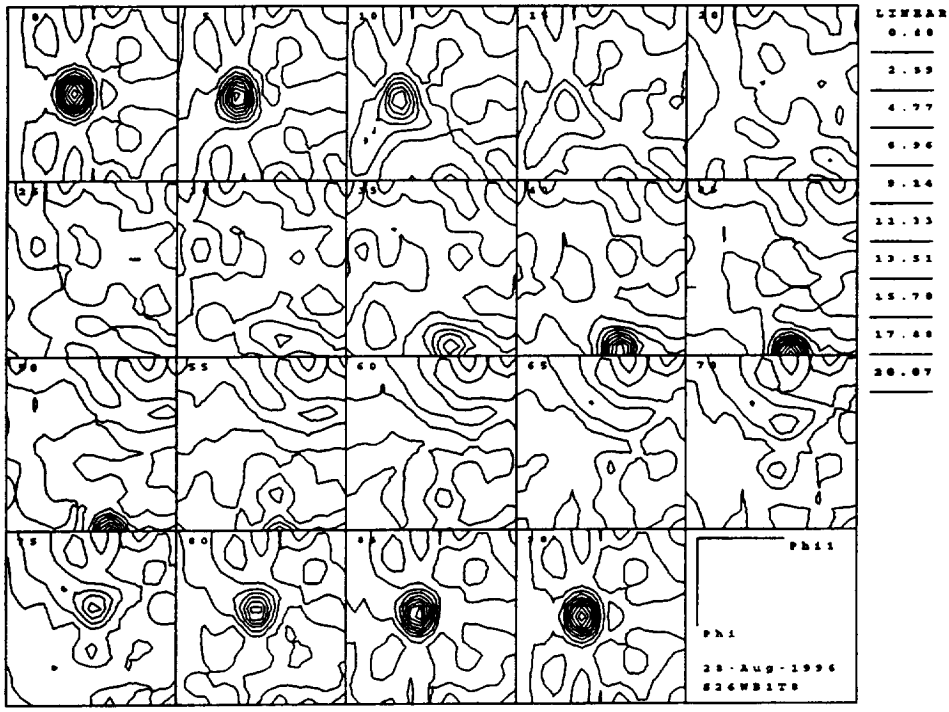

(b) Sections: φ_2= 45°; φ_2= 90°

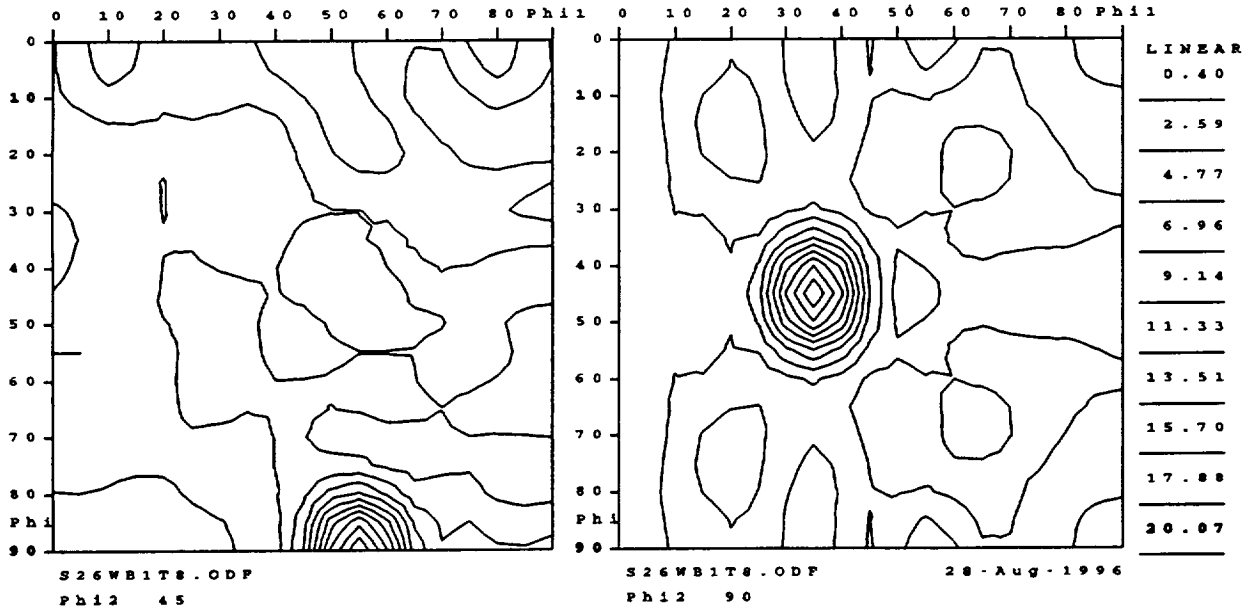

Figure 94. CODF sections for the 2096-T3 extrusion in the web @ t/8; (a), Complete sections: φ_2= 0, 5, 10 ..... 90°; and (b), enlarged φ_2= 45° and φ_2= 90° sections. [Specimen plane perpendicular to (C)ircumferential axis]

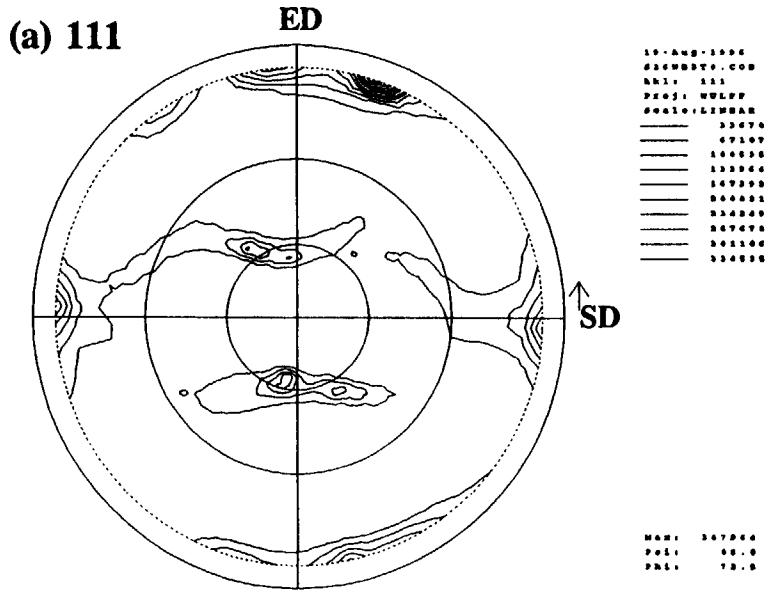

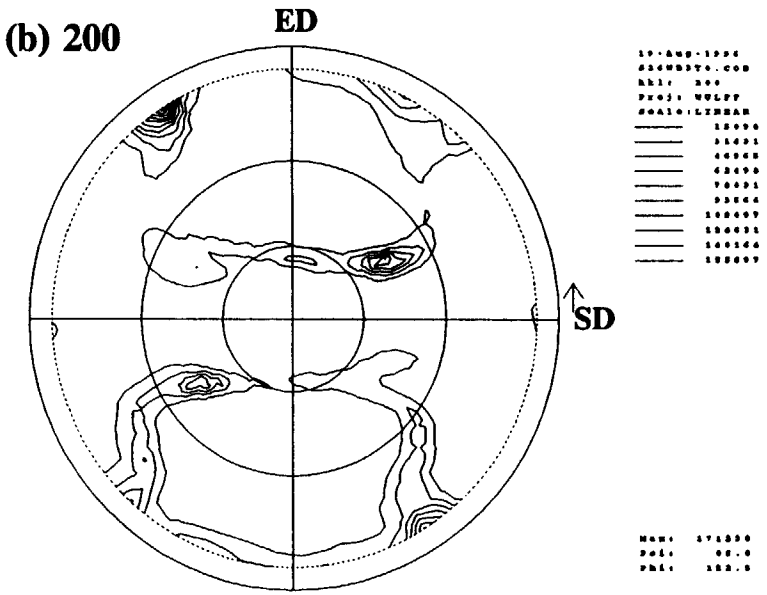

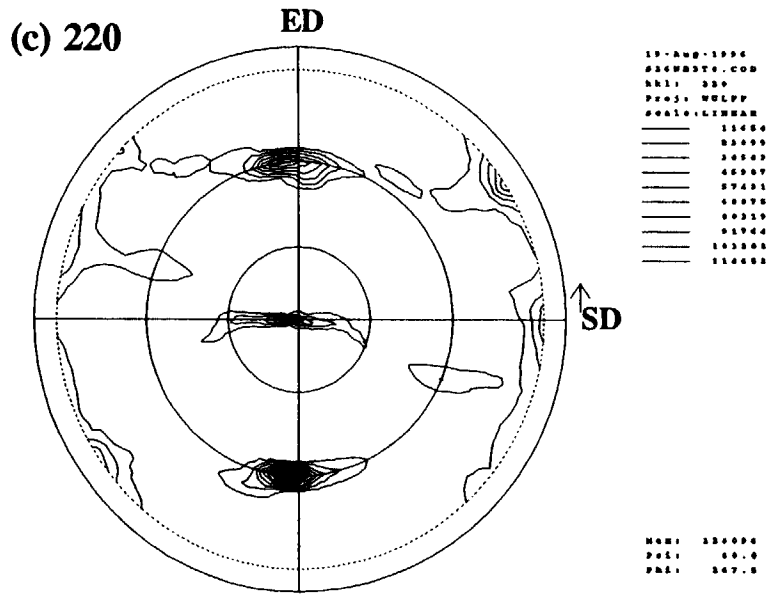

Figure 95.
Partial pole figures for the 2096-T3 extrusion in the web @ 3t/8: (a) (111); (b) (200); (c) (220). [Specimen plane perpendicular to (C)ircumferential axis]

(a) Sections: $\varphi_2 = 0 - 90°$

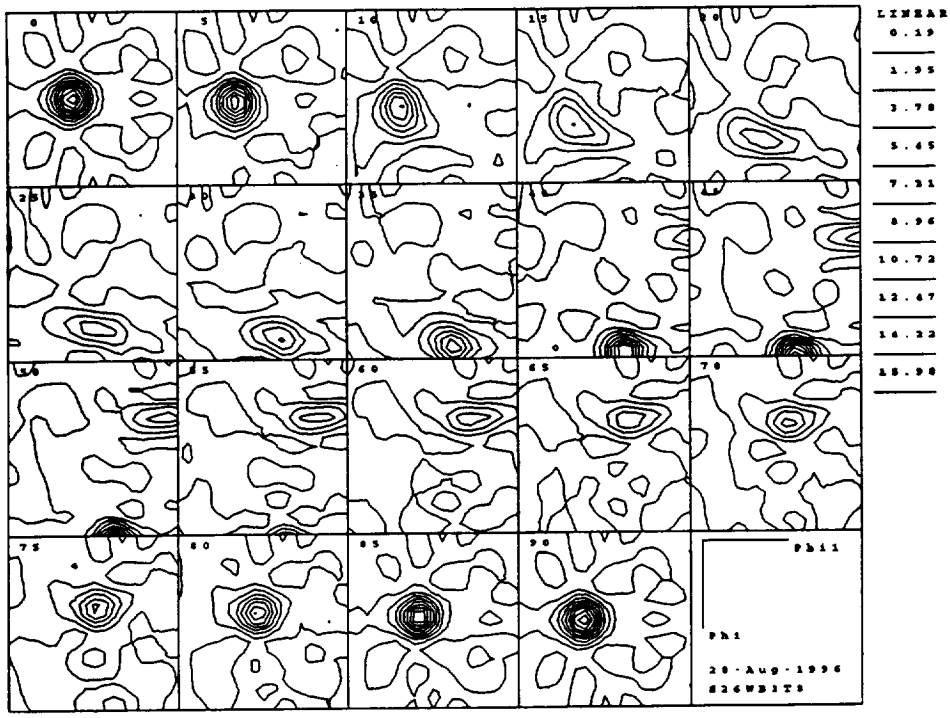

(b) Sections: $\varphi_2 = 45°$; $\varphi_2 = 90°$

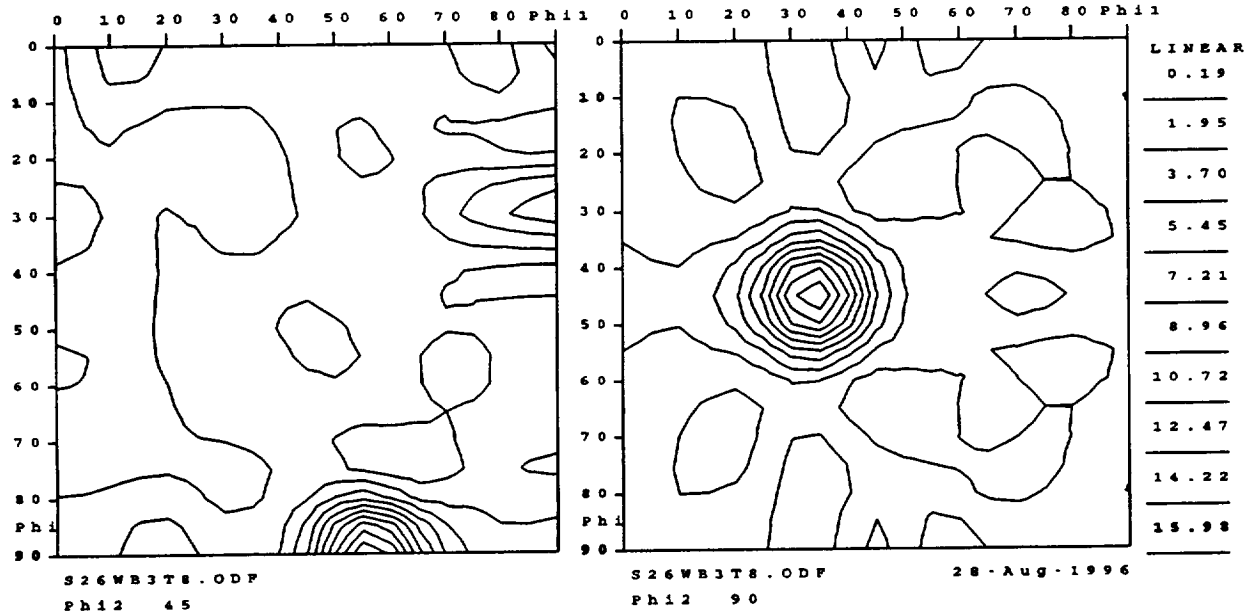

Figure 96. CODF sections for the 2096-T3 extrusion in the web @ 3t/8; (a), Complete sections: $\varphi_2 = 0, 5, 10 \ldots 90°$; and (b), enlarged $\varphi_2 = 45°$ and $\varphi_2 = 90°$ sections. [Specimen plane perpendicular to (C)ircumferential axis]

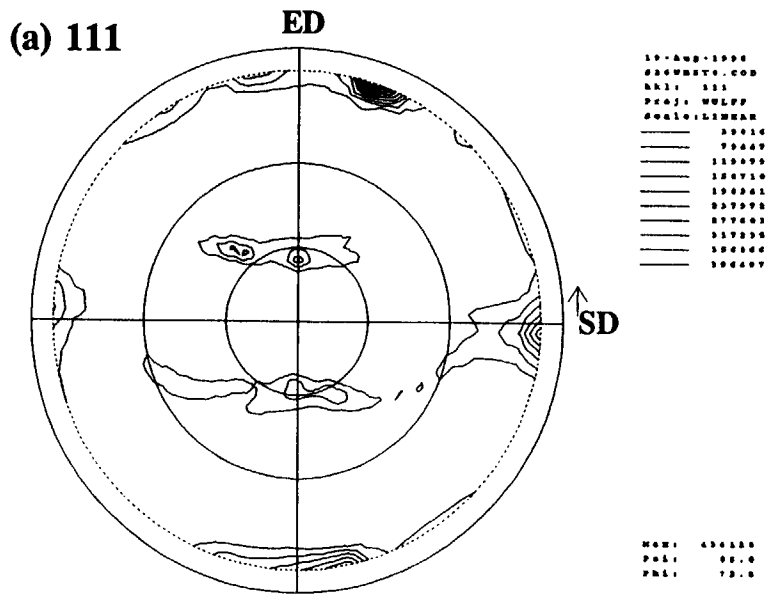

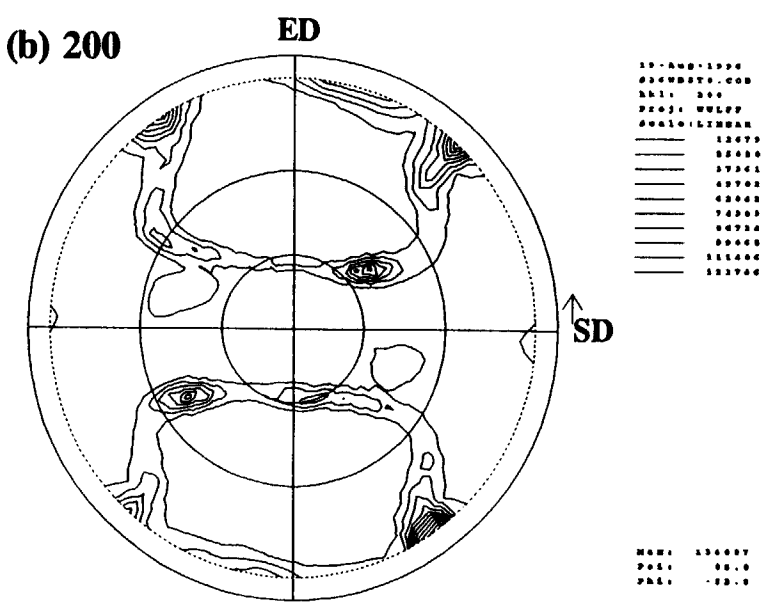

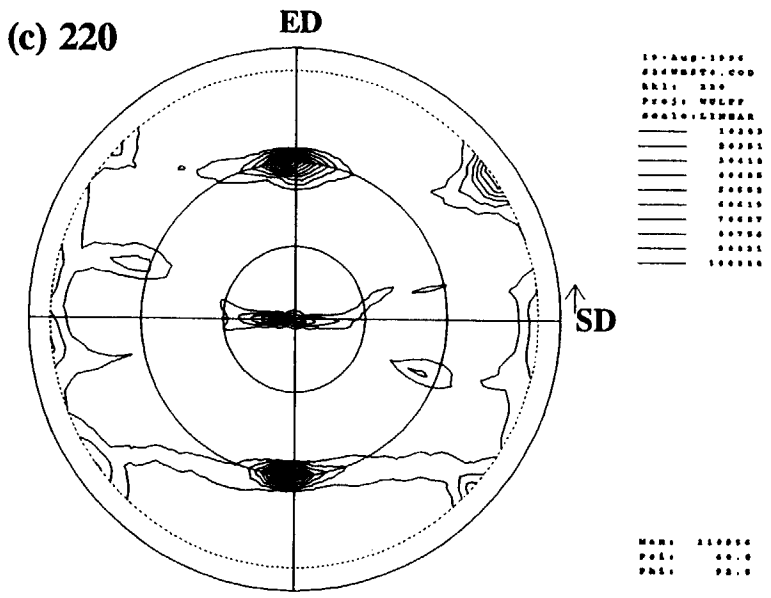

Figure 97.
Partial pole figures for the 2096-T3 extrusion in the web @ 5t/8: (a) (111); (b) (200); (c) (220). [Specimen plane perpendicular to (C)ircumferential axis]

(a) Sections: φ_2= 0 - 90°

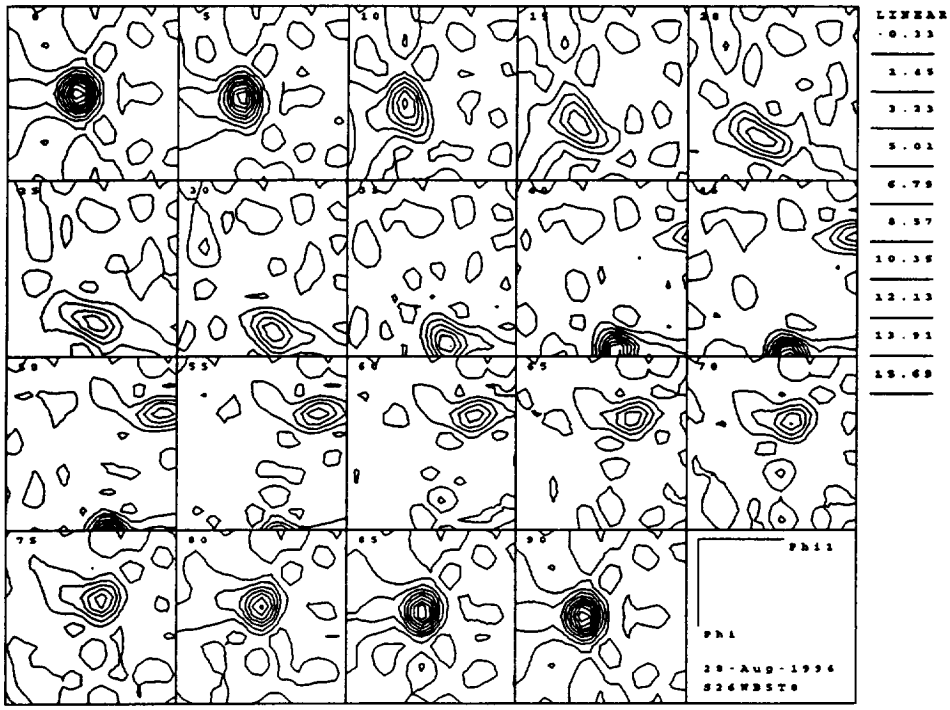

(b) Sections: φ_2= 45°; φ_2= 90°

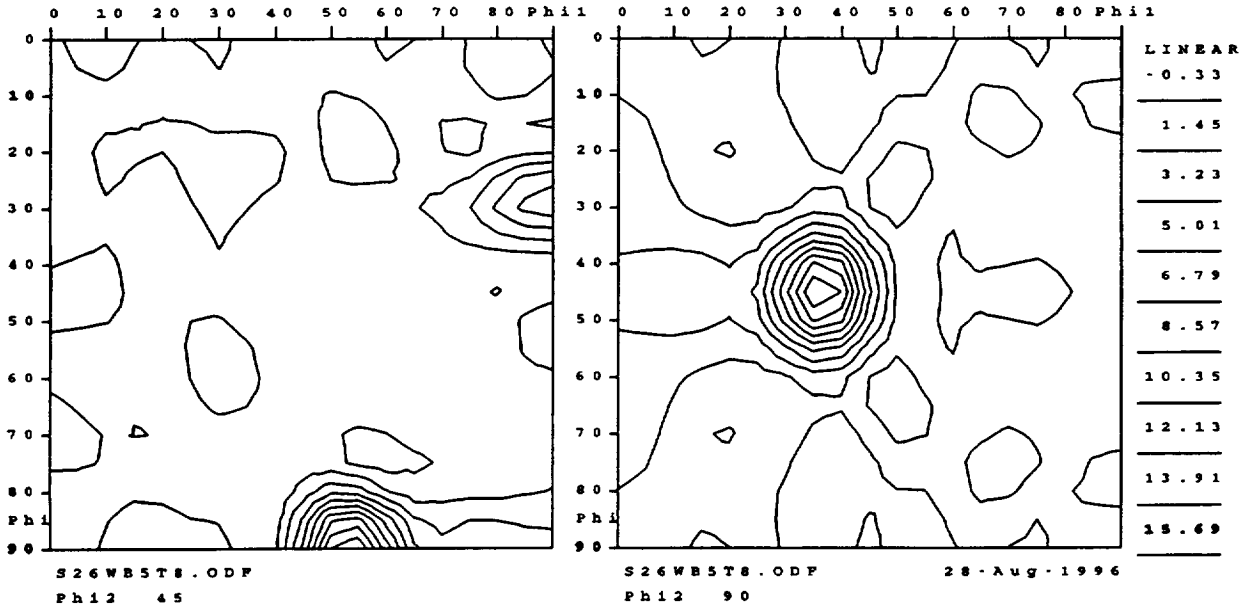

Figure 98. CODF sections for the 2096-T3 extrusion in the web @ 5t/8; (a), Complete sections: φ_2= 0, 5, 10 ..... 90°; and (b), enlarged φ_2= 45° and φ_2= 90° sections. [Specimen plane perpendicular to (C)ircumferential axis]

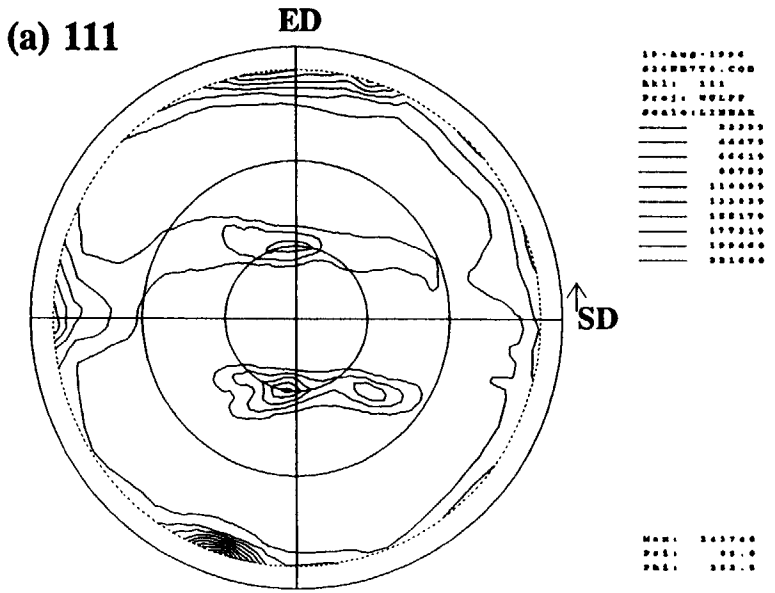

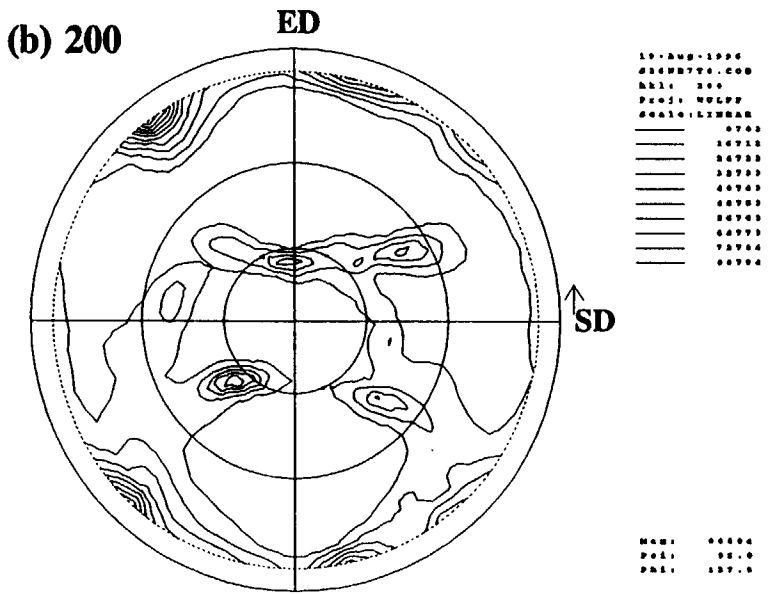

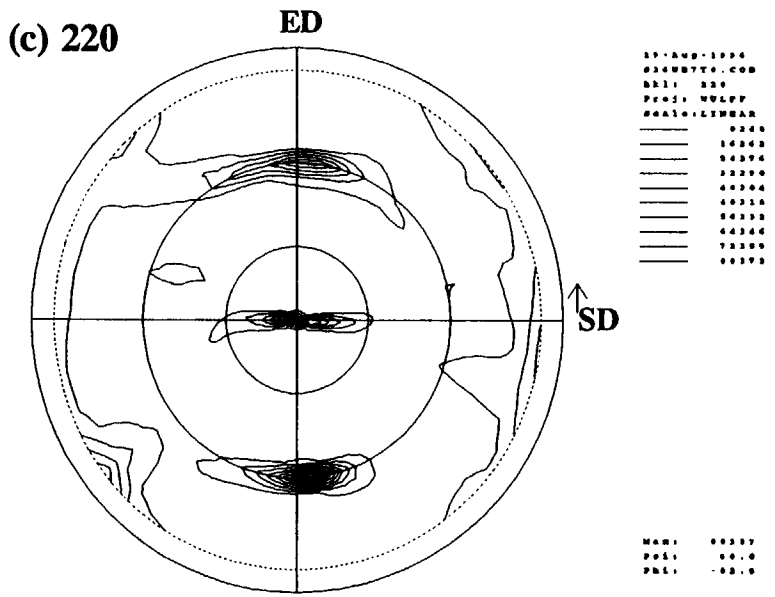

Figure 99.
Partial pole figures for the 2096-T3 extrusion in the web @ 7t/8: (a) (111); (b) (200); (c) (220). [Specimen plane perpendicular to (C)ircumferential axis]

(a) Sections: φ_2= 0 - 90°

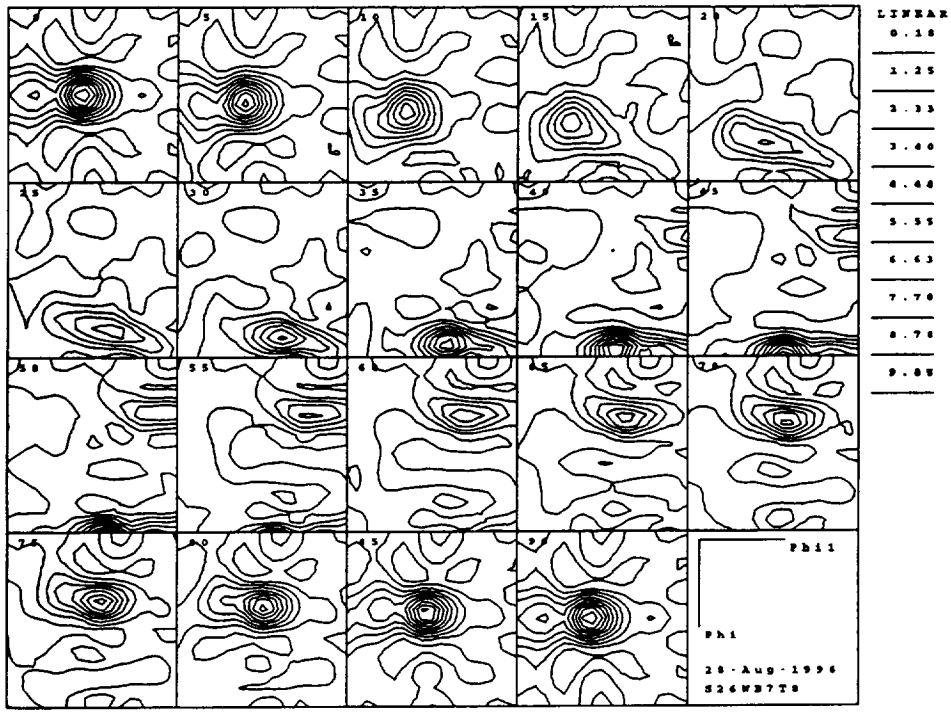

(b) Sections: φ_2= 45°; φ_2= 90°

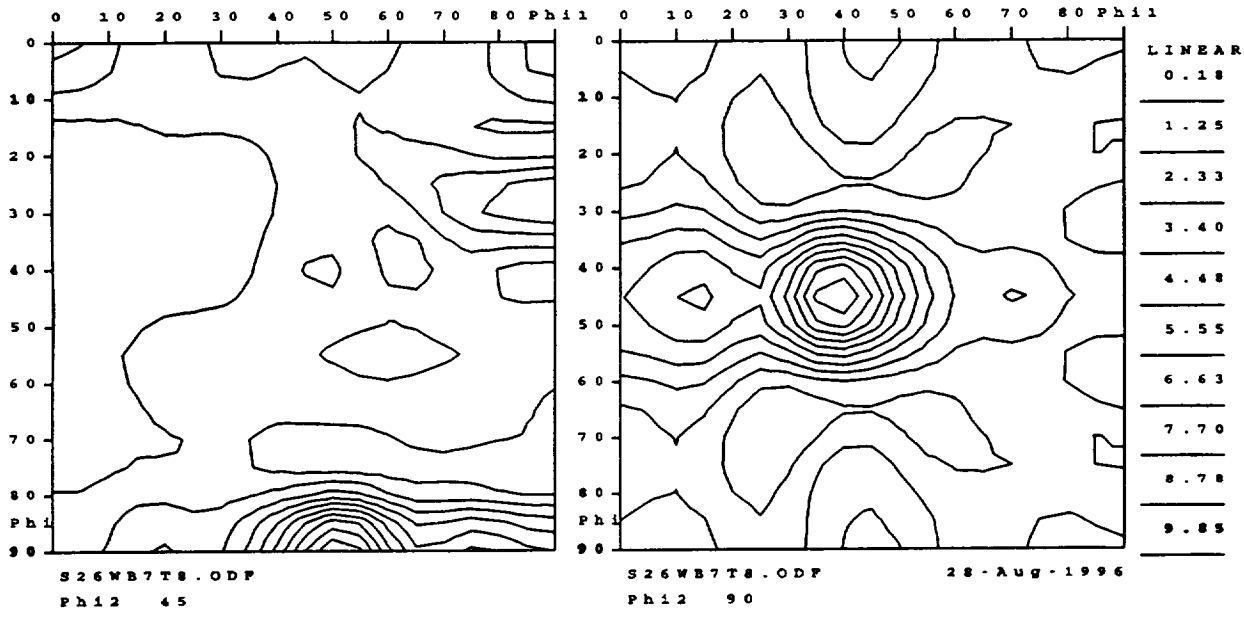

Figure 100. CODF sections for the 2096-T3 extrusion in the web @ 7t/8; (a), Complete sections: φ_2= 0, 5, 10 ..... 90°; and (b), enlarged φ_2= 45° and φ_2= 90° sections. [Specimen plane perpendicular to (C)ircumferential axis]

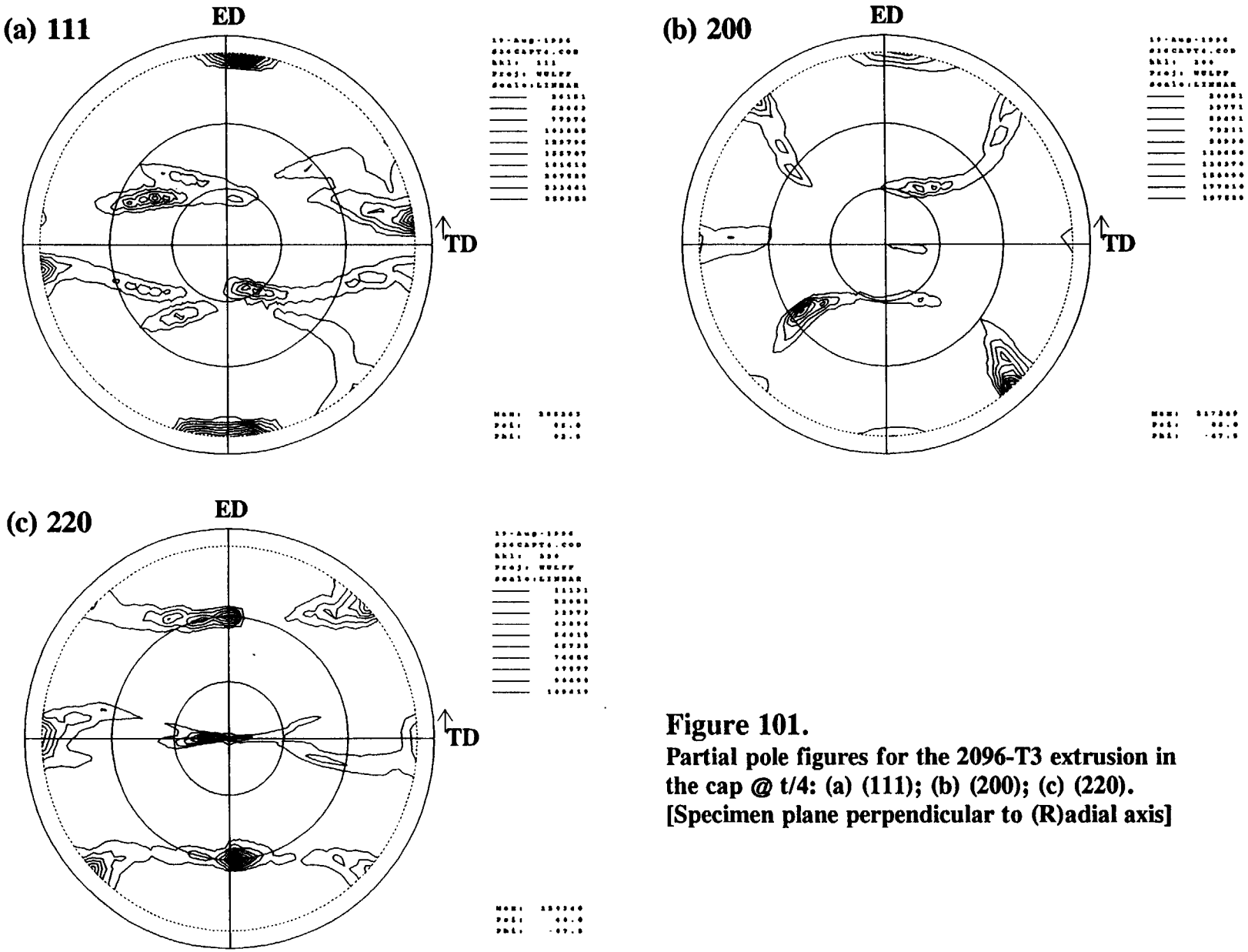

Figure 101.
Partial pole figures for the 2096-T3 extrusion in the cap @ t/4: (a) (111); (b) (200); (c) (220). [Specimen plane perpendicular to (R)adial axis]

(a) Sections: $\varphi_2 = 0 - 90°$

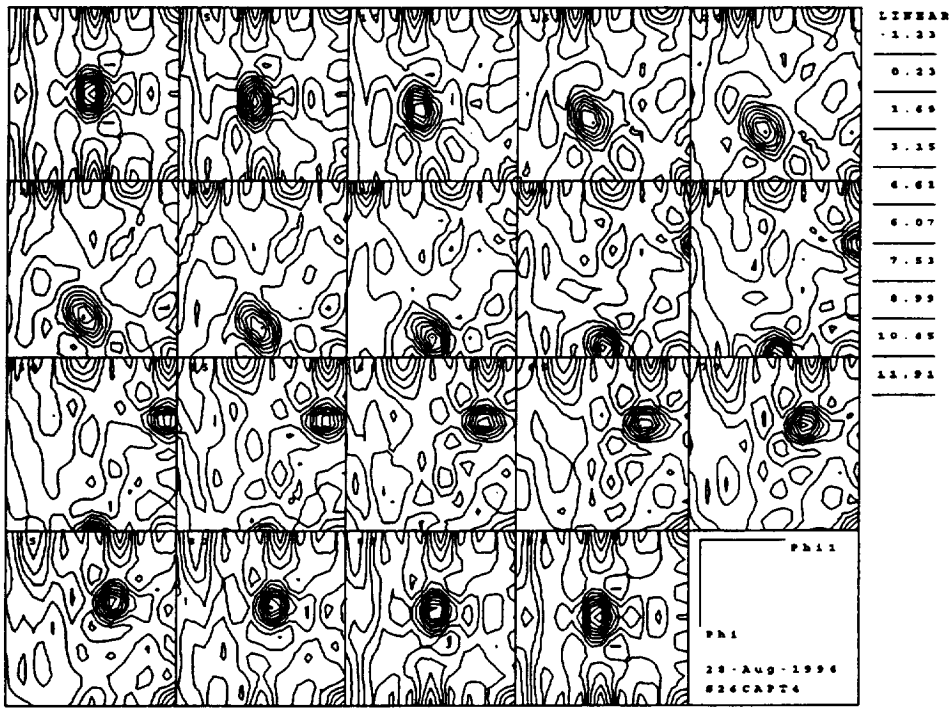

(b) Sections: $\varphi_2 = 45°$; $\varphi_2 = 90°$

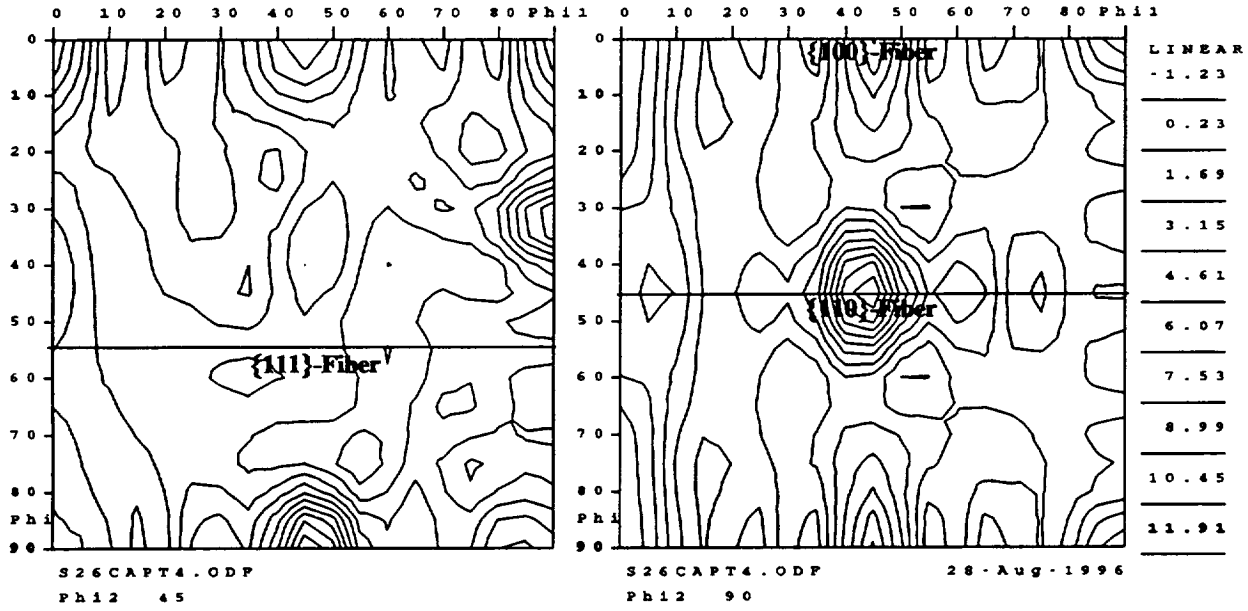

Figure 102. CODF sections for the 2096-T3 extrusion in the cap @ t/4; (a), Complete sections: $\varphi_2 = 0, 5, 10 \ldots 90°$; and (b), enlarged $\varphi_2 = 45°$ and $\varphi_2 = 90°$ sections. The locations of the {100}-fiber, {110}-fiber and {111}-fiber are shown.
[Specimen plane perpendicular to (R)adial axis]

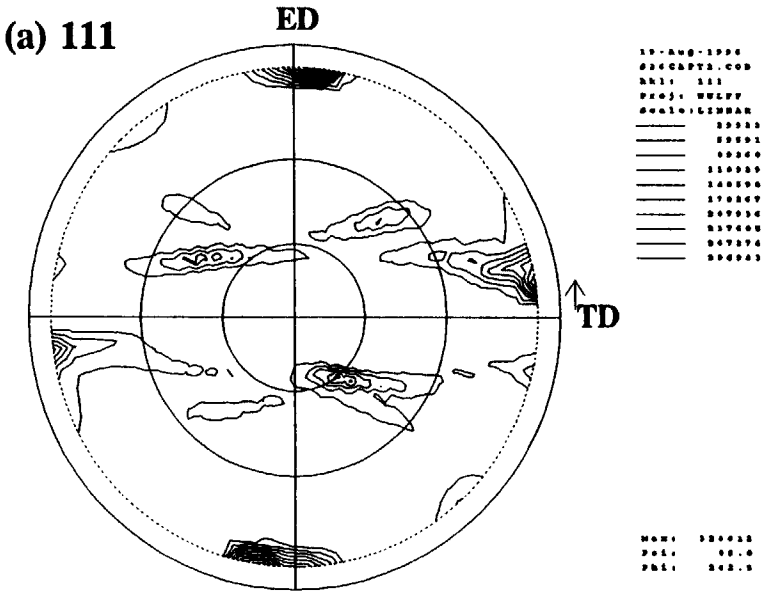

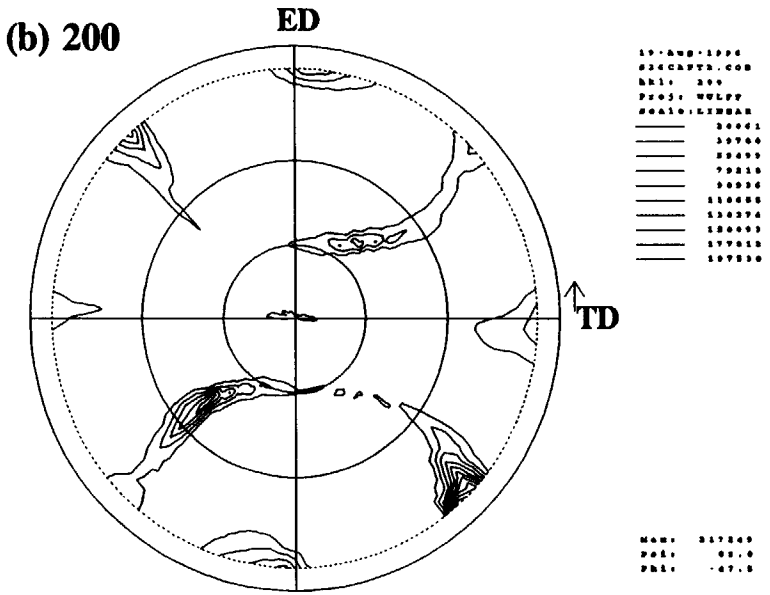

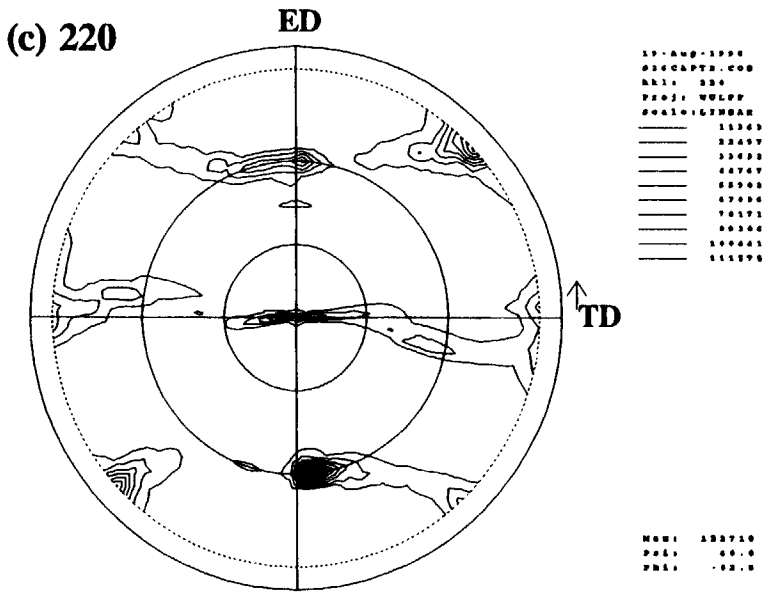

Figure 103.
Partial pole figures for the 2096-T3 extrusion in the cap @ t/2: (a) (111); (b) (200); (c) (220). [Specimen plane perpendicular to (R)adial axis]

(a) Sections: $\varphi_2 = 0 - 90°$

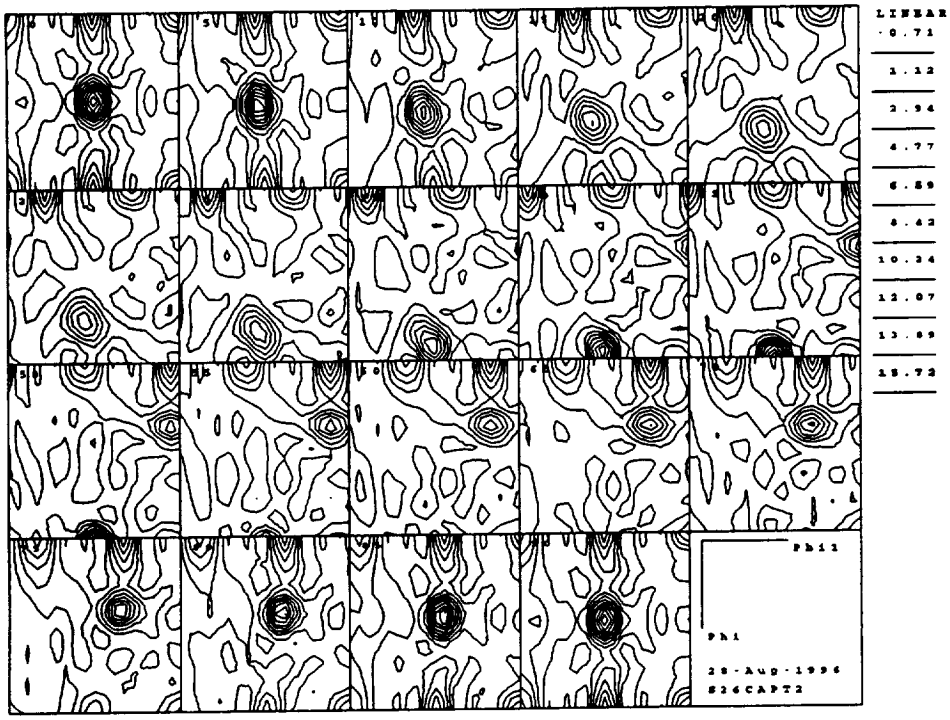

(b) Sections: $\varphi_2 = 45°$; $\varphi_2 = 90°$

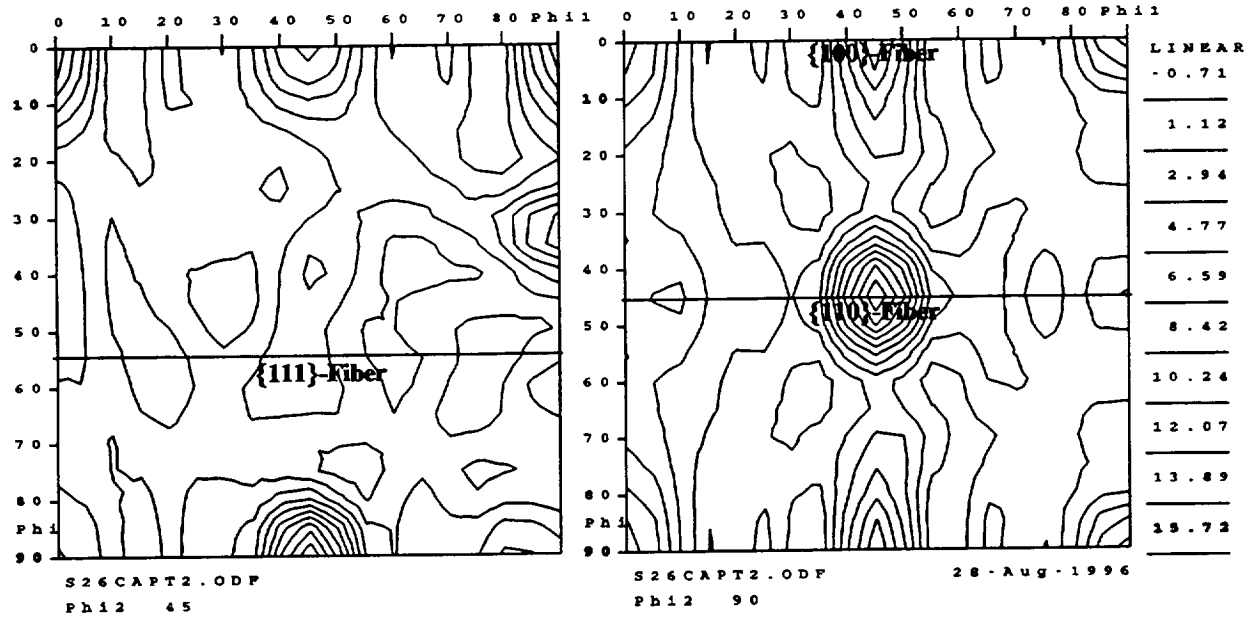

Figure 104. CODF sections for the 2096-T3 extrusion in the cap @ t/2; (a), Complete sections: $\varphi_2 = 0, 5, 10 \ldots 90°$; and (b), enlarged $\varphi_2 = 45°$ and $\varphi_2 = 90°$ sections. The locations of the {100}-fiber, {110}-fiber and {111}-fiber are shown.
[Specimen plane perpendicular to (R)adial axis]

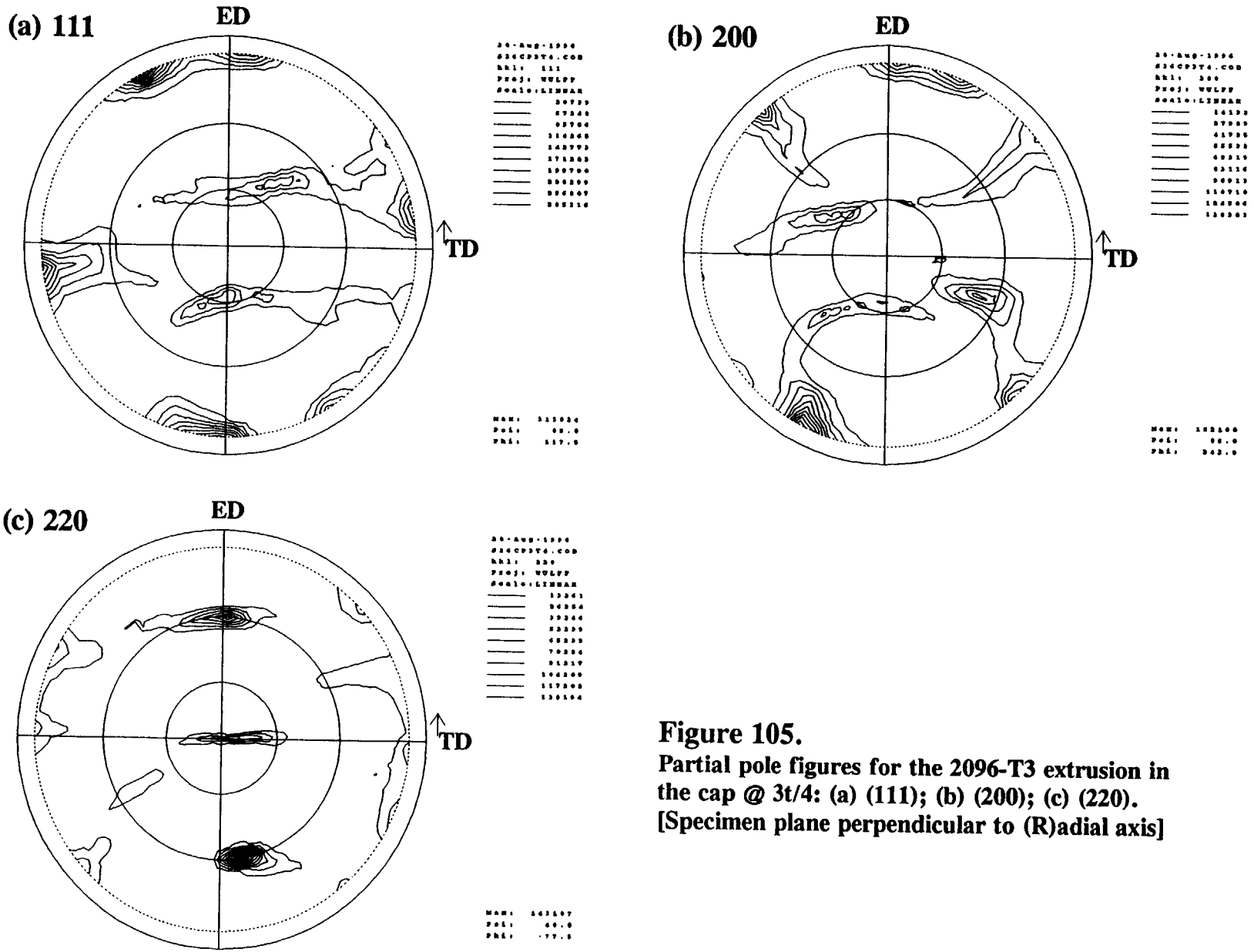

Figure 105.
Partial pole figures for the 2096-T3 extrusion in the cap @ 3t/4: (a) (111); (b) (200); (c) (220). [Specimen plane perpendicular to (R)adial axis]

(a) Sections: φ_2= 0 - 90°

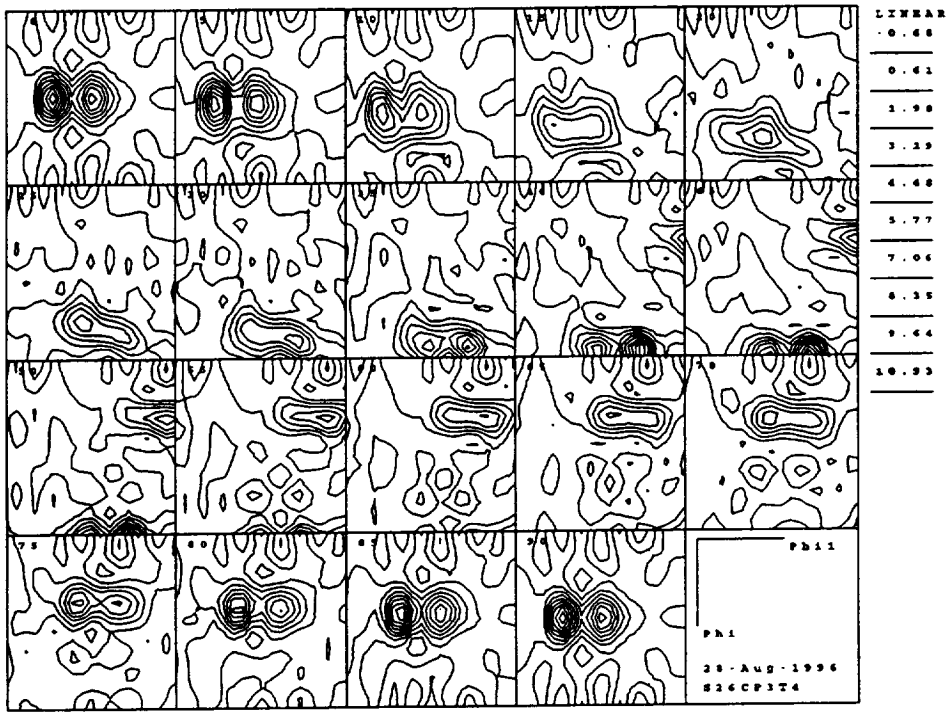

(b) Sections: φ_2= 45°; φ_2= 90°

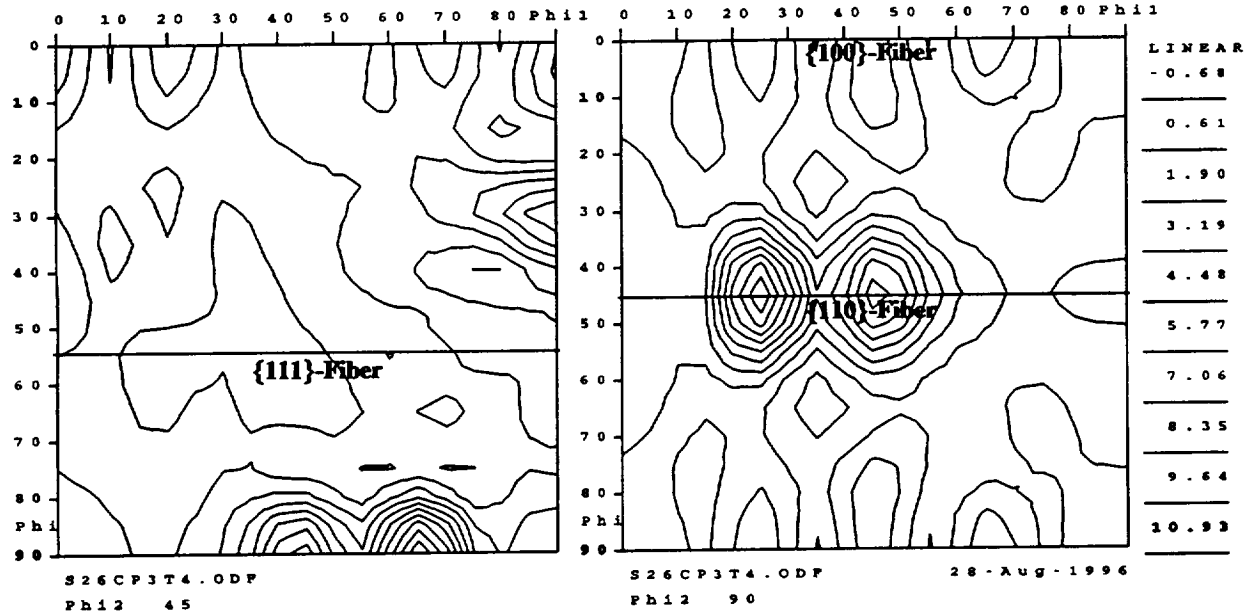

Figure 106. CODF sections for the 2096-T3 extrusion in the cap @ 3t/4; (a), Complete sections: φ_2= 0, 5, 10 ..... 90°; and (b), enlarged φ_2= 45° and φ_2= 90° sections. The locations of the {100}-fiber, {110}-fiber and {111}-fiber are shown.
[Specimen plane perpendicular to (R)adial axis]

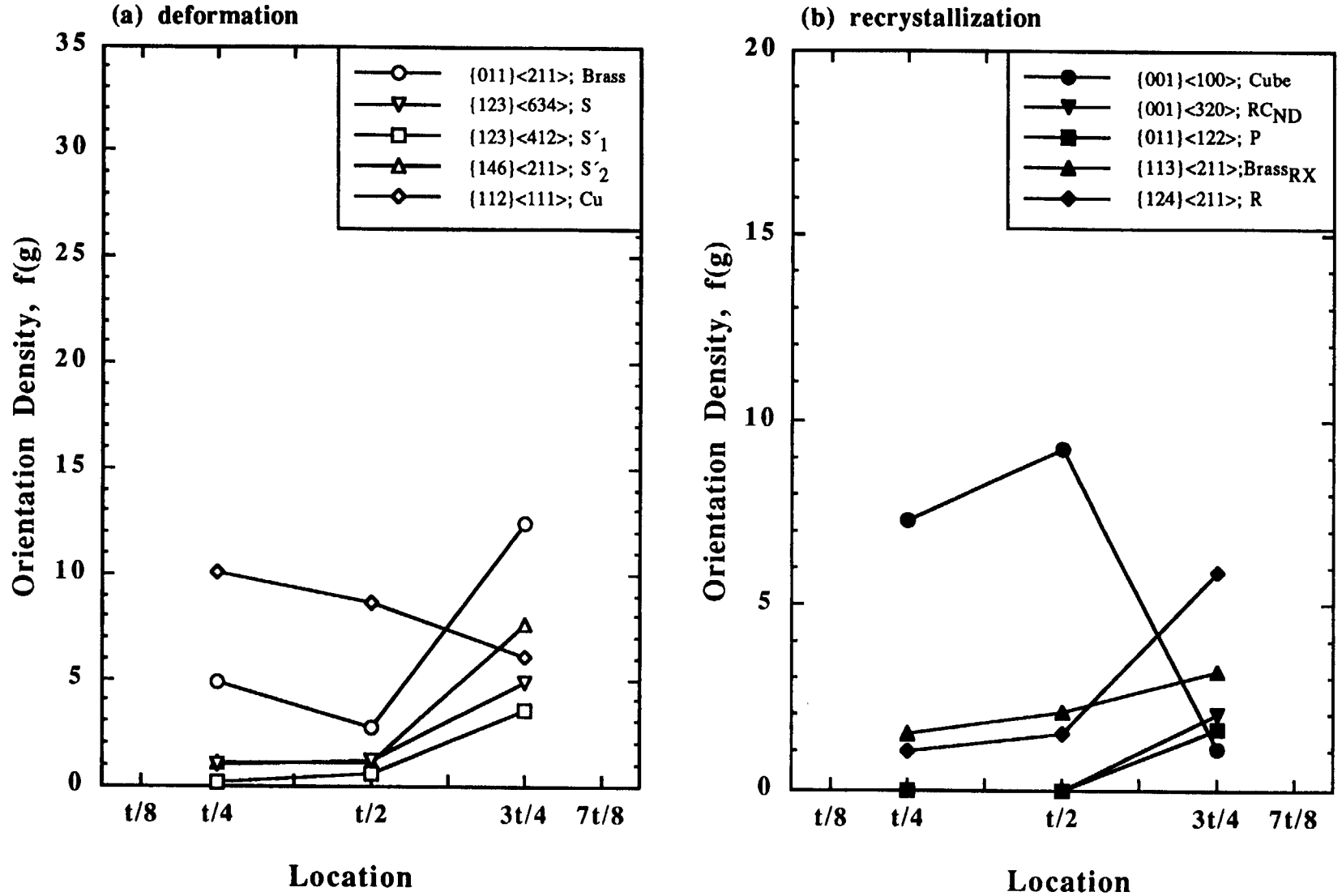

Figure 107. Orientation density, f(g), as a function of location through the cross-section for the 2096-T3 extrusion in the cap region: (a) Deformation-related components; (b) Recrystallization-related components.

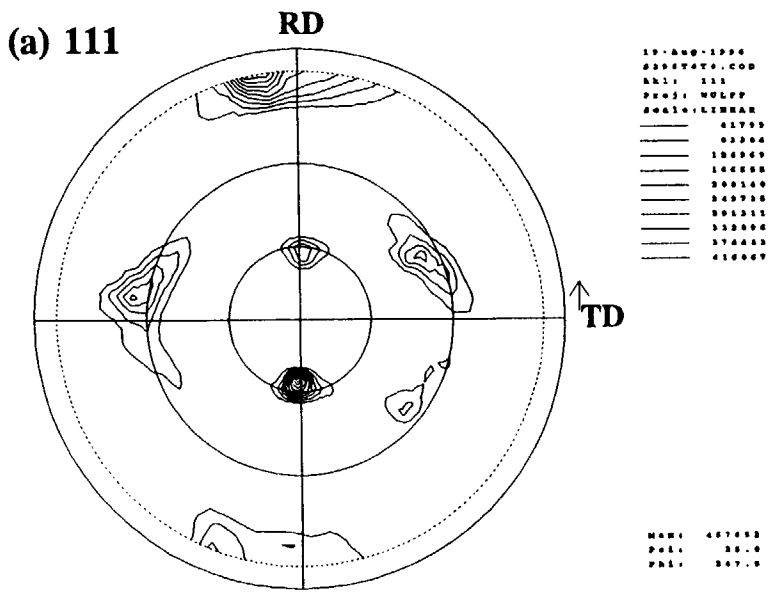

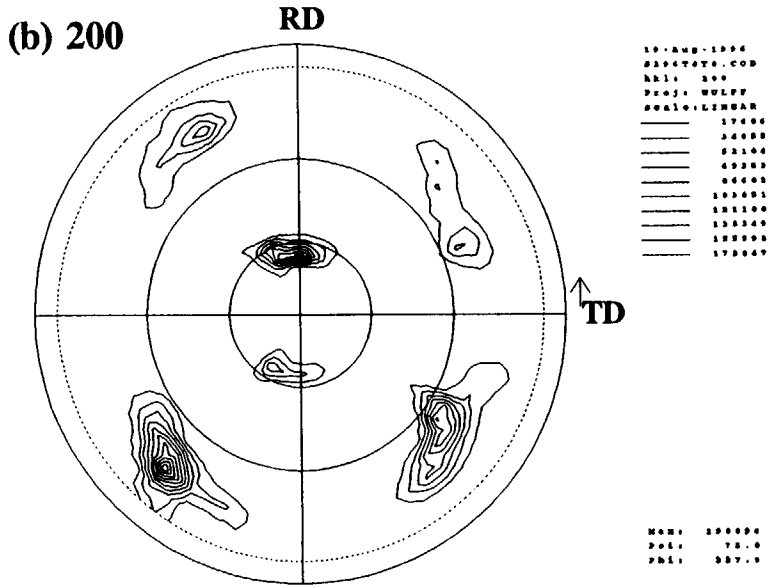

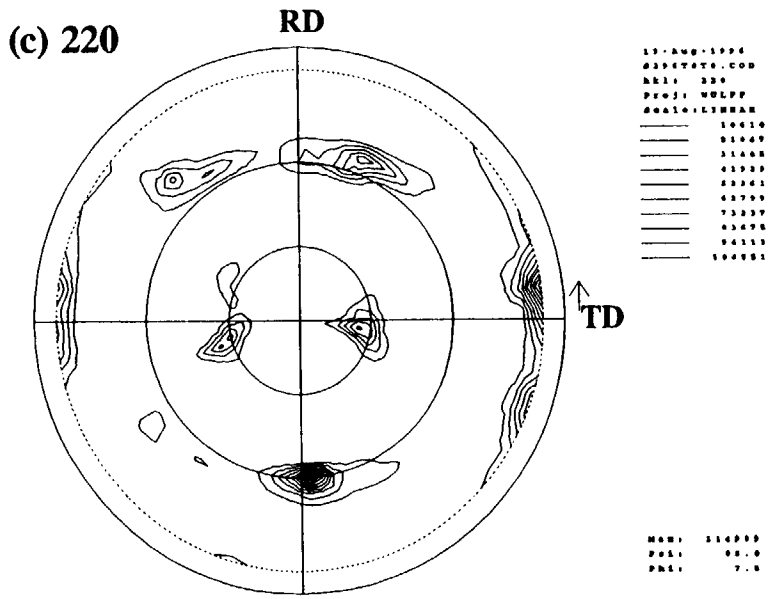

Figure 108.
Partial pole figures for 2096-T8 sheet @ t/8: (a) (111); (b) (200); (c) (220). [Specimen plane perpendicular to (S)hort-Transverse axis]

(a) Sections: φ_2= 0 - 90°

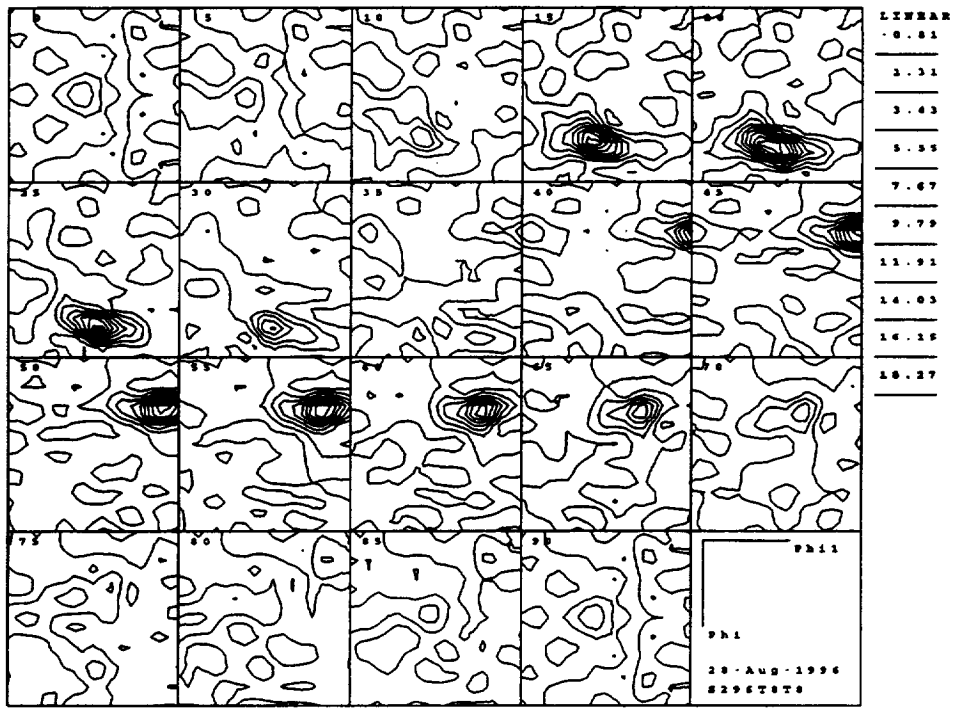

(b) Sections: φ_2= 45°; φ_2= 90°

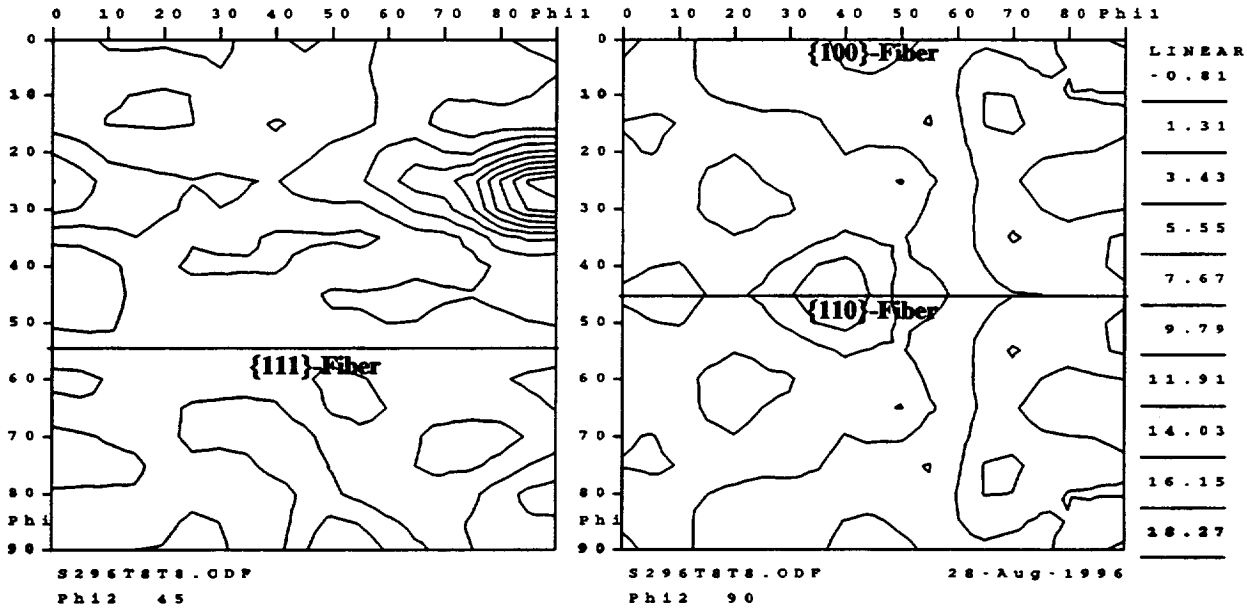

Figure 109. CODF sections for 2096-T8 sheet @ t/8; (a), Complete sections: φ_2= 0, 5, 10 ..... 90°; and (b), enlarged φ_2= 45° and φ_2= 90° sections. The locations of the {100}-fiber, {110}-fiber and {111}-fiber are shown.
[Specimen plane perpendicular to (S)hort-Transverse axis]

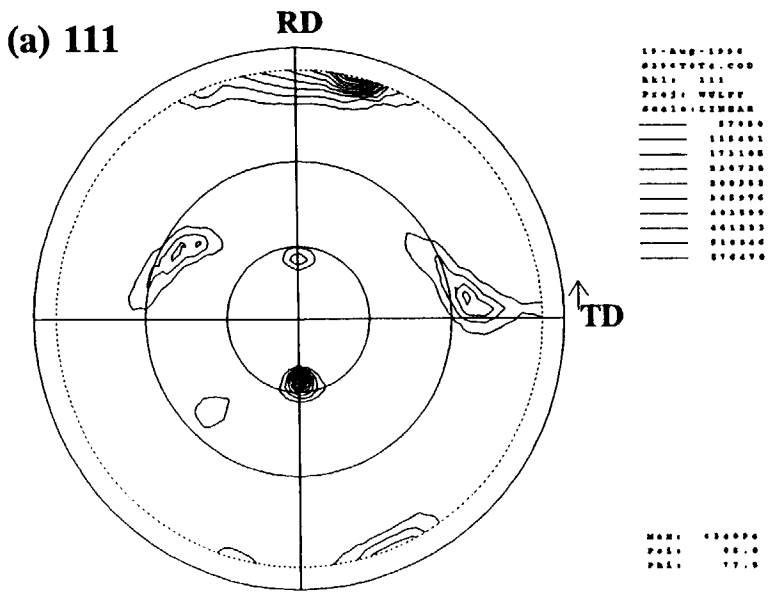

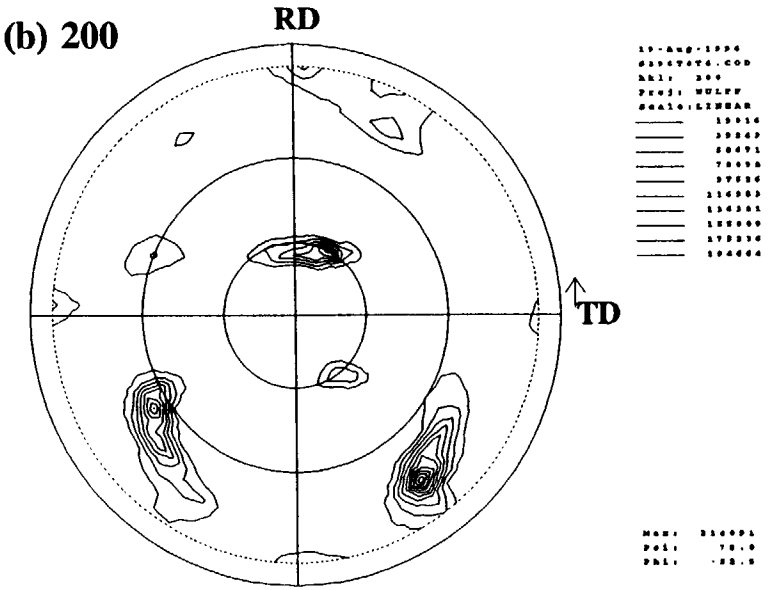

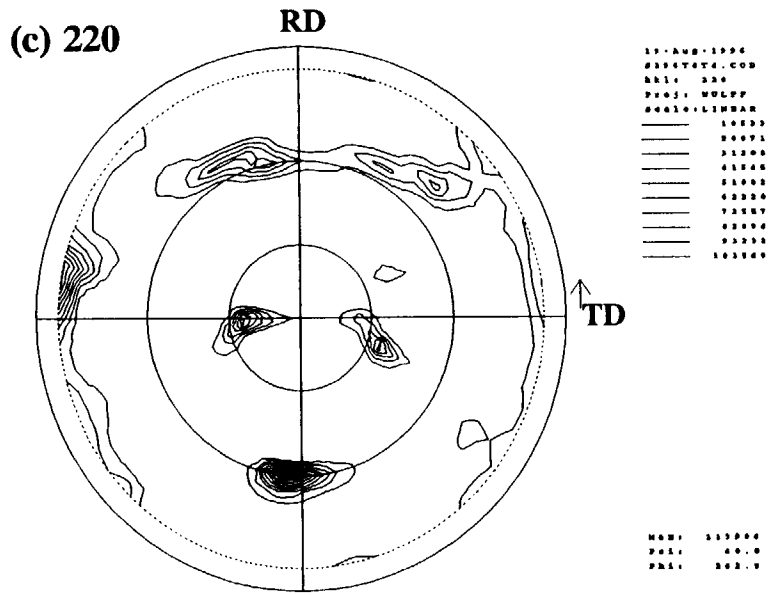

Figure 110.
Partial pole figures for 2096-T8 sheet @ t/4: (a) (111); (b) (200); (c) (220). [Specimen plane perpendicular to (S)hort-Transverse axis]

(a) Sections: φ_2= 0 - 90°

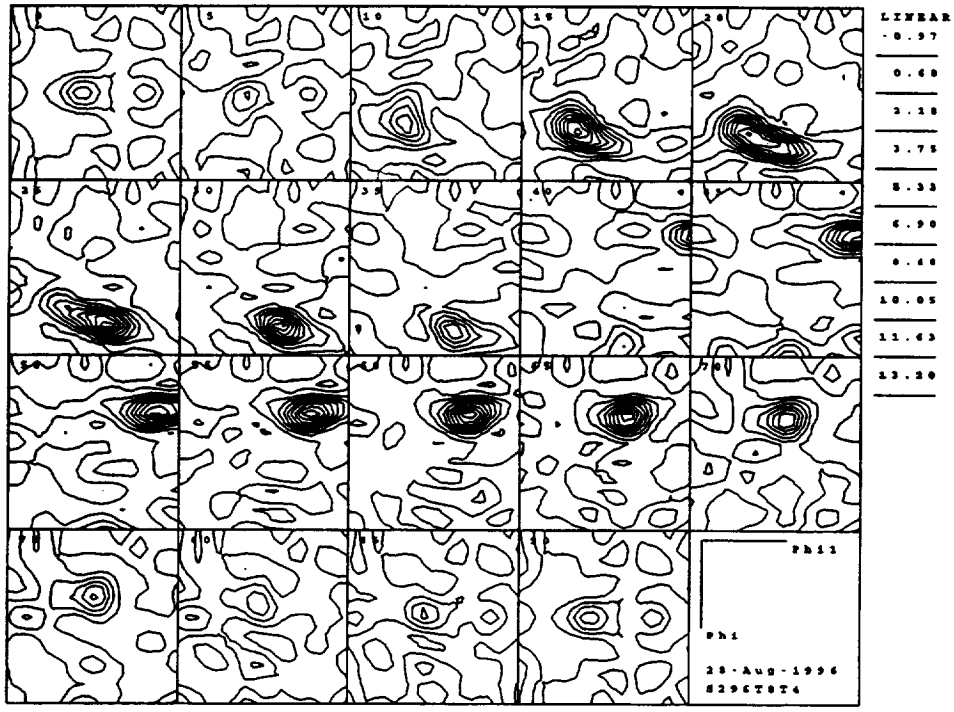

(b) Sections: φ_2= 45°; φ_2= 90°

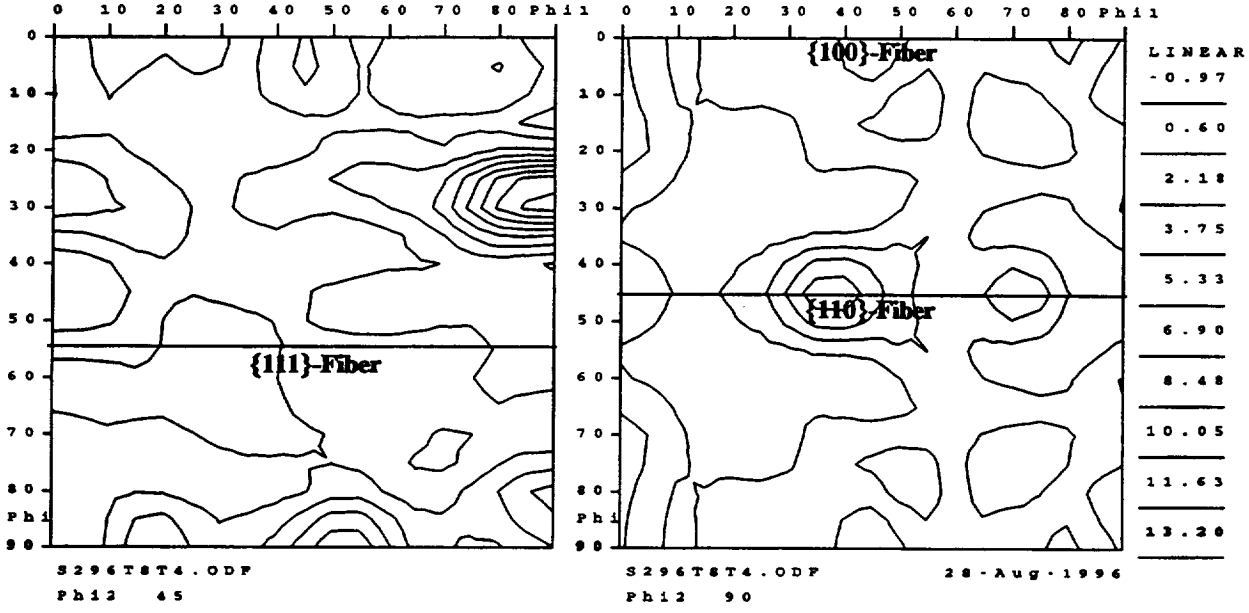

Figure 111. CODF sections for 2096-T8 sheet @ t/4; (a), Complete sections: φ_2= 0, 5, 10 ..... 90°; and (b), enlarged φ_2= 45° and φ_2= 90° sections. The locations of the {100}-fiber, {110}-fiber and {111}-fiber are shown.
[Specimen plane perpendicular to (S)hort-Transverse axis]

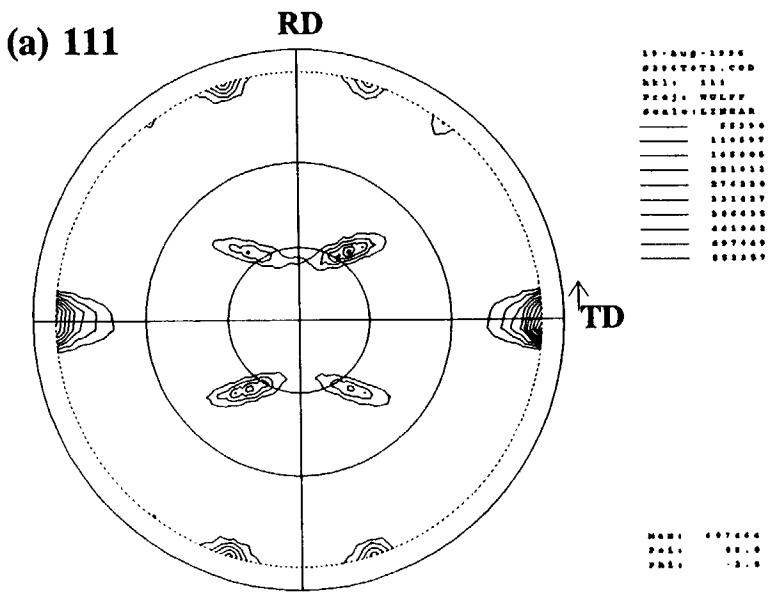

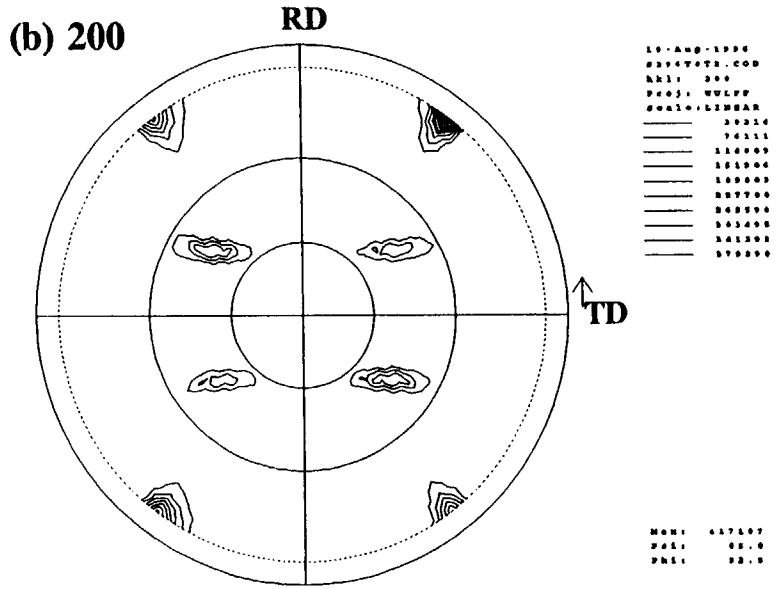

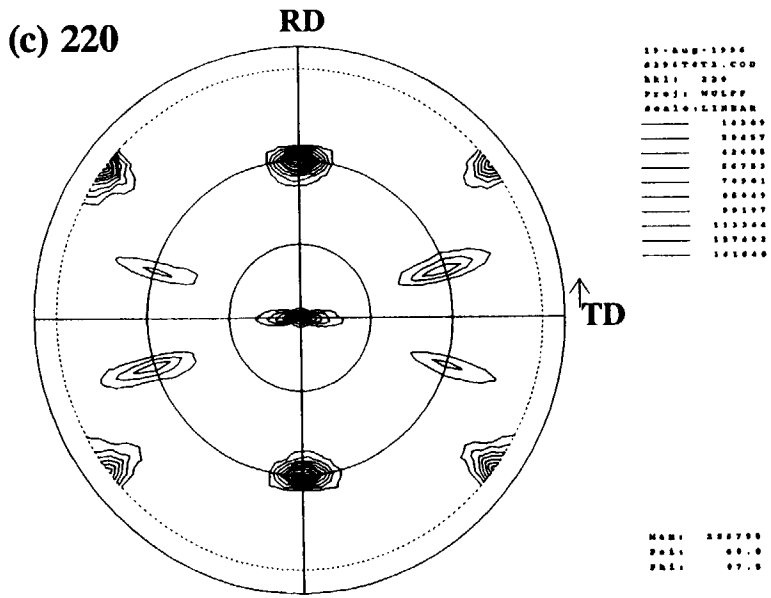

Figure 112.
Partial pole figures for 2096-T8 sheet @ t/2: (a) (111); (b) (200); (c) (220). [Specimen plane perpendicular to (S)hort-Transverse axis]

(a) Sections: φ_2= 0 - 90°

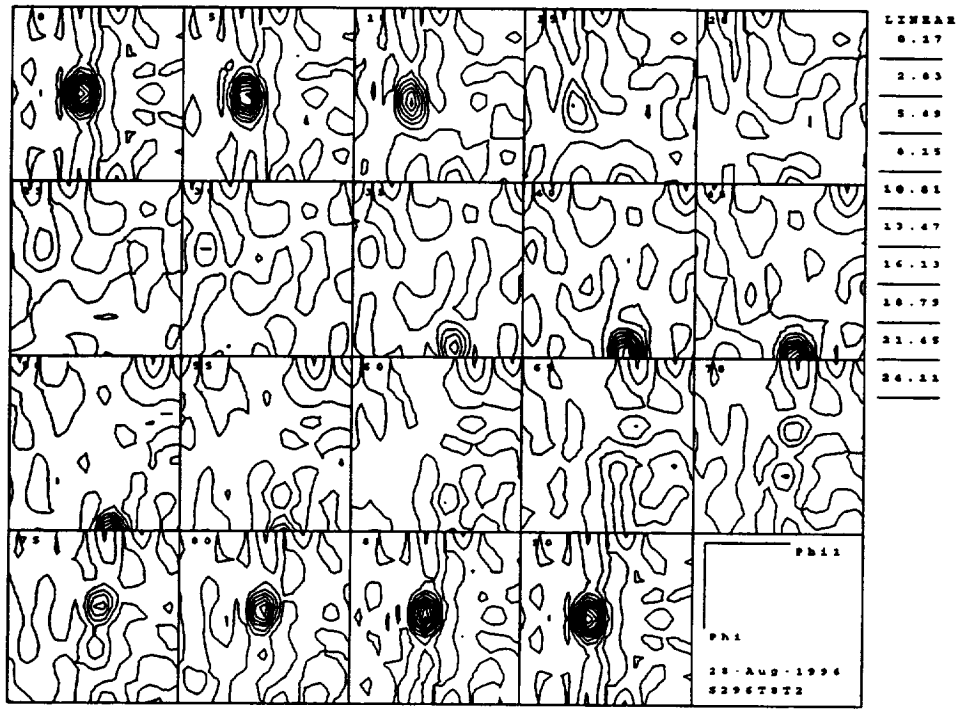

(b) Sections: φ_2= 45°; φ_2= 90°

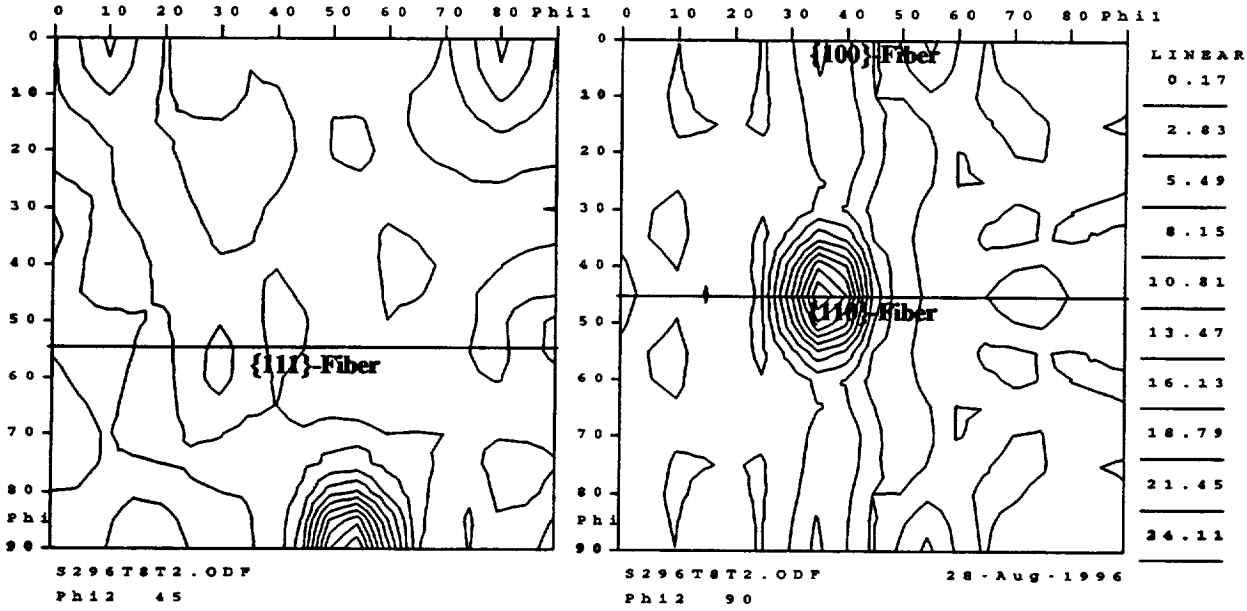

Figure 113. CODF sections for 2096-T8 sheet @ t/2; (a), Complete sections: φ_2= 0, 5, 10 ..... 90°; and (b), enlarged φ_2= 45° and φ_2= 90° sections. The locations of the {100}-fiber, {110}-fiber and {111}-fiber are shown.
[Specimen plane perpendicular to (S)hort-Transverse axis]

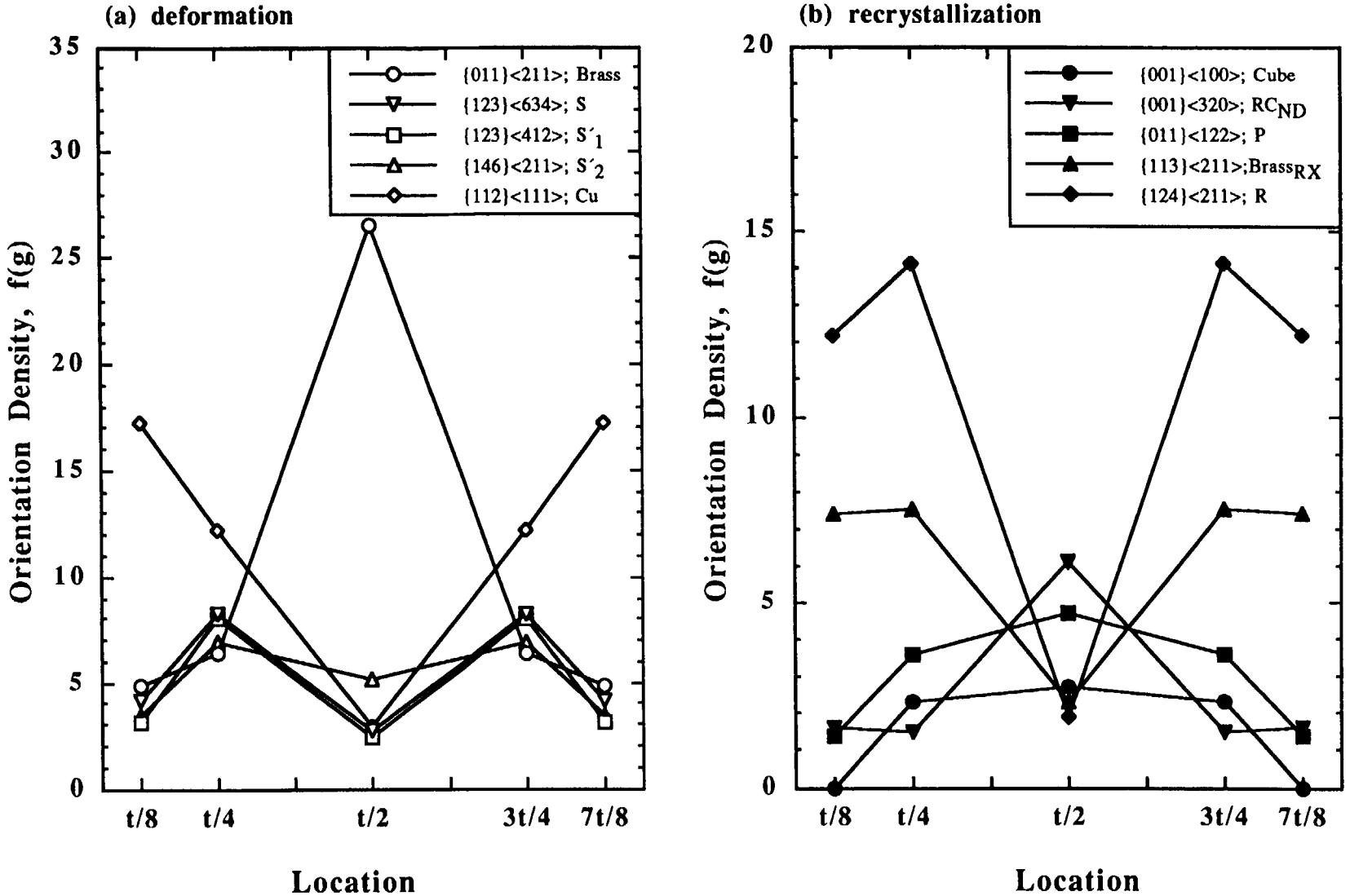

Figure 114. Orientation density, f(g), as a function of location through the cross-section for the 2096-T8 sheet: (a) Deformation-related components; (b) Recrystallization-related components.

4.4 Alloy 2195

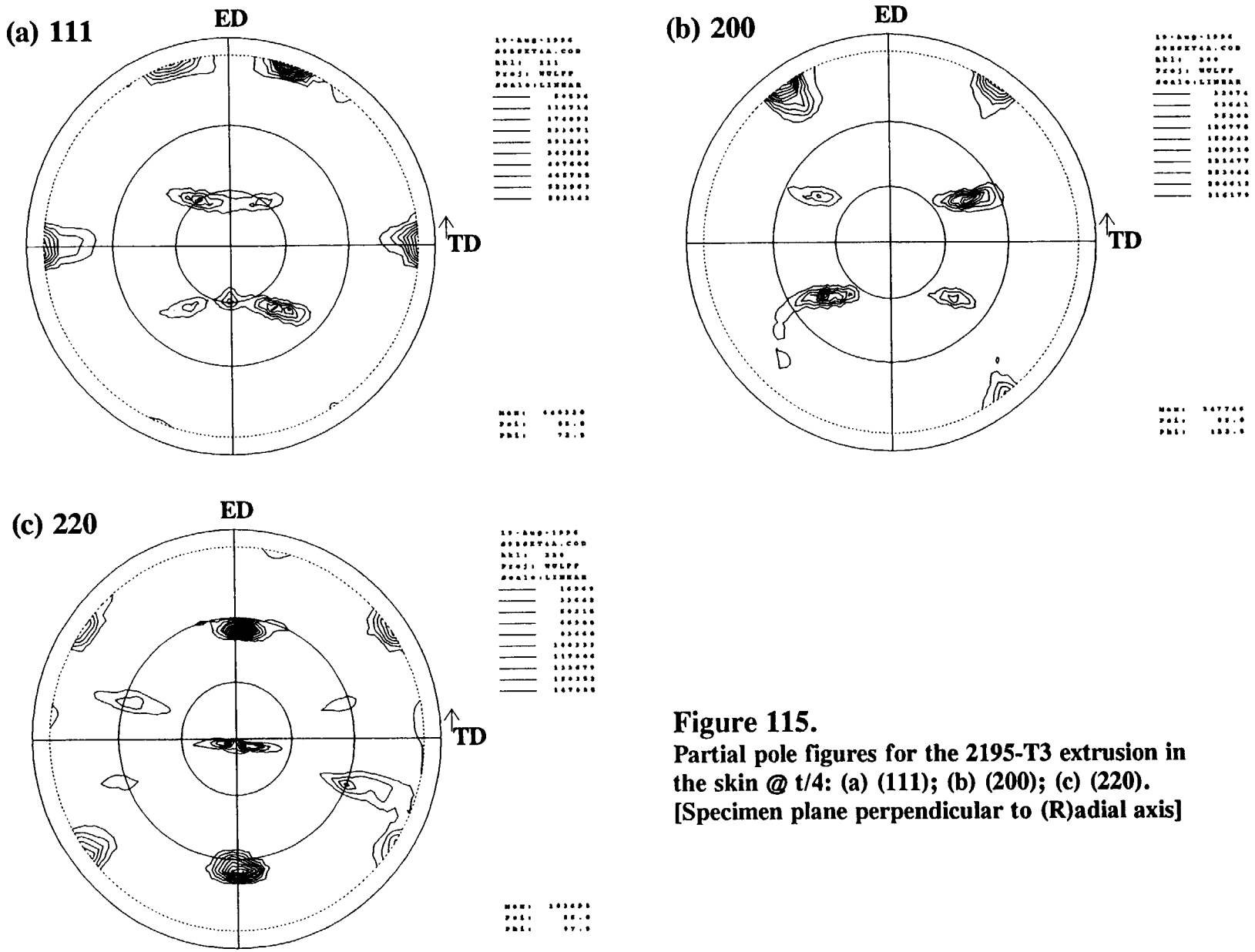

Figure 115.
Partial pole figures for the 2195-T3 extrusion in the skin @ t/4: (a) (111); (b) (200); (c) (220). [Specimen plane perpendicular to (R)adial axis]

(a) Sections: φ_2= 0 - 90°

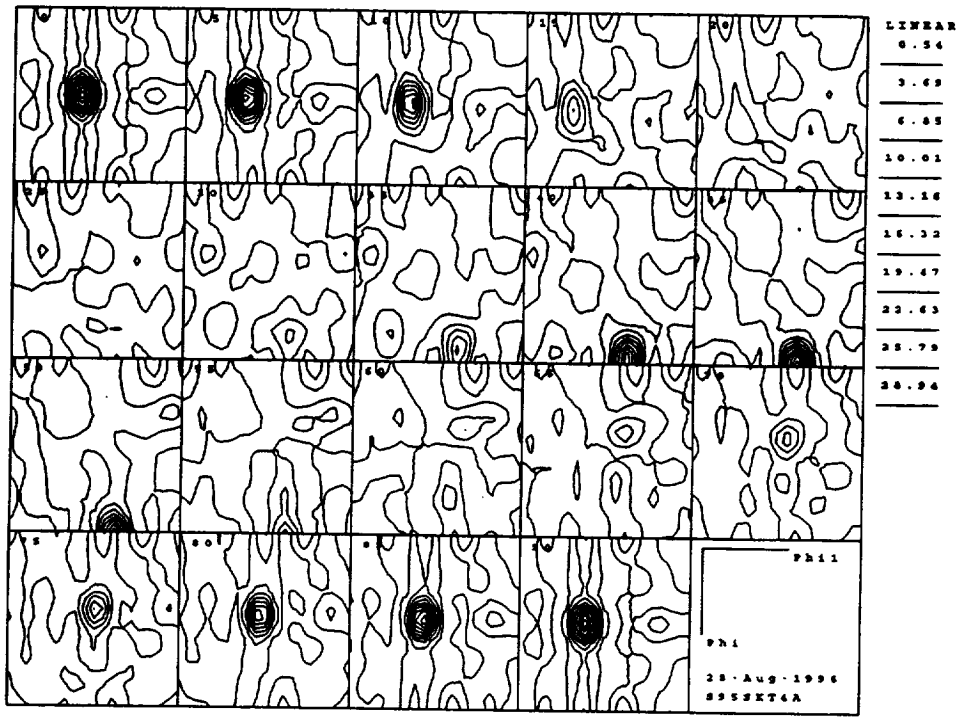

(b) Sections: φ_2= 45°; φ_2= 90°

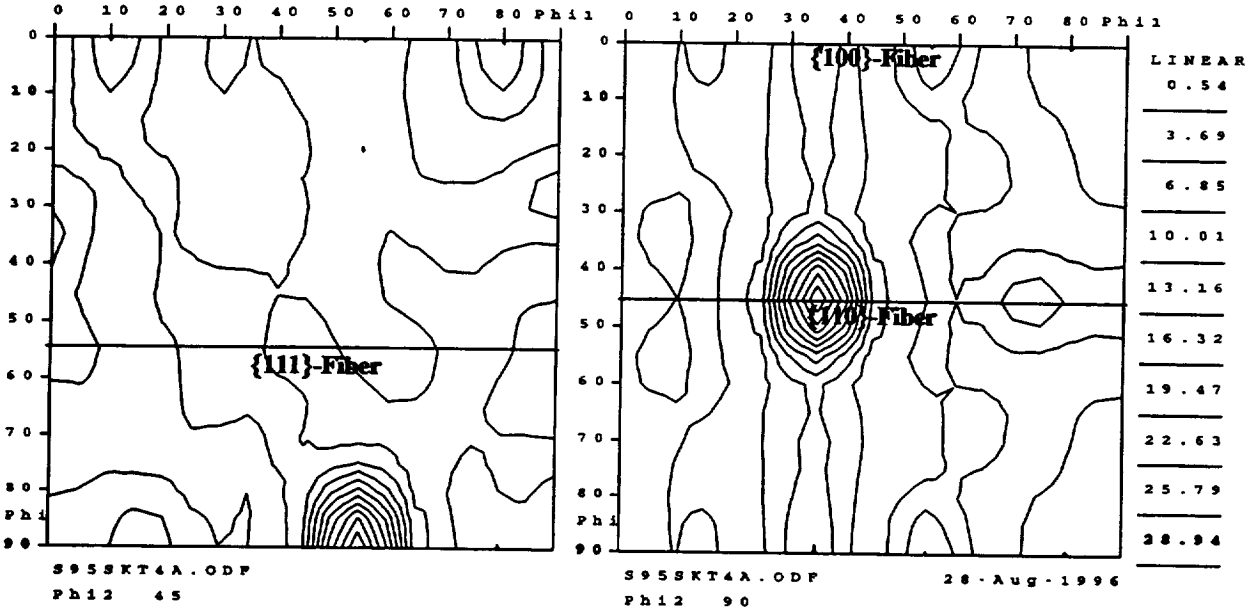

Figure 116. CODF sections for the 2195-T3 extrusion in the skin @ t/4; (a), Complete sections: φ_2= 0, 5, 10 ..... 90°; and (b), enlarged φ_2= 45° and φ_2= 90° sections. The locations of the {100}-fiber, {110}-fiber and {111}-fiber are shown.
[Specimen plane perpendicular to (R)adial axis]

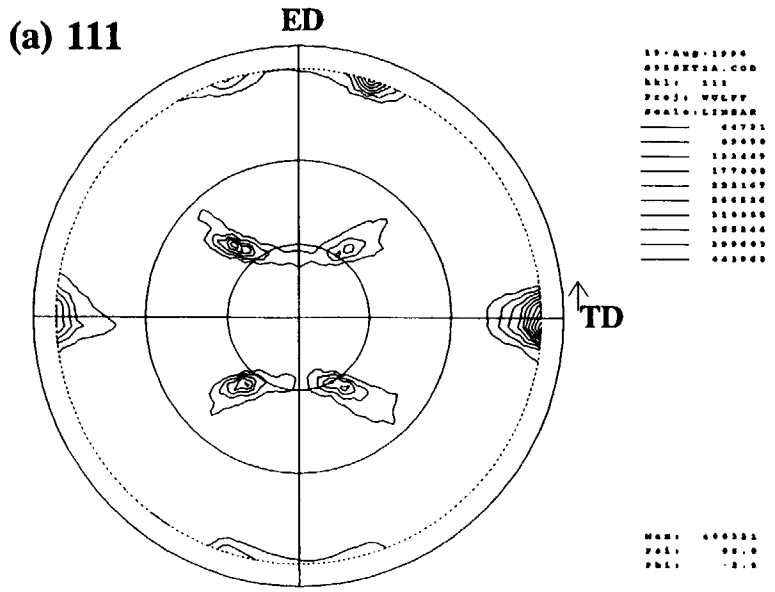

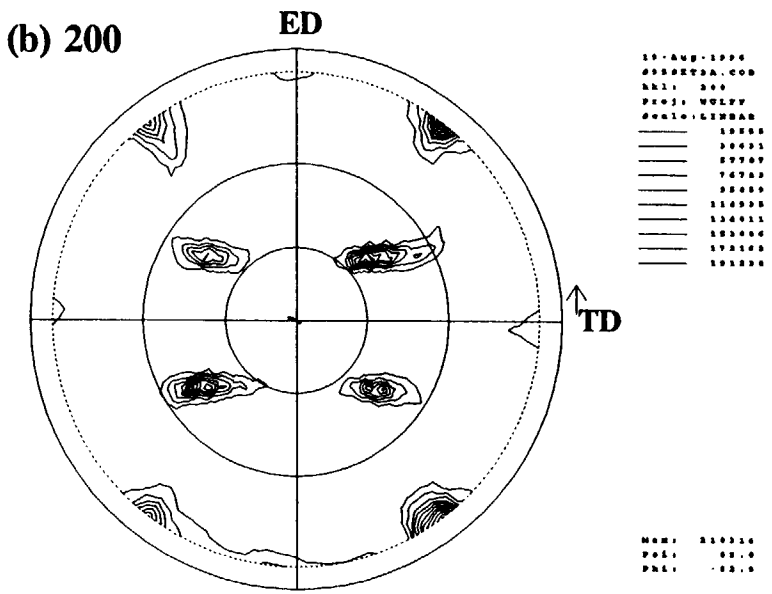

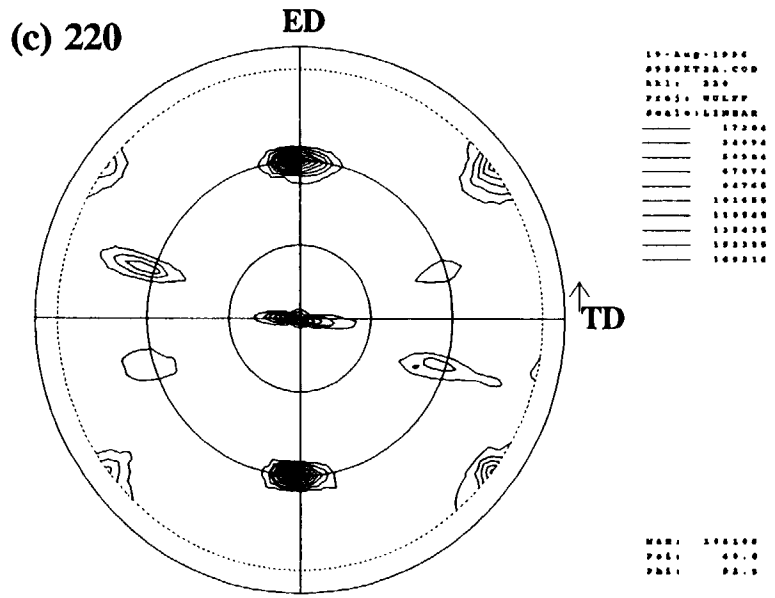

Figure 117.
Partial pole figures for the 2195-T3 extrusion in the skin @ t/2: (a) (111); (b) (200); (c) (220). [Specimen plane perpendicular to (R)adial axis]

(a) Sections: φ_2= 0 - 90°

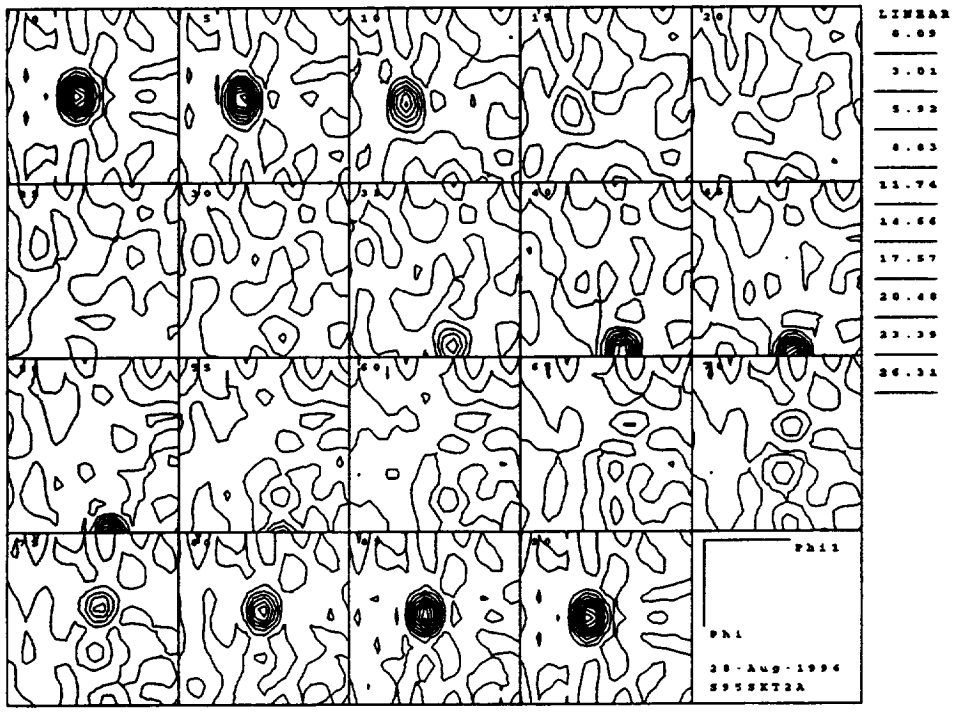

(b) Sections: φ_2= 45°; φ_2= 90°

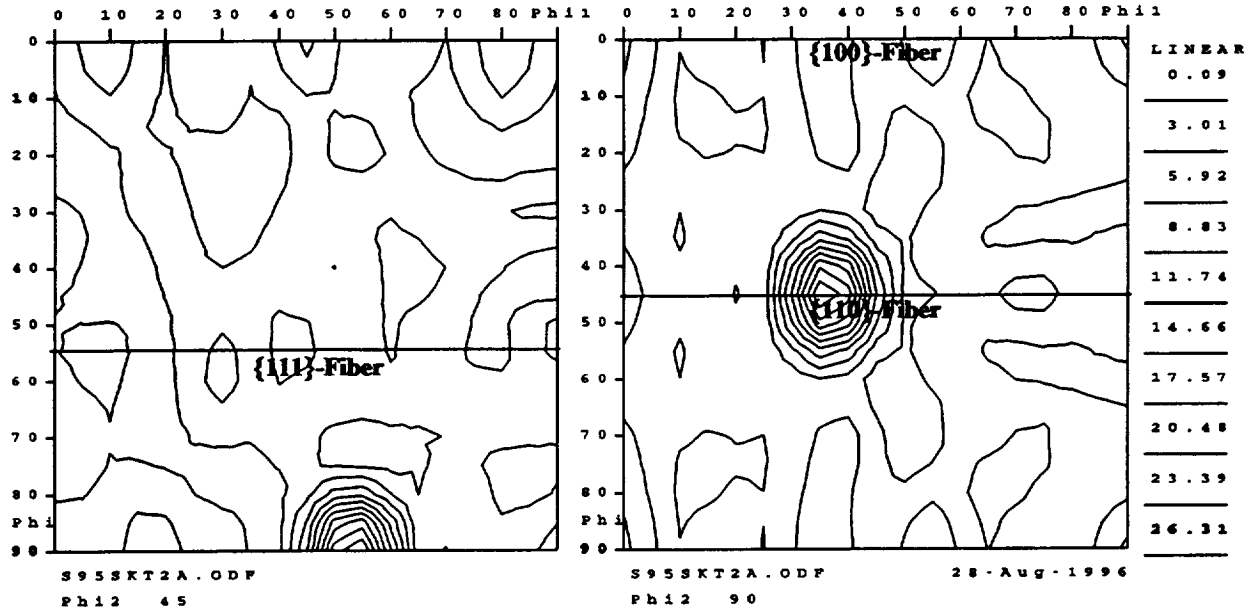

Figure 118. CODF sections for the 2195-T3 extrusion in the skin @ t/2; (a), Complete sections: φ_2= 0, 5, 10 ..... 90°; and (b), enlarged φ_2= 45° and φ_2= 90° sections. The locations of the {100}-fiber, {110}-fiber and {111}-fiber are shown.
[Specimen plane perpendicular to (R)adial axis]

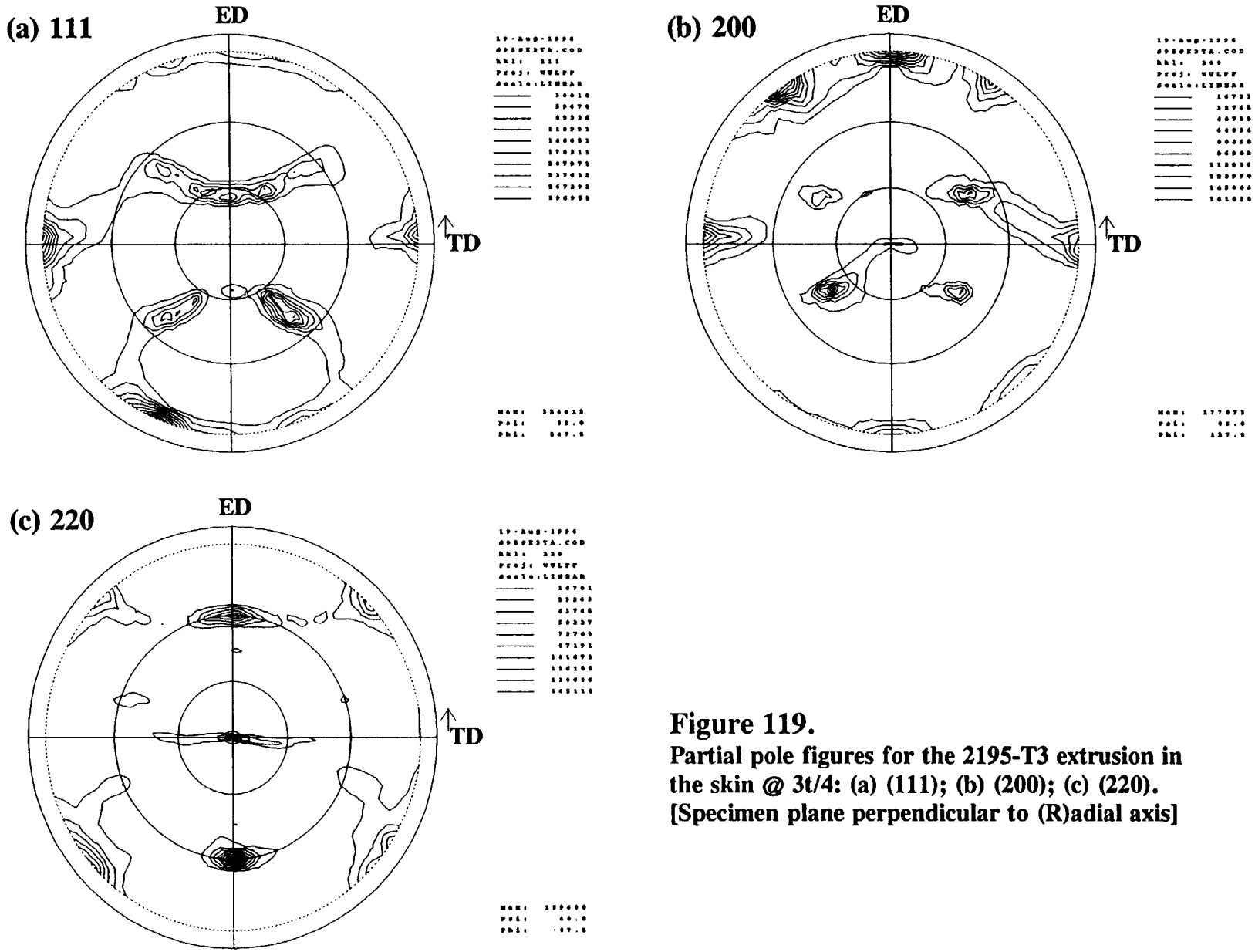

Figure 119.
Partial pole figures for the 2195-T3 extrusion in the skin @ 3t/4: (a) (111); (b) (200); (c) (220). [Specimen plane perpendicular to (R)adial axis]

(a) Sections: φ_2= 0 - 90°

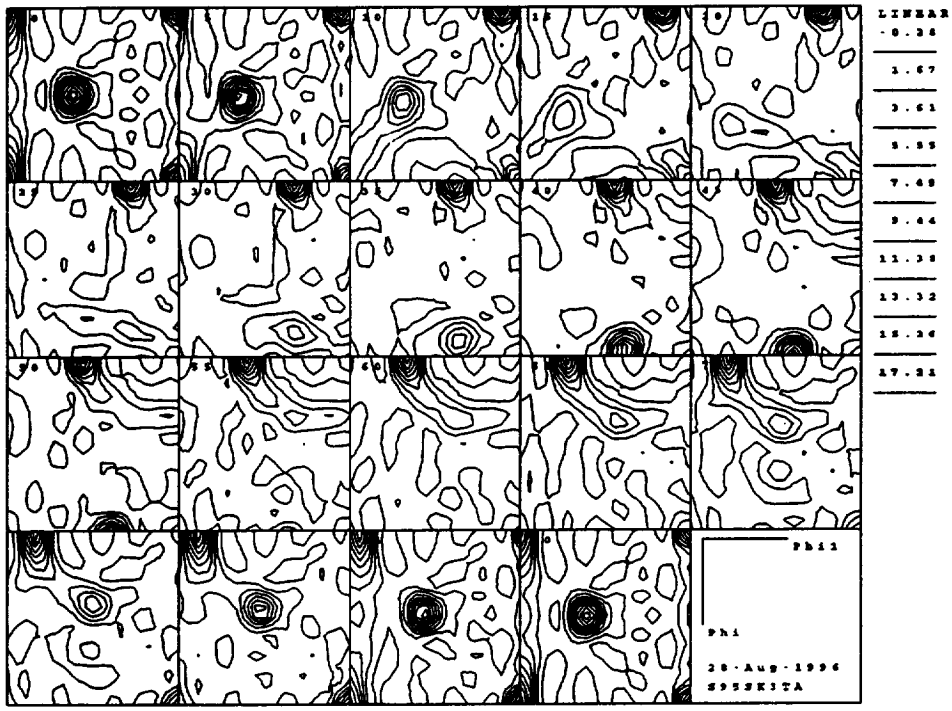

(b) Sections: φ_2= 45°; φ_2= 90°

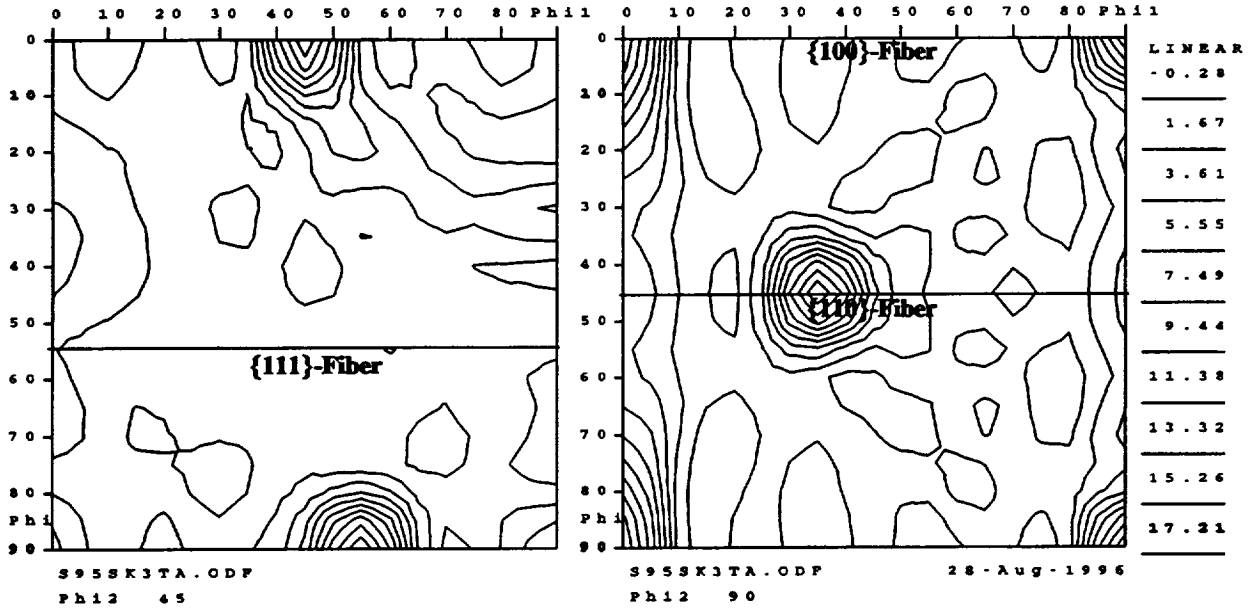

Figure 120. CODF sections for the 2195-T3 extrusion in the skin @ 3t/4; (a), Complete sections: φ_2= 0, 5, 10 ..... 90°; and (b), enlarged φ_2= 45° and φ_2= 90° sections. The locations of the {100}-fiber, {110}-fiber and {111}-fiber are shown.
[Specimen plane perpendicular to (R)adial axis]

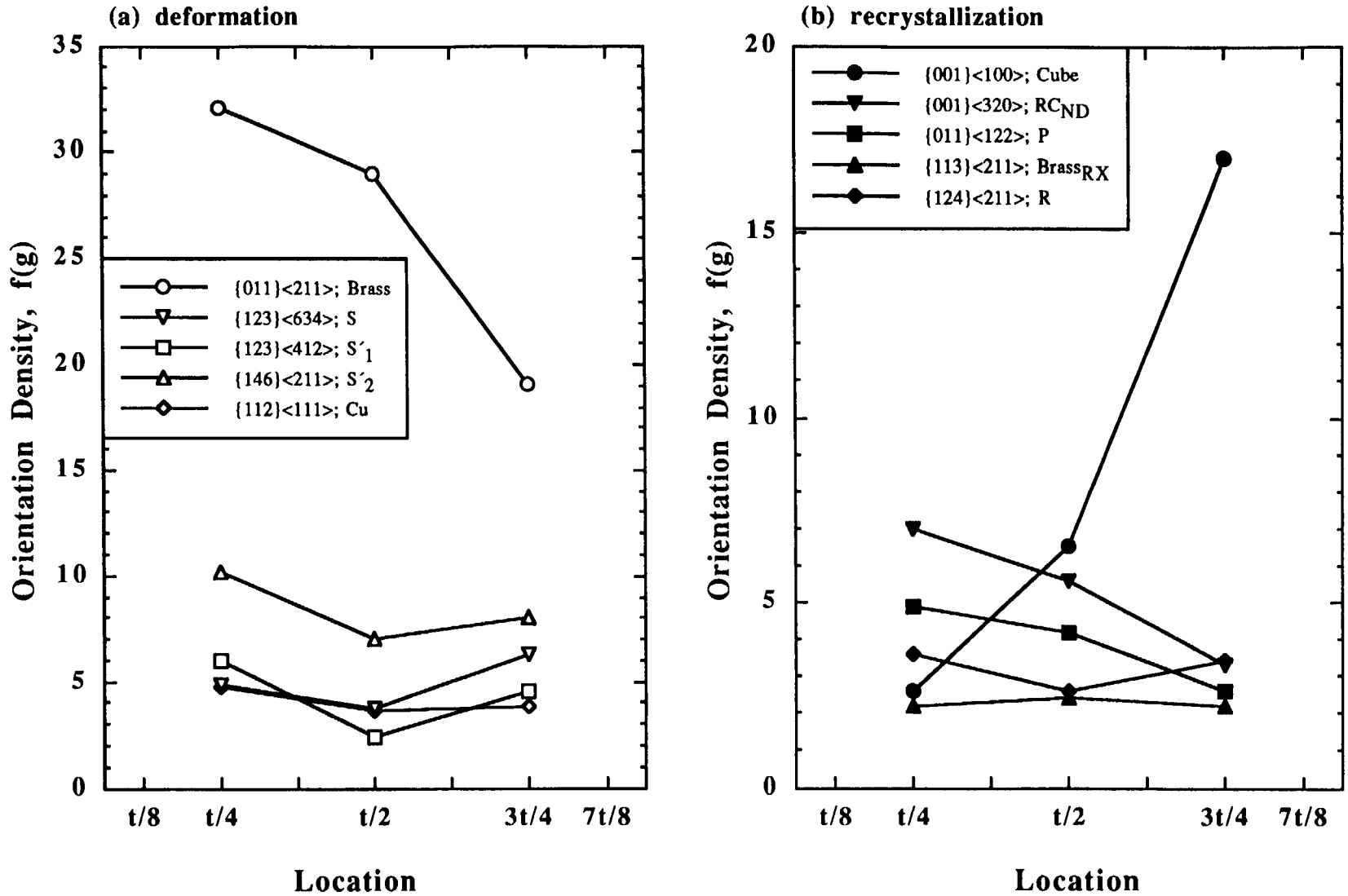

Figure 121. Orientation density, f(g), as a function of location through the cross-section for the 2195-T3 extrusion in the skin region: (a) Deformation-related components; (b) Recrystallization-related components.

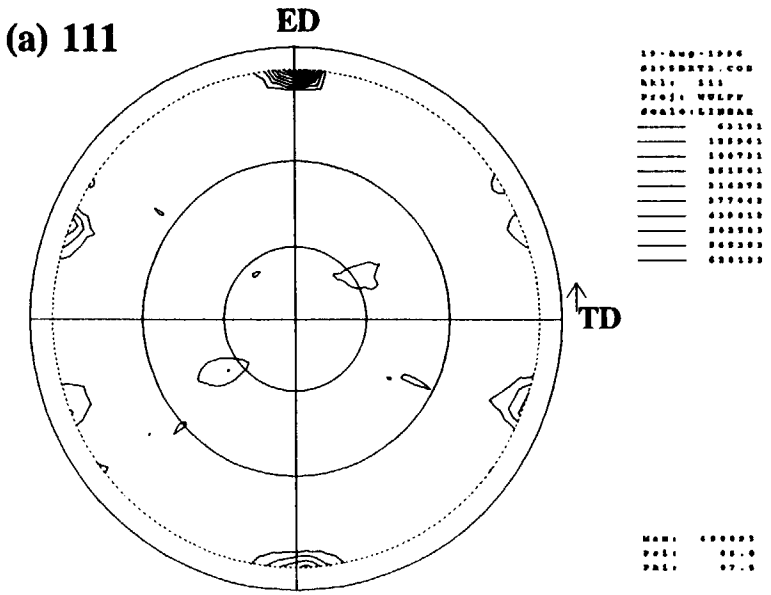

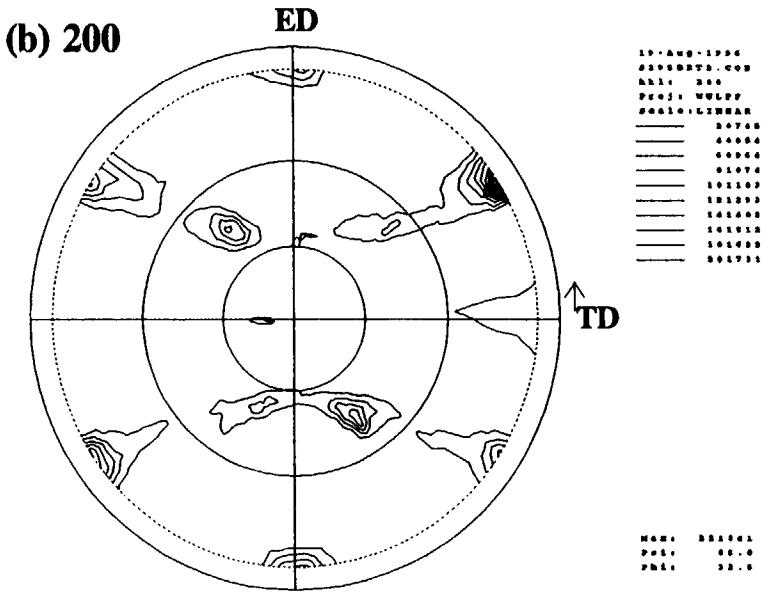

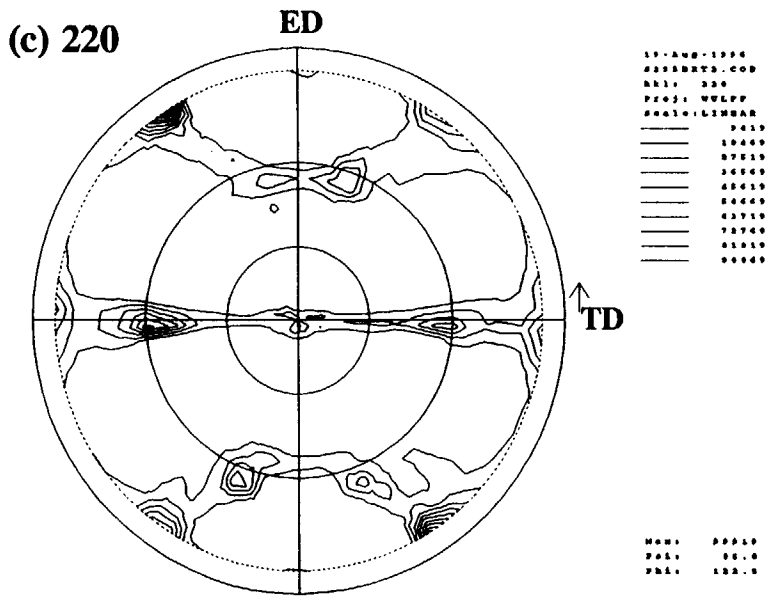

Figure 122.
Partial pole figures for the 2195-T3 extrusion in the base @ t/2: (a) (111); (b) (200); (c) (220). [Specimen plane perpendicular to (R)adial axis]

(a) Sections: φ_2= 0 - 90°

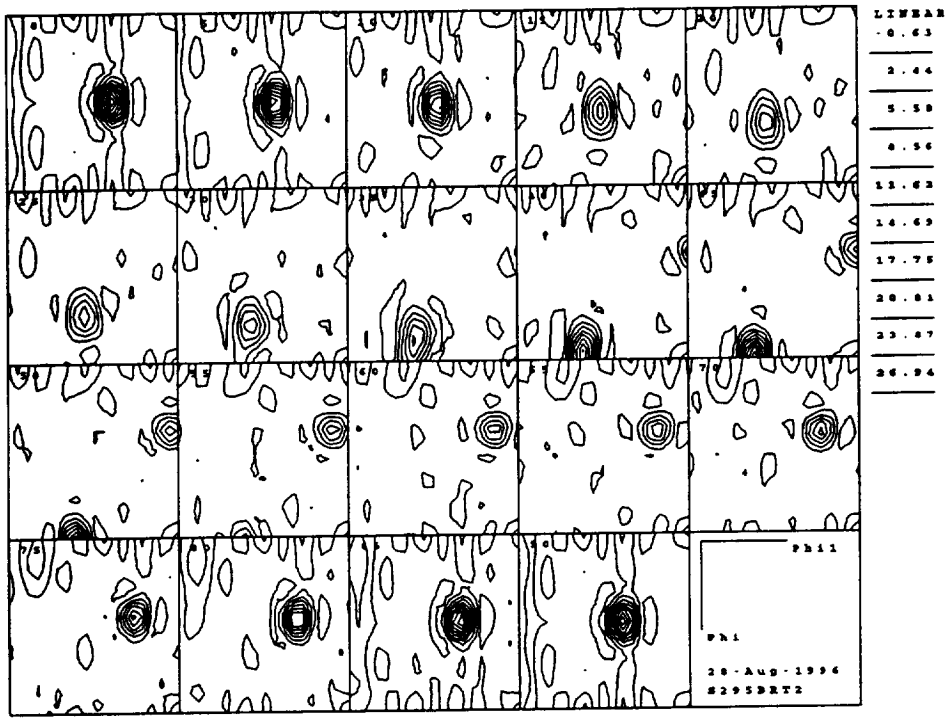

(b) Sections: φ_2= 45°; φ_2= 90°

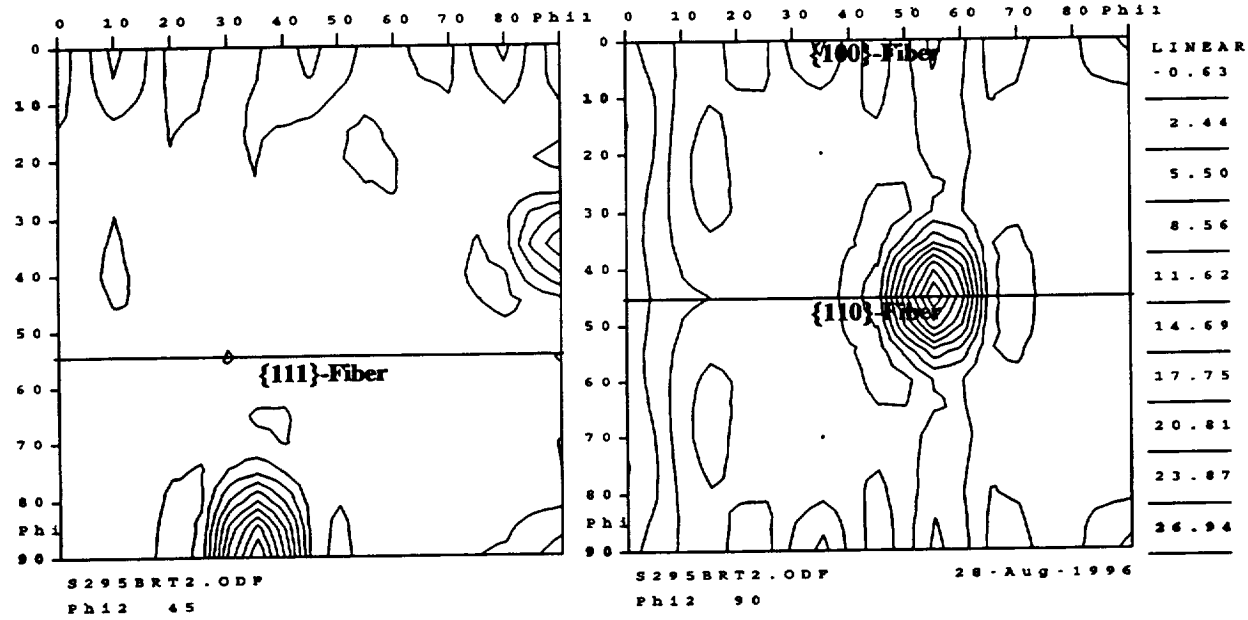

Figure 123. CODF sections for the 2195-T3 extrusion in the base @ t/2; (a), Complete sections: φ_2= 0, 5, 10 ..... 90°; and (b), enlarged φ_2= 45° and φ_2= 90° sections. The locations of the {100}-fiber, {110}-fiber and {111}-fiber are shown.
[Specimen plane perpendicular to (R)adial axis]

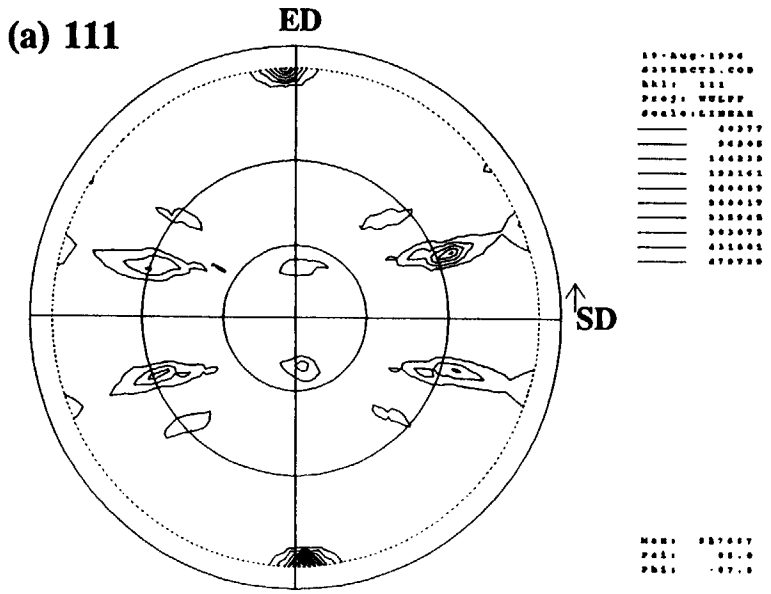

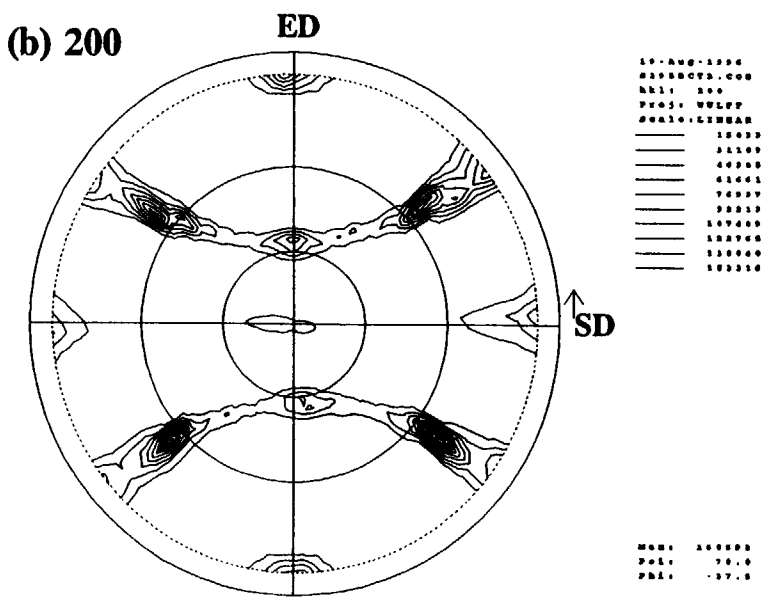

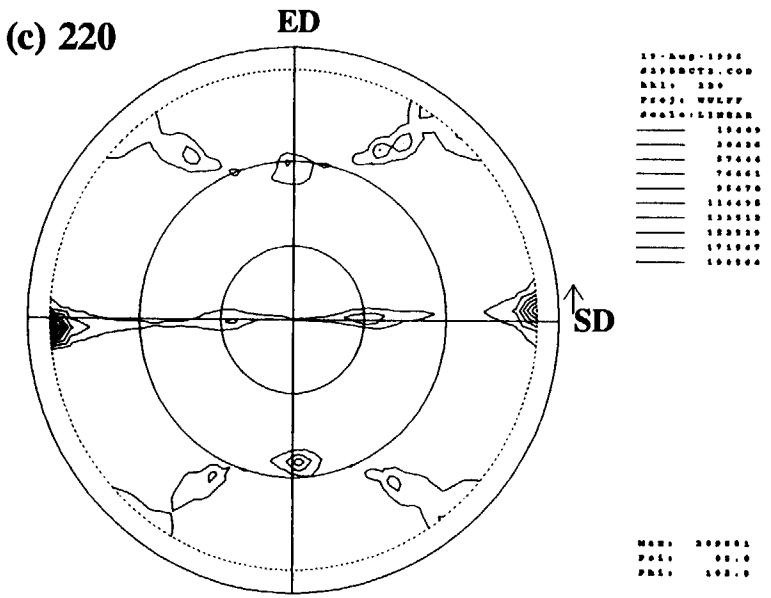

Figure 124.
Partial pole figures for the 2195-T3 extrusion in the base @ t/2: (a) (111); (b) (200); (c) (220). [Specimen plane perpendicular to (C)ircumferential axis]

(a) Sections: φ_2= 0 - 90°

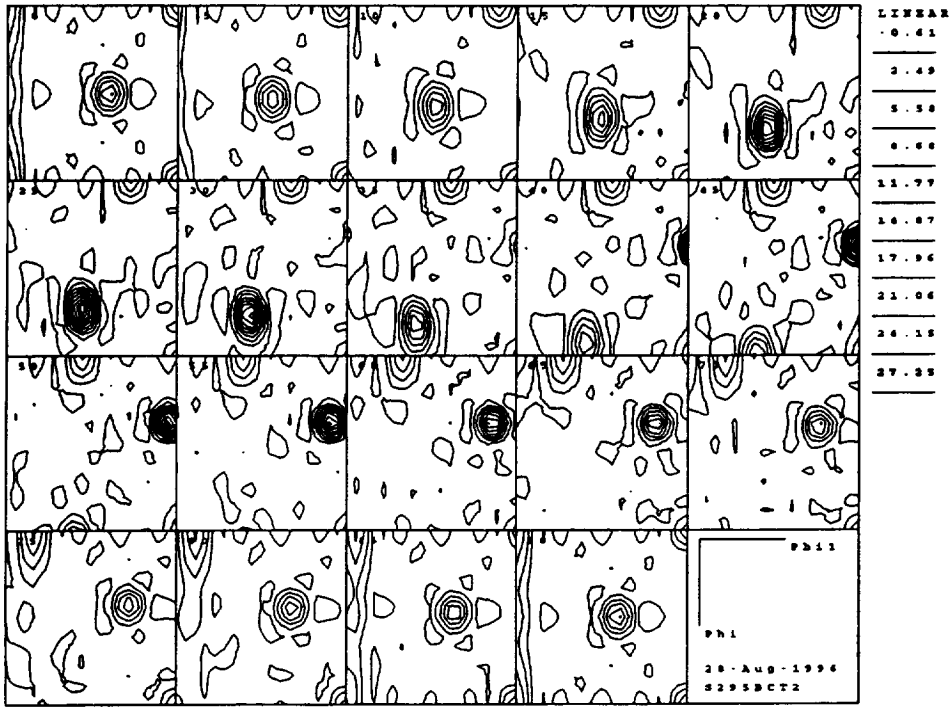

(b) Sections: φ_2= 45°; φ_2= 90°

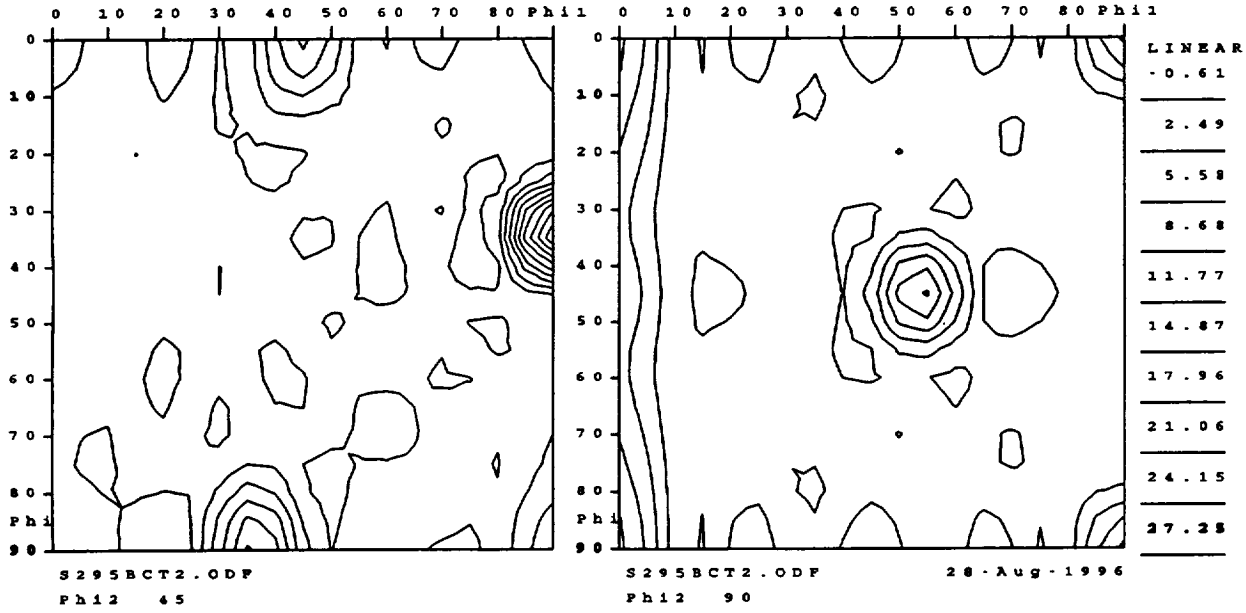

Figure 125. CODF sections for the 2195-T3 extrusion in the base @ t/2; (a), Complete sections: φ_2= 0, 5, 10 ..... 90°; and (b), enlarged φ_2= 45° and φ_2= 90° sections. [Specimen plane perpendicular to (C)ircumferential axis]

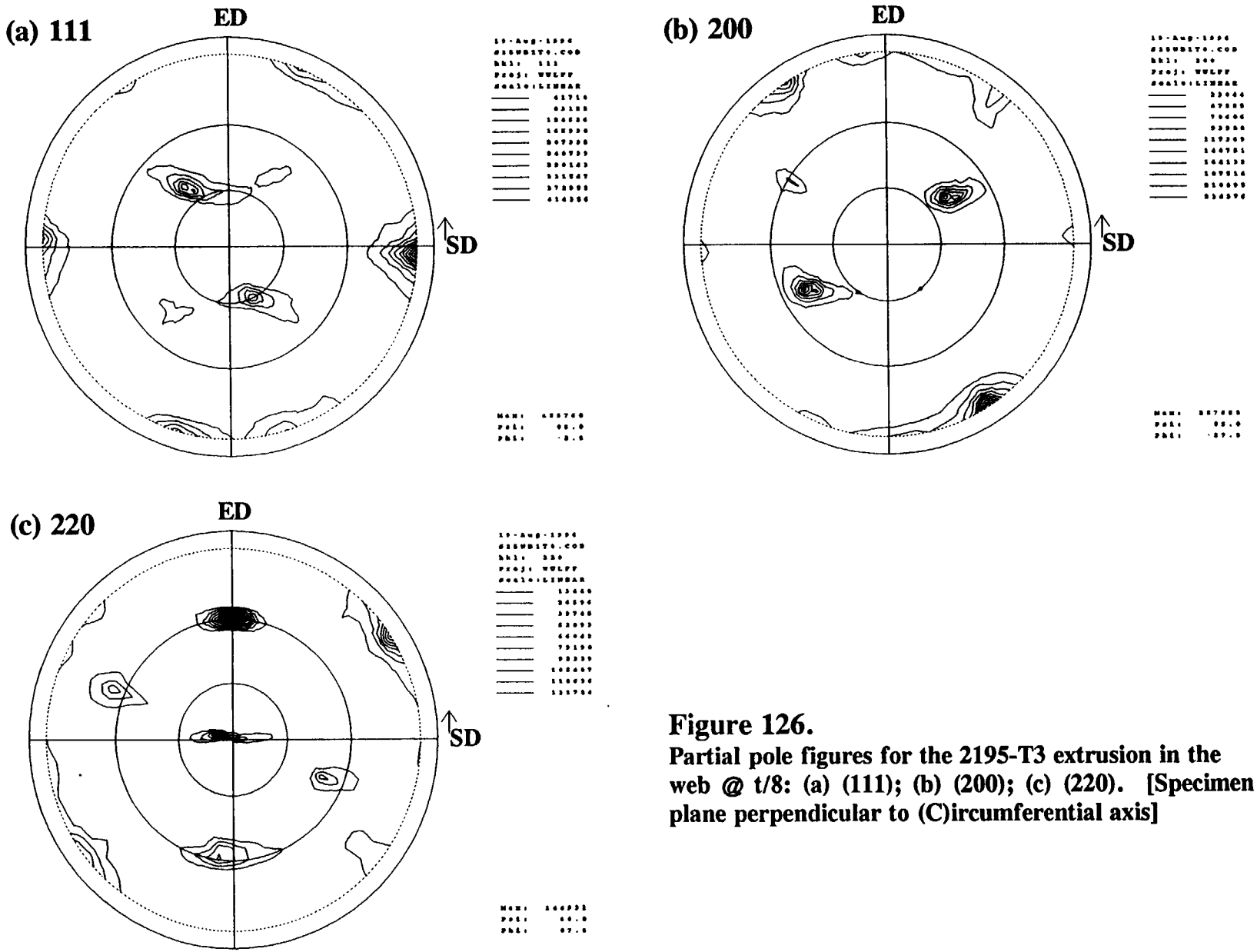

Figure 126.
Partial pole figures for the 2195-T3 extrusion in the web @ t/8: (a) (111); (b) (200); (c) (220). [Specimen plane perpendicular to (C)ircumferential axis]

(a) Sections: $\varphi_2 = 0 - 90°$

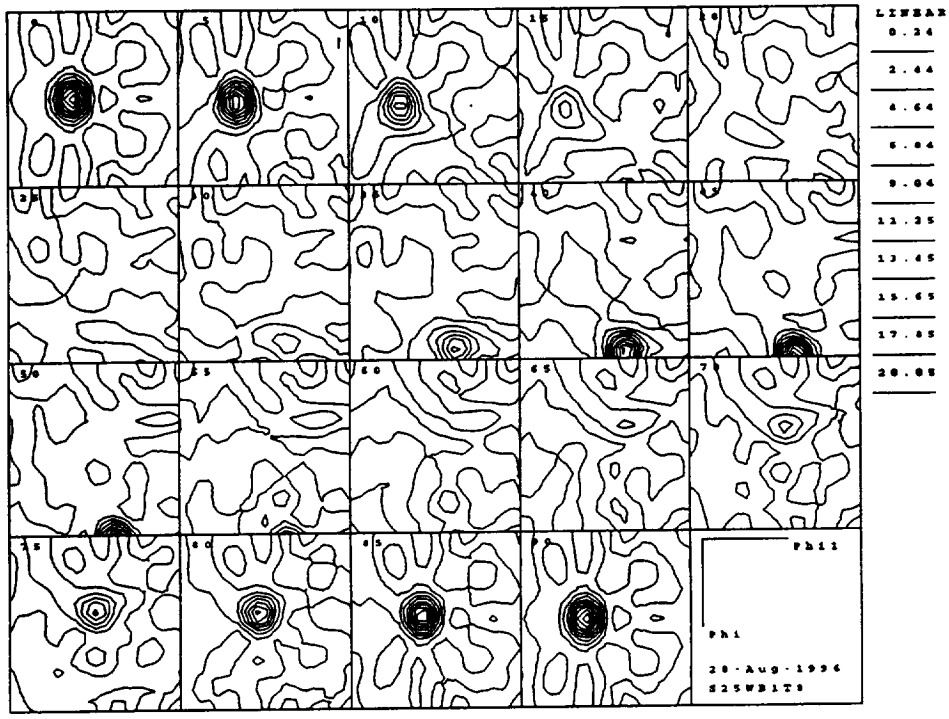

(b) Sections: $\varphi_2 = 45°$; $\varphi_2 = 90°$

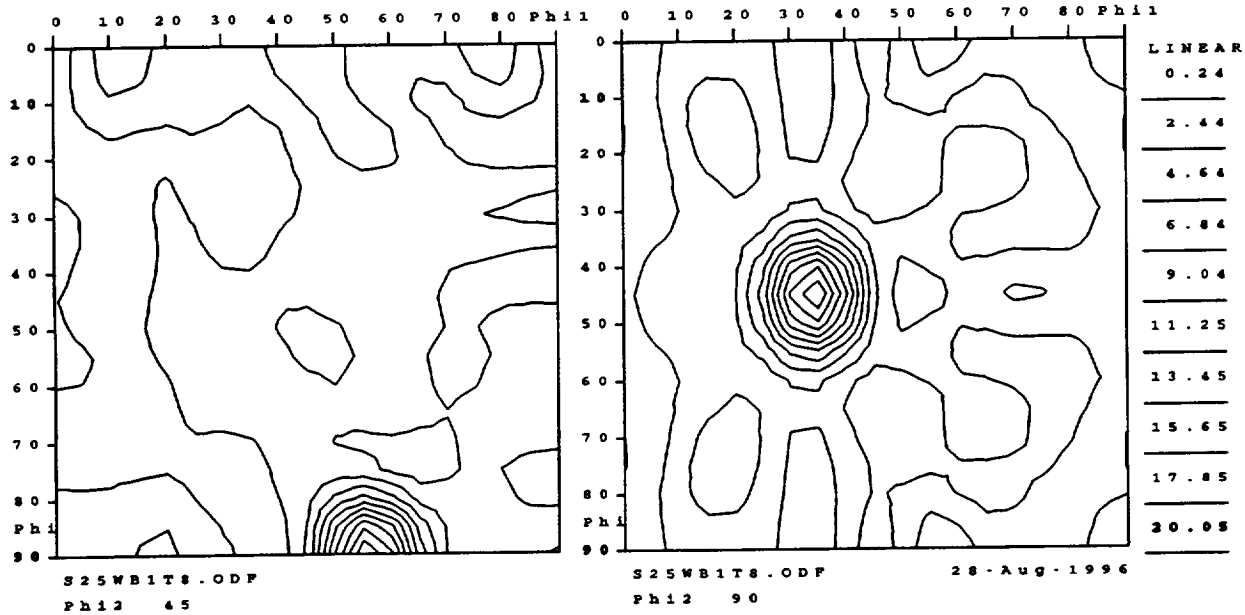

Figure 127. CODF sections for the 2195-T3 extrusion in the web @ t/8; (a), Complete sections: $\varphi_2 = 0, 5, 10 \ldots 90°$; and (b), enlarged $\varphi_2 = 45°$ and $\varphi_2 = 90°$ sections. [Specimen plane perpendicular to (C)ircumferential axis]

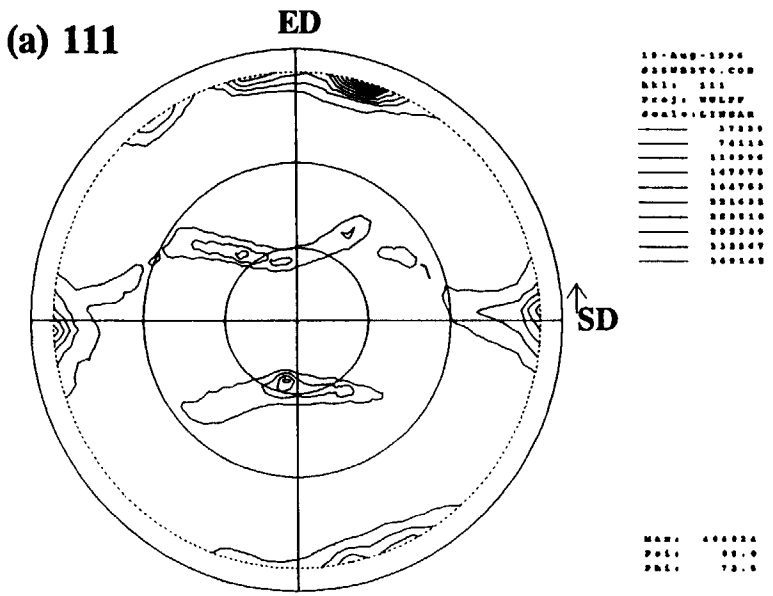

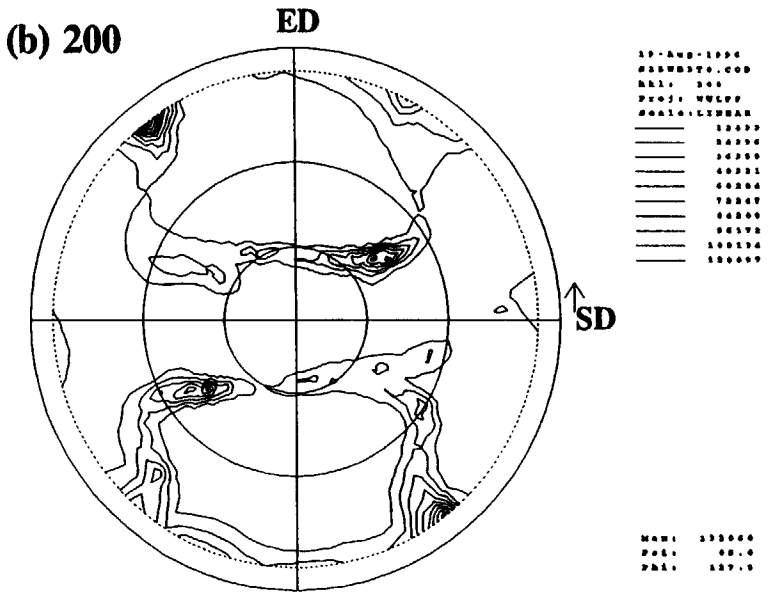

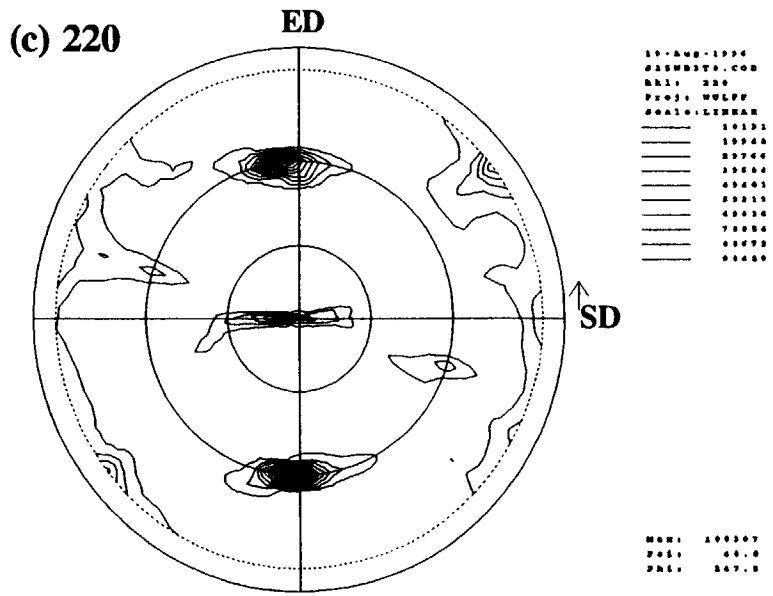

Figure 128.
Partial pole figures for the 2195-T3 extrusion in the web @ 3t/8: (a) (111); (b) (200); (c) (220). [Specimen plane perpendicular to (C)ircumferential axis]

(a) Sections: $\varphi_2 = 0 - 90°$

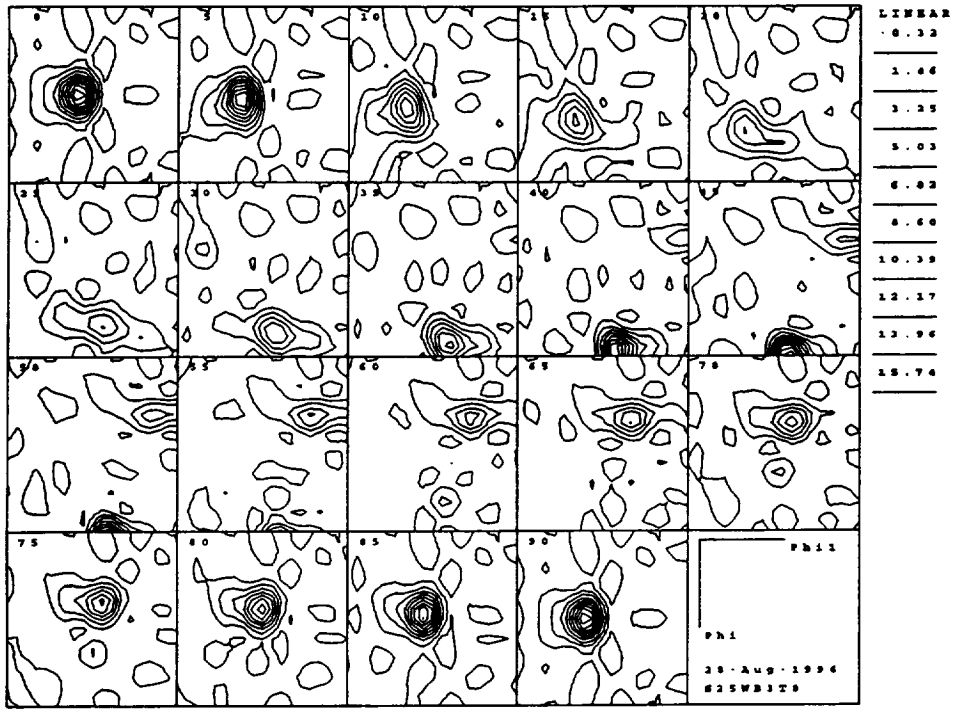

(b) Sections: $\varphi_2 = 45°$; $\varphi_2 = 90°$

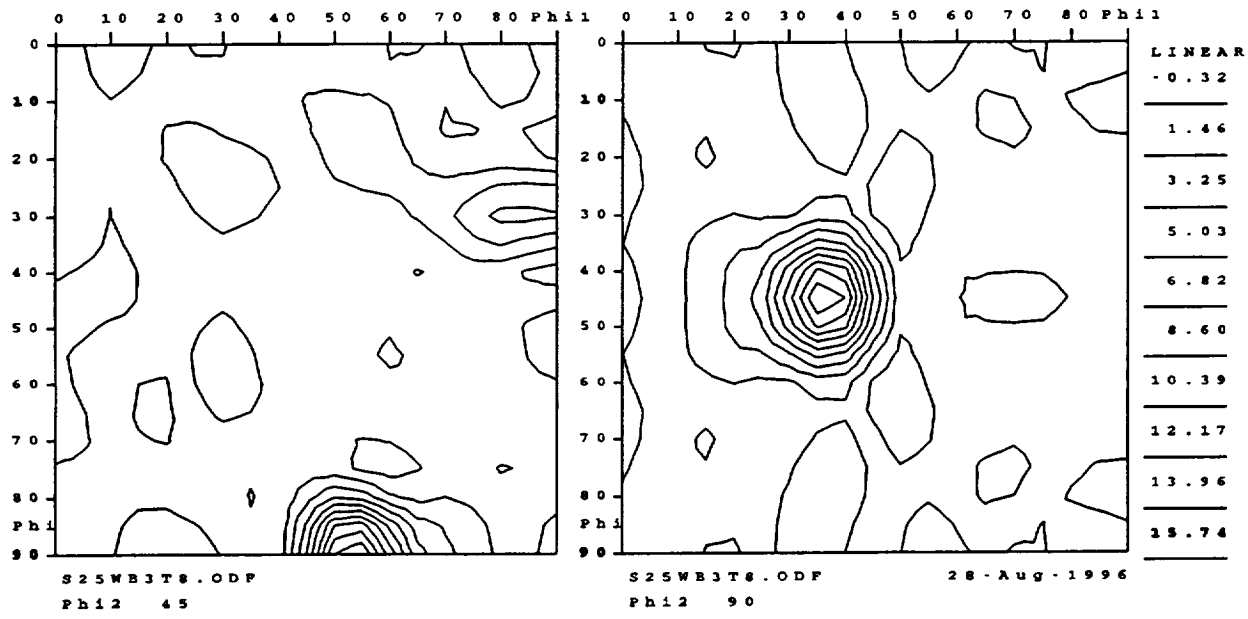

Figure 129. CODF sections for the 2195-T3 extrusion in the web @ 3t/8; (a), Complete sections: $\varphi_2 = 0, 5, 10 \ldots 90°$; and (b), enlarged $\varphi_2 = 45°$ and $\varphi_2 = 90°$ sections. [Specimen plane perpendicular to (C)ircumferential axis]

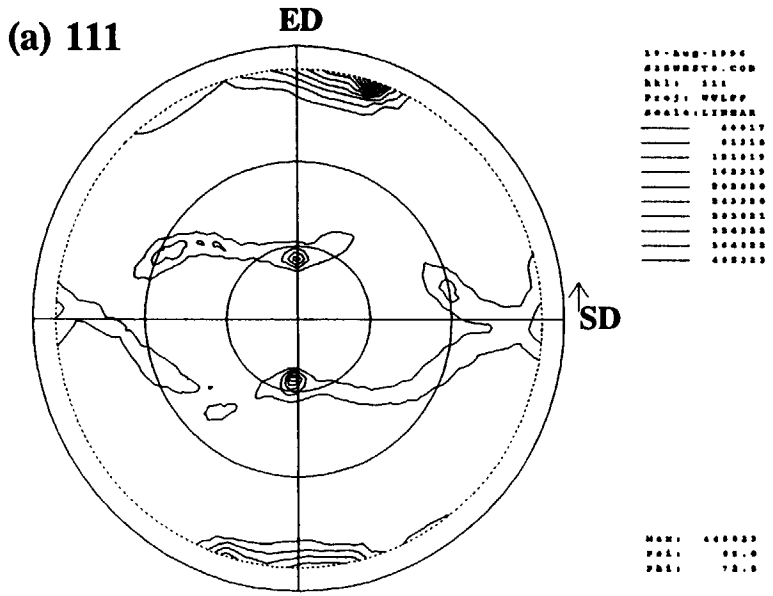

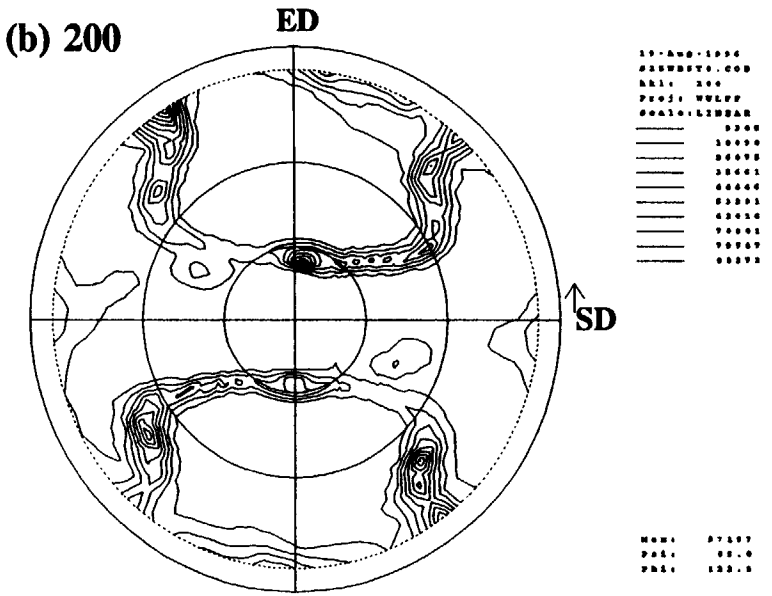

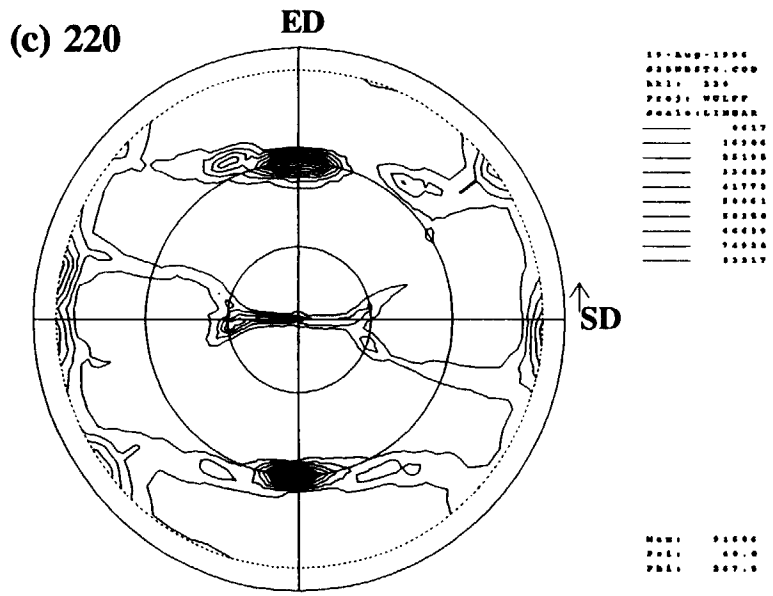

Figure 130.
Partial pole figures for the 2195-T3 extrusion in the web @ 5t/8: (a) (111); (b) (200); (c) (220). [Specimen plane perpendicular to (C)ircumferential axis]

(a) Sections: φ_2= 0 - 90°

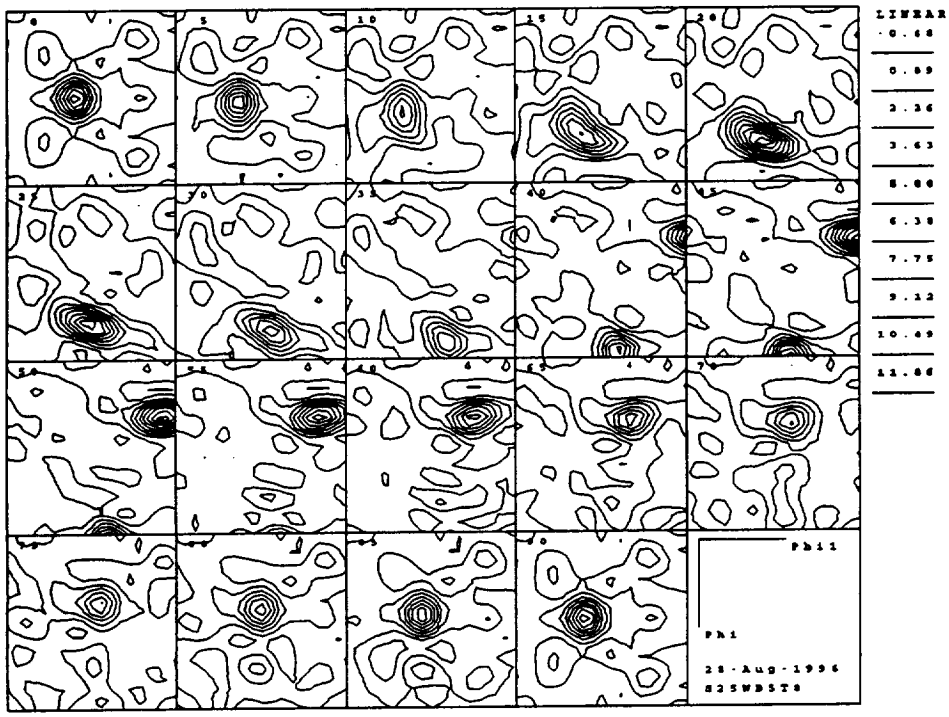

(b) Sections: φ_2= 45°; φ_2= 90°

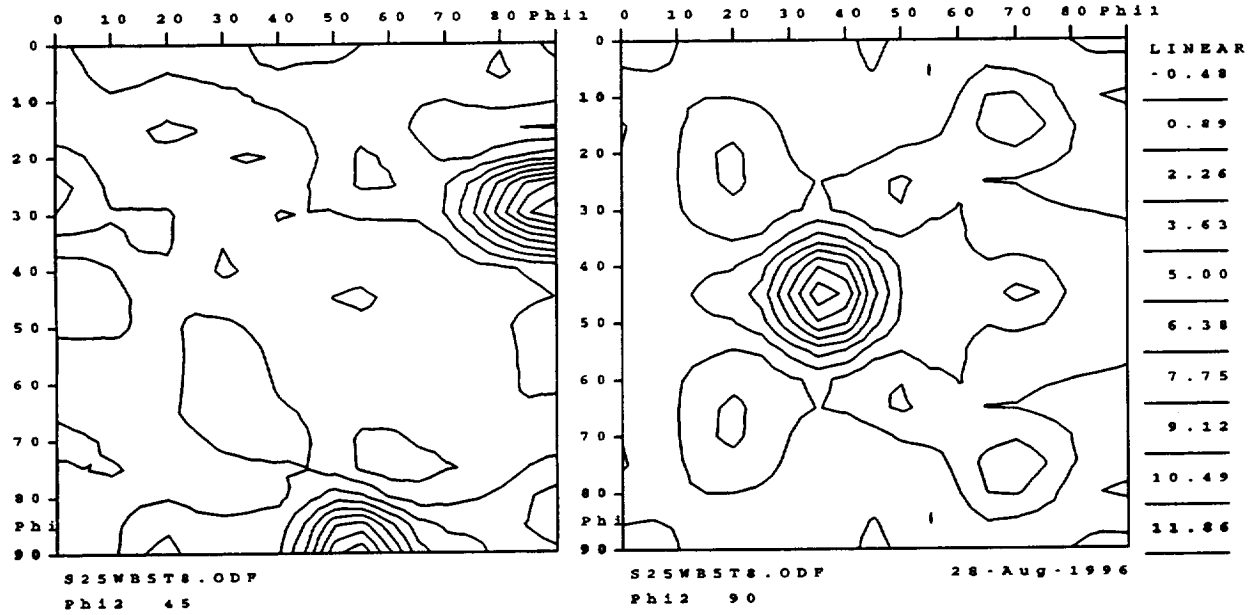

Figure 131. CODF sections for the 2195-T3 extrusion in the web @ 5t/8; (a), Complete sections: φ_2= 0, 5, 10 ..... 90°; and (b), enlarged φ_2= 45° and φ_2= 90° sections. [Specimen plane perpendicular to (C)ircumferential axis]

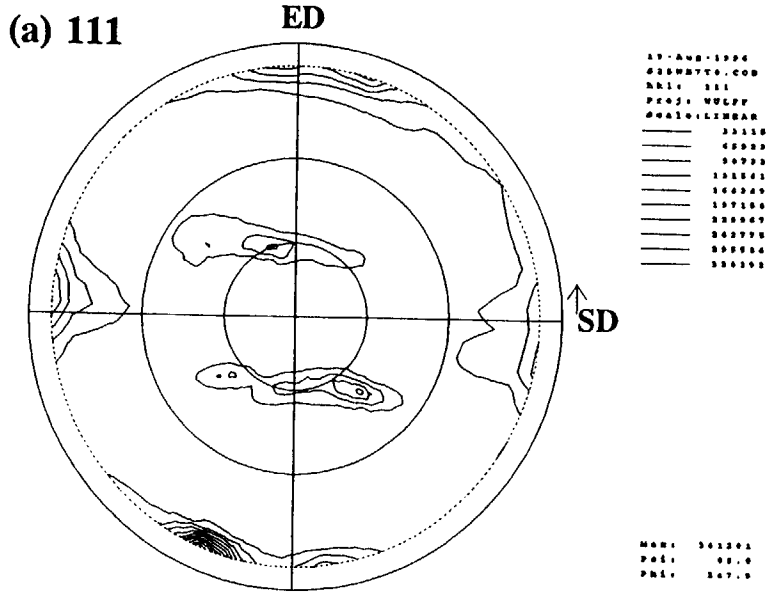

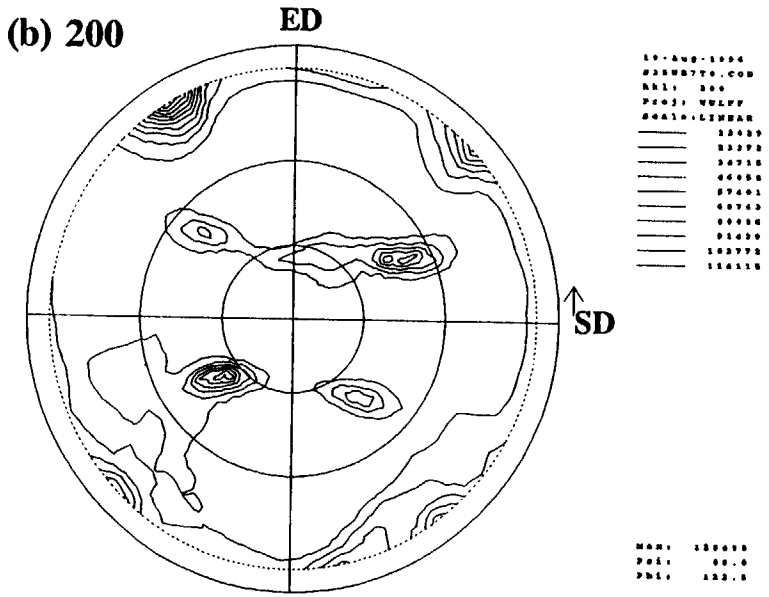

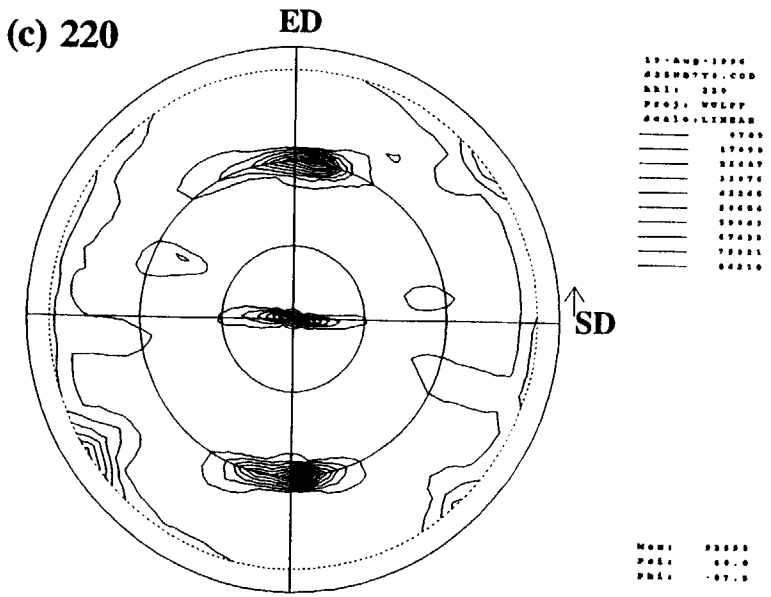

Figure 132.
Partial pole figures for the 2195-T3 extrusion in the web @ 7t/8: (a) (111); (b) (200); (c) (220). [Specimen plane perpendicular to (C)ircumferential axis]

(a) Sections: φ_2= 0 - 90°

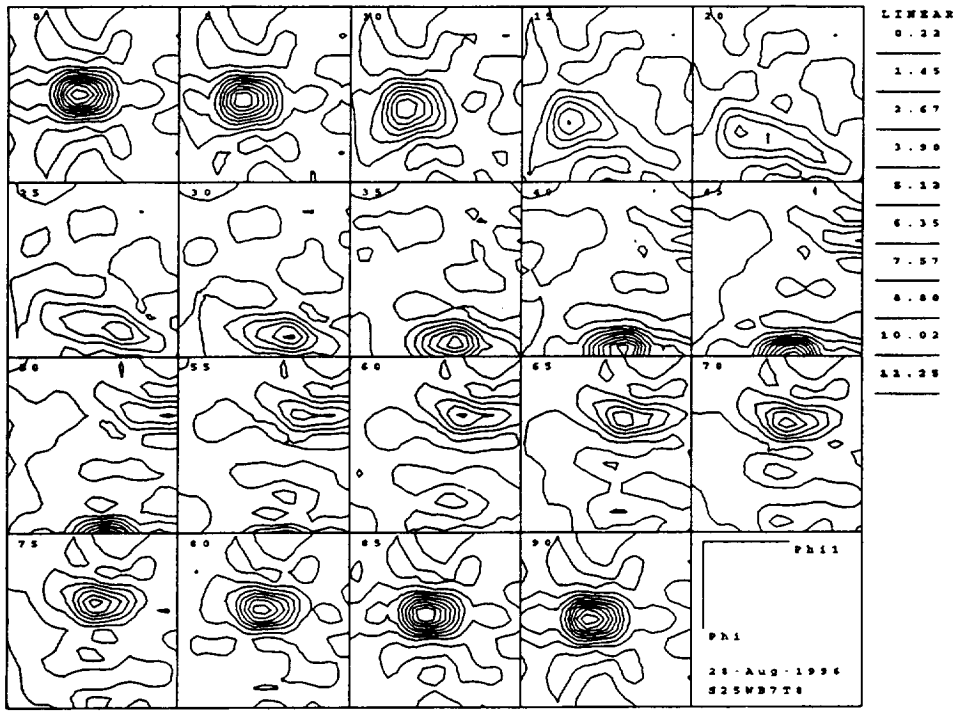

(b) Sections: φ_2= 45°; φ_2= 90°

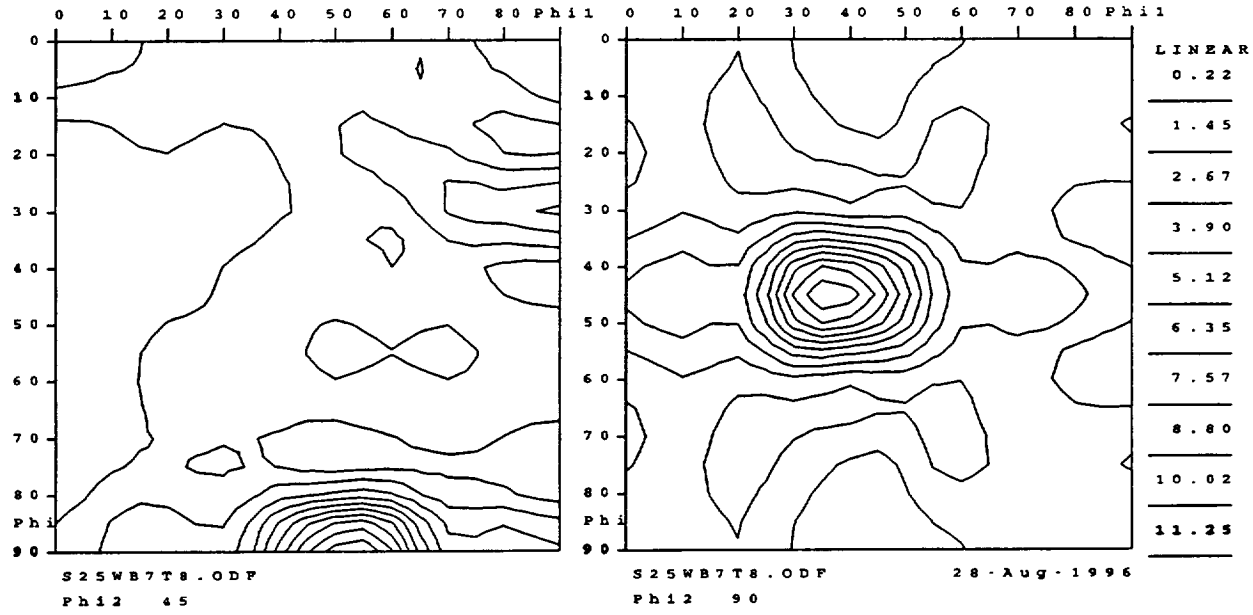

Figure 133. CODF sections for the 2195-T3 extrusion in the web @ 7t/8; (a), Complete sections: φ_2= 0, 5, 10 ..... 90°; and (b), enlarged φ_2= 45° and φ_2= 90° sections. [Specimen plane perpendicular to (C)ircumferential axis]

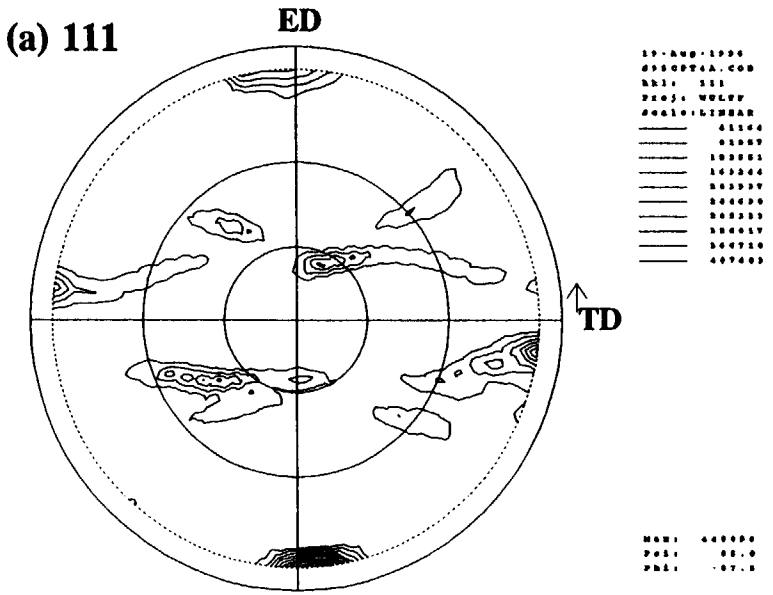

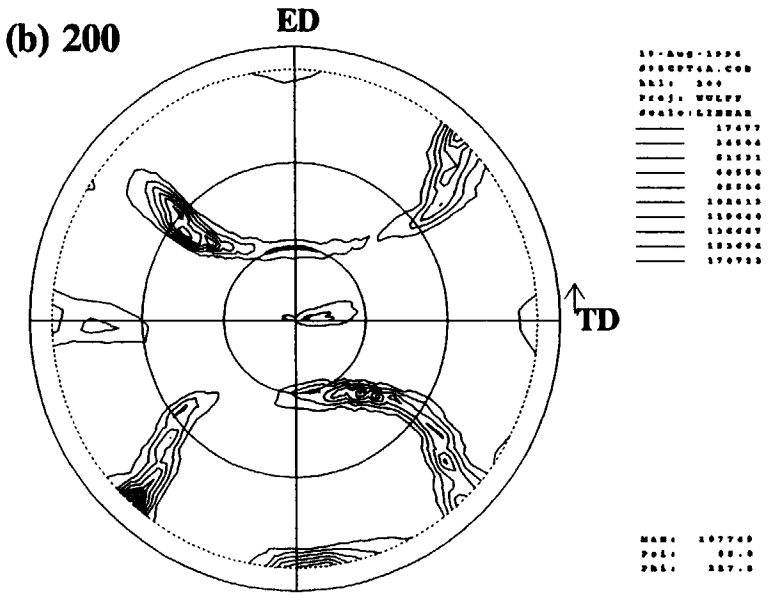

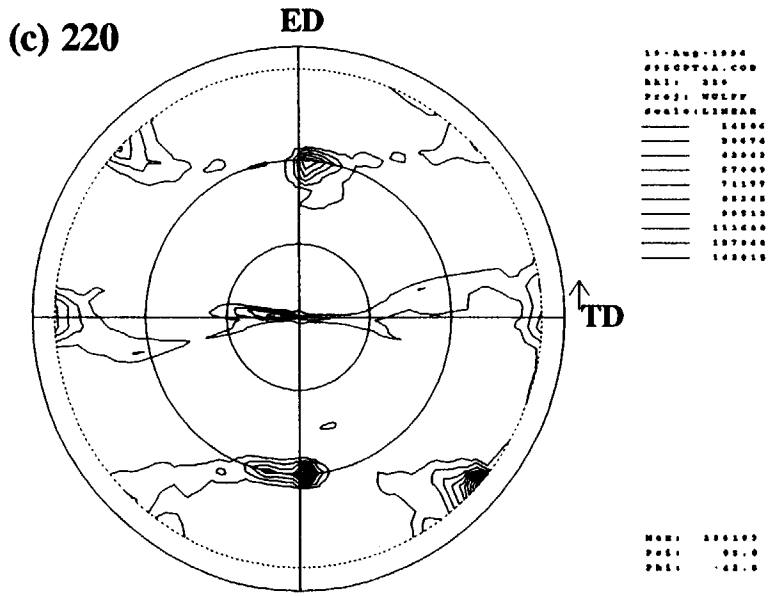

Figure 134.
Partial pole figures for the 2195-T3 extrusion in the cap @ t/4: (a) (111); (b) (200); (c) (220). [Specimen plane perpendicular to (R)adial axis]

(a) Sections: φ_2= 0 - 90°

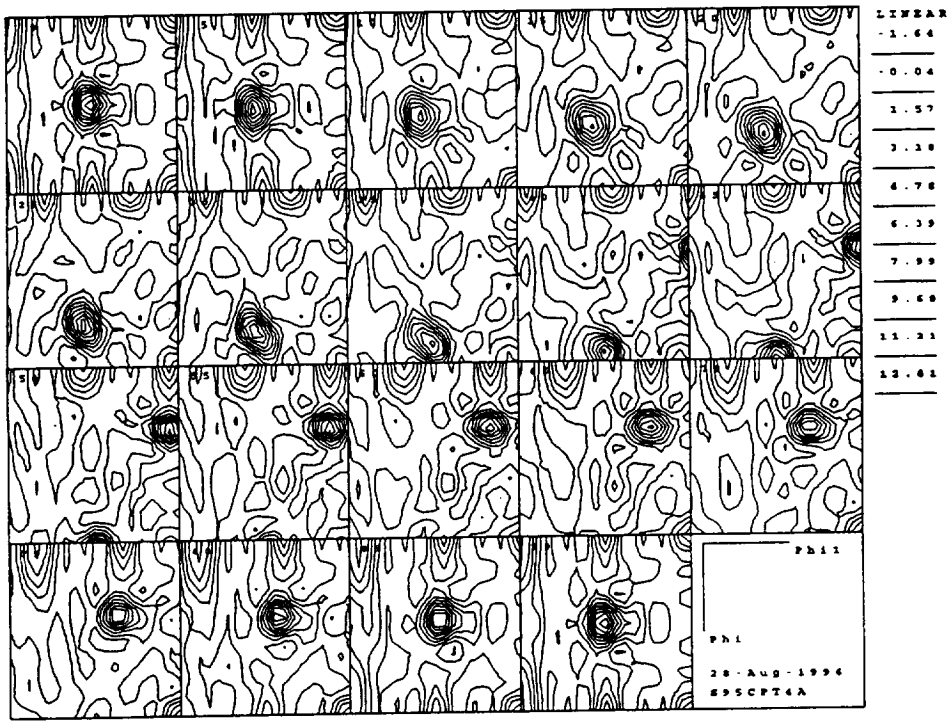

(b) Sections: φ_2= 45°; φ_2= 90°

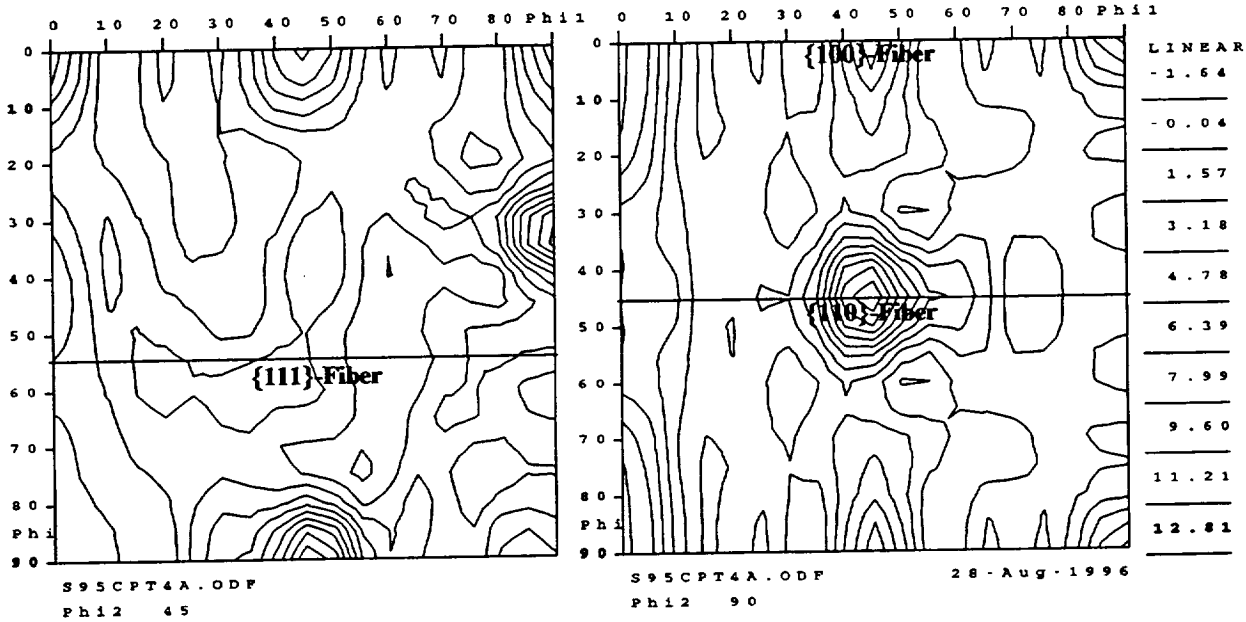

Figure 135. CODF sections for the 2195-T3 extrusion in the cap @ t/4; (a), Complete sections: φ_2= 0, 5, 10 ..... 90°; and (b), enlarged φ_2= 45° and φ_2= 90° sections. The locations of the {100}-fiber, {110}-fiber and {111}-fiber are shown.
[Specimen plane perpendicular to (R)adial axis]

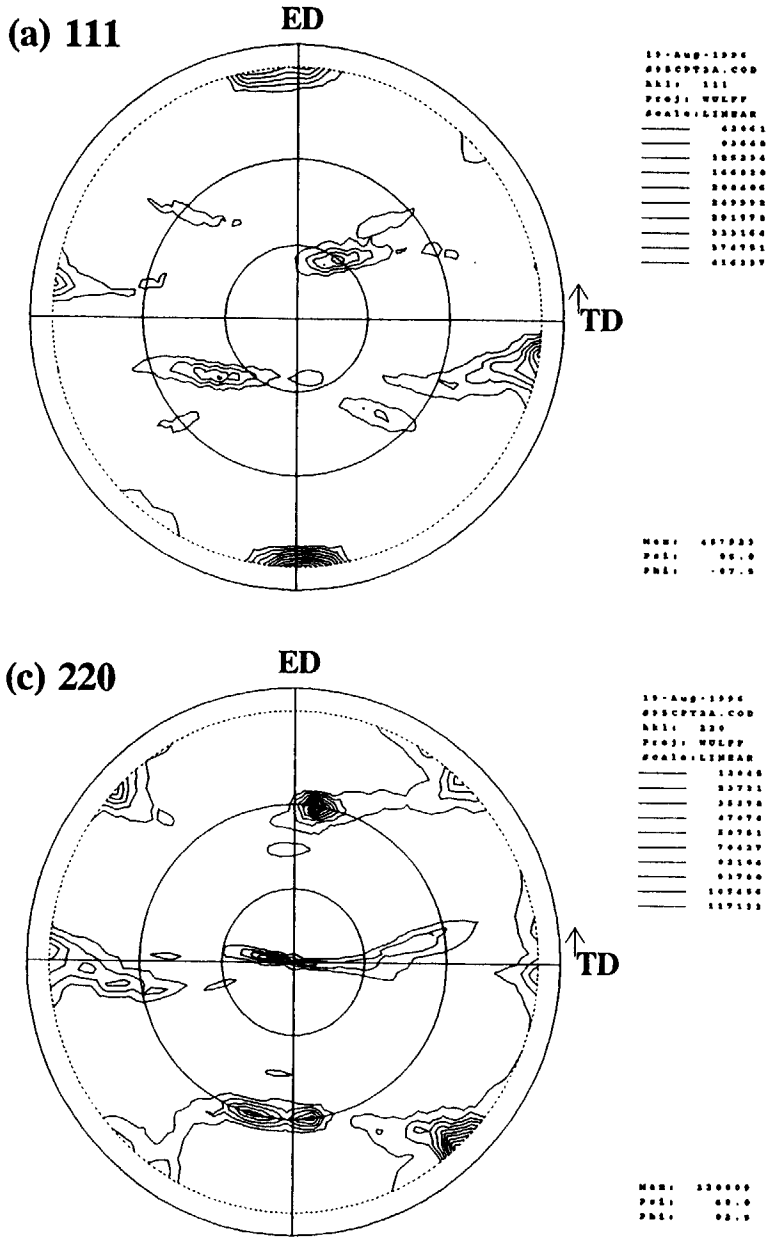

Figure 136.
Partial pole figures for the 2195-T3 extrusion in the cap @ t/2: (a) (111); (b) (200); (c) (220). [Specimen plane perpendicular to (R)adial axis]

(a) Sections: φ_2= 0 - 90°

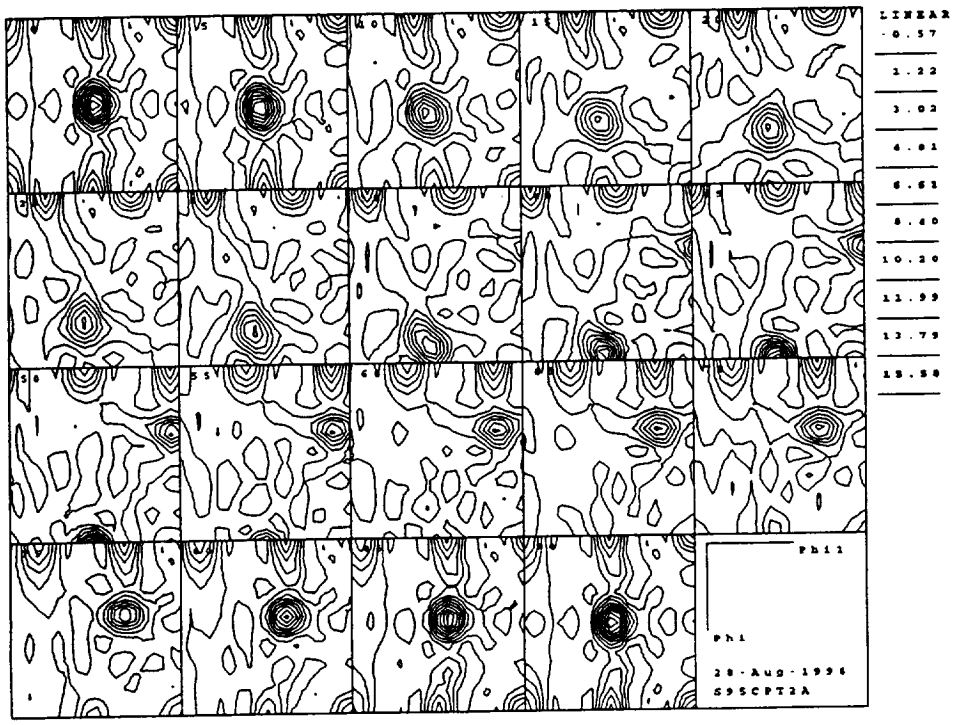

(b) Sections: φ_2= 45°; φ_2= 90°

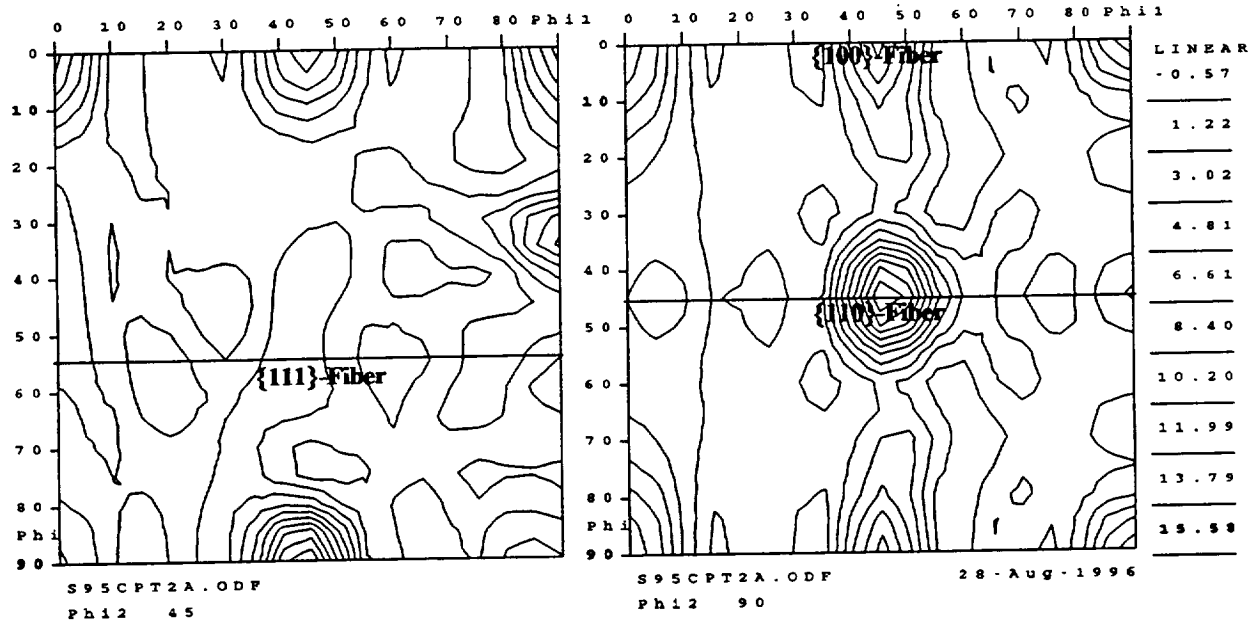

Figure 137. CODF sections for the 2195-T3 extrusion in the cap @ t/2; (a), Complete sections: φ_2= 0, 5, 10 ..... 90°; and (b), enlarged φ_2= 45° and φ_2= 90° sections. The locations of the {100}-fiber, {110}-fiber and {111}-fiber are shown.
[Specimen plane perpendicular to (R)adial axis]

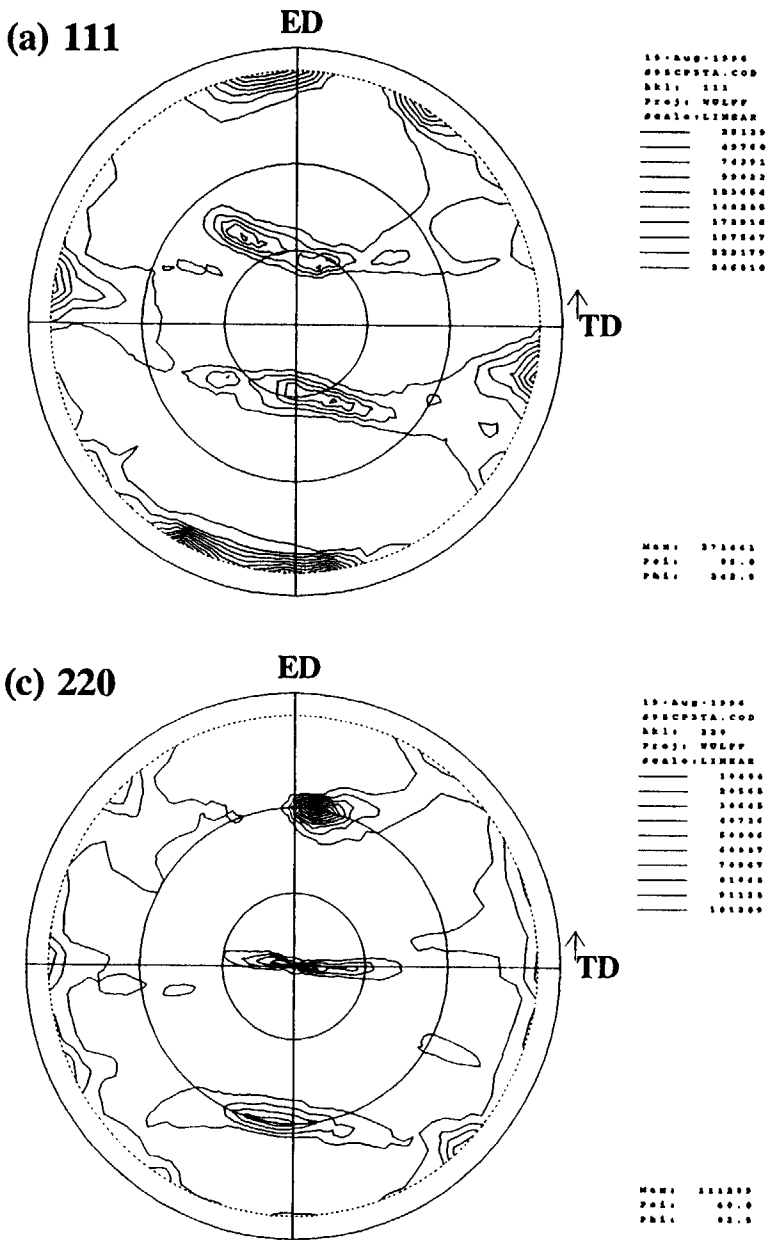

Figure 138.
Partial pole figures for the 2195-T3 extrusion in the cap @ 3t/4: (a) (111); (b) (200); (c) (220). [Specimen plane perpendicular to (R)adial axis]

(a) Sections: φ_2= 0 - 90°

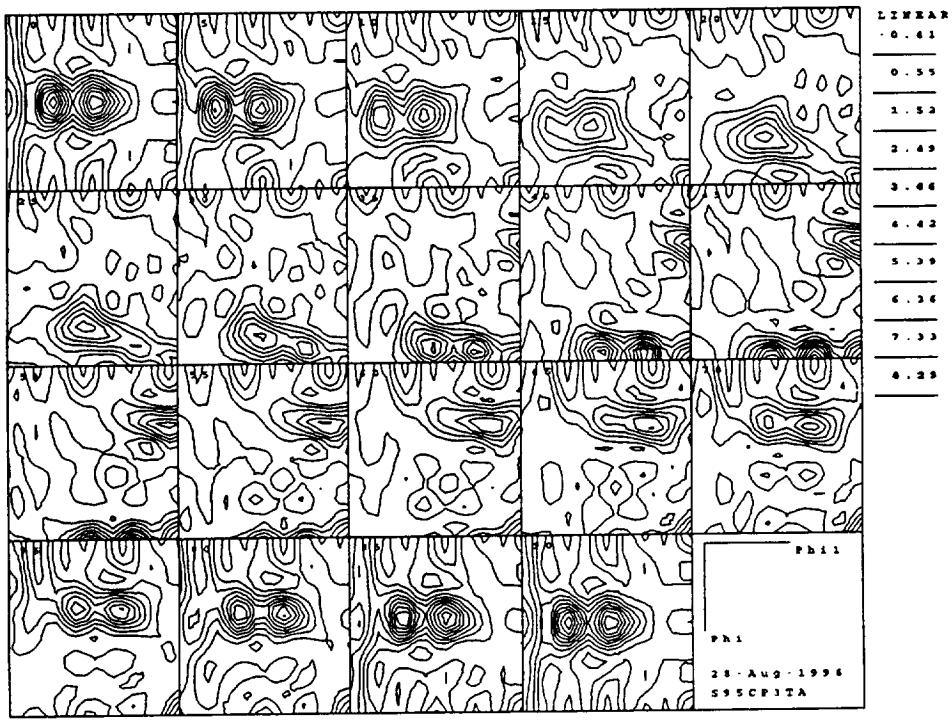

(b) Sections: φ_2= 45°; φ_2= 90°

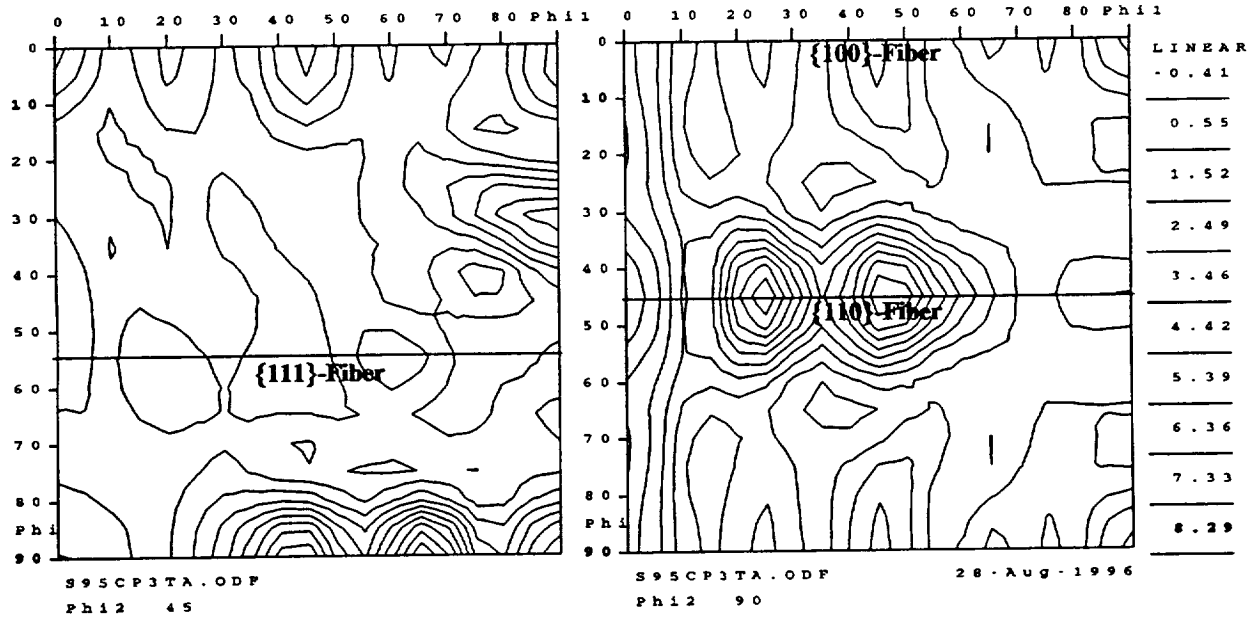

Figure 139. CODF sections for the 2195-T3 extrusion in the cap @ 3t/4; (a), Complete sections: φ_2= 0, 5, 10 ..... 90°; and (b), enlarged φ_2= 45° and φ_2= 90° sections. The locations of the {100}-fiber, {110}-fiber and {111}-fiber are shown.
[Specimen plane perpendicular to (R)adial axis]

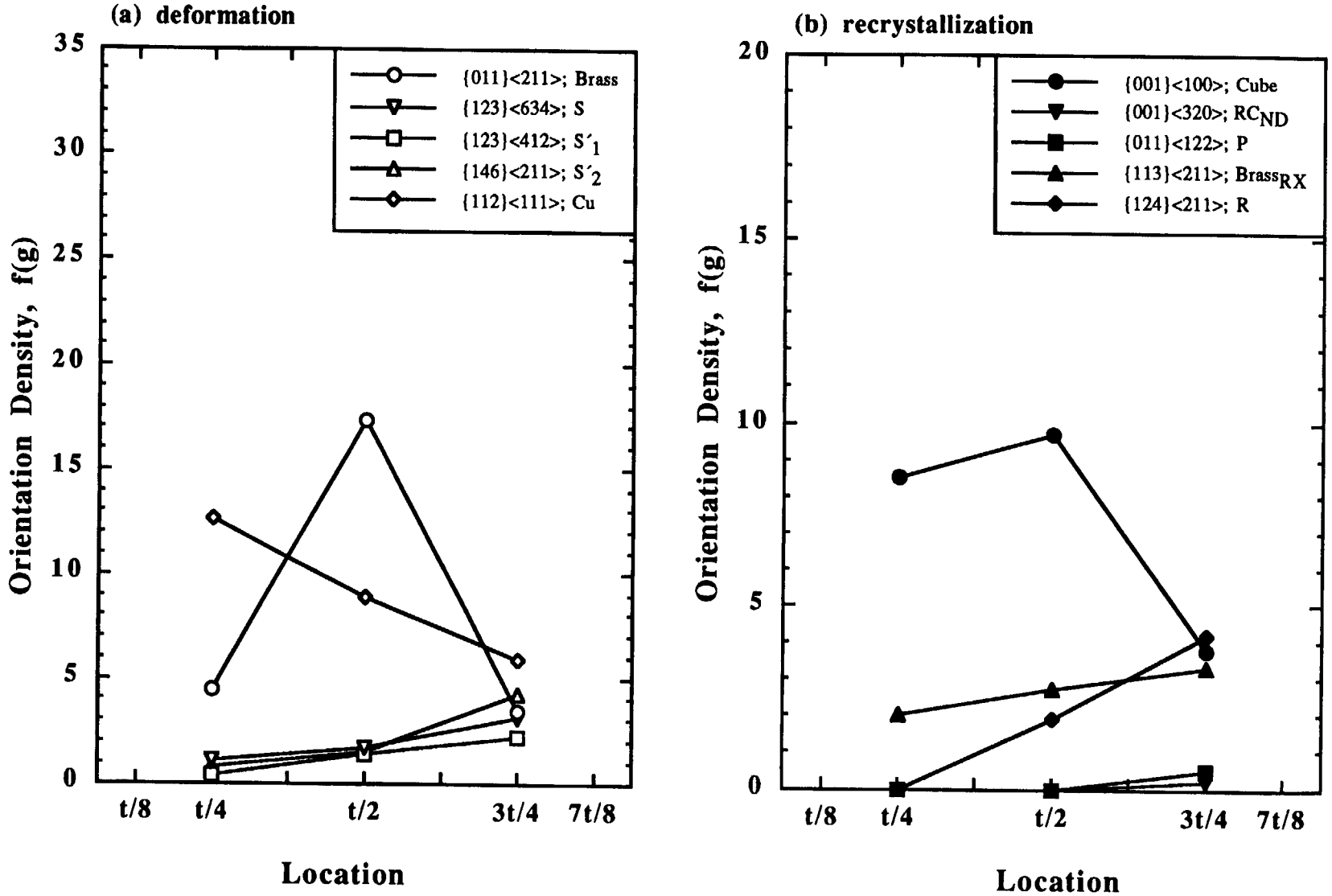

Figure 140. Orientation density, f(g), as a function of location through the cross-section for the 2195-T3 extrusion in the cap region: (a) Deformation-related components; (b) Recrystallization-related components.

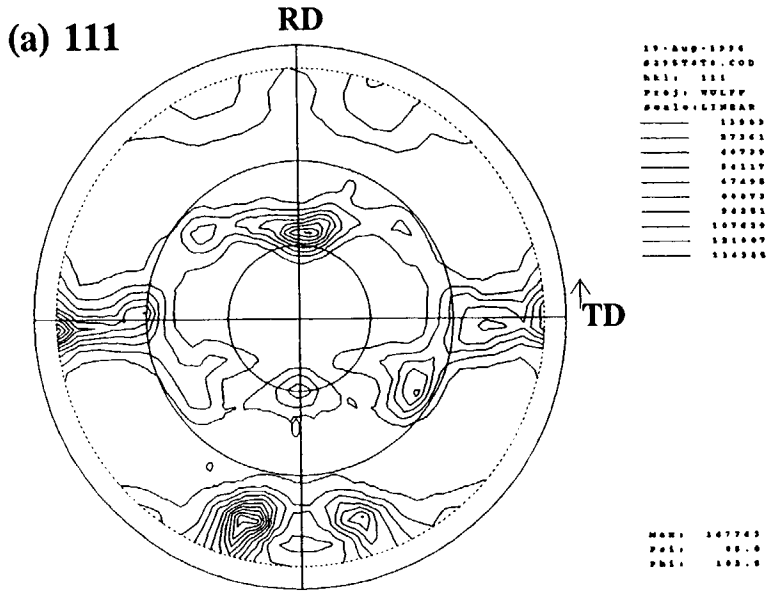

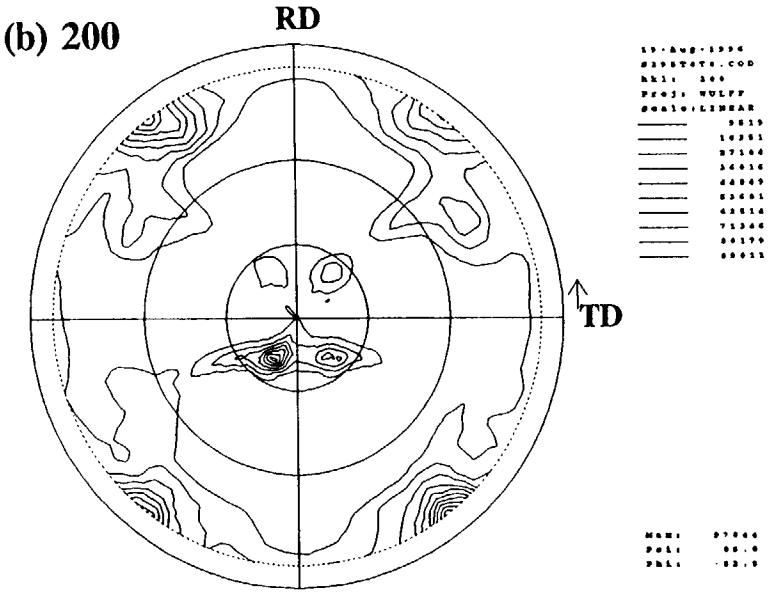

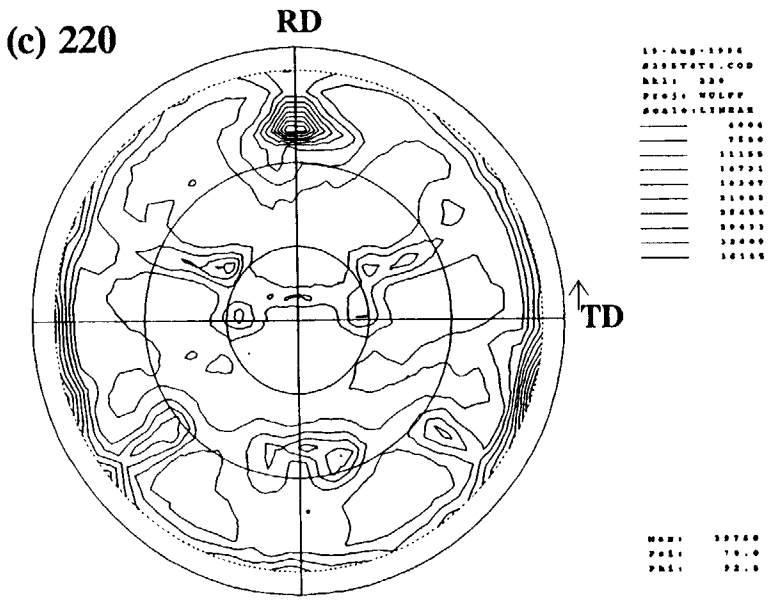

Figure 141.
Partial pole figures for 2195-T8 plate @ t/8: (a) (111); (b) (200); (c) (220). [Specimen plane perpendicular to (S)hort-Transverse axis]

(a) Sections: φ_2= 0 - 90°

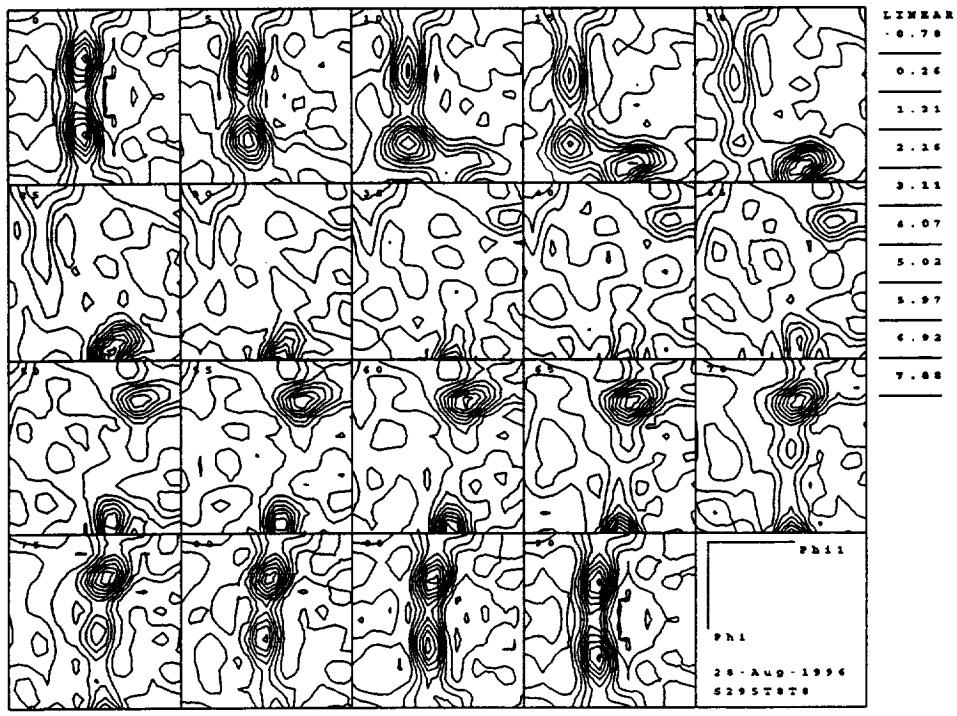

(b) Sections: φ_2= 45°; φ_2= 90°

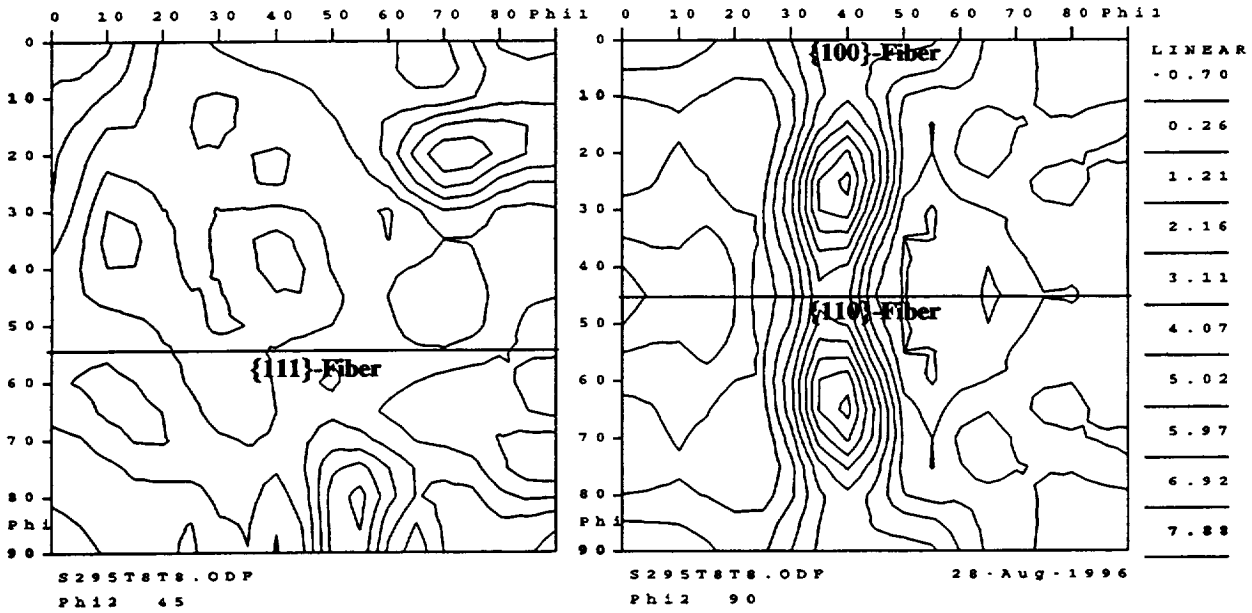

Figure 142. CODF sections for 2195-T8 plate @ t/8; (a), Complete sections: φ_2= 0, 5, 10 ..... 90°; and (b), enlarged φ_2= 45° and φ_2= 90° sections. The locations of the {100}-fiber, {110}-fiber and {111}-fiber are shown.
[Specimen plane perpendicular to (S)hort-Transverse axis]

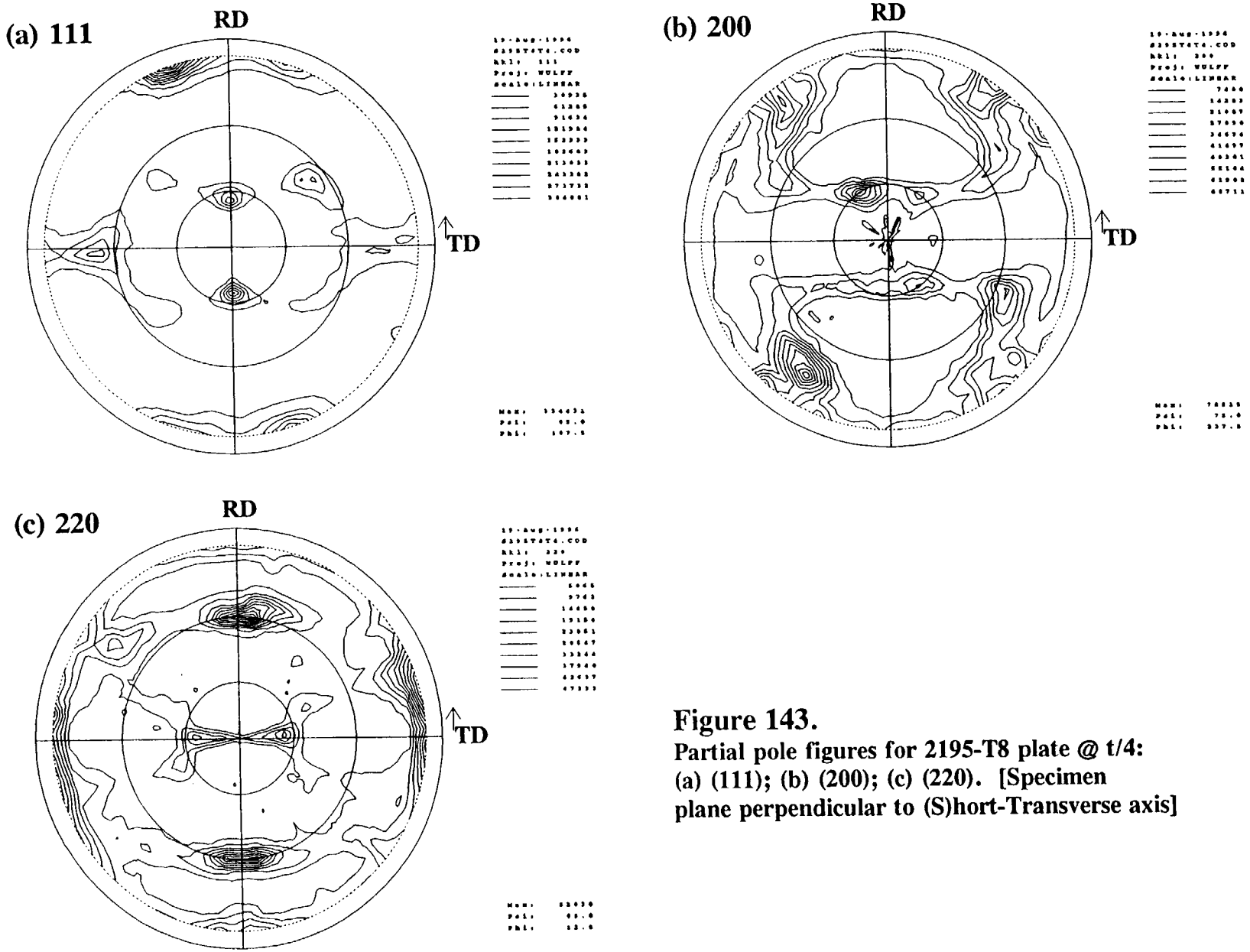

Figure 143.
Partial pole figures for 2195-T8 plate @ t/4: (a) (111); (b) (200); (c) (220). [Specimen plane perpendicular to (S)hort-Transverse axis]

(a) Sections: φ_2= 0 - 90°

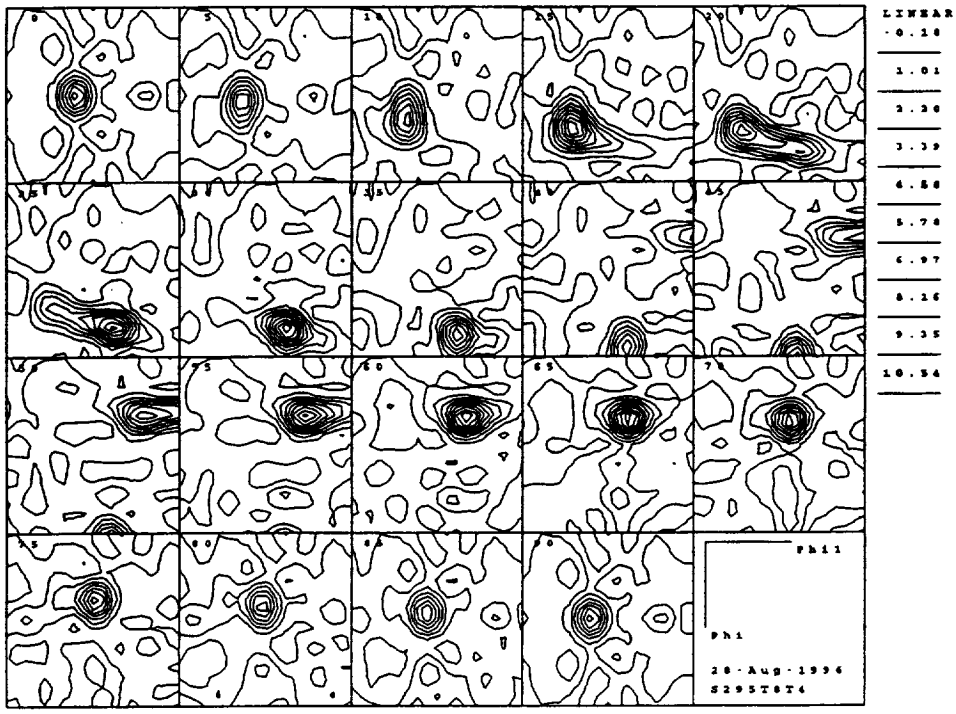

(b) Sections: φ_2= 45°; φ_2= 90°

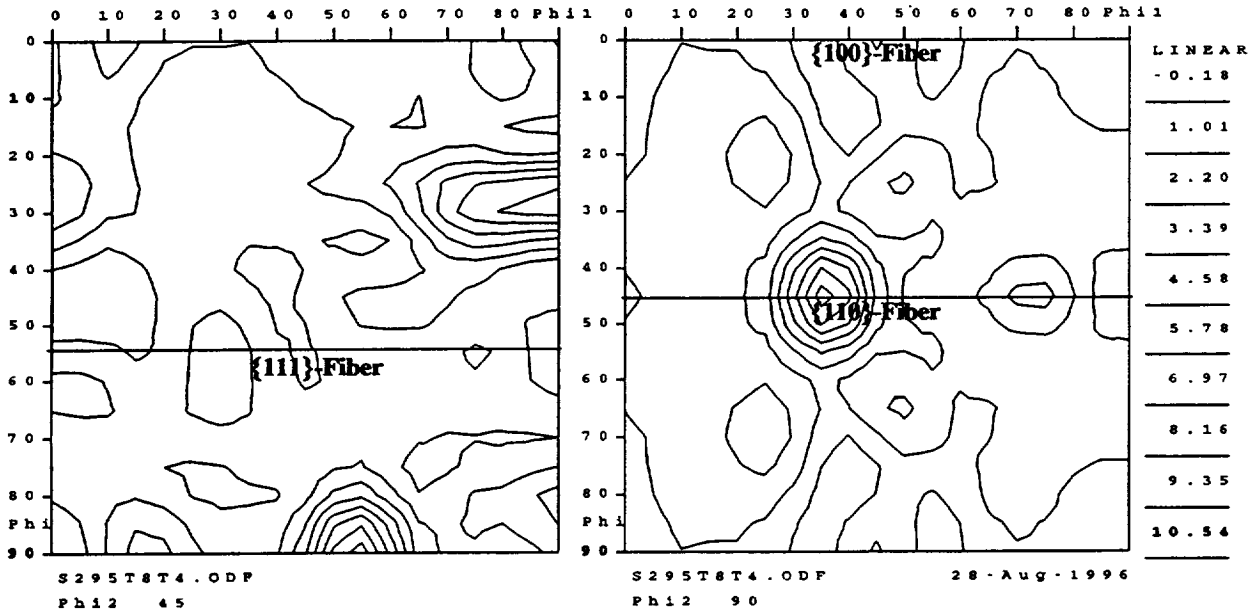

Figure 144. CODF sections for 2195-T8 plate @ t/4; (a), Complete sections: φ_2= 0, 5, 10 ..... 90°; and (b), enlarged φ_2= 45° and φ_2= 90° sections. The locations of the {100}-fiber, {110}-fiber and {111}-fiber are shown.
[Specimen plane perpendicular to (S)hort-Transverse axis]

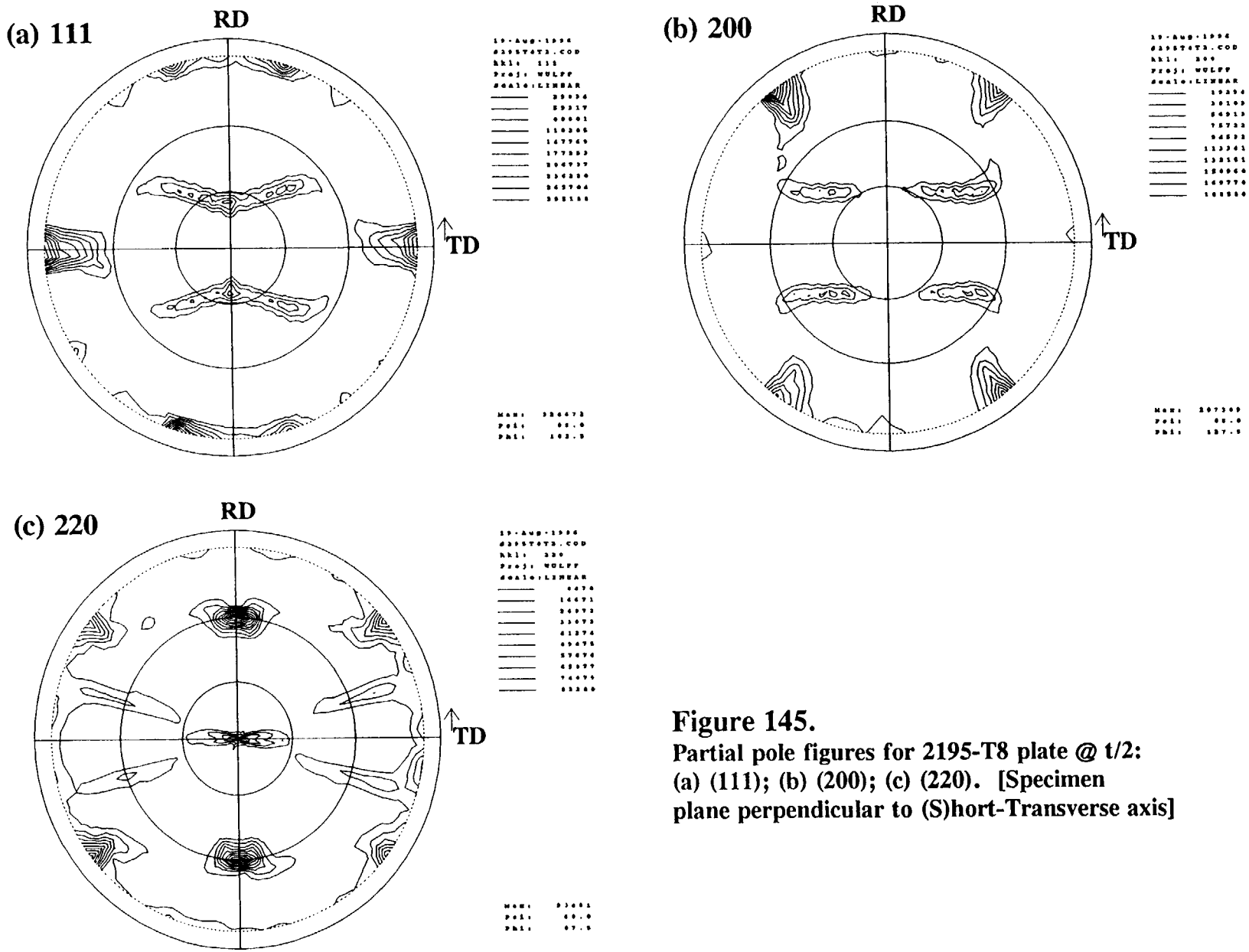

Figure 145.
Partial pole figures for 2195-T8 plate @ t/2: (a) (111); (b) (200); (c) (220). [Specimen plane perpendicular to (S)hort-Transverse axis]

(a) Sections: φ_2= 0 - 90°

(b) Sections: φ_2= 45°; φ_2= 90°

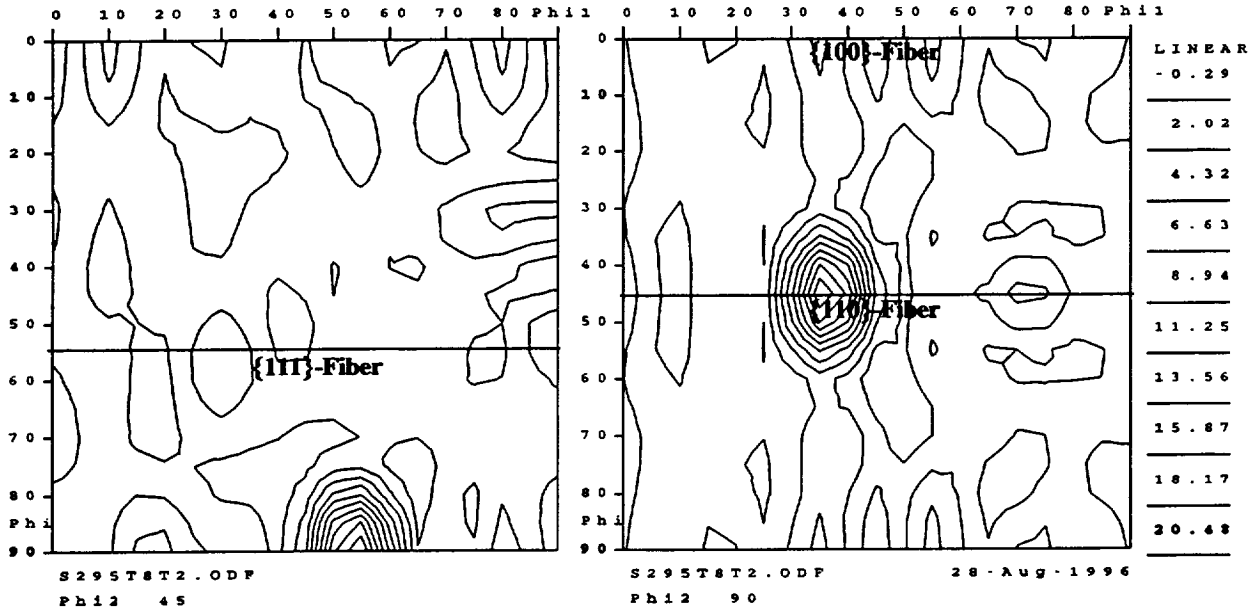

Figure 146. CODF sections for 2195-T8 plate @ t/2; (a), Complete sections: φ_2= 0, 5, 10 ..... 90°; and (b), enlarged φ_2= 45° and φ_2= 90° sections. The locations of the {100}-fiber, {110}-fiber and {111}-fiber are shown.
[Specimen plane perpendicular to (S)hort-Transverse axis]

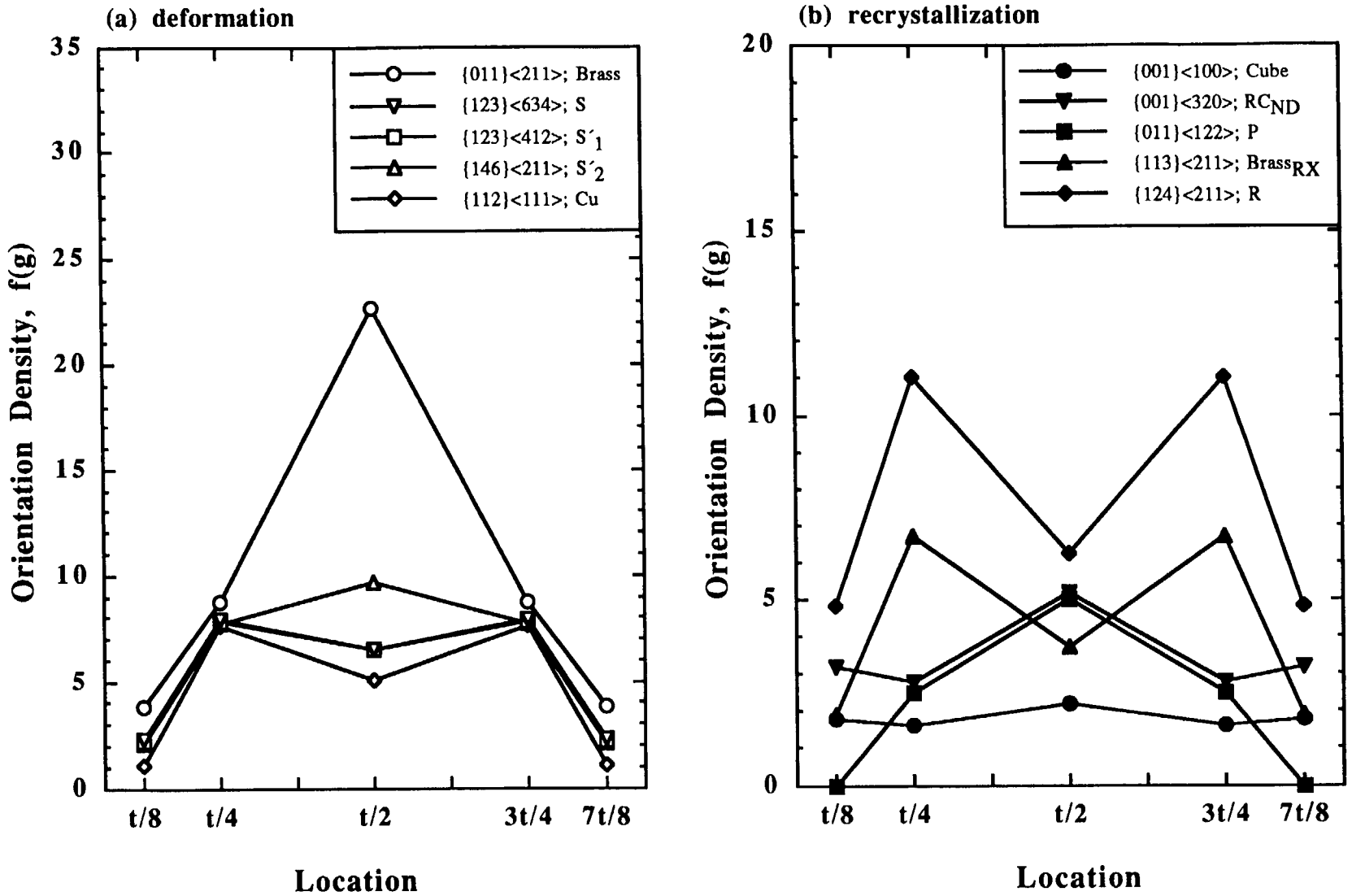

Figure 147. Orientation density, f(g), as a function of location through the cross-section for the 2195-T8 plate: (a) Deformation-related components; (b) Recrystallization-related components.

REPORT DOCUMENTATION PAGE

Form Approved
OMB No. 0704-0188

Public reporting burden for this collection of information is estimated to average 1 hour per response, including the time for reviewing instructions, searching existing data sources, gathering and maintaining the data needed, and completing and reviewing the collection of information. Send comments regarding this burden estimate or any other aspect of this collection of information, including suggestions for reducing this burden, to Washington Headquarters Services, Directorate for Information Operations and Reports, 1215 Jefferson Davis Highway, Suite 1204, Arlington, VA 22202-4302, and to the Office of Management and Budget, Paperwork Reduction Project (0704-0188), Washington, DC 20503.

1. AGENCY USE ONLY *(Leave blank)*	2. REPORT DATE	3. REPORT TYPE AND DATES COVERED
	February 1998	Contractor Report

4. TITLE AND SUBTITLE
Catalogue of X-Ray Texture Data for Al-Cu-Li Alloy 1460, 2090, 2096 and 2195 Near-Net-Shape Extrusions, Sheet and Plate

5. FUNDING NUMBERS
C NAS1-19708

522-12-51-01

6. AUTHOR(S)
Stephen J. Hales
Robert A. Hafley
Joel A. Alexa

7. PERFORMING ORGANIZATION NAME(S) AND ADDRESS(ES)
Analytical Services & Materials, Inc.
107 Research Drive
Hampton, VA 23666

8. PERFORMING ORGANIZATION REPORT NUMBER

9. SPONSORING / MONITORING AGENCY NAME(S) AND ADDRESS(ES)
National Aeronautics and Space Administration
Lanlgey Research Center
Hampton, VA 23681-2199

10. SPONSORING / MONITORING AGENCY REPORT NUMBER
NASA/CR-1998-206924

11. SUPPLEMENTARY NOTES
Langley Technical Monitor: R. Keith Bird

12a. DISTRIBUTION / AVAILABILITY STATEMENT
Unclassified - Unlimited
Subject Category 26
Distribution: Standard
Availability: NASA CASI (301) 621-0390

12b. DISTRIBUTION CODE

13. ABSTRACT *(Maximum 200 words)*

The effect of crystallographic texture on the mechanical properties of near-net-shape extrusions is of major interest if these products are to find application in launch vehicle or aircraft structures. The objective of this research was to produce a catalogue containing quantitative texture information for extruded product, sheet and plate. The material characterized was extracted from wide, integrally stiffened panels fabricated from the Al-Cu-Li alloys 1460, 2090, 2096 and 2195. The textural characteristics of sheet and plate products of the same alloys were determined for comparison purposes. The approach involved using X-ray diffraction to generate pole figures in combination with orientation distribution function analysis. The data were compiled as a function of location in the extruded cross-sections and the variation in the major deformation- and recrystallization-related texture components was identified.

14. SUBJECT TERMS
ODF, X-ray, texture, Al-Cu-Li, 1460, 2090, 2096, 2195, near-net-shape, extrusion

15. NUMBER OF PAGES
170

16. PRICE CODE
A08

17. SECURITY CLASSIFICATION OF REPORT	18. SECURITY CLASSIFICATION OF THIS PAGE	19. SECURITY CLASSIFICATION OF ABSTRACT	20. LIMITATION OF ABSTRACT
Unclassified	Unclassified	Unclassified	